FLEXIBLE BARS

R. Frisch-Fay

Lecturer in Civil Engineering
The University of New South Wales

LONDON
BUTTERWORTHS
1962

Suggested U.D.C. number 539. 384: 62–127

Printed in Great Britain by
R. J. Acford Ltd., Industrial Estate, Chichester, Sussex.

PREFACE

THE German mathematician Clebsch published his '*Theorie der Elasticiät fester Körper*' one hundred years ago. For a long time his book gave the only comprehensive treatment of elasticity in general and of deflections in particular. Saalschütz's '*Der belastete Stab*' in 1880 was the first attempt to give a complete description of the deflections of a bar in the linear as well as in the nonlinear field. No similar work appeared until 1948 when a Russian monograph '*Nonlinear problems in the statics of thin rods*' by E. P. Popov was published.

A large number of works dealing with Strength of Materials is available for undergraduate students and a much smaller number containing advanced topics for Engineers, Physicists and Applied Mathematicians. A few of these mention nonlinear deflections very briefly; generally speaking, however, nonlinear bending and deflections of a bar have so far been neglected, for apart from a nineteenth century German book only a Russian work is available. This book is intended to fill the gap.

This monograph is written for advanced students and research engineers. The majority of problems are developed in detail while in a very few cases the final results only are given. For the solution of many cases a knowledge of engineering mathematics up to graduate standard together with an understanding of elliptic functions and integrals has been assumed. In cases where solutions cannot be derived without going beyond this limit references to a more detailed discussion are given.

After an introductory chapter concerning basic derivations, Chapter 2 deals with the cantilever, Chapter 3 with the bar on two supports, and Chapter 4 with initially curved bars. Chapter 5 describes approximate methods for the analysis of those problems for which closed form solutions have not yet been suggested. Finally, Chapter 6 serves as an introduction to nonlinear deflections in three dimensions.

The author takes this opportunity to express his sincere appreciation to Mr. F. E. Archer, senior lecturer, and to Mr. I. J. Somervaille, lecturer in the School of Civil Engineering, The University of New South Wales, for their valuable help and criticism in the preparation of the final manuscript.

The author has pleasure in acknowledging permission from the Commonwealth Scientific and Industrial Research Organization, Melbourne (*Australian Journal of Applied Science*) to use illustrations and material in sections 2.5, 2.8, 3.1, 3.3, 4.7 and 4.10. The writer is also indebted to the Editors of the *Journal of Applied Mechanics* (American Society of Mechanical Engineers) and to Mr. A. E. Seames and Professor H. D. Conway for facilities in connection with sections 4.12 and 5.8; and to Professor M. Mizuno whose analysis of springs in the *Bulletin of Japan Society of Mechanical Engineers* was used extensively in section 6.6.

Ryde, New South Wales
January 1962

R. FRISCH-FAY

CONTENTS

1

BASIC EQUATIONS

1.1. The Concept of Linear and of Nonlinear Deflections

When investigating the deflections of a loaded bar, analysis usually begins with the Bernoulli–Euler law, according to which the bending moment at any point of the bar is proportional to the change in the curvature caused by the action of the load. The basic formula

$$\frac{1}{r} = \frac{M}{EI} = \frac{d\phi}{ds}$$

is immediately applicable when the equation of the deflection curve is given in the intrinsic form $s = f(\phi)$ where s is measured along the length of the arc and ϕ is the slope at s. In rectangular coordinates the curvature is expressed as

$$\frac{1}{r} = -\frac{d^2y/dx^2}{[1 + (dy/dx)^2]^{3/2}} \tag{1.1}$$

The negative sign can be explained by the fact that in assuming downward deflections as positive, an increase in x means a decrease in ϕ. Since the bending moment is a function of x we can write

$$M = \frac{EI}{r} = g(x) \tag{1.2}$$

The combination of (1.1) and (1.2) results in a second order nonlinear differential equation. In conventional engineering applications the relationship between bending moment and curvature is linearized by neglecting the square of the slope, $(dy/dx)^2$, in comparison with unity. This approach is justified provided the deflections are very small compared with the length of the bar, that is, when the deflection curve is very flat. This approximation is not permissible for slender bars and wires where the deflections are appreciable compared to the length. The elementary theory, therefore, is not applicable for the calculation of 'large deflections'. A simple example will illustrate this statement. By using the formula $\delta = Pl^3/3EI$ for the deflection of the free end of a horizontal cantilever loaded by a vertical force P at that point, absurd answers will result for slender bars; for, if $l = 100$ in., $P = 1$ lb, and $EI = 1000$ lb in.^{2}, we find that the deflection $\delta = 333$ in., 3·33 times the length of the cantilever.

The deflection curve of an elastic bar was first investigated by J. Bernoulli who tried to employ the recently developed infinitesimal calculus for the solution of physical problems. The first comprehensive study in the deflection of bars was written by Euler[1]. In the appendix of his book called *De Curvis Elasticis*, Euler explains that $(dy/dx)^2$ cannot be neglected in the expression for the curvature unless the deflections are small. For the horizontal cantilever subject to a vertical load at the free end, Euler finds $Cy''/[1+(y')^2]^{3/2} = Px$ which he integrates by series and shows that $C = Pl^2(2l - 3f)/6f$ where f is the deflection of the free end. Neglecting the term $3f$ in the bracket we get $f = Pl^3/3EI$. The neglected term allows for the shortening of the lever arm during the deflection.

The flexible bar was also analysed by Lagrange[2] in his work entitled *Sur la Force des Ressorts Pliès*. The solution, however, was erroneous as pointed out later by Plana[3].

In addition to giving inaccurate and sometimes absurd answers, the elementary theory gives no solution for the deflection in any direction other than the one normal to the original shape of the bar. This is shown in *Figure 1.1* where a simply supported beam carries

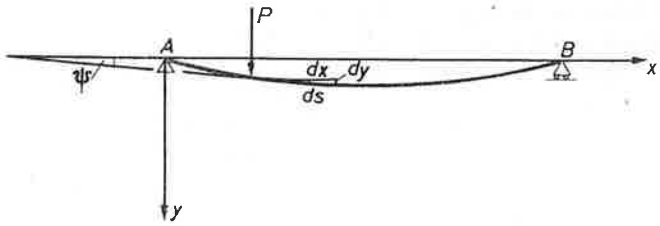

Figure 1.1

a load P. The conventional theory of deflections assumes here that $ds \approx dx$ and $\theta \approx \tan\theta$. As a result $\int dx = \int ds$, hence the rolling support at B will not move toward A. The curve is, of course, longer than the chord AB but as long as the curve is very flat (in other words, dy is of first order smallness) the difference between arc length and chord length is of second order smallness. This is of great importance for the usual engineering analysis because it means that the load P moves only in the y direction, hence the distances between the forces remain unchanged during deflection. In these circumstances the deflection is a linear function of the bending moment and of the load too. This is the basis of the principle of superposition.

With the increase of the slope the assumption of $ds = dx$ becomes less and less valid; the deflections are no longer a linear function of the bending moment or of the load, hence the principle of superposition is not applicable. This has far-reaching consequences in the analysis of large deflections. Every case involving large deflections has to be solved separately since load types that are a linear combination of types already solved cannot be analysed on the assumption that the final deflections are also a linear combination of the deflections previously obtained.

The nonlinear relationship between deflection and bending moment can easily be demonstrated on a cantilever carrying P at the free end. By gradually increasing P from zero to its final value the bar will deflect and its free end will begin to move toward the fixed end. Because of the shortening of the lever arm the bending moment will not increase at the same rate as the applied load.

It should be noted that systems undergoing large deflections are not the only ones to which the principle of superposition does not apply. For example, the central hinge C in the structure in *Figure 1.2* will deflect

$$CC' = \delta = l\left(\frac{P}{AE}\right)^{1/3}$$

indicating a nonlinear relationship between δ and P. This, furthermore, is true for small deflections only because the result was obtained by writing $\sec \alpha = 1 + \alpha^2/2$.

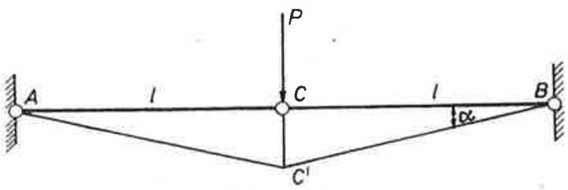

Figure 1.2

1.2. Nonlinear Differential Equations of the Second Order. Elliptic Functions and Integrals

Linear differential equations of the second order have two linearly independent solutions, that is, they are not proportional. Hence if y_1 is a solution and y_2 is also a solution of the same differential equation, then any linear combination $y = Ay_1 + By_2$ is also a solution. A and B are arbitrary multipliers which, for a particular case, can be determined from the boundary conditions, but the functions y_1 and y_2 remain unaffected. In the case of nonlinear second order differential equations, A and B are also found from boundary conditions but they are not mere multipliers. The solution y is a function of A and B, that is, of the boundary conditions[4].

While there is no general method for the solution of second order nonlinear differential equations, a certain type, called Newton's equation, may be solved by a simple procedure and will involve elliptic integrals. Newton's equation[5] contains the second derivative of the dependent variable and a nonlinear function of the same variable. It is of the form

$$\frac{d^2y}{dx^2} + a\Phi(y) = 0$$

The name 'elliptic integral' was used by Legendre to designate integrals of the types

$$\int \frac{dx}{\sqrt{X}}, \quad \int \frac{x^2 dx}{\sqrt{X}} \quad \text{and} \quad \int \frac{dx}{(x-b)\sqrt{X}},$$

where X is either of the third or fourth degree in x. These are called 'elliptic integrals' of the first, second, and third kind respectively. A comprehensive study of elliptic integrals and functions is given by Cayley[6] and by Hancock[7]. A concise treatment on the subject is also presented by Bowman[8]. Tables for elliptic functions and integrals have been prepared by Milne-Thomson[9], Pearson[10], and by Jahnke and Emde[11].

For the present discussion (with the exception of Chapter 6) only the first and second kind elliptic integrals are of importance. Suitable transformation turns these into

$$\int_0^x \frac{dx}{[(1-x^2)(1-p^2x^2)]^{\frac{1}{2}}} \quad \text{and} \quad \int_0^x \frac{(1-p^2x^2)^{\frac{1}{2}}dx}{(1-x^2)^{\frac{1}{2}}}$$

Writing $x = \sin\phi$, we get Legendre's standard form of the first kind:

$$F(p, \phi) = \int_0^\phi \frac{d\phi}{(1-p^2\sin^2\phi)^{\frac{1}{2}}}$$

and of the second kind:

$$E(p, \phi) = \int_0^\phi (1 - p^2 \sin^2 \phi)^{\frac{1}{2}} d\phi$$

$F(p, \phi)$ is a function of p, the modulus, and of the limit ϕ. Let

$$u = \int_0^\phi \frac{d\phi}{(1 - p^2 \sin^2 \phi)^{\frac{1}{2}}} = F(p, \phi)$$

Considering p a constant we express the inverse function of u as $\phi = \text{am } u = \text{amplitude of } u$.

Considered as a function of u,

$$\begin{aligned}
x &= \sin \phi = \sin \text{am } u = \text{sn } u \\
(1 - x^2)^{\frac{1}{2}} &= \cos \phi = \cos \text{am } u = \text{cn } u \\
(1 - p^2x^2)^{\frac{1}{2}} &= \Delta \phi = \Delta \text{ am } u = \text{dn } u
\end{aligned}$$

where sn u, cn u, and dn u are Jacobi's elliptic functions. The relationship between x and the elliptic functions is more readily understood if it is compared with circular functions.

Thus,

$$u = \int_0^x \frac{dx}{(1 - x^2)^{\frac{1}{2}}} = \sin^{-1} x,$$

while

$$u = \int_0^x \frac{dx}{[(1 - x^2)(1 - p^2x^2)]^{\frac{1}{2}}} = \text{sn}^{-1} x$$

Putting $x = 1$ for the upper limit,

$$u = \int_0^1 \frac{dx}{(1 - x^2)^{\frac{1}{2}}} = \sin^{-1} 1 = \pi/2$$

and

$$u = \int_0^1 \frac{dx}{[(1 - x^2)(1 - p^2x^2)]^{\frac{1}{2}}} = \int_0^{\pi/2} \frac{d\phi}{(1 - p^2 \sin^2 \phi)^{\frac{1}{2}}} = F(p, \pi/2) = K(p)$$

$K(p)$ is the 'complete elliptic integral' of the first kind and its value depends on p only. For $p = 0$, $K(0) = \pi/2$, and, as seen above, the circular sine and the elliptic sine are identical. Similarly, $\cos u = \text{cn}\, u$ if $p = 0$. If $p = 1$, we find:

$$\text{sn}\ u = \tanh u$$

and
$$\text{cn}\ u = \text{sech}\ u = \text{dn}\ u$$

The complete integral of the second kind is defined as

$$E(p, \pi/2) = \int_0^{\pi/2} (1 - p^2 \sin^2 \phi)^{\frac{1}{2}} d\phi = E(p)$$

Integrals of the type of F and E have a closed form solution for $p = 0$ and $p = 1$ only. In other cases they may be evaluated by series expansion[12].

1.3. Vertical Strut under Vertical Load

Let us assume a vertical strut, fixed at the bottom and subject to a vertical load P at the top. If the bar is sufficiently flexible it will take the shape in *Figure 1.3*. The flexural rigidity EI is constant, a

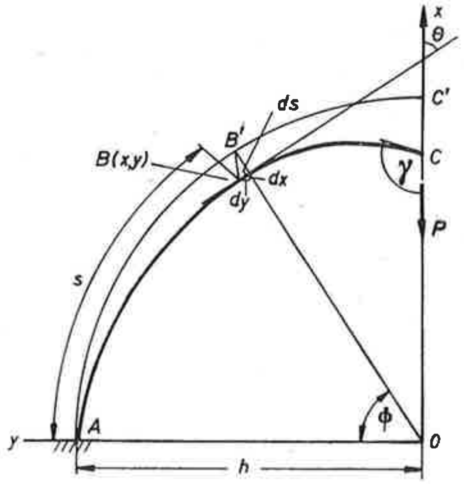

Figure 1.3

condition that will hold throughout this discussion. The bending moment at $B(x, y)$ due to P is $M = -Py = EI/r$

and
$$y = -\frac{EI}{Pr} = -\frac{1}{k^2 r} \tag{1.3}$$

where $k = (P/EI)^{\frac{1}{2}}$ and r is the radius of curvature. Using the accurate expression of $1/r$ we have

$$y = -\frac{d^2y/dx^2}{k^2[1 + (dy/dx)^2]^{3/2}} \tag{1.4}$$

Integrating with respect to x, equation (1.4) becomes

$$y^2 = \frac{2}{k^2[1 + (dy/dx)^2]^{\frac{1}{2}}} + C \tag{1.5}$$

From *Figure* 1.3, $dx/ds = \cos\theta$, hence $[1 + (dy/dx)^2]^{\frac{1}{2}} = 1/\cos\theta$ and equation (1.5) reduces to

$$y^2 = \frac{2}{k^2}\cos\theta + C = \frac{2}{k^2}[1 - 2\sin^2(\theta/2)] + C \tag{1.6}$$

Introducing
$$h^2 = 2/k^2 + C \tag{1.7}$$

we get
$$y^2 = h^2 - \frac{4}{k^2}\sin^2(\theta/2) \tag{1.8}$$

At the fixed end A, $\theta = 0$, hence $y = h = AO$. Since y^2 is positive, the solution of equation (1.8) will depend on the relative values of h and k.

First we assume
$$h^2 < 4/k^2$$

Let
$$h^2 = 4p^2/k^2 \tag{1.9}$$

where $p < 1$ and select ϕ such that

$$\sin(\theta/2) = p\sin\phi \tag{1.10}$$

In this case
$$y = h\cos\phi \tag{1.11}$$

Noting that $dy/d\phi = -h\sin\phi$ and $dy/ds = \sin\theta$, after some reductions,

$$ds = -\frac{hd\phi}{2p(1 - p^2\sin^2\phi)^{\frac{1}{2}}} = -\frac{d\phi}{k(1 - p^2\sin^2\phi)^{\frac{1}{2}}} \tag{1.12}$$

θ is negative as shown in *Figure 1.3*, hence ϕ is also negative. The negative sign in equation (1.12) means that ϕ is decreasing while s

increases. Integrating ds from 0 to s and disregarding the negative sign,

$$s = \frac{1}{k}\int_0^{\phi} \frac{d\phi}{(1 - p^2 \sin^2 \phi)^{\frac{1}{2}}} = \frac{1}{k} F(p, \phi) \tag{1.13}$$

This equation contains the unknowns p and ϕ. The modulus p will be calculated from the assumption that the length of the strut does not alter during bending. Hence

$$L = \frac{1}{k}\int_0^{\pi/2} \frac{d\phi}{(1 - p^2 \sin^2 \phi)^{\frac{1}{2}}} = \frac{1}{k} K(p) \tag{1.14}$$

the limits having been chosen such that ϕ sweeps the quadrant in *Figure 1.3* from AO to $C'O$. Since, from (1.10),

$$p = \frac{\sin(\theta/2)}{\sin \phi}$$

the slope at C is found from $\sin(\gamma/2) = p$ (1.15)

This is a fundamental relationship between the modulus governing the shape of the bar and the end slope. Equation (1.14) will yield p and the slope at B can be determined in terms of s. By solving equation (1.13) for ϕ, expression (1.10) will supply θ. Expressed in elliptic functions, the relationship between the angle of the tangent at B and the length of the arc AB is:

$$\sin(\theta/2) = p \operatorname{sn} ks \tag{1.16}$$

where the modulus of sn is p.

The total horizontal deflection of the bar is

$$AO = h = 2p/k$$

and the y coordinate of B

$$y = \frac{2p \cos \phi}{k} = \frac{2p}{k} \operatorname{cn} ks \tag{1.17}$$

The bending moment at B

$$M = -yP = -2pkEI \operatorname{cn} ks \tag{1.18}$$

Turning now to the vertical coordinate of B we note that

$$dx = ds\cos\theta = ds(1 - 2p^2\sin^2\phi) \tag{1.19}$$

Substituting ds from expression (1.12) in equation (1.19)

$$dx = \frac{(1 - 2p^2\sin^2\phi)\,d\phi}{k(1 - p^2\sin^2\phi)^{\frac{1}{2}}}$$

and

$$x = \frac{1}{k}\int_0^{\phi}\frac{d\phi}{(1 - p^2\sin^2\phi)^{\frac{1}{2}}} - \frac{2p^2}{k}\int_0^{\phi}\frac{\sin^2\phi\,d\phi}{(1 - p^2\sin^2\phi)^{\frac{1}{2}}}$$

The second integral equals

$$[F(p, \phi) - E(p, \phi)]/p^2$$

and we find for the vertical deflection at B

$$x = 2E(p, \phi)/k - F(p, \phi)/k \tag{1.20}$$

By substituting $\pi/2$ for the upper limit in the integrals of equation (1.20) we can write for the deflection CO

$$v = 2E(p)/k - L \tag{1.21}$$

As explained before, the first step in the analysis of the strut is to calculate p. The position of any point of the deflected shape can be obtained from solving equations (1.13, 11, and 20).

The force necessary to cause the deflection shown in *Figure 1.3* is:

$$P = EIK^2(p)/L^2 = 4P_{cr}K^2(p)/\pi^2$$

where $P_{cr} = EI\pi^2/4L^2 =$ Euler's critical load.

If we continue the strut ABC (*Figure 1.4(a)*) symmetrically about A downward until D we get the deflected shape of a bar CD, $2L$ long and acted upon by forces P at the two ends (*Figure 1.4(b)*). By engaging similar bars at the points of contraflexure C and D, we get a series of elastic lines called the 'undulating elastica'

(*Figures 1.4*(*a*) and (*c*)). Of the two, however, only the one in *Figure 1.4*(*c*) is stable.

A gradual increase of P in *Figure 1.3* will be followed by growing vertical and horizontal deflections. However, there must be a value of P that marks the maximum horizontal movement of C

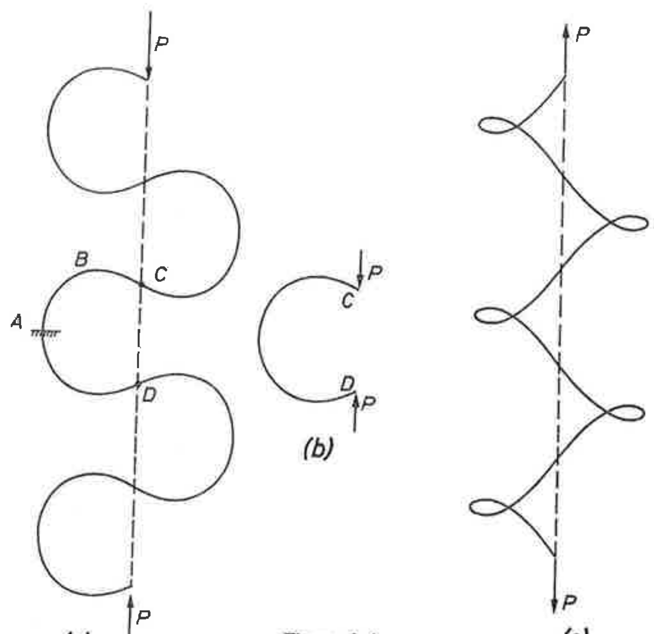

Figure 1.4

so that any further increase in P will mean a receding C. In order to find this force P, h/L must be made a maximum (*Figure 1.5*).

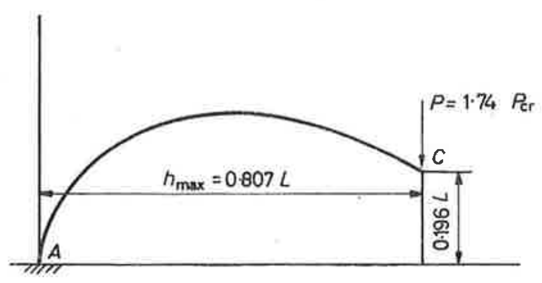

Figure 1.5

Since

$h/L = 2p/K(p) = \zeta(p)$ and $d[\zeta(p)]/dp = [2K(p) - 2pK'(p)]/K^2(p)$

the criterion of h/L being a maximum is

$$K(p) = pK'(p) = B(p)p^2/(1 - p^2)$$

where
$$B(p) = \int_0^{\pi/2} \frac{\cos^2 \phi \, d\phi}{(1 - p^2 \sin^2 \phi)^{\frac{1}{2}}}$$

This condition is satisfied by $p = 0{\cdot}837$, hence $h_{\max} = 0{\cdot}807L$ and is caused by $P = 1{\cdot}74P_{\text{cr}}$.

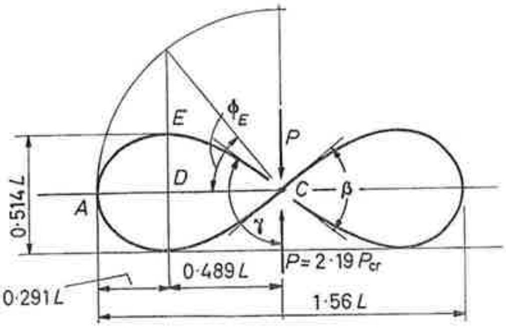

Figure 1.6

A wire of length $4L$ is bent elastically to take the form shown in *Figure 1.6*. To find its dimensions and the force necessary for holding it in equilibrium we observe that

$$v = 2E(p)/k - L = 0$$

This equation is solved by $p = 0{\cdot}908$, hence $h = 0{\cdot}78L$ and $P = 2{\cdot}19P_{\text{cr}}$. To find DE we note that $\theta = \pi/2$ at E so that

$$\sin \phi_E = \frac{\sin (\pi/4)}{p} = 0{\cdot}779$$

Applying equations (1.11 and 20), $CD = 0{\cdot}489L$ and $ED = 0{\cdot}257L$.

1.4. The Infinite Bar

In the previous section we discussed the elastic shape of a bar for which $h^2 < 4/k^2$. If $h^2 = 4/k^2$, that is, if $p = 1$, we have from equation (1.14)

$$L = \frac{1}{k}\int_0^{\pi/2} \frac{d\phi}{(1-\sin^2\phi)^{\frac{1}{2}}} = \frac{1}{k}\int_0^{\pi/2} \sec\phi\, d\phi$$

$$= \frac{1}{k}\,[\ln\tan(\pi/2) - \ln\tan(\pi/4)] = \infty \qquad (1.22)$$

Also from equation (1.9), $h = 2/k = 2\sqrt{(EI/P)}$ (finite) (1.23)

and $v = 2E(p)/k - L = -\infty$. Similar considerations lead to

$$s = \frac{1}{k}\int_0^{\phi} \frac{d\phi}{\cos\phi} = \frac{1}{k}\ln\tan(\phi/2 + \pi/4) = \frac{1}{k}(\lambda\phi)$$

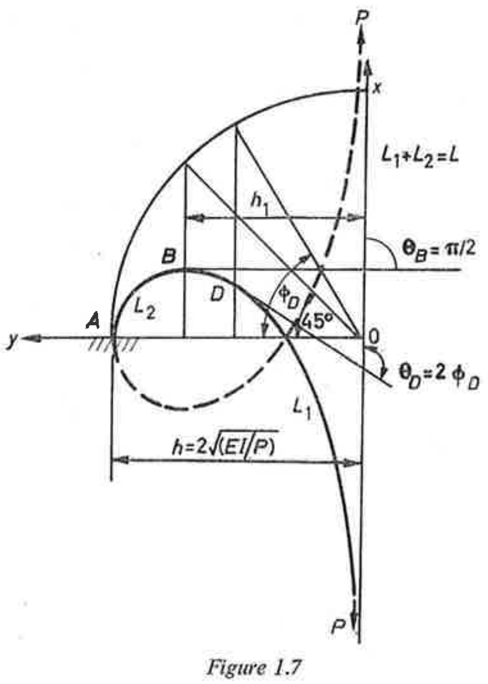

Figure 1.7

Hence the relationship between the slope and the bar length is $\phi = \theta/2 = \text{gd}\, ks$.

The last two functions were $\lambda(\phi) =$ Lambda function, and its inverse function, gd $ks =$ Gudermannian of ks. For these two functions the reader is referred to any standard textbook on advanced calculus. Hancock's work may also be consulted[13].

To find the vertical coordinate of a point in terms of $\phi = \theta/2$ we use the equations derived for the undulating elastica but set $p = 1$. Then

$$x = \frac{1}{k}\int_0^\phi \frac{d\phi}{\cos\phi} - \frac{2}{k}\int_0^\phi \frac{\sin^2\phi\, d\phi}{\cos\phi}$$
$$= \frac{2\sin\phi}{k} - \frac{\ln\tan(\phi/2 + \pi/4)}{k}$$

As ϕ approaches $\pi/2$, θ tends to π, and v approaches $-\infty$. This shows that the two branches of the loop in *Figure 1.7* are asymtotic to the vertical axis. The physical importance of the case is that the bar, although infinitely long, has a finite horizontal deflection.

1.5. Nodal Elastica

If, in equation (1.8) $h \leqslant 2/k$, y will vanish for certain values of x (for $h = 2/k$, y vanishes at $x = \pm\infty$). Since from $y = -1/k^2 r$, the curvature vanishes with y, it is clear that points of contraflexure occur whenever the curve passes through the x-axis. If, on the other hand, $h > 2/k$, y and the curvature will never vanish; in other words, there will be no points of contraflexure.

$$\text{Let } 4/k^2 = h^2 p^2, \qquad (p^2 < 1)$$

Then, from equation (1.8)

$$y = h[1 - p^2 \sin^2(\theta/2)]^{\frac{1}{2}} \tag{1.24}$$

Since $p^2 < 1$, y will not vanish for any real value of θ. We now select a parameter ϕ such that

$$\sin\phi = p\sin(\theta/2) \tag{1.25}$$

It follows at once that

$$y = h\cos\phi \tag{1.26}$$

Also, from

$$\frac{dy}{d\theta} = -\frac{hp^2 \sin\theta}{4[1 - p^2 \sin^2(\theta/2)]^{\frac{1}{2}}}$$

and from

$$\sin\theta = \frac{dy}{d\theta} \cdot \frac{d\theta}{ds}$$

we obtain

$$ds = -\frac{hp^2\, d(\theta/2)}{2[1 - p^2 \sin^2(\theta/2)]^{\frac{1}{2}}}$$

and

$$s = -\frac{hp^2}{2}\int_0^{\theta/2} \frac{d(\theta/2)}{[1 - p^2 \sin^2(\theta/2)]^{\frac{1}{2}}} = -\, hp^2 F(p, \theta/2)/2 \quad (1.27)$$

The reason for the negative sign is that θ is decreasing from the fixed end to the free end. In the following discussion s is taken positive.

To find x we note that

$$dx = \cos\theta\, ds = [1 - 2\sin^2(\theta/2)]\, ds$$

$$= \frac{hp^2\, d(\theta/2)}{2[1 - p^2 \sin^2(\theta/2)]^{\frac{1}{2}}} - \frac{hp^2 \sin^2(\theta/2)\, d(\theta/2)}{[1 - p^2 \sin^2(\theta/2)]^{\frac{1}{2}}}$$

(the negative sign in ds has been neglected). Integrating,

$$x = hp^2F(p, \theta/2)/2 - hp^2\int_0^{\theta/2} \frac{\sin^2(\theta/2)\, d(\theta/2)}{[1 - p^2 \sin^2(\theta/2)]^{\frac{1}{2}}}$$

$$= hE(p, \theta/2) - h(1 - p^2/2)F(p, \theta/2) \quad (1.28)$$

It follows from equation (1.24) that $y_{\max} = h$ and $y_{\min} = (1-p^2)^{\frac{1}{2}}$. This latter value of y occurs when $\theta = \pi$. Since $y_{\max}$ and $y_{\min}$ have the same sign, y cannot be zero: consequently P cannot act directly on the bar, because at P, $y = 0$. Therefore, the load can act only through a rigid lever which is equivalent to a couple $Ph \cos\phi$ and a direct load P. This is shown in *Figure 1.8*. The elastic shape of this bar is called the ‘ nodal elastica ’. *Figure 1.8* shows that ϕ will not reach $\pi/2$, hence complete elliptic integrals will not be used. If the length of the bar s, also P and M are given, from equation (1.24)

$$e = y = 2[1 - p^2 \sin^2(\theta/2)]^{\frac{1}{2}}/pk$$

where $e = M/P$. Combining this expression with equation (1.27) two equations are obtained with p and θ as unknowns. There are, however, certain ambiguous cases. Assuming for a moment that the levers (*b*) and (*c*) in *Figure 1.8* are equal, the slopes at C and D

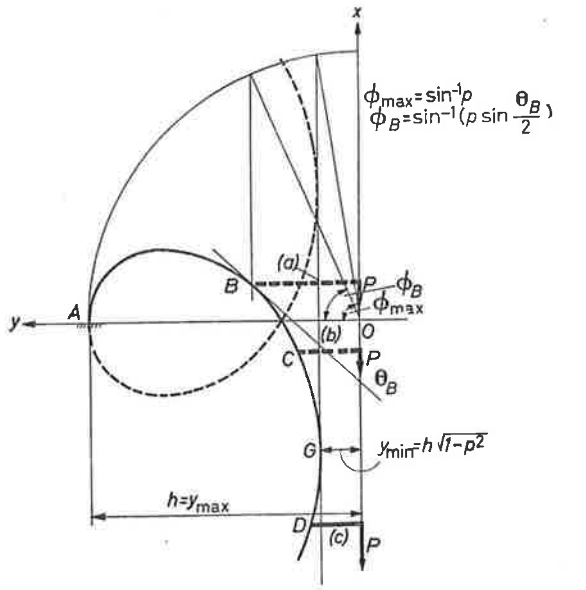

Figure 1.8

are $\pi - \alpha$ and $\pi + \alpha$ respectively. If these values are inserted in equation (1.24) we find that $\sin^2(\theta/2)$ is the same for both cases. It should be noted that the length $ABCG$ in *Figure 1.8* is the length of one half of a revolution of the nodal elastica and that it equals $L_\pi = hp^2F(p, \pi/2)/2 = pK(p)/k$. Equation (1.27) is applicable only for a bar of length less than $ABCG$. If the conditions of equilibrium call for a deflected shape $ABCGD$ (which, of course, cannot be known in advance) we trace the nodal elastica to a full revolution and deduct the missing part from this length. Thus the length of the nodal elastica measured from A, when θ varies from 0 to 2π, is $L_{2\pi} = 2pK(p)/k$, hence

$$L = ABCGD = L_{2\pi} - hp^2F(p, \theta_D/2)/2 \qquad (1.29)$$

It may be pointed out here that any of the three load positions shown in *Figure 1.8* are capable of holding the bar in the same general shape with overlapping segments of AB, ABC, and $ABCD$ respectively. Furthermore, it is not possible to tell in advance whether the bar will reach its equilibrium in position (*a*) (*Figure 1.8*) or one (or more) full revolutions later. Hence, the correct equation for the solution of a bar subject to a direct force and a couple has to be established by trial and error; only the correct equation can be solved for a real p.

Regarding the bending moment, we have from

$$\theta/2 = \operatorname{am}(ks/p)$$

$$\sin(\theta/2) = \operatorname{sn}(ks/p)$$

and

$$\cos\phi = [1 - p^2 \sin^2(\theta/2)]^{\frac{1}{2}} = \operatorname{dn}(ks/p)$$

$$\frac{M}{EI} = \frac{Ph\cos\phi}{EI} = \frac{2k}{p}\operatorname{dn}(ks/p)$$

1.6. Kirchhoff's Dynamical Analogy. The Pendulum

For the bending moment of a point (x, y) on the bar in *Figure 1.3* we have the differential equation

$$EI\frac{d\theta}{ds} + Py = 0$$

or

$$\frac{d^2\theta}{ds^2} + k^2 \sin\theta = 0 \tag{1.30}$$

Referring now to the simple pendulum in *Figure 1.9*, its movement is governed by the equation

$$\frac{d^2\theta}{dt^2} + \frac{g}{l}\sin\theta = 0 \tag{1.31}$$

Equations (1.30) and (1.31) are formally identical. This was first noticed by Kirchhoff and is known as Kirchhoff's Analogy[14]. According to this theory, the tangent of an elastica performs pendulum oscillations on each side of the line of action of the applied force as the point on the curve moves with a constant velocity.

In order to compare the movement of a mathematical pendulum with the elastic shape of a thin bar let us assume a weightless rod of length l, suspended from one end and having a bob attached to the other. This pendulum moves freely under gravity (in a vertical plane). At the time t the velocity of the bob is v and θ is the angle between the rod and the vertical through the point of suspension (*Figure 1.9*). If the bob starts from rest by giving it a jerk the initial conditions are

$$(v)_{t=0} = v_0 \text{ and } (\theta)_{t=0} = 0$$

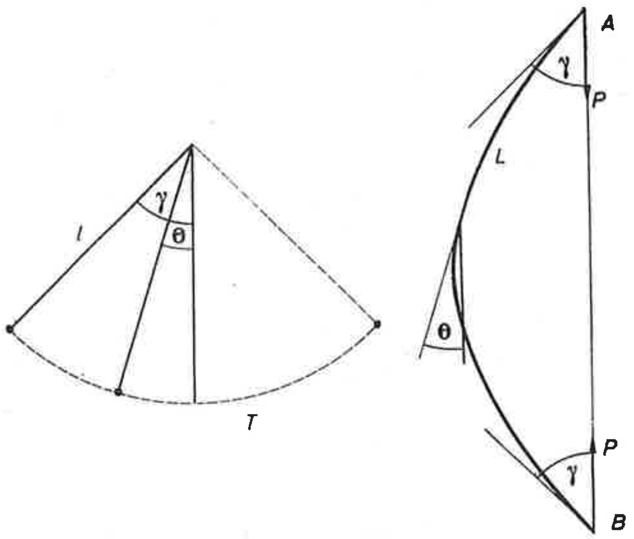

Figure 1.9

Equating the kinetic energy with the potential energy of the bob,

$$(v_0^2 - v^2)/2 = gl\,(1 - \cos\theta)$$

or
$$v^2 = v_0^2 - 4gl\sin^2(\theta/2) \tag{1.32}$$

Noting that $v = l\,d\theta/dt$ and letting $w^2 = g/l$, equation (1.32) reduces to

$$\left(\frac{d\theta}{dt}\right)^2 = 4w^2\left(\frac{v_0^2}{4gl} - \sin^2(\theta/2)\right) \tag{1.33}$$

The solution of this nonlinear differential equation depends on the relative values of v_0^2 and $4gl$.

The maximum potential energy of the bob is $2lgm$, where m is the mass of the bob. If

$$v_0^2\, m/2 < 2lgm$$

or

$$v_0^2 < 4gl,$$

the bob will not reach the height $2l$, hence the rod will oscillate. Let $p^2 = v_0^2/4gl$, so that $p^2 < 1$. If the amplitude of the pendulum is γ, the boundary condition is $(v)_{\theta=\gamma} = 0$. For these values of v and θ equation (1.32) becomes

$$p^2 = v_0^2/4gl = \sin^2(\gamma/2)$$

Since $d\theta/dt$ changes sign at $\theta = \pm\gamma$ (oscillating rod) we have from equation (1.33)

$$w\,dt = \pm\frac{d\theta}{2[p^2 - \sin^2(\theta/2)]^{\frac{1}{2}}} \tag{1.34}$$

Let $\sin(\theta/2) = p \sin\phi = \sin(\gamma/2)\sin\phi$. ϕ will then oscillate between $+\pi/2$ and $-\pi/2$ while θ varies from $+\gamma$ to $-\gamma$. We wish to express t as a function of ϕ. After some reductions we find

$$w\,dt = \pm\frac{p\cos\phi\, d\phi}{\cos(\theta/2)(p^2 - p^2\sin^2\phi)^{\frac{1}{2}}} = \pm\frac{d\phi}{(1 - p^2\sin^2\phi)^{\frac{1}{2}}} \tag{1.35}$$

It follows immediately that

$$\left.\begin{aligned} \sin\phi &= \operatorname{sn} wt \\ \sin(\theta/2) &= p \operatorname{sn} wt \\ \text{and the angular velocity}\quad d\theta/dt &= \pm\, 2pw \operatorname{cn} wt \end{aligned}\right\} \tag{1.36}$$

The modulus of the elliptic functions is p.

The time necessary for the bob to move from $\theta = 0$ to $\theta = +\gamma$, then to $-\gamma$, back to $\theta = 0$ is the complete period T. We find without difficulty

$$wT = 4w\int dt = 4\int_0^{\pi/2}\frac{d\phi}{(1 - p^2\sin^2\phi)^{\frac{1}{2}}}$$

or

$$T = 4K(p)/w \tag{1.37}$$

For small values of γ (between 0° and 5°) $K \approx \pi/2$, hence the complete period for small oscillations is

$$T = 2\pi/w = 2\pi(l/g)^{\frac{1}{2}} \tag{1.38}$$

Comparing now equations (1.36) and (1.37) with (1.16) and (1.14) we find that they become identical if we put $L = T/4$ and $k = w$, also, t has the same meaning for the pendulum as has s for the undulating elastica. We notice also that if the two γ's in *Figure 1.9* are equal, the moduli for the pendulum and the bar are the same. The similarity between equations (1.14) and (1.37) is shown in *Figure 1.10*. If L is the length AB in *Figure 1.10* (*b*) and $T = 2\pi\,(l/g)^{\frac{1}{2}}$ is the complete period of a pendulum with a small amplitude (*Figure 1.10* (*a*)), then

$$L : L_1 : L_2 : L_3 : \ldots . = T : T_1 : T_2 : T_3 : \ldots$$

where L_1, L_2, etc., are the lengths of a slender bar hinged between A and B with end slopes γ_1, γ_2, etc., and T_1, T_2, etc., are the complete periods of a pendulum with an amplitude of γ_1, γ_2, etc.

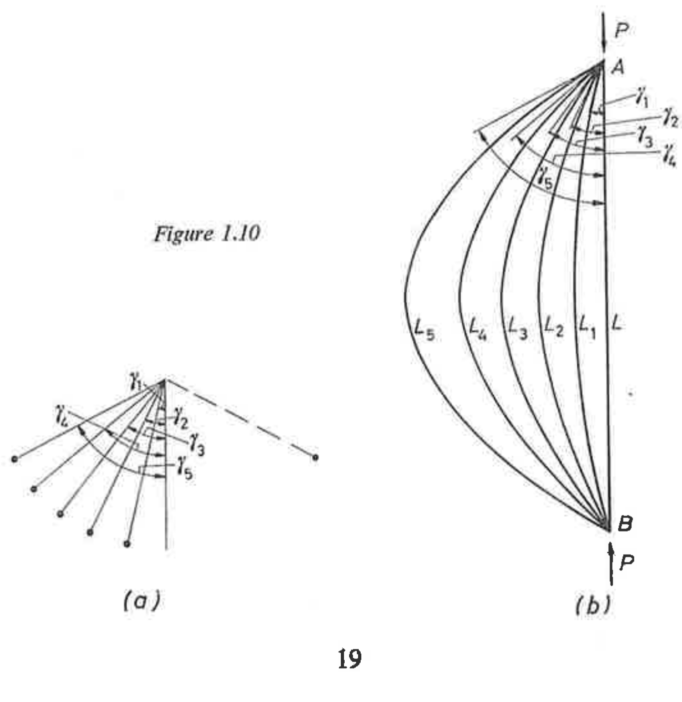

Figure 1.10

Further increase in the initial velocity v_0 will bring us to the stage where the kinetic energy of the bob equals the potential energy $2lgm$. This will happen when

$$v_0^2 = 4gl$$

or

$$p^2 = v_0^2/4gl = 1$$

Putting $p = 1$ in equation (1.37) results in

$$T = 4[\ln\tan(\pi/2) - \ln\tan(\pi/4)]/w = \infty \tag{1.39}$$

The rod never quite reaches the upward vertical position. In this case the angular velocity, $\omega = d\theta/dt = 2w$ sech wt. The $y =$ sech wt function decreases as wt increases and reaches the t-axis asymptotically, in other words, the angular velocity becomes zero after an infinitely long time.

Increasing v_0 further still brings us to the revolving pendulum. It can readily be proven for this case that

$$\left.\begin{aligned} T &= 2pK(p)/w \\ \theta/2 &= \mathrm{am}(wt/p) \\ \text{and} \qquad \omega = d\theta/dt &= +2w\,\mathrm{dn}(wt/p)/p \end{aligned}\right\} \tag{1.40}$$

These results have been obtained from

$$p^2 = 4gl/v_0^2 < 1$$

This shows that when v_0^2 increases indefinitely, p^2 tends to zero. Since dn is unity for $p = 0$, the speed becomes $2w/p$, an infinitely large speed. However, for small values of p, dn is very nearly unity, hence the pendulum will revolve at a constant velocity and the time of a complete revolution is

$$T = \pi p(l/g)^{\frac{1}{2}} \tag{1.41}$$

The similarity between the three types of elastic bars and the pendulum is shown in *Table 1*. The length of the nodal elastica, $L_{2\pi}$, refers to a complete revolution; the same applies to the complete period $T_{2\pi}$ of the revolving pendulum. The pendulum corresponding to the infinite bar is neither oscillating nor is it revolving: the bob starts from the lowest position and reaches the top after an infinitely long time.

Table 1. Comparison of the elastica and the pendulum

Elastica		Pendulum	
Undulating	$\phi = \text{am } ks$ $\sin(\theta/2) = p \text{ sn } ks$ $M/EI = 2pk \text{ cn } ks$ $L = K(p)/k$	Oscillating	$\phi = \text{am } wt$ $\sin(\theta/2) = p \text{ sn } wt$ $\omega = d\theta/dt = \pm 2pw \text{ cn } wt$ $T = 4K(p)/w$
Infinite Bar	$\phi = \text{gd } ks$ $\sin(\theta/2) = \tanh ks$ $M/EI = 2k \text{ sech } ks$ $L = \infty$	$v_0^2 = 4gl$	$\phi = \text{gd } wt$ $\sin(\theta/2) = \tanh wt$ $\omega = d\theta/dt = 2w \text{ sech } wt$ $T = \infty$
Nodal	$\theta/2 = \text{am } (ks/p)$ $\sin(\theta/2) = \text{sn } (ks/p)$ $M/EI = \frac{2k}{p} \text{ dn } (ks/p)$ $L_{2\pi} = \frac{2p}{k} K(p)$	Revolving	$\theta/2 = \text{am } (wt/p)$ $\sin(\theta/2) = \text{sn } (wt/p)$ $\omega = d\theta/dt = \frac{2w}{p} \text{ dn } (wt/p)$ $T_{2\pi} = \frac{2p}{w} K(p)$

1.7. Deflection of a Compressed Bar[15]

According to the linear theory of buckling, the bar in *Figure 1.11* remains straight if $P < P_{cr}$ and for $P = P_{cr}$, δ becomes small but

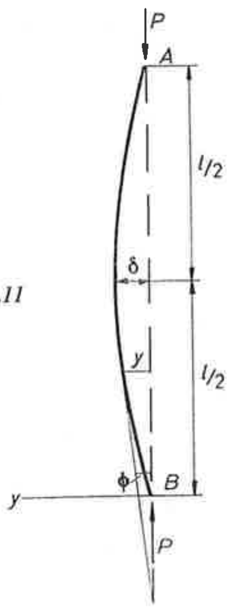

Figure 1.11

indeterminate. For $P > P_{cr}$ the linear theory fails to give an answer. Experiments show, however, that for slender bars there is a definite lateral deflection δ after the load has past the critical value ($P_{cr} = \pi^2 EI/l^2$). To find an expression for δ in terms of P, let the deflection y be a function of the length s, that is, $y = f(s)$. After two differentiations we get

$$\frac{dy^2}{ds^2} = -k^2 y \cos\phi \tag{1.42}$$

in which ϕ is the slope of the elastic line and $k^2 = P/EI$. We substitute

$$\cos\phi = 1 - \phi^2/2 \text{ and } \phi \approx \sin\phi = dy/ds = y'$$

in equation (1.42) and obtain

$$y'' + k^2 y = k^2 (y')^2 y/2 \tag{1.43}$$

Since the right-hand side of equation (1.43) is of the third degree in y an approximation for y will be sufficient. We have recourse to the linear theory and assume

$$y = c\sin(\pi s/l) \tag{1.44}$$

for the elastic line. We note immediately that in order to satisfy the boundary conditions $(y)_{s=0} = 0$ and $(y)_{s=l} = 0$, $\pi/l = k$, that is, $P = P_{cr}$. There is, however, a slight difference between P and P_{cr} in the buckled shape and hence between π/l and k too. Allowing for this difference and letting $\pi/l = k_0$, the right-hand side of equation (1.43) becomes

$$(c^3 k_0^4 \cos^2 k_0 s \sin k_0 s)/2 = c^3 k_0^4 (\sin k_0 s + \sin 3k_0 s)/8$$

Equation (1.43) now becomes

$$y'' + k^2 y = c^3 k_0^4 (\sin k_0 s + \sin 3k_0 s)/8 \tag{1.45}$$

and is solved by

$$\left.\begin{aligned} y &= c\sin k_0 s + c_1 \sin 3k_0 s \\ \text{where} \quad c^2 &= \frac{8(k^2 - k_0^2)}{k_0^4} = \frac{8l^2}{\pi^2}\left(\frac{P}{P_{cr}} - 1\right) \\ \text{and} \quad c_1 &= -\frac{k_0^2}{64} c^3 \end{aligned}\right\} \tag{1.46}$$

c_1 was obtained by writing $k^2 \approx k_0^2$.

We now have a solution for δ since, from equation (1.46)

$$\delta = (y)_{s=l/2} = c - c_1$$

c_1 is of third order smallness if c is assumed to be of the first, hence we can write with sufficient accuracy

$$\delta = c = 0{\cdot}900l\left(\frac{P}{P_{cr}} - 1\right)^{\frac{1}{2}} \tag{1.47}$$

Accordingly, if $P = 1{\cdot}01\ P_{cr}$, $\delta = 0{\cdot}09\ l$
and if $P = 1{\cdot}05\ P_{cr}$, $\delta = 0{\cdot}20\ l$

Equation (1.46) tells us how the shape of the buckled bar deviates from a true sine curve. Toward the ends of the bar the deflection is less, while at the middle it is somewhat more than indicated in the assumed curve of expression (1.44).

Elliptic integrals can also be used for the analysis of the lateral movement of a bar for $P > P_{cr}$. Take, for example, the strut in *Figure 1.3*. The force necessary to cause the deflection shown in *Figure 1.3* is (see page 9)

$$P = EI\,K^2(p)/L^2 = 4P_{cr}\,K^2(p)/\pi^2 \tag{1.48}$$

Equation (1.48) shows that in order to have an elastic line different from a vertical fixed at A, $P > P_{cr}$ since $K(p)$ cannot be less than $\pi/2$ [16].

$K(p)$ can be expanded in terms of p as follows:

$$K(p) = \frac{\pi}{2}\left[1 + \left(\frac{1}{2}\right)^2 p^2 + \left(\frac{1.3}{2.4}\right)^2 p^4 + \left(\frac{1.3.5}{2.4.6}\right)^2 p^6 + \ldots\right]$$

For slight horizontal deflections, γ and p are small since $p = \sin(\gamma/2)$. By taking the first two terms only in the series of $K(p)$ we get for p

$$p = 2[2K(p)/\pi - 1]^{\frac{1}{2}}$$

Remembering that the horizontal deflection $h = 2p/k$, from (1.9), we obtain finally

$$h = \frac{8L}{\pi}[\sqrt{(1/n)} - (1/n)]^{\frac{1}{2}} \tag{1.49}$$

where $n = P/P_{cr}$. If P is only slightly above P_{cr} we may write

$$h = \frac{8L}{\pi}\sqrt{(\Delta/2)} \tag{1.50}$$

in which $\Delta = n - 1$.

It is seen from (1.49) that $(dn/dh)_{n=1} = 0$, hence the tangent of the curve showing the relationship between n and h is parallel to the h-axis at $n = 1$. This is shown in *Figure 1.12*. Employing equation (1.50),

for $\Delta = 0{\cdot}001$ $\quad h/L = 0{\cdot}055$

and for $\Delta = 0{\cdot}01$ $\quad h/L = 0{\cdot}17$.

These values are based on $K(p) \approx \pi/2 + \pi p^2/8$. For larger values of Δ this expression is no longer sufficiently accurate.

$$\gamma = \left(\frac{dy}{dx}\right)_{x=l} = \delta\frac{\pi}{2l} \tag{1.51}$$

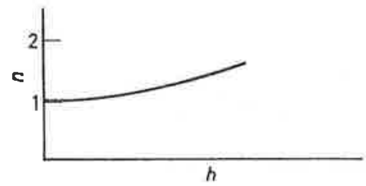

Figure 1.12

In the approximate theory $y = \delta[1 - \cos(x\pi/2l)]$ (*Figure 1.13*) and where δ is an indeterminate horizontal deflection. The accurate horizontal deflection is

$$h = \frac{2p}{k} = 4L\frac{\sin(\gamma/2)}{\pi} = \gamma\frac{2L}{\pi} \tag{1.52}$$

provided γ is small, $P = P_{cr}$, and $l \approx L$.

The approximate theory of buckling, based on $y'' = 1/r$, defines P_{cr} as the load capable of keeping the bar in any slightly (though indeterminately) buckled shape. The inability of this theory to give a definite answer to the lateral deflection can be remedied by applying the rigorous expression of $1/r$. It has been shown that, contrary to the results of the approximate theory, there is a unique relationship between load and deflection and consequently the criterion for the critical load may be rephrased.

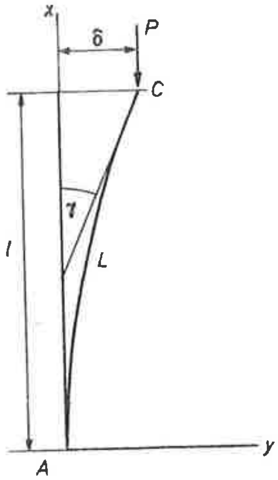

Figure 1.13

Consider a load P placed on the vertical bar in *Figure 1.13* capable of holding it in a bent shape. Gradual diminishing of P will lead to a straightening out of the strut. When the bar has reached its original straight form the load P will equal the critical load. In other words, P_{cr} is reached 'from above' instead of 'from below' as in the conventional definition. According to the latter there is an infinite number of equilibrium positions (the straight one included) at P_{cr}. On the other hand, the exact theory states that the straight line is the only form for P_{cr}. If $P > P_{cr}$ acts on the bar, the approximate theory recognizes the straight form as the only possible equilibrium position but that is unstable; the exact analysis gives one stable equilibrium position with a definite lateral displacement (*Figure 1.12*) for each value of P.

The shape assumed by an elastic strut when loaded by $P > P_{cr}$ was shown in *Figure 1.3*. This shape, however, is not the only possible equilibrium shape of a flexible bar. According to Saalschuetz[17], the equations governing the shape of a strut shown in *Figure 1.14* are

$$\left.\begin{aligned} v &= [2E(p) - 2E(p, \phi_0) - K(p) + F(p, \phi_0)]/k \\ \text{and} \qquad h &= \frac{2p}{k}\cos\phi_0 \end{aligned}\right\} \qquad (1.53)$$

where p and ϕ_0 must satisfy

$$\left.\begin{aligned} p\sin\phi_0 &= 0 \\ \text{and} \qquad K(p) - F(p, \phi_0) &= kL \end{aligned}\right\} \qquad (1.54)$$

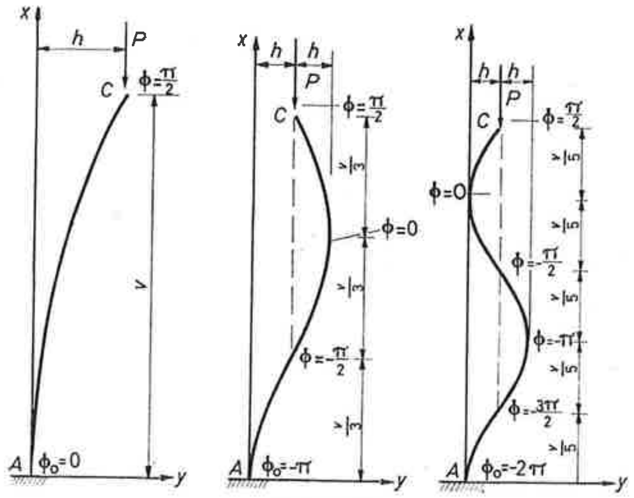

Figure 1.14

According to equations (1.54) we have either $p = 0$ or $\sin\phi_0 = 0$. If $p = 0$ the bar is straight. If $\sin\phi_0 = 0$ we can have $\phi_0 = 0$, or $\phi_0 = -n\pi$ ($n = 0, 1, 2, 3, \ldots$) and equations (1.53 and 54) read

$$\left.\begin{aligned} v &= [2(2n+1)E(p) - (2n+1)K(p)]/k \\ h &= 2p/k \\ kL &= (2n+1)K(p) \end{aligned}\right\} \qquad (1.55)$$

The smallest value of $K(p)$ is $\pi/2$ and this occurs when $p = 0$. If $p \neq 0$, that is if the bar is curved, we find p from the third expression in equations (1.55) for $n = 1, 2, 3$, etc. n is limited by virtue of $K(p) \geqslant \pi/2$. As shown in *Figure 1.14* a bar of given length L and EI can carry different loads P according to their elastic shapes. The coordinates of the elastic line are

$$\left.\begin{aligned} x &= \{2E(p,\phi) - F(p,\phi) + 2n[2E(p) - K(p)]\}/k \\ \text{and} \qquad y &= \frac{2}{k}\left|p[(-1)^n - \cos\phi]\right| \end{aligned}\right\} \qquad (1.56)$$

in which ϕ varies from $-n\pi$ to $+\pi/2$.

The lateral movement, given as the ratio h/L can be expressed as a function of PL^2/EI for $n = 1, 2, 3$, etc.[18]. This is shown in the graph on *Figure 1.15*. There is a branch for every value of $n = 0, 1, 2$, etc. It follows from the nature of $K(p)$ that the branches belonging to different values of n can never intersect, for this would mean that for a given k and h (and hence for a given p) the function $K(p)$ could assume two or more different values. The inscribed rectangle $a'\ b'\ c'\ d'$ is proportional to the maximum bending moment in the bar for the force P that belongs to the value k^2L^2 on the abscissa.

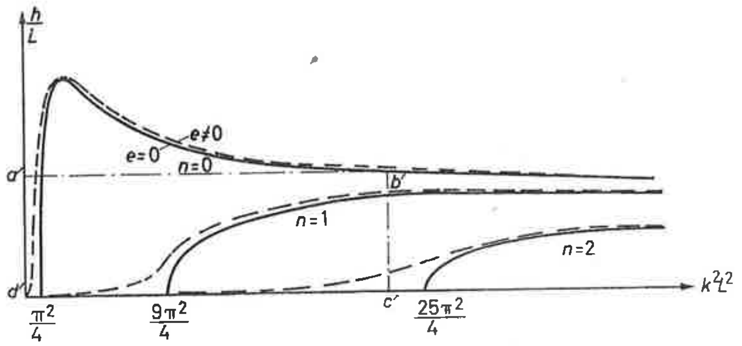

Figure 1.15 (According to Malkin[18])

1.8. Eccentric Loading of Flexible Strut

The question arises now as to how and to what extent a given eccentricity of the load will affect our previous results. It should be realized first that the elastic shape remains unchanged if the load, instead of acting directly on the strut, acts through a rigid lever. This can be seen from *Figure 1.16*. The solution of this strut depends upon

$$\left.\begin{aligned} ke &= \frac{2p\cos\phi_B}{1 - 2p^2\sin^2\phi_B} \\ \text{and} \qquad s &= F(p, \phi_B)/k \end{aligned}\right\} \qquad (1.57)$$

For a given e, s, and P the equations (1.57) will yield p and ϕ_B. The lateral movement of the top of the bar is then found from

$$y_B = 2p(1 - \cos\phi_B)/k$$

One is interested usually in small eccentricities. If e is small then, from equations (1.57), either p or $\cos\phi_B$ or both must be small too[19].

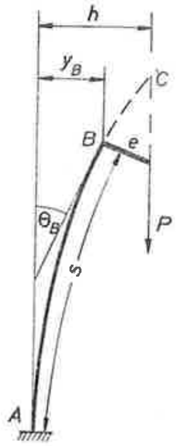

Figure 1.16

If $p = \varepsilon$ where ε is a small positive value, we have for the bar's top

$$y_B = e(1/\cos ks - 1)$$

The deflection y_B and the eccentricity e are of the same order of magnitude.

If $\cos\phi_B = 2\delta$ where 2δ is small, we may write

$$e = [4\delta p/(1 - 2p^2)]/k$$
$$s = [K(p) - 2\delta(1 - p^2)^{-\frac{1}{2}}]/k$$

and

$$y_B = 2p(1 - 2\delta)/k$$

If, finally, both $p = \varepsilon$ and $\cos\phi_B = 2\delta$ are small, we have, after neglecting terms of second order smallness and higher,

$$e = 4\delta a/k, \qquad s = (\pi/2 - 2\delta)/k$$

and

$$y_B = 2\varepsilon(1 - 2\delta)/k$$

In this case ϕ_B is nearly $\pi/2$ and y_B, though of the order of ε, is still large compared to e.

The dotted lines in *Figure 1.15* refer to a small eccentricity. It can be seen clearly that the greatest difference between $e = 0$ and

$e \neq 0$ occurs near the critical point. Past P_{cr} the two lines are nearly identical.

1.9. Strain Energy of a Flexible Bar due to Bending

The work done in bending an originally straight bar into a circular shape of radius r is

$$U = \frac{EI}{2r^2} L$$

This shows that the equation expressing the strain energy stored in a bar bent from straight into circular form, is the same for rigid and flexible bars alike, since in both cases the deformation is due to a couple that remains constant during bending. The same cannot be said for strain energy caused by forces instead of couples. The reason is that, in the conventional analysis, the strain energy due to bending,

$$U = \int_0^l \frac{EI}{2} \left(\frac{d^2y}{dx^2}\right)^2 dx$$

is based on $y'' = 1/r$.

The work done in bending an elemental length ds from a straight into a curved form (*Figure 1.13*) is

$$dU = \frac{EI}{2r^2} ds$$

where $1/r$ is the curvature of the final shape. From equation (1.3) $1/r = -yk^2$, hence $dU = (y^2Pk^2/2)ds$.

For the undulating elastica ($p < 1$)

$$dU = 2P \frac{p^2 \cos^2 \phi \, d\phi}{k(1 - p^2 \sin^2 \phi)^{\frac{1}{2}}} \tag{1.58}$$

and the strain energy stored in the bar between A and B (*Figure 1.3*) is

$$\begin{aligned} U &= \frac{2Pp^2}{k} \int_0^{\phi} \frac{\cos^2 \phi \, d\phi}{(1 - p^2 \sin^2 \phi)^{\frac{1}{2}}} \\ &= \frac{2P}{k} [E(p, \phi) - (1 - p^2)F(p, \phi)] \end{aligned} \tag{1.59}$$

Since $s = F(p, \phi)/k$, and since from equation (1.20) $x = 2E(p, \phi)/k - s$, the expression for the strain energy is

$$U = P[x + (2p^2 - 1)s] \tag{1.60}$$

For the strain energy in the infinite bar we note that $p = 1$. Therefore, from equation (1.58)

$$dU = \frac{2P}{k} \cos \phi \, d\phi$$

and
$$U = \frac{2P}{k} \sin \phi = \frac{2P}{k} \tanh ks = P(x + s) \tag{1.61}$$

This is the strain energy stored in the bar in *Figure 1.7* along a length s, measured from A.

The strain energy in a nodal elastica may be calculated as follows. For an elemental length ds

$$dU = (Py^2k^2/2)ds.$$

The elemental length $ds = \dfrac{hp^2\, d(\theta/2)}{2[1 - p^2 \sin^2(\theta/2)]^{\frac{1}{2}}}$,

hence
$$dU = Ph[1 - p^2 \sin^2(\theta/2)]^{\frac{1}{2}}\, d(\theta/2)$$

and
$$U = PhE(p, \theta/2) = P[x + (2/p^2 - 1)\, s] \tag{1.62}$$

This follows from equations (1.27 and 28).

As an example, consider a flexible straight bar, $4L$ long, bent into three different shapes as shown on *Figure 1.17*. On the larger circle the ends of the bar are secured by a joint that will permit the transmission of a moment, shear, and axial force, but not of a torque. By twisting the circle about a diameter, shape (*b*) has been obtained (*Figure 1.17*). If we fold shape (*b*) to bring its extreme points together the bar will assume the double circle of shape (*c*) (the torsional resistance of the bar is assumed to be very small compared to its resistance against bending). The strain energies of the three different shapes are found as follows.

We see at once that the energy of the large circle is

$$U_a = 2LP_{cr}$$

and that of the small double circle is

$$U_c = 8LP_{cr}, \text{ where } P_{cr} = EI\pi^2/4L^2$$

As for shape (*b*) it has been found in section 1.3 that for this particular case of bending $p = 0{\cdot}908$ and $P = 2{\cdot}19P_{cr}$. Inserting these values in the strain energy equation of the undulating elastica, we get

$$U_b = 5{\cdot}65\,P_{cr}L$$

Hence the strain energies of the shapes (*a*), (*b*) and (*c*) are in the ratio $1 : 2\sqrt{2} : 4$.

When calculating U_b the incomplete elliptic integrals in equation (1.59) have been replaced by $K(p)$ and $E(p)$.

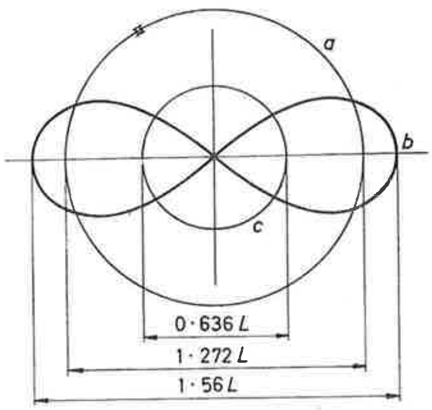

Figure 1.17

REFERENCES

1. Euler. *Methodus Inveniendi Lineas Curvas*, 1744
2. Lagrange. *Sur la Force des Ressorts Pliès*, Mém. Acad. Berlin, 1770
3. Plana. *Equation de la courbe fermèe par une lame élastique*, Mem. R. Soc. Turin, 1809
4. McLachlan, N. W. *Ordinary Nonlinear Differential Equations in Engineering*, Clarendon Press, Oxford, 1950
5. Salvadori, M. G. and Schwarz, R. J. *Differential Equations in Engineering Problems*, p. 324, Prentice-Hall, New York, 1954
6. Cayley, A. *Elliptic Functions*, G. Bell and Sons, London, 1895
7. Hancock, H. *Elliptic Integrals*, Wiley, New York, 1917

[8] Bowman, F. *Introduction to Elliptic Functions*, English University Press, London, 1953
[9] Milne-Thomson, L. M. *Jacobian Elliptic Functions*, Dover Publications
[10] Pearson, K. *Tables of the Complete and Incomplete Elliptic Integrals*, Cambridge University Press, London, 1934
[11] Jahnke, E. and Emde, F. *Tables of Functions*, Dover Publications, New York, 1945
[12] Jahnke, E. and Emde, F. *ibid.*
[13] Hancock, H. *ibid.* p. 28
[14] Kirchhoff, G. R. On the equilibrium and the movements of an infinitely thin bar, *Crelles Journal*, 56, 1859
[15] Mises, R. Ausbiegung eines auf Knicken beanspruchten Stabes, *Z. angew. Math. Mech. 4*, 5 (1924) 435
[16] Frisch-Fay, R. On large deflections, *Aust. J. appl. Sci. 10*, 4 (1959) 418
[17] Saalschuetz. *Der belastete Stab*, Teubner, Leipzig, 1880
[18] Malkin, I. Formaenderung eines axial gedrueckten duennen Stabes, *Z. angew. Math. Mech. 6*, (1926) 73
[19] Malkin, I. *ibid.*

2
CANTILEVER

2.1. Equations of Equilibrium of a Bent Elastic Rod

Let T, S, and M be the tension, shear and bending moment acting at P (*Figure 2.1*) and $T + dT$, $S + dS$, and $M + dM$ the tension, shear, and bending moment at Q, a point distant ds from P. Let ψ be the angle between the tangent at P and the x-axis. PQ is part of a slender, originally straight bar. Corresponding to the length ds, the change in slope from P to Q is $d\psi$, hence the angle at Q is $\psi+d\psi$. q is the external load per unit length, hence the load qds acts on the element in question. Denote the normal and the tangential components of q by q_n and q_t. Resolving the forces acting along the tangent and the normal at P and taking moments about P, the equations of equilibrium are as follows:

$$\left.\begin{aligned} -T + (T + dT)\cos d\psi - (S + dS)\sin d\psi + q_t\,ds &= 0 \\ -S + (S + dS)\cos d\psi + (T + dT)\sin d\psi + q_n\,ds &= 0 \\ -M + (M + dM) + (S + dS)\,ds &= 0 \end{aligned}\right\} \quad (2.1)$$

If the above equations are divided by ds, proceeding to the limit, and remembering that $d\psi/ds=1/r$ equations (2.1) reduce to

$$\left.\begin{aligned} \frac{dT}{ds} - \frac{S}{r} + q_t &= 0 \\ \frac{dS}{ds} + \frac{T}{r} + q_n &= 0 \\ \frac{dM}{ds} + S &= 0 \end{aligned}\right\} \quad (2.2)$$

From the last equation in (2.2) we find

$$S= -dM/ds, \quad \text{and hence} \quad dS/ds= -d^2M/ds^2.$$

Substituting these values in (2.2) we get

$$\left.\begin{aligned} \frac{dT}{ds} + \frac{1}{r}\frac{dM}{ds} + q_t &= 0 \\ -\frac{d^2M}{ds^2} + \frac{T}{r} + q_n &= 0 \end{aligned}\right\} \quad (2.3)$$

Multiplying the first equation by $\cos\psi$ and the second by $-\sin\psi$, and adding them together we have

$$\frac{d}{ds}\left[\left(T-\frac{M}{r}\right)\cos\psi\right]+\frac{d^2}{ds^2}(M\sin\psi)+q_x=0$$

where q_x is the component of q in the x direction.

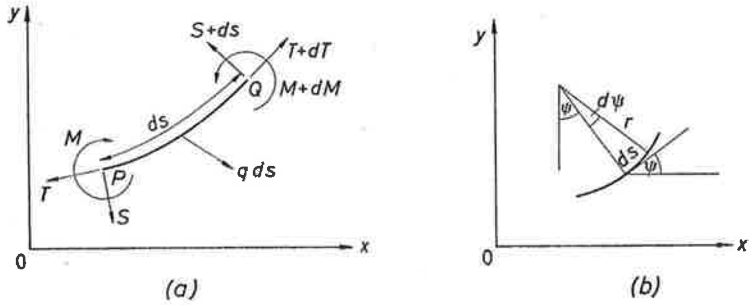

Figure 2.1

Further, multiplying the first equation of (2.3) by $\sin\psi$ and the second by $\cos\psi$ and adding together we have

$$\frac{d}{ds}\left[\left(T-\frac{M}{r}\right)\sin\psi\right]-\frac{d^2}{ds^2}(M\cos\psi)+q_y=0$$

where q_y is the y component of q.

On integrating, the last two equations become

$$\left.\begin{aligned}\left(T-\frac{M}{r}\right)\cos\psi+\frac{d}{ds}(M\sin\psi)&=-\int q_x\,ds=Q_x\\ \left(T-\frac{M}{r}\right)\sin\psi-\frac{d}{ds}(M\cos\psi)&=-\int q_y\,ds=Q_y\end{aligned}\right\}\qquad(2.4)$$

Multiplying again the first equation by $\sin\psi$, the second by $-\cos\psi$ and adding, one obtains

$$\frac{dM}{ds}=Q_x\sin\psi-Q_y\cos\psi$$

or

$$M=\int Q_x\,dy-\int Q_y\,dx=EI\,\frac{d^2y/dx^2}{[1+(dy/dx)^2]^{3/2}}\qquad(2.5)$$

This differential equation expresses the equilibrium of a slender rod under general load conditions. It will be seen later in the discussion that only for a limited number of cases can the problem be solved in a closed form, so that recourse will have to be made to numerical methods.

If, instead of resolving the forces tangentially and normally to the element, they are resolved in the x and y directions, the following equations result (*Figure 2.1*)

$$\left.\begin{aligned} &d(T\cos\psi) - d(S\sin\psi) = -q_x\,ds \\ \text{and}\quad &d(T\sin\psi) + d(S\cos\psi) = q_y\,ds \end{aligned}\right\} \tag{2.6}$$

Integration of these two equations yields

$$\left.\begin{aligned} T\cos\psi - S\sin\psi &= T_0 - q_x s \\ T\sin\psi + S\cos\psi &= S_0 + q_y s \end{aligned}\right\} \tag{2.7}$$

where T_0 and S_0 are the tension and the shear force at the origin of s. Taking moments about P, the same $S = -dM/ds$ will result. Eliminating T from (2.7),

$$-S = dM/ds = (T_0 - q_x s)\sin\psi - (S_0 + q_y s)\cos\psi$$

Since $M = EI\,d\psi/ds$, it follows that

$$EI\,d^2\psi/ds^2 - (T_0 - q_x s)\sin\psi + (S_0 + q_y s)\cos\psi = 0 \tag{2.8}$$

For the solution of a particular problem the initial values T_0 and S_0 must be found first. Equation (2.8) will be used later in the discussion for solving the cantilever under a distributed load.

2.2. Horizontal Cantilever with a Vertical Point Load at the Free End

The cantilever in *Figure 2.2* which is fixed at B, is L long, and its flexural rigidity is EI. Take the origin of the x and y axes at B and let x, y be the coordinates of point Q. The bending moment at this point is

$$M = EI\frac{d\psi}{ds} = P(L - x - \Delta) \tag{2.9}$$

Differentiating (2.9) with respect to s

$$\frac{d^2\psi}{ds^2} = -\frac{P}{EI}\frac{dx}{ds} = -\frac{P}{EI}\cos\psi \tag{2.10}$$

Integrating this equation will result in

$$\frac{1}{2}\left(\frac{d\psi}{ds}\right)^2 = -\frac{P}{EI}\sin\psi + C \tag{2.11}$$

The differentiation of (2.9) and the integration of the result was carried out in order to establish a differential equation containing one dependent variable only. In (2.9) the left side represents an intrinsic form while the right side is expressed in cartesian coordinates. Equation (2.10) is a nonlinear second order differential equation with a constant coefficient. The integration constant C

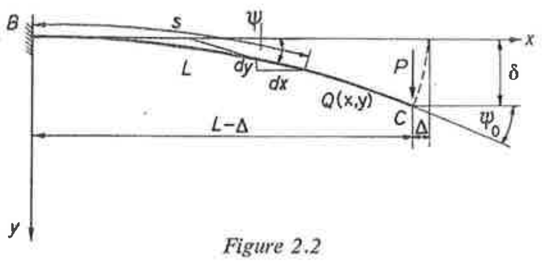

Figure 2.2

can be found from the boundary condition, which is, that the curvature at the loaded end is zero. If the end slope is ψ_0, we have

$$\left(\frac{d\psi}{ds}\right)_{\psi=\psi_0} = 0, \quad \text{hence} \quad C = \frac{P}{EI}\sin\psi_0$$

Substituting C into equation (2.11) will yield

$$\frac{d\psi}{ds} = \frac{2P}{EI}(\sin\psi_0 - \sin\psi)^{\frac{1}{2}} \tag{2.12}$$

The bar is assumed to be inextensible; in other words, it will not change its length during bending. Therefore, writing

$$\int_0^{\psi_0} ds = L \tag{2.13}$$

with $PL^2/EI = q^2$ and combining equations (2.12 and 13) the following expression results:

$$\int_0^{\psi_0} ds = L = \frac{L}{q}\int_0^{\psi_0} \frac{d\psi}{[2(\sin\psi_0 - \sin\psi)]^{\frac{1}{2}}}$$

or

$$q\sqrt{2} = \int_0^{\psi_0} \frac{d\psi}{(\sin\psi_0 - \sin\psi)^{\frac{1}{2}}} \tag{2.14}$$

In order to bring the right side of equation (2.14) to the standard form of elliptic integrals, a new variable, ϕ, is introduced to satisfy the following equation:

$$1 + \sin\psi = (1 + \sin\psi_0)\sin^2\phi$$

and let

$$p^2 = (1 + \sin\psi_0)/2 \qquad (2.15)^1$$

Differentiating the first equation in (2.15) with respect to ϕ results in

$$\cos\psi\,\frac{d\psi}{d\phi} = 4p^2\sin\phi\cos\phi$$

But $\cos\psi = (1 - \sin^2\psi)^{\frac{1}{2}} = (4p^2\sin^2\phi - 4p^4\sin^4\phi)^{\frac{1}{2}}$
$= 2p\sin\phi(1 - p^2\sin^2\phi)^{\frac{1}{2}}$

Also, $\sin\psi = 2p^2\sin^2\phi - 1$, and $\sin\psi_0 = 2p^2 - 1$

Substituting $d\psi$, $\sin\psi$, and $\sin\psi_0$ in equation (2.14) we obtain

$$q\sqrt{2} = \int_0^{\psi_0} \frac{4p^2\sin\phi\cos\phi\,d\phi}{2p\sin\phi\,[(1 - p^2\sin^2\phi)(2p^2 - 2p^2\sin^2\phi)]^{\frac{1}{2}}}$$
$$= \int_0^{\psi_0} \frac{\sqrt{2}\,d\phi}{(1 - p^2\sin^2\phi)^{\frac{1}{2}}}$$

Regarding the new limits, it will be seen from $\sin\psi = 2p^2\sin^2\phi - 1$, that if $\psi = 0$, $\sin\phi = 1/p\sqrt{2}$. Hence the lower limit

$$\phi_1 = \sin^{-1}\left(\frac{1}{p\sqrt{2}}\right)$$

If $\psi = \psi_0$, $1+\sin\psi = (1+\sin\psi_0)\sin^2\phi$, hence $\sin^2\phi = 1$ and the upper limit is $\pi/2$. Therefore,

$$q = \int_{\phi_1}^{\pi/2} \frac{d\phi}{(1 - p^2\sin^2\phi)^{\frac{1}{2}}} = K(p) - F\left[p, \sin^{-1}\left(\frac{1}{p\sqrt{2}}\right)\right] \qquad (2.16)^2$$

This equation has one unknown only, the modulus p. It can be found by trial and error by using the tables of elliptic integrals.

Since $dy = ds \sin\psi$, the vertical deflection is given by

$$dy = \frac{\sqrt{EI}\sin\psi\, d\psi}{[2P(\sin\psi_0 - \sin\psi)]^{\frac{1}{2}}} \qquad \text{(from (2.12))}$$

or

$$\delta = \int_0^{\psi_0} \frac{\sqrt{EI}\sin\psi\, d\psi}{[2P(\sin\psi_0 - \sin\psi)]^{\frac{1}{2}}}$$

By using the same substitutions for $\sin\psi$, $\sin\psi_0$, and $d\psi$ as before, δ may be expressed as

$$\delta = \left(\frac{EI}{P}\right)^{\frac{1}{2}} \int_{\phi_1}^{\pi/2} \frac{(2p^2\sin^2\phi - 1)d\phi}{(1 - p^2\sin^2\phi)^{\frac{1}{2}}} \tag{2.17}$$

However, the integral in (2.17) equals

$$\int_{\phi_1}^{\pi/2} \frac{d\phi}{(1 - p^2\sin^2\phi)^{\frac{1}{2}}} - 2\int_{\phi_1}^{\pi/2} (1 - p^2\sin^2\phi)^{\frac{1}{2}}\, d\phi$$

and so $\delta = (EI/P)^{\frac{1}{2}}[K(p) - F(p,\phi_1) - 2E(p) + 2E(p,\phi_1)]$ (2.18)

in which $\phi_1 = \sin^{-1}(1/p\sqrt{2})$.

The horizontal displacement of C can be derived without difficulty. It is noted that $(\psi)_{x=0} = 0$, hence

$$P(L - \Delta) = M_0 = EI\left(\frac{d\psi}{ds}\right)_{\psi=0} = EI\left(\frac{2P\sin\psi_0}{EI}\right)^{\frac{1}{2}} \tag{2.19}$$

by employing equation (2.12).

However, $\sin\psi_0 = 2p^2 - 1$ (from equation (2.15)) and after some reductions the horizontal deflection is found

$$\Delta = L - \left[\frac{2EI(2p^2 - 1)}{P}\right]^{\frac{1}{2}} \tag{2.20}$$

At a point Q, distant s from B, the slope ψ_Q can be calculated from

$$\int_0^{\psi_Q} ds = s = \frac{1}{k}\int_0^{\psi_Q} \frac{d\psi}{[2(\sin\psi_0 - \sin\psi)]^{\frac{1}{2}}} \tag{2.21}$$

in which $k = (P/EI)^{\frac{1}{2}}$.

After introducing the parameter ϕ, equation (2.21) reduces to

$$s = \frac{1}{k}\int_{\phi_1}^{\phi_Q} \frac{d\phi}{(1 - p^2 \sin^2 \phi)^{\frac{1}{2}}}$$

where $$\phi_Q = \sin^{-1}\left[\frac{1}{p}\left(\frac{1 + \sin \psi_B}{2}\right)^{\frac{1}{2}}\right]$$

By writing $$s = [F(p, \phi_Q) - F(p, \phi_1)]/k \qquad (2.22)$$

the equation has ϕ_Q as the only unknown. Since ϕ_Q is a function of ψ_Q the slope at any point can be found from equation (2.22) in terms of s. The horizontal and vertical coordinates of point Q will be discussed in the next article.

As an example of the vertical deflection, consider the cantilever mentioned on page 2. As pointed out, the elementary theory gives a 333 in. vertical deflection. Using the equations derived in this article one finds from equation (2.16) $p = \sin 86° = 0{\cdot}99756$ and $\phi_1 = 45°8'$. Inserting these values of p and ϕ_1 in equation (2.18),

$$\delta = 81{\cdot}23 \text{ in.}$$

The horizontal displacement of the free end of the cantilever will be (from 2.20)

$$\Delta = 55{\cdot}50 \text{ in.}$$

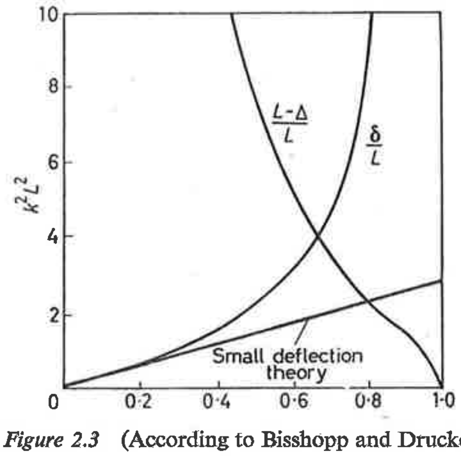

Figure 2.3 (According to Bisshopp and Drucker[1])

The end of this cantilever is nearly vertical since, from (2.15), $\sin \psi_0 = 2p^2 - 1 = 0{\cdot}99024$, hence $\psi_0 = 82°$.

Numerical results can be obtained quickly with the aid of graphs shown in *Figure 2.3* where the values of δ/L and $(L - \Delta)/L$ have been calculated as a function of PL^2/EI.

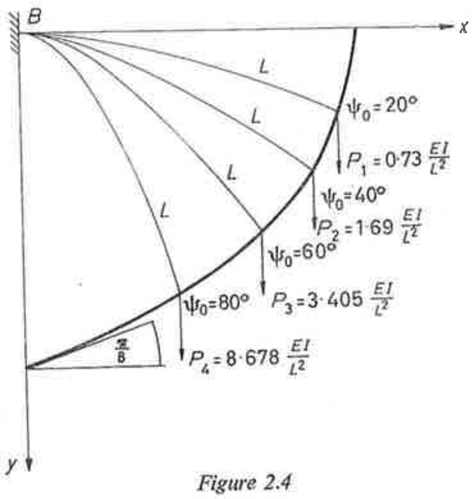

Figure 2.4

As the load increases continually, the locus of the free end will be the curve shown in *Figure 2.4*. The end slopes of the bars in *Figure 2.4* are $\psi_0 = 10°, 20°, \ldots 80°$. It can be shown that the locus makes a finite angle with the horizontal at the lowest point, corresponding to an infinite load[3]. This angle is $\pi/8$.

From $\quad p^2 = (1 + \sin \psi_0)/2$ it follows that

$$p = \sin(\pi/4 + \psi_0/2)$$

Hence, as the angle ψ_0 tends to $\pi/2$, p tends to 1, and ϕ_1 tends to $\pi/4$. However, for $p = 1$ the integral $E(1, \phi) = \sin \phi$; therefore

$$\lim_{\psi_0 \to \pi/2} \frac{L - \delta}{L - \Delta} = \lim_{p \to 1} \frac{2E(p) - 2E(p, \pi/4)}{[2(2p^2 - 1)]^{\frac{1}{2}}} = \sqrt{2} - 1 = \tan(\pi/8)$$

2.3. The Principle of Elastic Similarity

This principle[4] and its application will be explained on a horizontal cantilever carrying a vertical load at the free end. Consider the cantilever shown in *Figure 2.5.* By continuing the bar towards the left past B the dotted line will eventually become vertical. Let

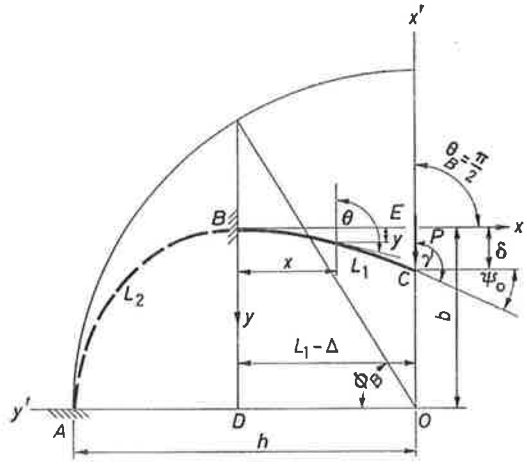

Figure 2.5

this happen at A and assume the bar to be clamped there. Then, by releasing the fixity at B, the cantilever will, together with its imaginary extension, remain unaltered in shape. However, the cantilever BC and its extension AB comprise together a vertical strut fixed at the bottom and subject to a vertical load at the top. This strut which will be called the basic strut for our purpose, has been dealt with in section 1.3. Since the shape of the basic strut is governed by the modulus p, and since the cantilever is a segment of the strut the modulus of the cantilever is also p.

Let L_1 be the length of the cantilever and L_2 the length of the imaginary extension. Then, from equation (2.14)

$$L = L_1 + L_2 = K(p)/k \tag{2.23}$$

The length L_1 can be found from the condition that at B the slope $\theta_B = \pi/2$ (in the basic strut the slope is measured from the vertical). The relationship between the slope and the parameter ϕ in the basic strut is

$$\sin(\theta_B/2) = p \sin \phi_B$$

and therefore,

$$\phi_B = \sin^{-1}(1/p\sqrt{2}),$$

where p is unknown for the time being. By inspection, L_2 is generated by rotating the radius of the quadrant from zero to ϕ_B, hence the remaining length L_1 is

$$L_1 = L - L_2 = \frac{1}{k} K(p) - \frac{1}{k} \int_0^{\phi_B} \frac{d\phi}{(1 - p^2 \sin^2 \phi)^{\frac{1}{2}}}$$

$$= \frac{1}{k} \left\{ K(p) - F\left[p, \sin^{-1}\left(\frac{1}{p\sqrt{2}} \right) \right] \right\} \tag{2.24}$$

This equation contains only p as unknown. It can be shown that equation (2.24) is identical with equation (2.16). This becomes obvious when it is realized that $p = \sin(\gamma/2)$ where γ is the end slope (measured from the vertical). Hence in terms of ψ_0 (measured from the horizontal) $\gamma = \pi/2 + \psi_0$. But

$$p = \sin(\gamma/2) = \sin(\pi/4 + \psi_0/2) = \frac{1}{\sqrt{2}}[\cos(\psi_0/2) + \sin(\psi_0/2)]$$

$$= [(1 + \sin\psi_0)/2]^{\frac{1}{2}} \tag{2.25}$$

which is identical with equation (2.15).

The radius of the auxiliary circle is given by

$$h = 2p/k \tag{2.26}$$

and the horizontal deflection at C

$$\Delta = L_1 - h\cos\phi_B = L_1 - \frac{2p}{k}(1 - p^2 \sin^2 \phi_B)^{\frac{1}{2}}$$

$$= L_1 - [2(2p^2 - 1)]^{\frac{1}{2}}/k \tag{2.27}$$

Comparing this equation with equation (2.20) it is seen that they are identical. The vertical deflection at C

$$\delta = BD - OC$$

These two dimensions can be found easily if it is remembered that the value of the parameter at point B is ϕ_B while that of C is $\pi/2$. Hence, by applying equation (1.20) we obtain

$$\delta = [2E(p, \phi_B) - F(p, \phi_B) - 2E(p) + K(p)]/k \tag{2.28}$$

The coordinates in the xy system will now be determined. The basic strut was solved in terms of the $x'y'$ coordinate system (*Figure 2.5*) but the x and y axes are better suited since their origin is at the fixed end of the cantilever.

In terms of the parameter ϕ the horizontal coordinate of any point

$$x = h\cos\phi_B - y' = h(\cos\phi_B - \cos\phi) \qquad (2.29)$$

The vertical coordinates may be found from

$$y = b - x' = [2E(p, \phi_B) - F(p, \phi_B) + F(p, \phi) - 2E(p, \phi)]/k \quad (2.30)$$

In equations (2.29) and (2.30), ϕ is the parameter of the point in question. The distance s of the point from B must be known. Then, in accordance with (2.22)

$$s = [F(p, \phi) - F(p, \phi_B)]/k \qquad (2.31)$$

This equation can be solved for ϕ, and θ may be determined from $p \sin\phi = \sin(\theta/2)$. For any given value of s the above equations which give x, y and θ, fully determine the point. Since θ is measured from the vertical it varies from $\pi/2$ to $\pi/2 + \psi_0$.

We have previously considered a flexible cantilever that gave an absurd answer when analysed within the linear framework. Take a cantilever now that will give a seemingly reasonable (though not accurate) answer when solved by the small deflection theory. Assume a cantilever $2\frac{1}{2}$ by $\frac{1}{4}$ in., 150 in. long with a vertical load $P = 5$ lb applied at the end. We find that $1/k = 139{\cdot}6$ ($E = 30 \times 10^6$ lb/in.^{2}). Substituting k in equation (2.24),

$$150 = 139{\cdot}6\{K(p) - F[p, \sin^{-1}(0{\cdot}707/p)]\}$$

This equation is solved by $p = 0{\cdot}866$, hence $L = 300$ in. and $h = 242$ in. The parameter at fixed end B is $\phi_B = \sin^{-1}(0{\cdot}707/0{\cdot}866) = 55°$. The horizontal movement of the end is

$$\Delta = L_1 - h\cos\phi_B = 11{\cdot}5 \text{ in.}$$

The vertical deflection of the same point

$$\delta = 139{\cdot}6[2E(0{\cdot}866, 55°) - F(0{\cdot}866, 55°) - \\ - E(0{\cdot}866) + K(0{\cdot}866)] = 50{\cdot}2 \text{ in.}$$

According to the small deflection theory, $\delta = 56{\cdot}7$ in.

The explanation for the larger value when using the elementary theory is that when the load increases from 0 to 5 lb the bending moment increases at a slower rate because of the horizontal movement of the end of the cantilever toward the fixed end. This slower rate of increase is ignored in the small deflection theory.

For an infinitely long cantilever $p = 1$. The bending moment at the fixed end is, however, finite because the bar will deflect until a finite lever arm can balance the flexural resistance of the bar. By applying the principle of elastic similarity, *Figure 1.7* shows that $\phi_B = 45°$ and

$$h_1 = h \cos 45° = \frac{\sqrt{2}}{k} \qquad \text{(finite)} \qquad (2.32)$$

A formal expression for the length of the cantilever is

$$L_1 = \frac{1}{k}[\ln \tan(\pi/2) - \ln \tan(3\pi/8)] = \infty$$

Likewise, the vertical deflection is also infinite.

2.4. Horizontal Cantilever with a Load and a Couple Applied at the Free End

If a force and a clockwise couple are applied at C (*Figure 2.6*) they can be replaced by a force acting on a rigid lever. The length

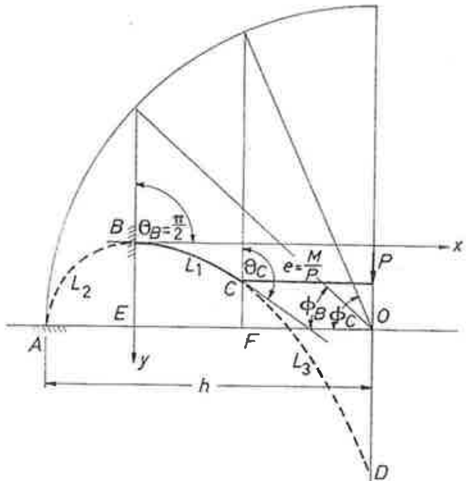

Figure 2.6

of this lever is $e = M/P$. To solve this problem the cantilever may be converted into a basic strut by continuing the bar past B until at A it becomes tangential to the vertical. Consider also that the bar extends past C until it intersects the line of action of P (placed on the lever). Let this point be D. The total length of the strut is

$$L = L_1 + L_2 + L_3$$

but for the time being only L_1 is known. On the other hand

$$\frac{e}{h} = \cos\phi_C = \frac{ek}{2p} \tag{2.33}$$

Also,
$$\sin\phi_B = \frac{\sin(\pi/2)}{p} = \frac{1}{p\sqrt{2}}$$

With the aid of the parameters ϕ_B and ϕ_C the segment L_1 may be expressed by the following equation

$$L_1 = \frac{1}{k}\left\{F\left[p, \cos^{-1}\left(\frac{ek}{2p}\right)\right] - F\left[p, \sin^{-1}\left(\frac{1}{p\sqrt{2}}\right)\right]\right\} \tag{2.34}$$

which can be solved for the unknown p. Once p is known, all other dimensions of the loaded bar can be obtained. From

$$\cos\phi_C = \frac{ek}{2p}$$

we obtain
$$\sin(\theta_C/2) = p\sin\phi_C$$

The relationship between the arc length (measured from B to the point in question) and the angle θ can be expressed as

$$s = [F(p,\phi) - F(p,\phi_B)]/k \tag{2.35}$$

where
$$\phi = \sin^{-1}\left(\frac{\sin(\theta/2)}{p}\right)$$

for values of $\pi/2 < \theta < \theta_C$.
In terms of the parameter ϕ the coordinates of a point (x, y) are

$$x = 2p(\cos\phi_B - \cos\phi)/k \tag{2.36}$$

and
$$y = [2E(p,\phi_B) - F(p,\phi_B) + F(p,\phi) - 2E(p,\phi)]/k \tag{2.37}$$

The deflection at C can be determined by putting $\phi = \phi_C$ in equations (2.36 and 37).

It should be noted that it is by no means certain that CD (*Figure 2·6*) can be extended until the curve intersects the line of action of P. Suppose, for example, that a small force and a large couple is applied on the bar. In this case e is large and P acts so far from the fixed end that the line of P will bypass the elastica. It will be remembered that even for an infinitely long cantilever the horizontal deflection is finite (2.32). Hence for this type of problem the elastic shape can be either the undulating or the nodal elastica. Unfortunately, we cannot tell in advance which one it will be and some numerical work is necessary to establish the type of curve which must be dealt with.

It is seen from equation (2.34) that

$$\frac{ek}{2p} \leqslant 1 \qquad \text{and} \qquad \frac{1}{p\sqrt{2}} \leqslant 1$$

are the two inequalities to be satisfied in order that ϕ should be real. It also follows that if $M^2/P > 2EI$, the curve cannot be an undulating elastica. It will be noticed that the length of the bar is not involved in the above stipulation. Hence the opposite, that is, $M^2/P < 2EI$, does not necessarily mean that the elastic shape will be an undulating elastica for it is possible that no real p will satisfy equation (2.34).

As an example let us consider a cantilever 100 in. long with a flexural rigidity of $EI = 10{,}000$ lb in.^{2}, acted upon by a force $P = 1$ lb and a couple $M = 50$ lb in. Since $M^2/P < 2EI$ the curve could be an undulating elastica. Trying equation (2.34),

$$100 = 100\left\{F\left[p, \cos^{-1}\left(\frac{1}{4p}\right)\right] - F\left[p, \sin^{-1}\left(\frac{0{\cdot}707}{p}\right)\right]\right\}$$

This equation is solved by $p = 0{\cdot}974 = \sin 77°$ (approximately). Hence the equations of the undulating elastica apply and the deflections of the end are $x_C = 83{\cdot}9$ in. and $y_C = 47{\cdot}3$ in., while the end slope is $\theta_C = 139°30'$.

Consider now the same cantilever with $P = 1$ lb and $M = 100$ lb in. Here again $M^2/P < 2EI$, but we find that the equation

$$100 = 100\left\{F\left[p, \cos^{-1}\left(\frac{1}{2p}\right)\right] - F\left[p, \sin^{-1}\left(\frac{0{\cdot}707}{p}\right)\right]\right\}$$

cannot be solved for $0 < p < 1$. Hence the cantilever will be a segment of a nodal elastica and the next step will be to investigate this type of curve.

It is seen at once that for a given L_1 and e the nodal elastica can assume a shape similar to BC, that is, ending with $\theta_C < \pi$, or it can be similar to shape $BCLD$ (*Figure 2.7*). The curve can also assume a shape $BC + nL_{2\pi}$ or a shape $BCLD + nL_{2\pi}$ respectively. The

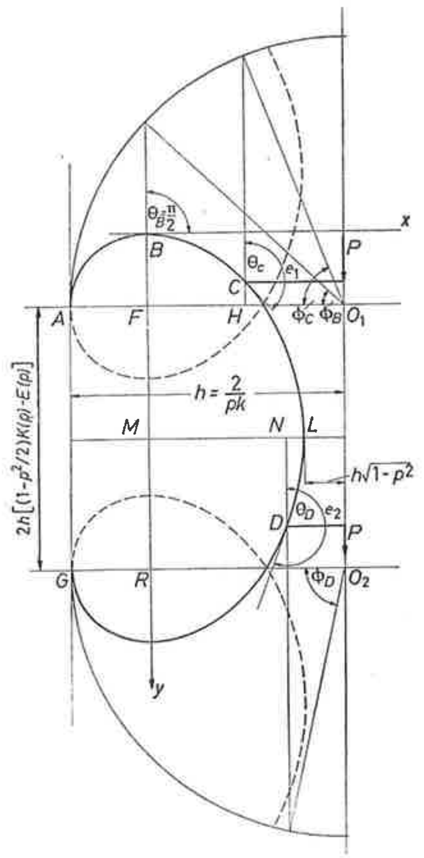

Figure 2.7

term $nL_{2\pi}$ indicates that the elastica can have any number of full revolutions in addition to its characteristic shape. If the bar will come to rest in a shape similar to BC one may write for the length

$$AC = pF(p, \theta_C/2)/k \tag{2.38}$$

This equation follows from equation (1.27). Since the bar begins at B, the length BC is

$$L = p[F(p, \theta_C/2) - F(p, \pi/4)]/k \tag{2.39}$$

$\theta_C/2$ can be found from

$$e_1 = h\cos\phi_C \quad \text{and} \quad \sin\phi_C = p\sin(\theta_C/2)$$

Hence
$$e_1 = \frac{2[1 - p^2\sin^2(\theta_C/2)]^{\frac{1}{2}}}{pk}$$

and
$$\sin(\theta_C/2) = \left(\frac{1}{p^2} - \frac{e_1 k^2}{4}\right)^{\frac{1}{2}}$$

Substituting this in equation (2.39) we obtain an equation with p as the only unknown.

If the end slope is more than π, but the bar does not cover one full revolution, the rigid lever is in the e_2 position (*Figure 2.7*). We have

$$e_2 = h\cos\phi_D \quad \text{and} \quad \sin\phi_D = p\sin(\pi - \theta_D/2) = p\sin(\theta_D/2)$$

and consequently, $\sin(\theta_D/2) = \left(\frac{1}{p^2} - \frac{e_2 k^2}{4}\right)^{\frac{1}{2}}$

and the length $BCLD$ is given by

$$L = \frac{p}{k}\left\{2K(p) - F\left[p, \sin^{-1}\left(\frac{1}{p^2} - \frac{e_2 k^2}{4}\right)^{\frac{1}{2}}\right] - F(p, \pi/4)\right\} \tag{2.40}$$

If the force acts on e_1 the connection between arc length s and slope θ is

$$s = p[F(p, \theta/2) - F(p, \pi/4)]/k$$

and the coordinates are

$$\left.\begin{aligned} x &= \frac{2}{kp}(\cos\phi_B - \cos\phi) \\ \text{and} \quad y &= h[E(p, \pi/4) - (1 - p^2/2)F(p, \pi/4) - \\ &\quad - E(p, \theta/2) + (1 - p^2/2)F(p, \theta/2)] \\ \text{where } \cos\phi &= [1 - p^2\sin^2(\theta/2)]^{\frac{1}{2}} \\ \text{and} \quad & \pi/2 < \theta < \theta_C \end{aligned}\right\} \tag{2.41}$$

If the bar ends with a slope $2\pi > \theta_D > \pi$, the modulus p will be found from equation (2.40). The appropriate equations of s, x and y are those of equation (2.41) for $\pi/2 < \theta < \pi$. For $\theta > \pi$ we have,

$$\left.\begin{aligned} s &= p[2K(p) - F(p, \pi/4) - F(p, \theta/2)]/k \\ x &= 2(\cos\phi_B - \cos\phi)/kp \\ y &= h[[E(p, \pi/4) - 2E(p) + E[p, (\pi - \theta/2)] + \\ &\qquad + (1 - p^2/2)\{2K(p) - F(p, \pi/4) - \\ &\qquad - F[p, (\pi - \theta/2)]\}]] \end{aligned}\right\} \quad (2.42)$$

For a nodal elastica that makes one or more full revolutions in addition to the lengths BC and $BCLD$ respectively, the basic equations to be solved for p are as follows:

$$\left.\begin{aligned} L &= p[2nK(p) + F(p, \theta_C/2) - F(p, \pi/4)]/k \\ \text{and} \quad L &= p\{(2n+2)K(p) - F[p, (\pi - \theta_D/2)] - \\ &\qquad - F(p, \pi/4)\}/k \end{aligned}\right\} \quad (2.43)$$

in which n is the number of revolutions.

The horizontal coordinates remain unchanged but for y the quantity $AG = 2h\ [(1-p^2/2)\,K(p) - E(p)]$ has to be added for every full revolution to the values calculated from equations (2.41 and 42) respectively.

The cantilever that could not be solved previously for $0<p<1$ when applying equation (2.34) will now be analysed by using the appropriate nodal equations. It is found that equation (2.39) is satisfied by $p = 0{\cdot}903$. It is known, therefore, that the cantilever will assume a shape similar to BC in *Figure 2.7*.

From $\quad \sin(\theta_C/2) = (1/p^2 - 1/4)^{\frac{1}{2}}$; $\theta_C = 162°\,12'$,

$\phi_B = \sin^{-1}[p \sin(\pi/4)] = 39°42'$ and $\phi_C = \sin^{-1}(p \sin 81°06') = 63°06'$. The deflection at C is calculated from equation (2.41) giving $x_C = 71{\cdot}68$ in., and $y_C = 80{\cdot}79$ in.

2.5. Cantilevers with Identical Lever Arms

If a cantilever of finite length is subject to gradually increasing loads applied vertically at the end of the bar, the free end will move toward the fixed end. If a constant lever arm is required, the length of the cantilever will have to be increased as the load grows. *Figure 2.8* depicts different shapes of the same cantilever loaded with increasing forces P, P_1, P_2, etc., at a constant distance l from A. The problem is to find a relationship between the load and the length of the cantilever belonging to that particular load.

The bending moment at $B(x, y)$ may be expressed as follows:

$$EI\,\frac{d\psi}{ds} = P(l - x) \tag{2.44}$$

Differentiating equation (2.44) with respect to s,

$$\frac{d^2\psi}{ds^2} = -P\,\frac{\cos\psi}{EI} \tag{2.45}$$

is obtained. Integration yields

$$\frac{1}{2}\left(\frac{d\psi}{ds}\right)^2 = \frac{P}{EI}\,(\sin\psi_0 - \sin\psi) \tag{2.46}$$

where the constant of the integration has been found from the boundary condition

$$\left(\frac{d\psi}{ds}\right)_{\psi=\psi_0} = 0$$

Since

$$\int_0^L dx = l,$$

equation (2.46) yields

$$dx = \frac{\cos\psi\, d\psi}{\left[\dfrac{2P}{EI}\,(\sin\psi_0 - \sin\psi)\right]^{\frac{1}{2}}} \tag{2.47}$$

Integrating the left and right sides of this equation from 0 to l and from 0 to ψ_0 respectively, we obtain

$$\int_0^{\psi_0} \frac{\cos\psi\, d\psi}{(\sin\psi_0 - \sin\psi)^{\frac{1}{2}}} = \left(\frac{2Pl^2}{EI}\right)^{\frac{1}{2}} \tag{2.48}$$

Let the independent parameter ϕ satisfy

$$1 + \sin\psi = 2p^2\sin^2\phi = (1 + \sin\psi_0)\sin^2\phi$$

and change the variable from ψ to ϕ. In terms of the new variable,

$$l = \frac{2p}{k} \int_{\phi_1}^{\pi/2} \sin \phi \, d\phi \tag{2.49}$$

where $\phi_1 = \sin^{-1} (1/p\sqrt{2})$. It follows from equation (2.49) that the relationship between l and p is

$$l = \frac{2p}{k} \cos \phi_1 \tag{2.50}$$

Having found p, the length L for the different loads P follows immediately:

$$L = [K(p) - F(p, \phi_1)]/k \tag{2.51}$$

This equation is based on equation (2.24).

The principle of elastic similarity can be usefully employed in this problem. As seen from *Figure 2.5*

$$l = h \cos \phi_B = \frac{2p}{k} \cos \phi_B \tag{2.52}$$

where $\sin \phi_B = 1/p\sqrt{2}$. Equations (2.50) and (2.52) are identical.

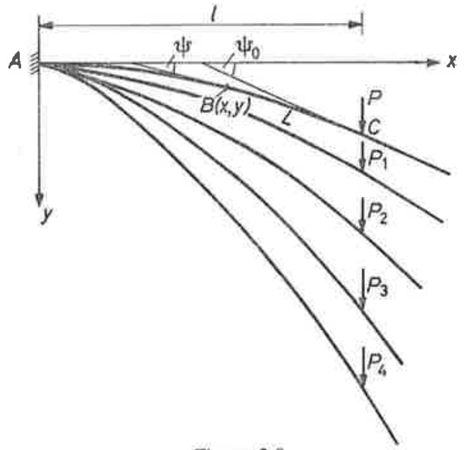

Figure 2.8

2.6. Horizontal Cantilever with an Inclined Load

Let α be the angle of inclination between the load and the x-axis. The bending moment at $Q(x, y)$ is (*Figure 2.9*)

$$M = EI\frac{d\psi}{ds} = P_1(x_C - x) + P_2(y_C - y) \tag{2.53}$$

where $P_1 = P\sin\alpha$ and $P_2 = P\cos\alpha$.

Differentiation of equation (2.53) with respect to s yields

$$EI\frac{d^2\psi}{ds^2} = -P_1\cos\psi - P_2\sin\psi \tag{2.54}$$

In order to solve equation (2.54) the following substitutions are introduced:

$$u = s/L \quad \text{and} \quad \theta = \psi + \alpha \tag{2.55}$$

It is found from equation (2.55) that

$$\frac{d^2\psi}{ds^2} = \frac{1}{L^2}\frac{d^2\theta}{du^2}$$

This follows from $\dfrac{d\theta}{du} = L\dfrac{d\psi}{ds}$

and $$\frac{d}{du}\left[\frac{d\psi}{ds}\right]L = \frac{d}{ds}\left[\frac{d\psi}{ds}\right]L\frac{ds}{du} = \frac{d^2\psi}{ds^2}L^2$$

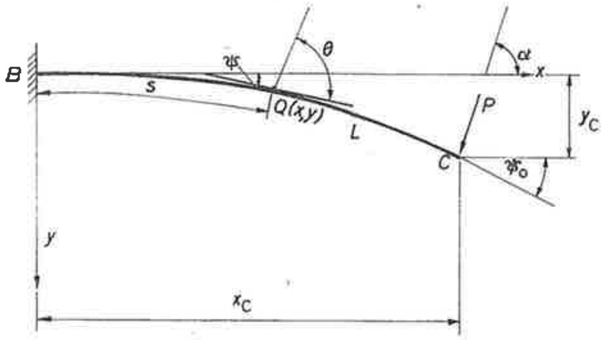

Figure 2.9

Also, for the right side of equation (2.54) one can write

$$P\left(\frac{P_1}{P}\cos\psi + \frac{P_2}{P}\sin\psi\right) = P\sin(\psi + \alpha) = P\sin\theta$$

These substitutions reduce equation (2.54) to

$$\frac{d^2\theta}{du^2} + c\sin\theta = 0 \tag{2.56}$$

in which $$c = \frac{L^2 P}{EI} = L^2 k^2$$

The boundary conditions are

$$(\psi)_{s=0} = 0 \qquad \text{or, } (\theta)_{u=0} = \alpha$$

and $$\left(\frac{d\psi}{ds}\right)_{s=L} = 0 \qquad \text{or, } \left(\frac{d\theta}{du}\right)_{\theta=\psi_0+\alpha} = 0 \tag{2.57}$$

Multiplying both sides of equation (2.56) by $2d\theta$ and integrating, yields

$$\left(\frac{d\theta}{du}\right)^2 = 2c\left[\cos\theta - \cos(\psi_0 + \alpha)\right]$$

Hence $$du = \frac{ds}{L} = \frac{d\theta}{\{2c\left[\cos\theta - \cos(\psi_0 + \alpha)\right]\}^{\frac{1}{2}}}$$

Integrating ds from $\psi = 0$ to $\psi = \psi_0$ means a lower limit $\theta = \alpha$ and an upper limit $\theta = \psi_0 + \alpha$ in terms of θ. Therefore,

$$L = \int_{\alpha}^{\psi_0+\alpha} ds = \frac{L}{\sqrt{2c}}\int_{\alpha}^{\psi_0+\alpha} \frac{d\theta}{\left[\cos\theta - \cos(\psi_0 + \alpha)\right]^{\frac{1}{2}}}$$

and $$1 = \frac{1}{\sqrt{2c}}\left\{-\int_0^{\alpha}\frac{d\theta}{\left[\cos\theta - \cos(\psi_0 + \alpha)\right]^{\frac{1}{2}}} + \right.$$
$$\left. + \int_0^{\psi_0+\alpha}\frac{d\theta}{\left[\cos\theta - \cos(\psi_0 + \alpha)\right]^{\frac{1}{2}}}\right\}$$

or $$1 = \frac{1}{2\sqrt{c}}\left\{-\int_0^{\alpha}\frac{d\theta}{\{\sin^2\left[(\psi_0 + \alpha)/2\right] - \sin^2(\theta/2)\}^{\frac{1}{2}}} + \right.$$
$$\left. + \int_0^{\psi_0+\alpha}\frac{d\theta}{\{\sin^2\left[(\psi_0 + \alpha)/2\right] - \sin^2(\theta/2)\}^{\frac{1}{2}}}\right\} \tag{2.58}$$

Let $p = \sin[(\psi_0 + \alpha)/2]$ and select ϕ such that

$$p \sin\phi = \sin(\theta/2) \tag{2.59}$$

Differentiating,
$$d\theta = \frac{2p\cos\phi\, d\phi}{(1 - p^2\sin^2\phi)^{\frac{1}{2}}} \tag{2.60}$$

The substitution of equation (2.60) in equation (2.58) results in

$$1 = \frac{1}{\sqrt{c}}\left\{\int_0^{\pi/2} \frac{d\phi}{(1 - p^2\sin^2\phi)^{\frac{1}{2}}} - \int_0^m \frac{d\phi}{(1 - p^2\sin^2\phi)^{\frac{1}{2}}}\right\} \tag{2.61}$$

where
$$m = \sin^{-1}\left(\frac{\sin(\alpha/2)}{p}\right)$$

and since $\sqrt{c} = Lk$, we have from equation (2.61)

$$L = [K(p) - F(p, m)]/k \tag{2.62}$$

Equation (2.62) yields p, the modulus that governs the deflected shape and from p we find ψ_0. The relationship between s and ψ can be derived similarly. Since $s = \int ds$, and the integration has to be performed between the limits $\psi = 0$ and $\psi = \psi_0$ (that is, from α to $\psi + \alpha$) one finds

$$s = [F(p, n) - F(p, m)]/k,$$

where
$$n = \sin^{-1}\left[\frac{\sin[(\psi + \alpha)/2]}{p}\right] \tag{2.63}$$

It is noted that

$$ds = \frac{L\, d\theta}{2\sqrt{c}\{\sin^2[(\psi_0 + \alpha)/2] - \sin^2(\theta/2)\}^{\frac{1}{2}}} = \frac{d\phi}{k(1 - p^2\sin^2\phi)^{\frac{1}{2}}}$$

As
$$\frac{dx}{ds} = \cos\psi, \quad dx = \frac{\cos(\theta - \alpha)\, d\phi}{k(1 - p^2\sin^2\phi)^{\frac{1}{2}}} \tag{2.64}$$

Expanding $\cos(\theta - \alpha)$ and noting that

$$\cos\theta = 1 - 2\sin^2(\theta/2) = 1 - 2p^2\sin^2\phi$$

the following expression for dx is obtained,

$$dx = \frac{\cos\alpha}{k}\left\{\frac{d\phi}{(1-p^2\sin^2\phi)^{\frac{1}{2}}} - \frac{2p^2\sin^2\phi\, d\phi}{(1-p^2\sin^2\phi)^{\frac{1}{2}}}\right\} + \frac{\sin\alpha}{k}2p\sin\phi\, d\phi$$

Again, by changing the variable from θ to ϕ the limits of the integration become m and n. Hence

$$x = \frac{1}{k}\{\cos\alpha\,[F(p,m) - F(p,n) + 2E(p,n) - 2E(p,m)] + \\ + 2p\sin\alpha(\cos m - \cos n)\} \qquad (2.65)$$

The horizontal coordinate of the end of the cantilever can be found by substituting $\psi = \psi_0$. In this case $n = \pi/2$. Therefore,

$$x_C = \frac{1}{k}\{\cos\alpha\,[F(p,m) - K(p) + 2E(p) - 2E(p,m)] + \\ + 2p\sin\alpha\cos m\} \qquad (2.66)$$

A similar procedure can be adopted for the derivation of the vertical coordinate.

$$dy = ds\sin\psi = ds\sin(\theta-\alpha)$$

By expanding $\sin(\theta-\alpha)$ and expressing $\sin\theta$ and $\cos\theta$ in terms of ϕ, the above expression leads to

$$dy = \frac{\cos\alpha}{k}2p\sin\phi\, d\phi - \frac{\sin\alpha}{k}\left[\frac{d\phi}{(1-p^2\sin^2\phi)^{\frac{1}{2}}} - \frac{2p^2\sin^2\phi\, d\phi}{(1-p^2\sin^2\phi)^{\frac{1}{2}}}\right]$$

Integrating between the same limits as for the horizontal deflection we obtain

$$y = \frac{1}{k}\{2p\cos\alpha(\cos m - \cos n) - \sin\alpha\,[F(p,m) - F(p,n) + \\ + 2E(p,n) - 2E(p,m)]\} \qquad (2.67)$$

Further,

$$y_C = \frac{1}{k}\{2p\cos\alpha\cos m - \sin\alpha\,[F(p,m) - K(p) + \\ + 2E(p) - 2E(p,m)]\} \qquad (2.68)$$

The same problem may be solved by considering the cantilever as a segment of the undulating elastica. The cantilever is converted into the basic strut by extending it past B to a point where the tangent to the elastic curve is parallel to P (*Figure 2.10*). Consider the bar ABC. The connection between the slope θ and the parameter is

$$\sin\phi_B = \frac{\sin(\theta_B/2)}{p}$$

Since $\quad L_1 + L_2 = K(p)/k, \quad \text{and} \quad L_2 = F(p,\phi_B)/k,$

$$L_1 = \left\{K(p) - F\left[p, \sin^{-1}\left(\frac{\sin(\theta_B/2)}{p}\right)\right]\right\}\Big/k. \qquad (2.69)$$

This equation is identical with equation (2.62).

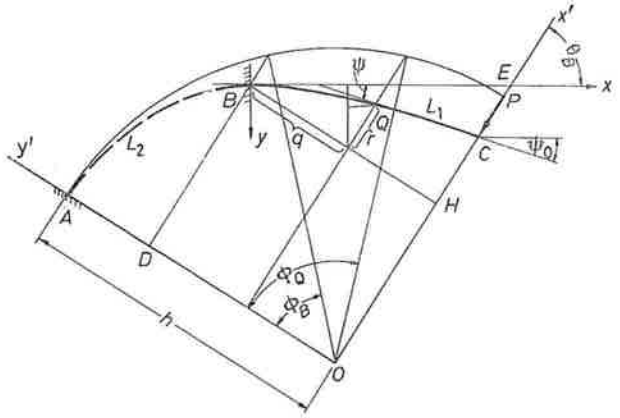

Figure 2.10

The length of the arc $BQ = s = ABQ - AB$. By using the incomplete elliptic integrals between the limits ϕ_B and ϕ_Q one obtains

$$s = \frac{1}{k}\left\{F\left[p, \sin^{-1}\left(\frac{\sin[(\psi + \theta_B)/2]}{p}\right)\right] - F\left[p, \sin^{-1}\left(\frac{\sin(\theta_B/2)}{p}\right)\right]\right\} \qquad (2.70)$$

since $$\sin\phi_Q = \frac{\sin[(\psi + \theta_B)/2]}{p}$$

Equation (2.70) is identical with (2.63).

The horizontal and vertical components of the deflection of the point $Q(x, y)$ can be found in terms of the xy system. From *Figure 2.10*,

$$r = [F(p,m) - F(p,n) + 2E(p,n) - 2E(p,m)]/k$$

and $$q = 2p(\cos m - \cos n)/k.$$

Hence
$$\left.\begin{aligned} x &= r\cos\theta_B + q\sin\theta_B \\ y &= q\cos\theta_B - r\sin\theta_B \end{aligned}\right\} \qquad (2.71)$$
and

These two equations are identical with equations (2.65) and (2.67) respectively if $\theta_B = \alpha$.

As an example of this type of problem consider a horizontal cantilever with a 5 lb load applied at an angle $\theta_B = 45°$ at the end. The cantilever is 260 in. long and has a $2\frac{1}{2} \times \frac{1}{4}$ in. cross section. From equation (2.69)

$$260 = 139{\cdot}6\left\{K(p) - F\left[p, \sin^{-1}\left(\frac{0{\cdot}385}{p}\right)\right]\right\}$$

for which $p = 0{\cdot}906$. Also, from $\phi_B = 25°$ the deflections at the free end are: $x_C = 124$ in., $y_C = 199$ in.

2.7. Cantilever under Two Vertical Loads

Let $L = L_1 + L_2$ be the length of the cantilever in *Figure 2.11*. The bending moment at a point U between B and C may be written as[5],

$$M = EI\frac{d\psi}{ds} = P_2(a + b - x) \qquad (2.72)$$

Differentiating, $$\frac{d^2\psi}{ds^2} = -\frac{P_2}{EI}\frac{dx}{ds} = -\frac{P_2}{EI}\cos\psi \qquad (2.73)$$

hence $$\frac{1}{2}\left(\frac{d\psi}{ds}\right)^2 = -\frac{P_2}{EI}\sin\psi + C_1 \qquad (2.74)$$

From the boundary condition $\left(\frac{d\psi}{ds}\right)_{\psi=\psi_2} = 0$

$$\frac{d\psi}{ds} = k_2[2(\sin\psi_2 - \sin\psi)]^{\frac{1}{2}}$$

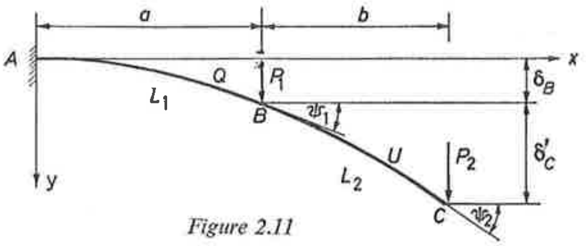

Figure 2.11

where $k_2 = (P_2/EI)^{\frac{1}{2}}$ and ψ_2 is the end slope. The length L_2 remains unchanged during deflection; this enables us to write

$$L_2 = \int_{\psi_1}^{\psi_2} ds = \frac{1}{k_2\sqrt{2}} \int_{\psi_1}^{\psi_2} \frac{d\psi}{(\sin\psi_2 - \sin\psi)^{\frac{1}{2}}} \qquad (2.75)$$

This elliptic integral contains the unknowns ψ_1 and ψ_2. To bring equation (2.75) to Legendre's standard form let

$$1 + \sin\psi = 2p_2^2 \sin^2\phi = (1 + \sin\psi_2)\sin^2\phi \qquad (2.76)$$

In terms of the new variable ϕ equation (2.75) reduces to

$$L_2 = \frac{1}{k_2}\int_{\phi_1}^{\pi/2} \frac{d\phi}{(1 - p_2^2 \sin\phi)^{\frac{1}{2}}} = \frac{1}{k_2}[K(p_2) - F(p_2, \phi_1)] \quad (2.77)$$

Here $\sin\phi_1 = [(1 + \sin\psi_1)/2]^{\frac{1}{2}}/p_2$ and p_2 is the modulus that governs the shape between B and C. Equation (2.77) has two unknowns, p_2 and ϕ_1, hence further equations are necessary. These can be obtained by considering the bending moment at Q. We have

$$EI\frac{d\psi}{ds} = P_2(a + b - x) + P_1(a - x) \qquad (2.78)$$

Similar operations to those carried out in equations (2.73) and (2.74) lead to

$$\frac{1}{2}\left(\frac{d\psi}{ds}\right)^2 = -k^2 \sin\psi + C_2 \qquad (2.79)$$

in which
$$k = \left(\frac{P_1 + P_2}{EI}\right)^{\frac{1}{2}}$$

It is seen that at B the bending moment is

$$\frac{P_2 b}{EI} = \left(\frac{d\psi}{ds}\right)_{\psi=\psi_1} = k_2[2(\sin\psi_2 - \sin\psi_1)]^{\frac{1}{2}} \qquad (2.80)$$

hence, from equation (2.79)

$$\frac{1}{2}\left(\frac{P_2 b}{EI}\right)^2 = -k^2\sin\psi_1 + C_2$$

and

$$C_2 = \frac{P_2^2 b^2}{2(EI)^2} + (P_1 + P_2)\frac{\sin\psi_1}{EI}$$

Thus equation (2.79) reduces to

$$\frac{d\psi}{ds} = \sqrt{2}\left[k^2(\sin\psi_1 - \sin\psi) + \frac{P_2^2 b^2}{2(EI)^2}\right]^{\frac{1}{2}} \qquad (2.81)$$

However, $\dfrac{P_2^2 b^2}{2(EI)^2} = k_2(\sin\psi_2 - \sin\psi_1)$ (from equation (2.80))

Therefore, equation (2.81) further reduces to

$$\frac{d\psi}{ds} = k\sqrt{2}\left[\sin\psi_1 - \sin\psi + \frac{k_2^2}{k^2}(\sin\psi_2 - \sin\psi_1)\right]^{\frac{1}{2}} \qquad (2.82)$$

Also equation (2.80) provides an expression for the horizontal projection of L_2 since

$$b = \frac{\sqrt{2}}{k_2}(\sin\psi_2 - \sin\psi_1)^{\frac{1}{2}} \qquad (2.83)$$

Again, L_1 does not alter during deflection

hence

$$L_1 = \int_0^{\psi_1} ds = \frac{1}{k\sqrt{2}}\int_0^{\psi_1}\frac{d\psi}{(2p^2 - 1 - \sin\psi)^{\frac{1}{2}}} \qquad (2.84)$$

if p is selected such that

$$\frac{k_2^2}{k^2}(\sin\psi_2 - \sin\psi_1) = 2p^2 - 1 - \sin\psi_1 \qquad (2.85)$$

A new variable ζ is introduced, satisfying

$$1 + \sin\psi = 2p^2\sin^2\zeta$$

This change is necessary to bring equation (2.84) to Legendre's standard elliptic integral. Substitution into equation (2.84) results in

$$L_1 = \frac{1}{k}\int_{\zeta_0}^{\zeta_1} \frac{d\zeta}{(1-p^2\sin^2\zeta)^{\frac{1}{2}}} = [F(p,\zeta_1) - F(p,\zeta_0)]/k \quad (2.86)$$

where $\sin\zeta_0 = \dfrac{1}{p\sqrt{2}}$ and $\sin\zeta_1 = \dfrac{1}{p}\left(\dfrac{1+\sin\psi_1}{2}\right)^{\frac{1}{2}}$

The modulus p decides the shape between A and B.

The deflected shape has, therefore, only three unknowns, namely p, p_2, and ψ_1. ψ_2 is dependent upon p_2 because, from (2.76), $\sin\psi_2 = 2p_2^2-1$. Equations (2.78, 85 and 86) are sufficient for the determination of the three unknowns.

Having found p, p_2, and ψ_1 the horizontal and vertical deflections of B and C are available at once. Since $(\psi)_{x=0} = 0$,

$$M_A = P_1 a + P_2(a+b) = EI\left(\frac{d\psi}{ds}\right)_{\psi=0} = EI\,k[2(2p^2-1)]^{\frac{1}{2}} \quad (2.87)$$

But b is already known from (2.83), which may be reduced to

$$b = [2(2p_2^2 - 1 - \sin\psi_1)]^{\frac{1}{2}}/k_2$$

Introducing this value of b into (2.87) one finds

$$a = \sqrt{2}[\sqrt{(2p^2-1)} - \sqrt{(2p^2-1-\sin\psi_1)}]/k \quad (2.88)$$

Since $dy = ds \sin\psi$, one can write

$$\delta_B = \int_0^{\psi_1} dy = \frac{1}{k\sqrt{2}}\int_0^{\psi_1} \frac{\sin\psi\, d\psi}{(2p^2-1-\sin\psi)^{\frac{1}{2}}} \quad (2.89)$$

The introduction of ζ reduces (2.89) to

$$\delta_B = \left[\int_{\zeta_0}^{\zeta_1} \frac{d\zeta}{(1-p^2\sin^2\zeta)^{\frac{1}{2}}} - 2\int_{\zeta_0}^{\zeta_1} (1-p^2\sin^2\zeta)d\zeta\right]\Big/k$$
$$= [F(p,\zeta_1) - F(p,\zeta_0) - 2E(p,\zeta_1) + 2E(p,\zeta_0)]/k \quad (2.90)$$

If dy is integrated between the limits ψ_1 and ψ_2 we obtain δ_C'. Hence, after introducing ϕ,

$$\delta_C' = [K(p_2) - 2E(p_2) - F(p_2,\phi_1) + 2E(p_2,\phi_1)]/k_2 \quad (2.91)$$

The coordinates of a point Q between A and B are found as follows. Let $AQ = s_Q$ and change equation (2.86) into

$$\begin{aligned} s_Q &= \frac{1}{k}\int_{\zeta_0}^{\zeta_Q} \frac{d\zeta}{\sqrt{(1-p^2 \sin^2 \zeta)}} \\ &= [F(p, \zeta_Q) - F(p, \zeta_0)]/k \end{aligned} \tag{2.92}$$

Equation (2.92) can be solved for ζ_Q and since

$$\sin \zeta_Q = \frac{1}{p}[(1 + \sin \psi_Q)/2]^{\frac{1}{2}},$$

ψ_Q may also be determined. Further,

$$\left.\begin{aligned} x_Q &= \sqrt{2}\,[\sqrt{(2p^2 - 1)} - \sqrt{(2p^2 - 1 - \sin \psi_Q)}]/k \\ \text{and}\quad y_Q &= [F(p, \zeta_Q) - F(p, \zeta_0) - 2E(p, \zeta_Q) + \\ &\qquad + 2E(p, \zeta_0)]/k \end{aligned}\right\} \tag{2.93}$$

For a point U between B and C the arc length

$$s_U = [F(p_2, \phi_U) - F(p_2, \phi_1)]/k_2 \tag{2.94}$$

where s_U is the distance BU measured along the arc and

$$\begin{aligned} \sin \phi_U &= [(1 + \sin \psi_U)\,2]^{\frac{1}{2}}/p_2 \\ &\quad [(1 + \sin \phi_U)/2]^{\frac{1}{2}} \end{aligned}$$

Equation (2.94) is solved for ϕ_U, from which ψ_U can be found. The coordinates of U are

$$\left.\begin{aligned} x_U &= a + [2(2p_2^2 - 1 - \sin \psi_U)]^{\frac{1}{2}}/k_2 \\ \text{and}\quad y_U &= \delta_B + [F(p_2, \phi_U) - F(p_2, \phi_1) - 2E(p_2, \phi_U) + \\ &\qquad + 2E(p_2, \phi_1)]/k_2 \end{aligned}\right\} \tag{2.95}$$

Before attempting to solve the cantilever numerically the slope ψ_1 must be assumed as the first step in the trial and error. Equations (2.77 and 86) will yield p_2 and p and these moduli must satisfy equation (2.85).

This problem shows clearly the difficulties encountered in non-linear deflections when more than one load acts on the bar. The elliptic integrals, set up in terms of the slopes, must be changed into Legendre's standard forms. To do this, new variables have to be found and the moduli must be selected such as to satisfy the boundary conditions. These difficulties can be bypassed by applying the principle of elastic similarity. This is shown in *Figure 2.12.*

After equilibrium is reached, the horizontal projection of L_2 is b. Replace P_1 and P_2 by their resultant $P = P_1 + P_2$ acting at a distance $b_r = bg$ from B, where $g = P_2/P$. This change will leave the bending moment in part L_1 unaltered. Hence the elastic shape of AB remains the same whether the cantilever is acted upon by P_1 and P_2 or by P alone.

Assume now that the resultant P is acting instead of P_1 and P_2 and extend portion AB (which, as explained before, remains unaltered) toward the right to D, also, continue past A toward the left until the slope becomes vertical. This occurs at G where the bar will be clamped. Thus we have arrived at a strut $GABD$, acted upon by P at the end. The length of the first portion of the cantilever is $L_1 = GAB - AG$ or, in elliptical integrals,

$$L_1 = [F(p, \zeta_B) - F(p, \zeta_A)]/k \tag{2.96}$$

where $\zeta_B = \sin^{-1}\left(\dfrac{\sin(\theta_B/2)}{p}\right)$, $\zeta_A = \sin^{-1}\left(\dfrac{\sin(\pi/4)}{p}\right)$,

and $$k = \left(\frac{P_1 + P_2}{EI}\right)^{\frac{1}{2}}$$

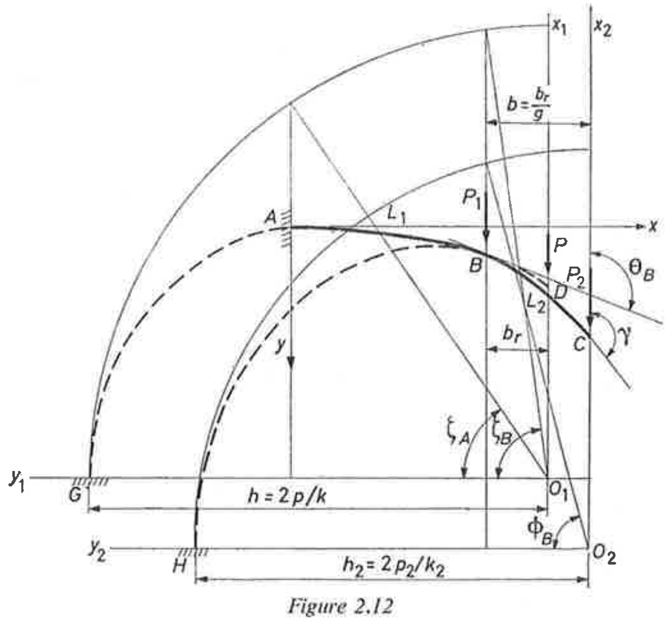

Figure 2.12

The unknowns in this equation are the modulus p and the slope at B, θ_B. The second portion of the cantilever, BC, is now considered. Assuming BC to be clamped at B it may be extended into a strut HBC, remembering, however, that at B the slope is the same θ_B as before. Now, $L_2 = HBC - HB$, and therefore,

$$L_2 = [K(p_2) - F(p_2, \phi_B)]/k_2 \tag{2.97}$$

where $k_2 = \left(\dfrac{P_2}{EI}\right)^{\frac{1}{2}}$ and $\phi_B = \sin^{-1}\left(\dfrac{\sin(\theta_B/2)}{p_2}\right)$

Since the shape of the strut (and of portion L_2) is governed by the modulus p_2 this is a new unknown. One more equation will, therefore, be necessary. This third equation can be had from geometric considerations. It is seen from *Figure 2.12* that

$$b_r = h\cos\zeta_B \text{ and } b = \frac{b_r}{g} = h_2\cos\phi_B$$

It follows that

$$h\cos\zeta_B = h_2\, g\cos\phi_B \tag{2.98}$$

Noting that $h = \dfrac{2p}{k}$, $h_2 = \dfrac{2p_2}{h_2}$, and $g = \dfrac{k_2^2}{k^2}$

equation (2.98) reduces to

$$\frac{k}{k_2} = \frac{p_2}{p}\left(\frac{1 - \dfrac{\sin^2(\theta_B/2)}{p_2^2}}{1 - \dfrac{\sin^2(\theta_B/2)}{p^2}}\right)^{\frac{1}{2}} \tag{2.99}$$

The problem is now basically solved; the simultaneous equations (2.96, 97 and 99) will yield p, p_2, and θ_B. A value for θ_B must first be assumed, and then p and p_2 calculated from (2.96) and (2.97) respectively. p and p_2 thus found must satisfy (2.99).

These results are identical with those obtained from purely analytical considerations. We note that the two portions L_1 and L_2 are governed by two different moduli p and p_2 respectively and that $p_2 = \sin(\gamma/2)$. When comparing the results obtained by using these two methods it should be remembered that $\theta = \pi/2 + \psi$, $\theta_B = \pi/2 + \psi_1$, and $\gamma = \pi/2 + \psi_2$. The parameters ζ and ϕ are identical, also, k, k_2, p, and p_2 have the same meaning in both methods. Note also that $\zeta_0 = \zeta_A$. It can be shown without difficulty that with the above substitutions equations (2.85) and (2.99) become identical.

The coordinates of the points on the deflected shape can now be calculated. Take the horizontal component of B (*Figure 2.12*):

$$x_B = 2p(\cos\zeta_A - \cos\zeta_B)/k \tag{2.100}$$

Now, $\sin\zeta_A = \dfrac{1}{p\sqrt{2}}$ and $\sin\zeta_B = \dfrac{\sin(\theta_B/2)}{p}$

but $\sin(\theta_B/2) = \sin(\pi/4 + \psi_1/2) = [(1 + \sin\psi_1)/2]^{\frac{1}{2}}$

hence $\cos\zeta_A = \left(1 - \dfrac{1}{2p^2}\right)^{\frac{1}{2}}$ and $\cos\zeta_B = \left(1 - \dfrac{1 + \sin\psi_1}{2p^2}\right)^{\frac{1}{2}}$

Therefore $x_B = \sqrt{2}\,[\sqrt{(2p^2 - 1)} - \sqrt{(2p^2 - 1 - \sin\psi_1)}]/k = a$

which is identical with equation (2.88). The horizontal coordinate is $x = 2p\,(\cos\zeta_A - \cos\zeta)/k$ for a point between A and B where $\sin\zeta = [\sin(\theta/2)]/p$ for a point between B and C the abscissa is

$$x = x_B + 2p_2(\cos\phi_B - \cos\phi)/k_2 \quad \text{where} \quad \sin\phi = \frac{\sin(\theta/2)}{p_2}$$

The relationship between slope and arc length is identical with equations (2.92 and 94) while the vertical coordinates have been given in equations (2.93 and 95).

As an example of a flexible cantilever subject to two vertical loads consider a bar 102·75 in. long with a 2 by 0·1 in. cross section. A load $P_2 = 1{\cdot}35$ lb is acting at the end and $P_1 = 0{\cdot}85$ lb is placed at 52·03 in. from the fixed end. Equations (2.96, 97 and 99) are solved by

$$\theta_B/2 = 70°, \quad p = \sin 72°\,55', \text{ and } \quad p_2 = \sin 75°$$

The deflections at the first load are $x_B = 43{\cdot}75$ in. and $y_B = 25{\cdot}14$ in. At the free end the deflections are $x_C = 71{\cdot}74$ in. and $y_C = 67{\cdot}32$ in. The end slope $\gamma = 150°$.

2.8. Cantilever under *n* Concentrated Loads

The analysis of the cantilever in the previous section has shown the difficulties encountered in finding the moduli, which determine the shape for the different parts of the bar. It can be shown that in the nonlinear framework a cantilever carrying n concentrated loads has $2n - 1$ unknowns, n moduli and $n - 1$ slopes at the points of application of the forces. The end slope θ_1 is not counted as an unknown since $p_1 = \sin(\theta_1/2)$.

No attempt will be made in this discussion to solve this problem by writing bending moment equations and solving them after having been reduced to Legendre's standard elliptic forms. The difficulties involved in finding new variables and in adjusting the integration constants so as to satisfy the boundary conditions have been demonstrated in the case of a cantilever subject to two vertical loads; a case that contained three unknowns only. The present problem, however, will need the setting up of $2n-1$ equations hence the principle of elastic similarity will be employed[6].

Consider a cantilever (*Figure 2.13*) on which the parallel forces $P_1, P_2, P_{r-1}, P_r, P_{n-1}$ and P_n act. These forces are applied at points

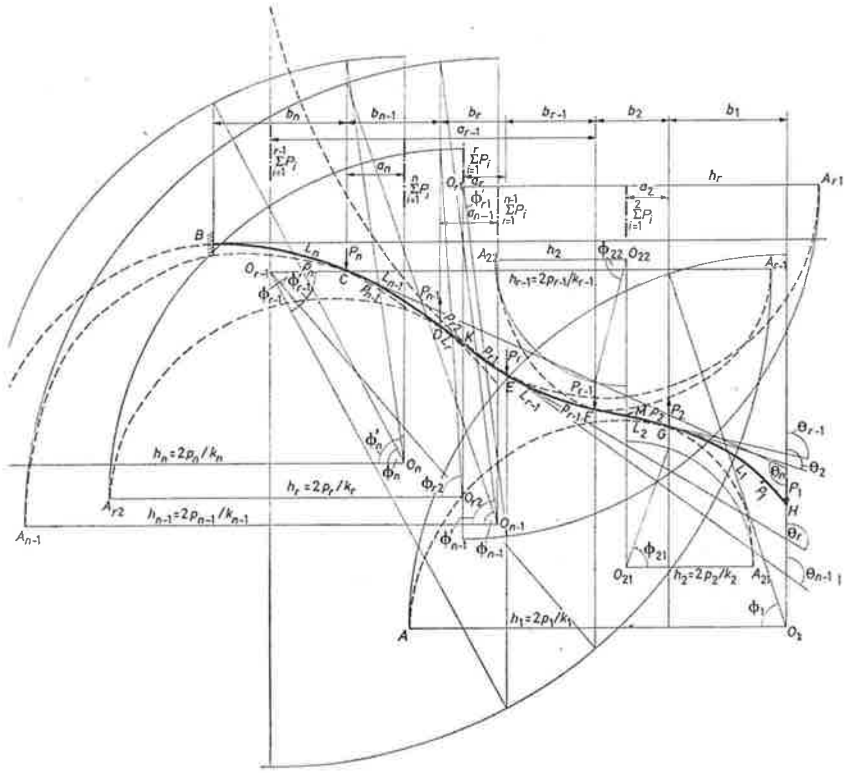

Figure 2.13

H, G, F, E, D, and C, the distance between these points being L_1, $L_2, \ldots L_{n-1}$ and the last distance between P_n and the fixed end is L_n. The slopes at the points of application of the forces $P_1, \ldots P_n$ are θ_1, $\theta_2 \ldots \theta_n$. Under the action of these loads the cantilever assumes its shape as shown and the distances between the applied loads (measured on the horizontal projection) are b_1, b_2, $b_{r-1}, \ldots b_n$.

The problem will be solved by transforming it to an equivalent set of basic strut problems; each portion, BC, CD, $DE, \ldots GH$, is replaced by a vertical strut fixed at the bottom, free at the top, with a vertical load applied at the free end.

Consider now a typical portion of the cantilever, say CD. This portion does not change the sign of its curvature. The resultant of forces $P_1, P_2, \ldots\ldots P_{n-1}$, that is, the resultant of all forces acting to the right of D, is at a distance a_{n-1} from D. Portion CD can be considered as a part of the vertical strut fixed at A_{n-1}, passing through C and D and ending on the line of action of $\sum_{i=1}^{n-1} P_i$. The shape of portion CD is governed by the modulus p_{n-1}. The quadrant is drawn from centre 0_{n-1} with a radius $h_{n-1} = 2p_{n-1}/k_{n-1}$, where

$$k_{n-1} = \left(\sum_{i=1}^{n-1} \frac{P_i}{EI}\right)^{\frac{1}{2}}$$

With regard to the values of the parameter ϕ we note that

$$\sin \phi'_{n-1} = \frac{\sin(\theta_{n-1}/2)}{p_{n-1}} \quad \text{and} \quad \sin \phi_{n-1} = \frac{\sin(\theta_n/2)}{p_{n-1}}$$

Considering now portion DE, this part of the cantilever is also a typical element of the whole although it falls into a different category from CD. As seen, there is a point of contraflexion at K, and L_r can be made up of a left and right part, L_{r2} and L_{r1}. There is, of course, $L_r = L_{r1} + L_{r2}$. Two moduli, p_{r1} and p_{r2} govern the shape. The resultant $\sum_{i=1}^{r} P_i$ acts through the vertical at K (hence the point of contraflexion at K). Extending KE into the basic strut it will begin at A_{r1}, pass through E, and end at K. Inspecting the curve $A_{r2}DKEA_{r1}$, its symmetry about K is obvious. Hence $p_{r1} = p_{r2} = p_r$ and

$$\sin \phi_{r1} = \frac{\sin(\theta_r/2)}{p_r}, \quad \sin \phi_{r2} = \frac{\sin(\theta_{n-1}/2)}{p_r}$$

2.8. CANTILEVER UNDER n CONCENTRATED LOADS

A cantilever subject to n forces has n portions. The equations relating to the lengths, moduli p, and angles θ are as follows:

$$\left.\begin{aligned}
L_n &= \frac{1}{k_n}\{F[p_n, \sin^{-1}(\sin\tfrac{1}{2}\theta_n/p_n)] - \\
&\qquad - F[p_n, \sin^{-1}(0{\cdot}707/p_n]\}, \\
L_{n-1} &= \frac{1}{k_{n-1}}\{F[p_{n-1}, \sin^{-1}(\sin\tfrac{1}{2}\theta_{n-1}/p_{n-1})] - \\
&\qquad - F[p_{n-1}, \sin^{-1}(\sin\tfrac{1}{2}\theta_n/p_{n-1})]\}, \\
L_r &= \frac{1}{k_r}\{2K(p_r) - F[p_r, \sin^{-1}(\sin\tfrac{1}{2}\theta_r/p_r)] - \\
&\qquad - F[p_r, \sin^{-1}(\sin\tfrac{1}{2}\theta_{n-1}/p_r)]\}, \\
L_{r-1} &= \frac{1}{k_{r-1}}\{F[p_{r-1}, \sin^{-1}(\sin\tfrac{1}{2}\theta_{r-1}/p_{r-1})] - \\
&\qquad - F[p_{r-1}, \sin^{-1}(\sin\tfrac{1}{2}\theta_r/p_{r-1})]\}, \\
L_2 &= \frac{1}{k_2}\{2K(p_2) - F[p_2, \sin^{-1}(\sin\tfrac{1}{2}\theta_2/p_2)] - \\
&\qquad - F[p_2, \sin^{-1}(\sin\tfrac{1}{2}\theta_{r-1}/p_2)]\}, \\
L_1 &= \frac{1}{k_1}\{K(p_1) - F[p_1, \sin^{-1}(\sin\tfrac{1}{2}\theta_2/p_1)]\}
\end{aligned}\right\} \quad (2.101)$$

There are n equations in (2.101). The number of unknowns for p is n and for θ it is $n-1$, altogether $2n-1$ unknowns. Further equations can be obtained by considering the relationship between a and b. From *Figure 2.13*

$$\left.\begin{aligned}
b_1 &= h_1\cos\phi_1 = 2p_1(\cos\phi_1)/k_1, \\
b_2 &= 2p_2(\cos\phi_{21} + \cos\phi_{22})/k_2, \\
b_{r-1} &= 2p_{r-1}(\cos\phi_{r-1} - \cos\phi'_{r-1})/k_{r-1}, \\
b_r &= 2p_r(\cos\phi_{r1} + \cos\phi_{r2})/k_r, \\
b_{n-1} &= 2p_{n-1}(\cos\phi_{n-1} - \cos\phi'_{n-1})/k_{n-1}, \\
b_n &= 2p_n(\cos\phi_n - \cos\phi'_n)/k_n,
\end{aligned}\right\} \quad (2.102)$$

where $k_r = \left(\sum_{i=1}^{r} P_i/EI\right)^{\frac{1}{2}}$,

$$
\left.
\begin{aligned}
\cos\phi_1 &= (1-\sin^2 \tfrac{1}{2}\theta_2/p_1^2)^{\frac{1}{2}},\\
\cos\phi_{21} &= (1-\sin^2 \tfrac{1}{2}\theta_2/p_2^2)^{\frac{1}{2}},\\
\cos\phi_{22} &= (1-\sin^2 \tfrac{1}{2}\theta_{r-1}/p_2^2)^{\frac{1}{2}},\\
\cos\phi_{r-1} &= (1-\sin^2 \tfrac{1}{2}\theta_{r-1}/p_{r-1}^2)^{\frac{1}{2}},\\
\cos\phi'_{r-1} &= (1-\sin^2 \tfrac{1}{2}\theta_r/p_{r-1}^2)^{\frac{1}{2}},\\
\cos\phi_{r1} &= (1-\sin^2 \tfrac{1}{2}\theta_r/p_r^2)^{\frac{1}{2}},\\
\cos\phi_{r2} &= (1-\sin^2 \tfrac{1}{2}\theta_{n-1}/p_r^2)^{\frac{1}{2}},\\
\cos\phi_{n-1} &= (1-\sin^2 \tfrac{1}{2}\theta_n/p_{n-1}^2)^{\frac{1}{2}},\\
\cos\phi'_{n-1} &= (1-\sin^2 \tfrac{1}{2}\theta_{n-1}/p_{n-1}^2)^{\frac{1}{2}},\\
\cos\phi_n &= (1-\sin^2 \tfrac{1}{2}\theta_B/p_n^2)^{\frac{1}{2}} = (1-0{\cdot}5/p_n^2)^{\frac{1}{2}},\\
\text{and}\quad \cos\phi'_n &= (1-\sin^2 \tfrac{1}{2}\theta_n/p_n^2)^{\frac{1}{2}}
\end{aligned}
\right\} \quad (2.103)
$$

It should be noted that if the centre of curvature is below the bar (negative bending moment) the subscript of ϕ' and of θ is the same, the subscript of ϕ on the other hand is lower than that of θ. If, however, the centre of curvature is above the bar (positive bending moment) the subscript of ϕ and of θ is identical and the subscript of ϕ' is lower than that of θ. For portions having a point of contraflexion the rule can be established without difficulty by comparing *Figure 2.13* with equations (2.103).

The distance a_i measured from P_i to $\sum_{r=1}^{r=i} P_i$ can be expressed as follows:

$$
\left.
\begin{aligned}
a_1 &= 0,\\
a_2 &= \frac{b_1 P_1}{\sum_1^2 P_i},\\
a_3 &= \frac{b_1 P_1 + b_2 \sum_1^2 P_i}{\sum_1^3 P_i},\\
&\vdots\\
a_r &= \frac{b_1 P_1 + b_2 \sum_1^2 P_i + b_3 \sum_1^3 P_i + \ldots + b_{r-1} \sum_1^{r-1} P_i}{\sum_1^r P_i}
\end{aligned}
\right\} \quad (2.104)
$$

However, these a's can also be expressed as (*Figure 2.13*)

$$\left.\begin{aligned} a_2 &= h_2 \cos\phi_{21} = 2p_2 \cos\phi_{21}/k_2, \\ a_{r-1} &= 2p_{r-1} \cos\phi_{r-1}/k_{r-1}, \\ a_r &= 2p_r \cos\phi_{r1}/k_r, \\ a_{n-1} &= 2p_{n-1} \cos\phi_{n-1}/k_{n-1}, \\ \text{and} \qquad a_n &= 2p_n \cos\phi_n/k_n \end{aligned}\right\} \quad (2.105)$$

a_2, a_{r-1}, and a_r, as shown on *Figure 2.13*, are negative, while a_{n-1}, and a_n are positive. Equation (2.104) will give the values of a with the correct sign if the clockwise moments are taken negative. In equations (2.105) the cosines are positive if the rotation of ϕ (from 0 to $\pi/2$) traces the arc of the circle in the direction of the positive a.

If equations (2.102) are substituted in equations (2.104) and the equations thus obtained compared with equations (2.105), we create $n-1$ equations without producing new unknowns. Hence the total number of available equations is now $2n-1$, the same as the number of unknowns.

Before numerical work on the solution can begin, the approximate shape of the cantilever must be assumed including the position of the points of contraflexion. The next step is to assume values for the θ's; the moduli will then be found from equations (2.101). After that p_1, p_2, etc., will be substituted in equations (2.103) together with the assumed θ's; this will yield the cosines of the parameter, and equations (2.102) can be solved. Having found the b's, their substitution in equations (2.104) and equations (2.105) must give identical values, for a_2, a_3, etc., . . . a_n.

A particular case of the problem just treated on a general level is the cantilever subject to equal vertical loads evenly spaced. Let

$$P_1 = P_2 = P_3 = \ldots. = P_n = P$$

and

$$L_1 = L_2 = L_3 = \ldots. L/n = s$$

Then

$$\sum_{i=1}^{i=r} P_i = rP$$

and

$$k_r = k\sqrt{r}, \text{ where } k = \left(\frac{P}{EI}\right)^{\frac{1}{2}}$$

The relationship between length, slope, and modulus is given by

$$\left.\begin{aligned} L_1 &= s = \frac{1}{k}\{K(p_1) - F[p_1, \sin^{-1}(\sin\tfrac{1}{2}\theta_2/p_1)]\}, \\ L_r &= s = \frac{1}{k\sqrt{r}}\{F[p_r, \sin^{-1}(\sin\tfrac{1}{2}\theta_r/p_r)] - \\ &\qquad - F[p_r, \sin^{-1}(\sin\tfrac{1}{2}\theta_{r+1}/p_r)]\}, \\ L_n &= s = \frac{1}{k\sqrt{n}}\{F[p_n, \sin^{-1}(\sin\tfrac{1}{2}\theta_n/p_n)] - \\ &\qquad - F[p_n, \sin^{-1}(0{\cdot}707/p_n)]\} \end{aligned}\right\} \quad (2.106)$$

There are n equations in (2.106). The remaining $n - 1$ equations are obtained as explained above. However, the fact that all forces are equal and that they are evenly spaced allows for some simplifications. This results in the following $n - 1$ equations:

$$\left.\begin{aligned} 2p_2^2 &= p_1^2 + \sin^2(\theta_2/2) \\ 3p_3^2 &= p_1^2 + \sin^2(\theta_2/2) + \sin^2(\theta_3/2) \\ \cdot &= \cdot\ \cdot\ \cdot\ \cdot\ \cdot\ \cdot\ \cdot\ \cdot\ \cdot\ \cdot \\ rp_r^2 &= p_1^2 + \sum_{k=2}^{r} \sin^2(\theta_k/2) \\ \cdot &= \cdot\ \cdot\ \cdot\ \cdot\ \cdot\ \cdot\ \cdot\ \cdot\ \cdot\ \cdot \\ np_n^2 &= p_1^2 + \sum_{k=2}^{n} \sin^2(\theta_k/2) \end{aligned}\right\} \quad (2.107)$$

Here again the assumed values for θ and the values of p as found from equations (2.106) must satisfy equations (2.107).

For the calculation of the deflection coordinates two types of equations will have to be considered. First take a portion with no point of contraflexion in it, say CD.

$$\left.\begin{aligned} x &= x_C + h_{n-1}(\cos\phi_{n-1} - \cos\phi) \\ y &= y_C + \frac{1}{k_{n-1}}[2E(p_{n-1}, \phi_{n-1}) - \\ &\qquad - F(p_{n-1}, \phi_{n-1}) + F(p_{n-1}, \phi) - \\ &\qquad\qquad - 2E(p_{n-1}, \phi)] \\ \text{and} \quad s_{n-1} &= L_n + \frac{1}{k_{n-1}}[F(p_{n-1}, \phi) - \\ &\qquad - F(p_{n-1}, \phi_{n-1})] \end{aligned}\right\} \quad (2.108)$$

where $\sin \phi = \dfrac{\sin (\theta/2)}{p_{n-1}}$ and x_C and y_C are the coordinates of point C (*Figure 2.14*). These coordinates can be obtained from equations similar to (2.108) by writing $\theta = \theta_n$, that is $\phi = \phi'_n$.

Different equations apply for portion DE since it has a point of contraflexion at K. For part DK one obtains

$$\left.\begin{aligned} x &= x_D + h_r(\cos\phi_{r2} - \cos\phi) \\ y &= y_D + \frac{1}{k_r}[2E(p_r, \phi_{r2}) - F(p_r, \phi_{r2}) + \\ &\qquad + F(p_r, \phi) - 2E(p_r, \phi)] \\ \text{and} \qquad s &= L_n + L_{n-1} + \frac{1}{k_r}[F(p_r, \phi) - F(p_r, \phi_{r2})] \end{aligned}\right\} \quad (2.109)$$

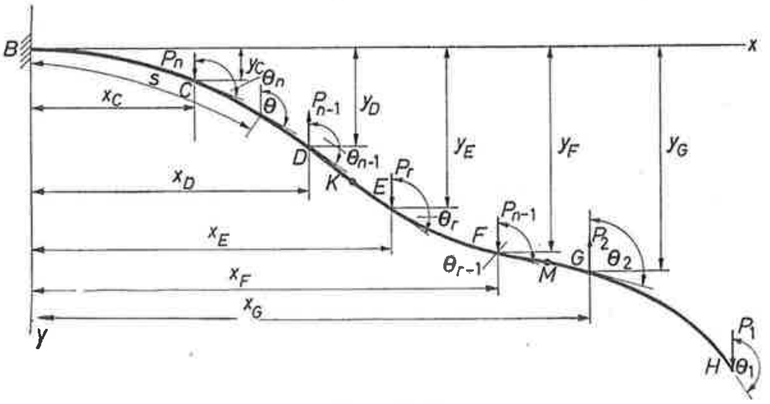

Figure 2.14

where $\sin \phi = \dfrac{\sin (\theta/2)}{p_r}$ and x_D and y_D are shown in *Figure 2.14*. For portion KE

$$\left.\begin{aligned} x &= x_K + h_r \cos\phi \\ y &= y_K + \frac{1}{k_r}[2E(p_r, \phi_{r1}) - F(p_r, \phi_{r1}) + \\ &\qquad + F(p_r, \phi) - 2E(p_r, \phi)] \\ \text{and} \qquad s &= L_n + L_{n-1} + s_K + \frac{1}{k_r}[K(p_r) - F(p_r, \phi)] \end{aligned}\right\} \quad (2.110)$$

where ϕ has the same meaning as for DK, and x_K, y_K and s_K can be found by substituting $\phi = \pi/2$ in equations (2.109).

The method outlined in this section can be further extended to solve any number of inclined forces by using inclined bases for the quadrants. The number of simultaneous equations remains $2n - 1$ for n inclined forces.

REFERENCES

[1] Bisshopp, K. E. and Drucker, D. C. Large deflections of cantilever beams, *Quart. appl. Math.* **3** (1945) 272

[2] Barten, H. J. On the deflection of a cantilever beam, *Quart. appl. Math.* **2** (1944) 168, and corrigenda in *Quart. appl. Math.* **3** (1945) 275

[3] Hummel, F. H. and Morton, W. B. On the large deflection of thin flexible strips and the measurement of their elasticity, *Phil. Mag. Ser. 7*, **4** (1927) 348

[4] Frisch-Fay, R. A new approach to the analysis of the deflection of thin cantilevers, *J. appl. Mech.* **28**, *Trans. ASME*, **83**, *Ser. E* (1961) 87

[5] Frisch-Fay, R. Large deflections of a cantilever under two concentrated loads, *J. appl. Mech.* **29**, *Trans. ASME*, **84**, *Ser. E* (1962)

[6] Frisch-Fay, R. Nonlinear bending of a cantilever under several concentrated loads, *Aust. J. appl. Sci.* **11** (1960) 233

3

BAR ON TWO SUPPORTS

3.1. Straight Bar on Unyielding Knife-edged Supports

The usual support of a statically determinate straight bar consists of a hinged and a roller support. The deflected shape of a rigid bar under these conditions is a very flat curve and, as it has been pointed out in section 1.1, the difference between chord length and arc length is of second order smallness. As a result, the conventional engineering analysis, while recognizing the usefulness of the roller support, considers the lateral movement of this support infinitesimal (*Figure 1.1*). In the nonlinear framework, on the other hand, the lateral movement of the roller support becomes finite. If a flexible bar is loaded at the centre by a vertical load P, the problem becomes identical with the one discussed in section 2.2 (for a non-symmetrical load see section 3.3).

An entirely different problem arises if A and B are fixed knife-edged supports and the bar assumes different lengths for different loads (*Figure 3.1*). It is easy to appreciate that by increasing P gradually the bar will sag more and more, requiring an increasing L and ψ_0.

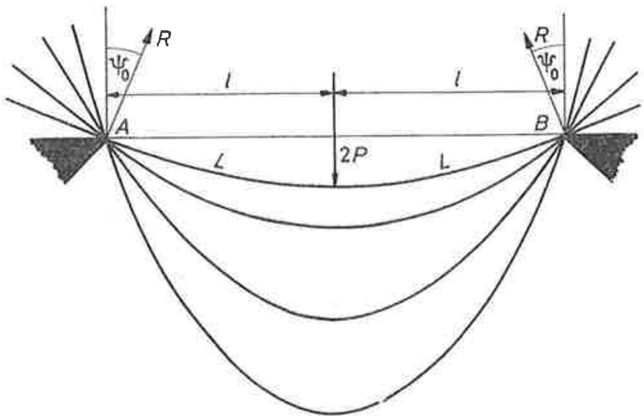

Figure 3.1

Let the distance between the supports be $2l$, the length of the bar $2L$, and let $2P$ be the load at the centre. Also, assume that the applied force is acting upward. We begin our investigations by neglecting the friction between the bar and the supports[1]. The reactions will then exert forces normal to the end tangent of the bar (*Figure 3.2*). The differential equation of the bar is

$$\frac{d\psi}{ds} = \frac{M}{EI} \tag{3.1}$$

where $M = P(l - x) + P \tan \psi_0 (y_{max} - y)$.

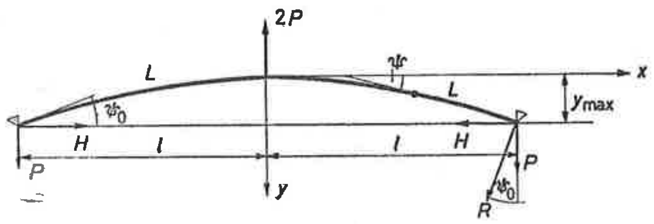

Figure 3.2

Taking the derivative of equation (3.1) with respect to s

$$\frac{d^2\psi}{ds^2} = -\frac{P}{EI}\frac{dx}{ds} - \frac{P}{EI}\tan\psi_0 \frac{dy}{ds} \tag{3.2}$$

Integrating,

$$\frac{1}{2}\left(\frac{d\psi}{ds}\right)^2 = -k^2 \sin\psi + k^2 \tan\psi_0 \cos\psi + C \tag{3.3}$$

From $\left(\frac{d\psi}{ds}\right)_{\psi=\psi_0} = 0, \quad C = 0,$

hence
$$\frac{d\psi}{ds} = k[2(\tan\psi_0 \cos\psi - \sin\psi)]^{\frac{1}{2}} \tag{3.4}$$

and
$$dy = \frac{\sin\psi \, d\psi}{k[2(\tan\psi_0 \cos\psi - \sin\psi)]^{\frac{1}{2}}} \tag{3.5}$$

We now introduce $\cos\phi = [\sin(\psi_0 - \psi)]^{\frac{1}{2}}$, $\cos\phi_0 = \sqrt{\sin\psi_0}$, and $p = \sin(\pi/4)$. It can be shown that by changing the variable from ψ

to ϕ, y/l and x/l can be expressed in terms of elliptic integrals. We obtain

$$\left.\begin{aligned} \frac{y}{l} &= \frac{\sqrt{2}\sin\psi_0\cos\phi - \cos\psi_0\,\Phi(p,\phi)}{\sqrt{2}\cos\psi_0\cos\phi_0 + \sin\psi_0\,\Phi(p,\phi_0)} \\ \frac{x}{l} &= \frac{\sqrt{2}\cos\psi_0\cos\phi + \sin\psi_0\,\Phi(p,\phi)}{\sqrt{2}\cos\psi_0\cos\phi_0 + \sin\psi_0\,\Phi(p,\phi_0)} \end{aligned}\right\} \tag{3.6}$$

where $\Phi(p,\phi) = F(p,\phi) - K(p) + 2E(p) - 2E(p,\phi)$

$$= 0{\cdot}8472 + F(p,\phi) - 2E(p,\phi)$$

and $\Phi(p,\phi_0) = 0{\cdot}8472 + F(p,\phi_0) - 2E(p,\phi_0)$

We also find that

$$l^2 = \frac{EI}{P}\cos\psi_0\left[\sqrt{2}\cos\psi_0\cos\phi_0 + \sin\psi_0\,\Phi(p,\phi_0)\right]^2 \tag{3.7}$$

The bar can go as far as $\psi_0 = \pi/2$ for, if $\psi_0 > \pi/2$, the vertical component of the reactions at A and B points in the same direction as the load $2P$, hence equilibrium becomes impossible. It follows from equations (3.5) and (3.6) that

$$\frac{y}{l} = \frac{(2\cos\psi)^{\frac{1}{2}}}{\Phi(p,0)} = 1{\cdot}6693\sqrt{\cos\psi} \tag{3.8}$$

and

$$\frac{x}{l} = \frac{\Phi(p,\phi)}{\Phi(p,0)} = 1{\cdot}1803\,\Phi(p,\phi) \tag{3.9}$$

From (3.7), Pl^2/EI can be expressed as a function of ψ_0. We find that $(Pl^2/EI)_{max} = 0{\cdot}834$ for $\psi_0 = 38{\cdot}301°$. The corresponding deflection is $y_{max}/l = 0{\cdot}4764$.

The functions $k^2l^2 = \Omega\,(\psi_0)$ and $y_{max}/l = \eta\,(\psi_0)$ are shown in *Figure 3.3*. The shape of the function Ω was expected from first principles. The load $2P$ is balanced by two vertical reactions, $P = R\cos\psi_0$ where R is the resultant reaction. By increasing the load more and more the bar will eventually assume a shape for which the vertical component (depending on a constantly decreasing $\cos\psi_0$) will no longer be sufficient to balance the load. When this happens, the bar will slip through between the supports. As seen from the graph, $k^2l^2 = \Omega(\psi_0)$, for every $P < P_{max}$ there are two ψ_0's. However, only one range is stable, as indicated on *Figure 3.3*. The behaviour of the function $\Omega(\psi_0)$ clearly shows that by giving the bar deflection an increment dy, the increment of the bar's strain energy is bigger than the work Pdy provided $P < P_{max}$, while in the unstable range the work Pdy is larger than the increment of the strain energy.

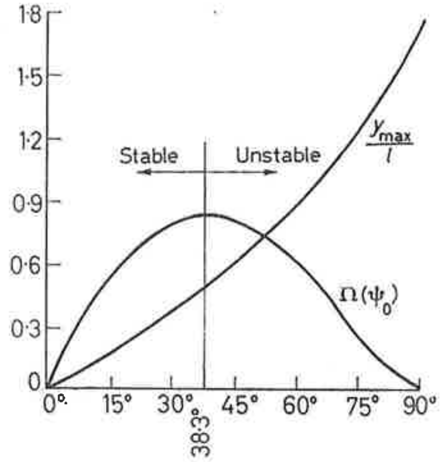

Figure 3.3 (From Gospodnetic[1])

This problem is, of course, in the province of large deflections. Within the framework of the small deflection theory this problem, while still nonlinear, can be approximated as follows. Consider a simply supported bar carrying $2P$ at the centre, subject to axial forces H, as shown in *Figure 3.4*. The deflection can be expressed by the fast converging series[2]

$$y = \frac{32\,Pl^3}{\pi^4 EI} \sum_{n=1,3,5}^{n=\infty} \left[n^2 \left(n^2 - \frac{4\,Hl^2}{\pi^2 EI} \right) \right]^{-1} \sin \frac{n\pi x}{2l} \qquad (3.10)$$

The condition for frictionless support on the knife edge stipulates

$$H = P \left(\frac{dy}{dx} \right)_{x=0} = Py_0'$$

After introducing the non-dimensional symbol,

$$\tau = \frac{4Pl^2}{\pi^2 EI}$$

equation (3.10), after one differentiation, reduces to

$$y_0' = \frac{4\tau}{\pi} \sum_{n=1,3,5}^{n=\infty} \frac{1}{n(n^2 - \tau y_0')} \tag{3.11}$$

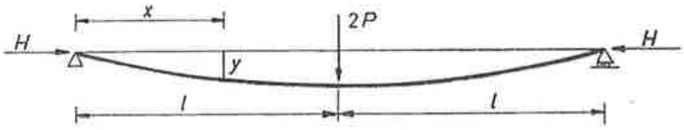

Figure 3.4

Taking the first term only of the series, we get

$$y_0' = \frac{4\tau}{\pi}\left(\frac{1}{1-\tau y_0'}\right) \text{ or, } y_0' = \frac{1}{2\tau} \pm \left(\frac{1}{4\tau^2} - \frac{4}{\pi}\right)^{\frac{1}{2}}$$

The derivative y_0' exists only as long as $1/4\tau^2 \geqslant 4/\pi$, otherwise no equilibrium is possible. We find the critical load from $\tau = \sqrt{\pi}/4$

hence $$P_{max} = \frac{\pi^2 EI\sqrt{\pi}}{16\, l^2} = \frac{1{\cdot}09}{l^2} EI \tag{3.12}$$

This is about 28 per cent higher than $0{\cdot}834\ EI/l^2$.

The same problem can also be analysed by making use of the formulae derived in section 2.6. Consider the right-hand side of the bar in *Figure 3.2* clamped at the centre (*Figure 3.5*). We note that whatever the shape of this cantilever may be, the inclined load R

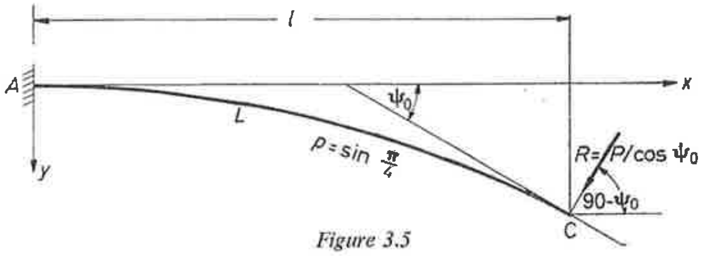

Figure 3.5

is always normal to the end tangent[3]. It follows from equation (1.15) that the modulus $p = \sin(\pi/4)$. Also, from equation (2.66) we find that the horizontal projection

$$l = \frac{1}{k}\{\cos(\pi/2 - \psi_0)\,[F(p, m) - K(p) + 2E(p) - $$
$$- 2E(p, m)] + 2p \sin(\pi/2 - \psi_0) \cos m\}$$

where

$$p = \sin(\pi/4),\ m = \sin^{-1}\left[\frac{\sin[(\pi/2 - \psi_0)/2]}{p}\right], \text{ and } k = \left(\frac{P}{EI\cos\psi_0}\right)^{\frac{1}{2}}$$

After some rearranging,

$$l = \frac{1}{k}\{\sin\psi_0\,\Phi(\pi/4, m) + \sqrt{2}\cos\psi_0\cos m\} \tag{3.13}$$

Here $m = \sin^{-1}[\cos(\psi_0/2) - \sin(\psi_0/2)]$ and k is the same as before. Equation (3.13) can be solved for ψ_0 and hence

$$L = \frac{1}{k}[K(\pi/4) - F(\pi/4, m)] \tag{3.14}$$

also, $$y_{max} = y_C = \frac{1}{k}[\sqrt{2}\sin\psi_0\cos m + \cos\psi_0\,\Phi(\pi/4, m)] \tag{3.15}$$

If P is expressed as a function of ψ_0, equation (3.7) will result. This follows from $\cos\phi_0 = \cos m = (1 - \sin^2 m)^{\frac{1}{2}} = (\sin\psi_0)^{\frac{1}{2}}$.

This analysis has been based on frictionless supports. When friction is taken into account the reactions consist of normal and tangential components and are inclined at an angle $\alpha = \pi/2 - (\psi_0 - \lambda)$ to the horizontal (*Figure 3.6*), where $\mu = \tan\lambda$ is the coefficient of friction. The vertical component of the

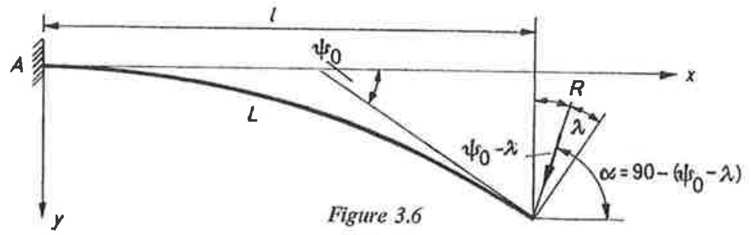

Figure 3.6

reaction R must balance P, hence $R = P/\cos(\psi_0 - \lambda)$. The same equations may be used again with the replacement of terms $(\pi/2 - \psi_0)$ by terms $[\pi/2 - (\psi_0 - \lambda)]$. Thus,

$$l = \frac{1}{k}[\sin(\psi_0 - \lambda)\,\Phi(p, n) + 2p\cos(\psi_0 - \lambda)\cos n] \qquad (3.16)$$

where $$k = \left[\frac{P}{EI\cos(\psi_0 - \lambda)}\right]^{\frac{1}{2}}, \quad p = \sin(\pi/4 + \lambda/2),$$

and $$n = \sin^{-1}\left[\frac{\cos[(\psi_0 - \lambda)/2] - \sin[(\psi_0 - \lambda)/2]}{\cos(\lambda/2) + \sin(\lambda/2)}\right]$$

The relationship between P and ψ_0 can be obtained by expressing P from equation (3.16)[3],

$$P = \Theta(\psi_0, \lambda) = \frac{EI}{l^2}\cos(\psi_0 - \lambda)[\sin(\psi_0 - \lambda)\,\Phi(p, n) + \\ + 2p\cos(\psi_0 - \lambda)\cos n]^2 \qquad (3.17)$$

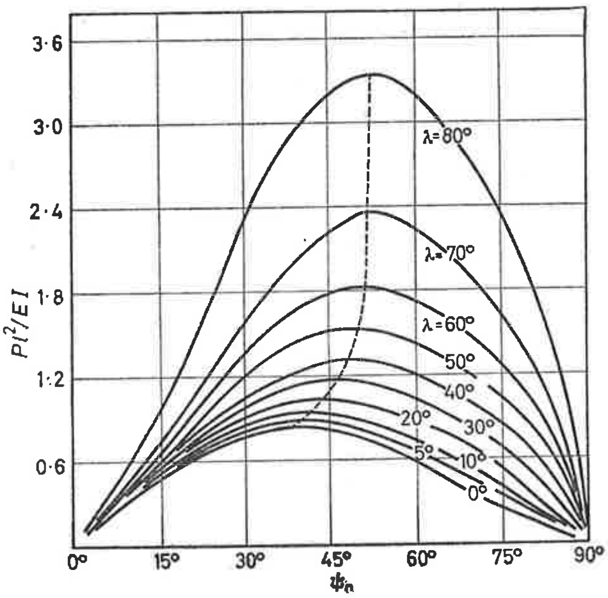

Figure 3.7

In *Figure 3.7* the function $Pl^2/EI = \Theta(\psi_0, \lambda)$ has been presented graphically for different values of λ. The dotted line connecting the peak values of the separate curves gives the relationship between the critical load P_{max} and the coefficient of friction in the form of $P_{max} = \beta\ EI/l^2$. The values of β are tabulated below.

Table 2

λ	0	5	10	20	30	40	50	60	70	80
β	0·8345	0·8848	0·9347	1·046	1·174	1·33	1·532	1·821	2·377	3·349

With the help of *Table 2* the friction coefficient between different metals, lubricated or otherwise, can be found. A simple experiment, such as shown in *Figure 3.8*, has to be carried out to measure the critical load of the bar, that is, the force P_{max} that will cause the bar to slip through between the supports. Three different elastic shapes are shown in *Figure 3.8*. The loads in the upper and lower positions are identical and less than P_{max}. The centre position shows the shape when the bar is about to slip under P_{max}.

The elastic shape of a bar resting on frictionless supports can also be analysed with the help of a circular arc whose length is identical with the length of the deflected shape $2L$. The circular arc in *Figure 3.9* is assumed to satisfy this condition. Let σ be half of the central angle and R the radius of the circle[4]. It can be shown that within a

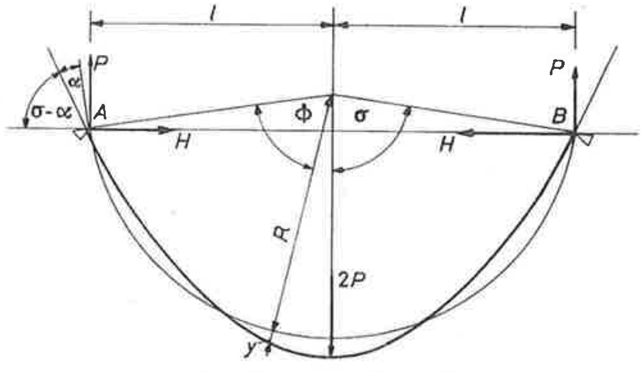

Figure 3.9 (From Sonntag[4])

certain range of deflections, the deviation of the elastic shape from the circle is of the same order as the difference between the straight and the loaded bar in the linear theory. Hence, if the radius of the

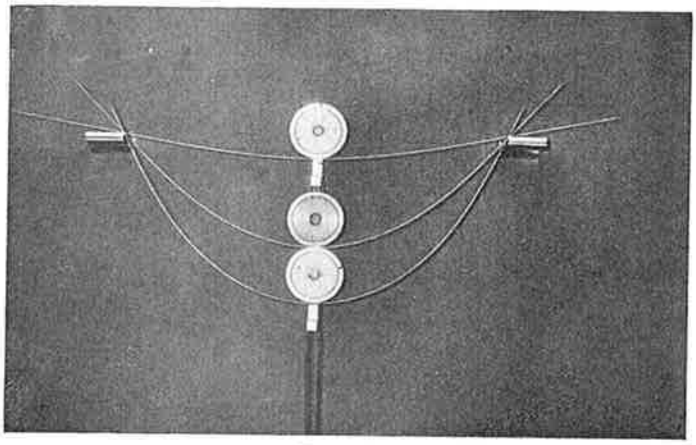

Figure 3.8

Facing page 80]

circle of equal length is known, the radial dimensions y (*Figure 3.9*) can be calculated with the help of linear differential equations.

The relationship between P and H is

$$\frac{H}{P} = \frac{(\Lambda_1 - \Lambda_2)/k^2l^2}{\Lambda_3}$$

where

$$k^2l^2 = \frac{Pl^2}{EI}$$

$$\Lambda_1 = \sin^2\sigma(\sin\sigma - \sigma\cos\sigma)$$
$$\Lambda_2 = \cos\sigma - \tfrac{3}{4}\cos 2\sigma - \tfrac{1}{2}\sigma\sin 2\sigma - \tfrac{1}{4}$$
$$\Lambda_3 = \tfrac{1}{2}\sigma\cos 2\sigma - \tfrac{3}{4}\sin 2\sigma + \sigma$$

There is also $H/P = \tan(\sigma - \alpha)$ where α is the difference between the end tangents belonging to the circle and the deflection line respectively. The combination of the two previous equations leads to

$$k^2l^2 = \frac{1}{\Lambda_3\tan(\sigma - \alpha) + \Lambda_2} \tag{3.18}$$

The angle α is the result of the rotation of the circular bar at the supports due to the applied load. Hence

$$\alpha = -\frac{R}{EI}\int_0^{\sigma} M_\phi\, d\phi$$

where M_ϕ is the bending moment expressed in terms of the angle ϕ. We have

$$M_\phi = -\frac{EI}{R} + PR[\sin\sigma - \sin(\sigma - \phi)] + HR[\cos(\sigma - \phi) - \cos\sigma]$$

Introducing the symbols

$$\Lambda_4 = \frac{\sigma\sin\sigma + \cos\sigma - 1}{\sin^2\sigma}$$

and

$$\Lambda_5 = \frac{\sin\sigma - \sigma\cos\sigma}{\sin^2\sigma}$$

we find

$$k^2l^2 = \frac{\sigma - \alpha}{\Lambda_4 + \Lambda_5\tan(\sigma - \alpha)} \tag{3.19}$$

The angle α is sufficiently small for writing $\tan \alpha \approx \alpha$, hence

$$\tan(\sigma - \alpha) = \frac{\tan \sigma - \alpha}{1 + \alpha \tan \sigma}$$

Combining this expression with equations (3.18 and 19) we get

$$\alpha = c + \sqrt{(c^2 + d)} \tag{3.20}$$

where $$c = \frac{\cos 2\sigma + \sigma \sin \sigma - (1 - \sigma^2/2)\cos\sigma}{3\sigma\cos\sigma - \sin 2\sigma - \sin\sigma}$$

and $$d = \frac{(2 - \sigma^2)\sin\sigma - \sin 2\sigma}{3\sigma\cos\sigma - \sin 2\sigma - \sin\sigma}$$

By assuming values for σ we find through equations (3.20) and (3.19) or (3.18) the corresponding k^2l^2 values, hence P becomes known. The equation of the deflected shape (measured radially from the circle) is

$$\frac{d^2 y}{d\phi^2} + y = -\frac{R^2}{EI} M_\phi \tag{3.21}$$

Introducing $$\frac{PR^3}{EI} = p, \quad \frac{HR^3}{EI} = h$$

$$t_0 = R + p \sin\sigma - h\cos\sigma$$

$$t_1 = p\sin\sigma - h\cos\sigma$$

$$t_2 = p\cos\sigma + h\sin\sigma$$

the solution of (3.21) is

$$y = D\sin\phi + t_0\cos\phi - t_0 + \tfrac{1}{2}t_1\phi\sin\phi + \tfrac{1}{2}t_2\phi\cos\phi \tag{3.22}$$

in which, from $$(y')_{\phi=\sigma} = 0,$$

$$D = -\frac{1}{\cos\sigma}[R\sin\sigma + \tfrac{1}{2}p\cos 2\sigma + \tfrac{1}{2}h(\sin 2\sigma - \sigma)]$$

These formulae give results within 1 per cent of the true value if $k^2l^2 \leqslant 0{\cdot}3$.

A graphical method for the derivation of the elastic shape of the frictionless bar has been suggested by Biezeno[5]. The method can be extended to a bar whose flexural rigidity varies symmetrically about the centre.

3.2. Flexible Bar Fixed at both Ends

The bar with uniform *EI*, fixed at both ends and subject to a vertical load at the centre is onefold statically indeterminate (*Figure 3.10(a)*). The bending moment at the ends *A* and *B* is $-Pl/2$ and at *C*, $M_C = +Pl/2$. Strictly speaking, these results apply only to a bar shown in *Figure 3.10(b)* where the joint at *B* is such that it will resist bending moment and shear force but will yield without resistance to an axial force. The bending moments and deflections of this bar are in a linear relationship with the load. However, this linear relationship is not present in a bar that is restrained at *A* and *B* with respect to horizontal movements[6]. The conventional theory does not take into account that the deflected curve is longer than the straight line between *A* and *B*. This elongation develops axial forces in the bar in addition to shear forces and bending moments.

It has been pointed out in section 1.1 that the approximate formula for the curvature cannot be used for flexible bars. In this problem, however, the emphasis is not on the deflections being *large* due to the flexibility of the bar but rather on the presence of longitudinal forces. The deflections of the bar in *Figure 3.10(a)* are, in fact, smaller than those of the bar in *Figure 3.10(b)*. Large deflections would mean a big difference between $2l$ and the length of the elastic line $2L$, hence a large S force would develop. In order to remain within the elastic range, S cannot exceed a certain value which in turn limits the deflection δ too. Therefore the problem will be analysed by using the approximate expression for the curvature.

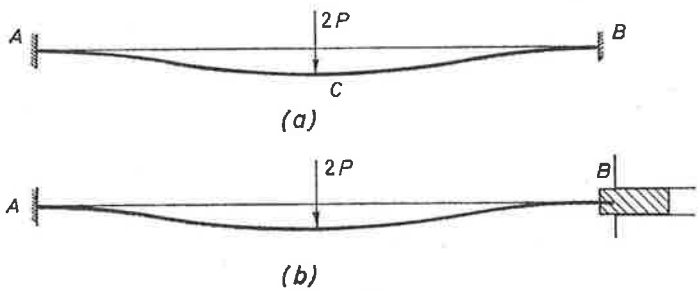

Figure 3.10

Consider the bar in *Figure 3.11*. For reasons of symmetry only the right-hand half will be analysed. The bending moment at a point (x, y) is

$$M = EI\frac{d^2y}{dx^2} = Sy + M_0 - P(l - x) \tag{3.23}$$

where M_0 is the fixing moment (clockwise) at E. The solution of (3.23) is

$$y = C_1 \cosh tx + C_2 \sinh tx + Ax + B \tag{3.24}$$

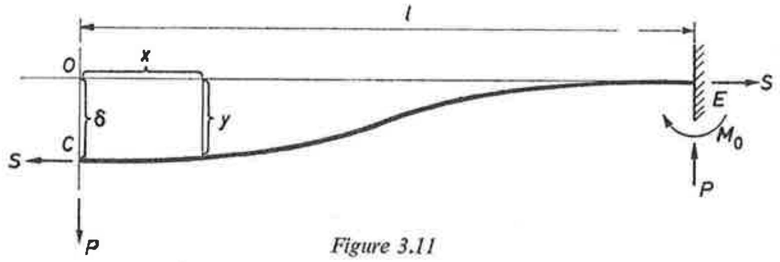

Figure 3.11

where C_1 and C_2 have to be found from boundary conditions. Substituting (3.24) in (3.23) we get

$$EI\, C_1 t^2 \cosh tx + EI\, C_2 t^2 \sinh tx = S\, C_1 \cosh tx + S\, C_2 \sinh tx + \\ + S\,Ax + S\,B + P\,x + M_0 - Pl \tag{3.25}$$

Comparing the coefficients of x in (3.25), we find

$$A = -\,P/S,\ B = (Pl - M_0)/S, \text{ and } t = \sqrt{(S/EI)} \tag{3.26}$$

From the boundary conditions

$$\left(\frac{dy}{dx}\right)_{x=0} = 0 \quad \text{and} \quad \left(\frac{dy}{dx}\right)_{x=l} = 0$$

$$C_1 = \frac{P}{S}\left(\frac{1 - \cosh tl}{t \sinh tl}\right) = -\frac{P}{tS}\tanh(tl/2)$$

and $$C_2 = -\frac{A}{t} = \frac{P}{tS}$$

To find the unknown M_0 we note that $(y)_{x=l} = 0$. Therefore,

$$-\frac{P}{tS}\tanh(tl/2)\cosh tl + \frac{P}{tS}\sinh tl - \frac{M_0}{S} = 0$$

and $$M_0 = -\frac{P}{t}\left[\frac{\cosh tl - 1}{\sinh tl}\cosh tl - \sinh tl\right]$$

$$= \frac{P}{t}\tanh(tl/2) \tag{3.27}$$

The equation of the elastic line can be had by inserting A, B, C_1, C_2, and M_0 in equation (3.24), giving

$$y = \frac{P}{St}\{\sinh tx - \tanh(tl/2)(1 + \cosh tx)\} + \frac{P}{S}(l - x) \tag{3.28}$$

At $x = 0$ the deflection becomes $y_{\max} = \delta$, and

$$\delta = \frac{Pl^3}{4EI}\,\eta(u) \tag{3.29}$$

where $$\eta(u) = \frac{u - \tanh u}{u^3}, \quad \text{and} \quad u = tl/2 \tag{3.30}$$

If $S = 0$, $t = 0$, and hence

$$\eta(u) = \lim_{u=0}\left(\frac{u - \tanh u}{u^3}\right) = \frac{1}{3}$$

It follows that $$\delta = \frac{Pl^3}{12\,EI}$$

which is the deflection according to the conventional theory (*Figure 3.10(b)*).

Equation (3.29) contains the unknown u which is a function of the equally unknown t. Therefore, to find δ, a further relationship is necessary. This can be found from the longitudinal expansion of the bar during deflection. It will be observed that for all previous problems the bar remained inextensible during deflection and this condition has supplied the equation necessary to evaluate the modulus of the shape.

The length of the curve $y = f(x)$ is

$$s = \int_0^l \left[1 + \left(\frac{dy}{dx}\right)^2\right]^{\frac{1}{2}} dx$$

As mentioned at the beginning of this article we are concerned with small deflections only, hence dy/dx is small compared with unity. Therefore,

$$s \approx \int_0^l \left[1 + \tfrac{1}{2}\left(\frac{dy}{dx}\right)^2\right] dx = l + \tfrac{1}{2}\int_0^l \left(\frac{dy}{dx}\right)^2 dx$$

The change in length is

$$\Delta l = s - l = \tfrac{1}{2}\int_0^l \left(\frac{dy}{dx}\right)^2 dx \tag{3.31}$$

Since the slope is small the axial force S can be considered constant along the bar. Hence

$$S = A_c E \frac{\Delta l}{l} = \frac{A_c E}{2l} \int_0^l \left(\frac{dy}{dx}\right)^2 dx \tag{3.32}$$

where A_c is the cross-sectional area of the bar.

Taking the first derivative of (3.24) and squaring it, substitution in (3.32) leads to

$$S = \frac{A_c E}{2l} \Big\{ (C_1^2 + C_2^2) \frac{t}{4} \sinh 2tl + (C_2^2 - C_1^2) t^2 \, l/2 + \\ + C_1 C_2 \, t (\cosh 2tl - 1)/2 + A^2 \, l + \\ + 2AC_1 (\cosh tl - 1) + 2AC_2 \sinh tl \Big\}$$

Introducing C_1, C_2, and A in this expression,

$$S^3 = \frac{A_c EP^2}{2} \left\{ \frac{1}{4tl} \xi(u) - \tfrac{1}{2} \tanh^2 u + \frac{3}{2} \right\} \tag{3.33}$$

where $\xi(u) = \tanh^2 (tl/2) \sinh 2tl + \sinh 2tl + 2 \tanh (tl/2) -$
$- 2 \tanh (tl/2) \cosh 2tl + 8 \tanh (tl/2) \cosh tl -$
$- 8 \tanh (tl/2) - 8 \sinh tl$

Since $\tanh (tl/2) = \dfrac{\cosh tl - 1}{\sinh tl} = \dfrac{\sinh tl}{\cosh tl + 1}$

$\xi(u)$ reduces to $-12 \tanh (tl/2)$.

Hence $$S^3 = \frac{A_c EP^2}{2} \left[\frac{3}{2} - \frac{1}{2} \tanh^2 u - \frac{3}{2} \frac{\tanh u}{u} \right]$$

and, since $S = EIt^2$,

$$P = \left(\frac{2S^3}{A_c E} \right)^{\frac{1}{2}} \left(\frac{3}{2} - \frac{1}{2} \tanh^2 u - \frac{3}{2} \frac{\tanh u}{u} \right)^{-\frac{1}{2}} \tag{3.34}$$

Equation (3.34) can be written as

$$P = \frac{8EI(2I/A_c)^{\frac{1}{2}}}{l^3} u^3 \left(\frac{3}{2} - \frac{1}{2} \tanh^2 u - \frac{3}{2} \frac{\tanh u}{u} \right)^{-\frac{1}{2}}$$

Combining this expression for P with equation (3.30)

$$\delta = 2\left(\frac{2I}{A_c}\right)^{\frac{1}{2}}(u - \tanh u)\left(\frac{3}{2} - \frac{1}{2}\tanh^2 u - \frac{3}{2}\frac{\tanh u}{u}\right)^{-\frac{1}{2}} \tag{3.35}$$

To find δ in terms of P we first assume values for u and calculate P from equation (3.34). The same value of u has to be used in equation (3.35) to find the deflection caused by P. These equations also show that there is no linearity between P and δ.

The bending moment at any point (x, y) may be calculated from

$$M_x = Sy + Px + M_0 - Pl$$

With equations (3.27) and (3.28) the bending moment reduces to

$$M_x = \frac{P}{t}[\sinh tx - \tanh u \cosh tx] \tag{3.36}$$

It follows at once from equation (3.36) that

$$(M)_{x=l/2} = 0$$

At $x = l$ the bending moment is

$$M_l = \frac{P}{t}[\sinh tl - \tanh u\,(2\cosh^2 u - 1)] = \frac{P}{t}\tanh u = M_0$$

To find the maximum stress in the bar, we superimpose $+\ S/A_c$ on a varying stress due to the bending moment. Since the maximum bending moment is M_0 we have at point E

$$f_{\max} = \frac{M_0}{Z} + \frac{S}{A_c} = \frac{Pl}{2Z}\frac{\tanh u}{u} + \frac{4EI}{A_c l^2}u^2$$

Consider now a bar with a rectangular cross section. If b is the width of the bar and h its depth, the maximum stress becomes

$$\begin{aligned} f_{\max} &= \frac{2Eh^2}{l^2\sqrt{6}}u^2\tanh u\left(\frac{3}{2} - \frac{1}{2}\tanh^2 u - \frac{3}{2}\frac{\tanh u}{u}\right)^{-\frac{1}{2}} + \frac{1}{3}E\left(\frac{h}{l}\right)^2 u^2 \\ &= \frac{1}{3}E\left(\frac{h}{l}\right)^2 u^2\left[1 + \sqrt{6}\tanh u\left(\frac{3}{2} - \frac{1}{2}\tanh^2 u - \frac{3}{2}\frac{\tanh u}{u}\right)^{-\frac{1}{2}}\right] \end{aligned} \tag{3.37}$$

The first term in the bracket is the contribution of the longitudinal force to the total stress and the second term is the share of the bending moment.

If $t = (S/EI)^{\frac{1}{2}} = \infty$, the second term tends to $\sqrt{6}$, hence the two stresses are in the ratio $1 : \sqrt{6}$. As t decreases, the share of the bending moment becomes larger and larger and if t tends to zero (very rigid bar), the effect of the axial force gradually disappears. It follows from the discussion that the value $\sqrt{6}$ in the second term of the bracket in (3.37) applies to rectangular cross-sections only.

As an example let us investigate a flat spring fixed at both ends and subject to $2P$ load at the centre. The length of the spring, $2l = 6$ in., and the cross-section is 0·25 by 0·02 in. The deflection δ for different values of P is required. The properties of the spring are $I = \frac{1}{6} \times 10^{-6}$ in.^{4}, $A_c = 5 \times 10^{-3}$ in.^{2}, and $E = 3 \times 10^7$ lb/in^2. We select for $u = tl/2$ the values $\frac{1}{2}$, 1, $1\frac{1}{2}$ and 2. Substituting these in (3.34, 35, and 37) we get P, δ and $f_{\max}$. The horizontal force $S = Elt^2 = 4EIu^2/l^2 = 2{\cdot}2\ u^2$. The deflections and stresses are represented in *Figure 3.12* as a function of P. The horizontal force is given too. Also, as a comparison, the deflections and stresses calculated from the conventional theory are shown by the dotted line.

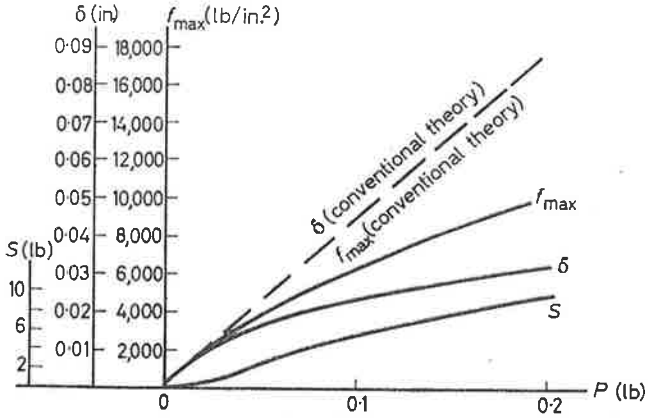

Figure 3.12

If, instead of a symmetrically placed concentrated load $2P$, a uniformly distributed load w acts on the bar in *Figure 3.11*, the basic differential equation to be solved is

$$M = EI\frac{d^2y}{dx^2} = Sy + M_0 - \tfrac{1}{2}w(l^2 - x^2) \qquad (3.38)$$

The particular solution of (3.38) which satisfies the boundary conditions relevant to the case is

$$y = \frac{wl}{St \sinh 2u} \cosh tx + \frac{(l^2 - x^2)}{2S} - \frac{wl}{St} \coth 2u \qquad (3.39)$$

where $\qquad t = (S/EI)^{\frac{1}{2}}, \quad \text{and} \quad u = tl/2.$

The fixed end moment is

$$M_0 = wl^2 \left(\frac{\coth 2u}{2u} - \frac{1}{4u^2} \right) \qquad (3.40)$$

The deflection at C is obtained by putting $x = 0$ in equation (3.39). Accordingly,

$$\delta = \frac{wl^4}{8EI} \frac{u - \tanh u}{u^3} = \frac{wl^4}{8EI} \eta(u) \qquad (3.41)$$

The function $\eta(u)$ is identical for both the concentrated load and the distributed load. For a rigid bar $S = t = 0$, hence $u = 0$. These values change equations (3.40) and (3.41) into

$$M_0 = \frac{wl^2}{3} \quad \text{and} \quad \delta = \frac{wl^4}{24EI} \quad \text{respectively.}$$

Both results are in agreement with the conventional analysis. From

$$S = A_c E \frac{\Delta l}{l} = \frac{A_c E}{2l} \int_0^l \left(\frac{dy}{dx} \right)^2 dx$$

we find $\quad S^3 = \dfrac{w^2 l^2 A_c E}{4} \left[\dfrac{2}{3} + \dfrac{1}{u^2} - \dfrac{3 \coth 2u}{2u} - \dfrac{1}{\sinh^2 2u} \right]$

Since $S = EIt^2$, this equation reduces to

$$wl^4 = 16 EIr_g u^3 \left(\frac{2}{3} - \frac{3 \coth 2u}{2u} - \frac{1}{\sinh^2 2u} + \frac{1}{u^2} \right)^{-\frac{1}{2}} \qquad (3.42)$$

where $r_g = (I/A_c)^{\frac{1}{2}}$ = radius of gyration in the plane of bending. Combining equations (3.41) and (3.42),

$$\delta = 2r_g (u - \tanh u) \left(\frac{2}{3} - \frac{3 \coth 2u}{2u} - \frac{1}{\sinh^2 2u} + \frac{1}{u^2} \right)^{-\frac{1}{2}} \qquad (3.43)$$

To find $\delta = \phi(w)$, different values of t have to be assumed first and w and δ found from (3.42) and (3.43) respectively.

The bending moment at a point (x, y) is

$$M_x = wl^2\left[\frac{\cosh tx}{2u\sinh 2u} - \frac{1}{4u^2}\right] \tag{3.44}$$

while at the centre of the bar

$$M_C = wl^2\left[\frac{1}{2u\sinh 2u} - \frac{1}{4u^2}\right] \tag{3.45}$$

The maximum tensile stress at E is

$$f_{\max} = \frac{wl^2}{Z}\left[\frac{\coth 2u}{2u} - \frac{1}{4u^2}\right] + \frac{EIt^2}{A_c}$$

In a bar having a rectangular cross section of width b and depth h, we find

$$f_{\max} = \frac{1}{3}E\left(\frac{h}{l}\right)^2 u^2\left[1 + \sqrt{12}(\coth 2u - 1/2u) \times \times\left(\frac{2}{3} - \frac{3\coth 2u}{2u} - \frac{1}{\sinh^2 2u} + \frac{1}{u^2}\right)^{-\frac{1}{2}}\right] \tag{3.46}$$

The first term in the bracket is the share of the longitudinal force to the total stress and the second term is the bending moment's contribution. If $t = \infty$ (very flexible bar), the second term tends to $3\sqrt{2}$, hence the two stresses are in the ratio $1 : 3\sqrt{2}$. With the decrease of t the influence of the bending moment becomes dominant.

When the bar was subject to $2P$ load at the centre the point of contraflexure was in a constant position ($x_0 = l/2$); this is not the case now. By setting equation (3.44) equal to zero, we obtain

$$x_0 = \frac{1}{t}\cosh^{-1}\left[\frac{\sinh 2u}{2u}\right] \tag{3.47}$$

As a numerical example of the case just treated let us investigate the behaviour of a flat spring fixed at both ends and subject to dead weight only. The spring has a cross-section of 0·25 by 0·02 in., is placed flat, and is $2l = 20$ in. long. With $E = 3 \times 10^7$ lb/in.^{2}, the flexural rigidity is $EI = 5$ lb/in^2. There is also $w = 0{\cdot}00142$ lb/in., and $r_g = 0{\cdot}00577$ in. The parameter t can be found by solving (3.42) for u. This equation is satisfied by $u = 2{\cdot}43$, hence $t = 0{\cdot}486$. The tensile force in the spring follows from $S = EIt^2 = 1{\cdot}161$ lb. To find the deflection at the centre, equation (3.41) or (3.43) may be applied; $\delta = 0{\cdot}0358$ in. According to the conventional approach which neglects the presence of tension, this deflection would be $\delta' = 0{\cdot}1183$ in. The maximum stress at the fixed end can be calculated from (3.46) and we find $f_{max} = 1620$ lb/in². According to the approximate analysis this stress would have risen to $f'_{max} = 2840$ lb/in². The position of the point of contraflexion is, from (3.47), $x_0 = 6{\cdot}725$ in. from the centre.

3.3. Simply Supported Bar with a Non-symmetrical Load

Consider a simply supported bar, ACB (*Figure 3.13*), subject to a force P at C. The length of the bar is $L_a + L_b = L$ and the load is applied at a distance L_a from the left support. The bar has one roller support and P acts upward. In the elementary theory, equations are set up for parts AC and CB, and the constants of integration found from $M_A = M_B = 0$ and from the fact that at C both the deflections and the slopes of the two parts are identical. The difficulty in our case is that owing to the unknowns a and b the reactions are functions of the deflected shape.

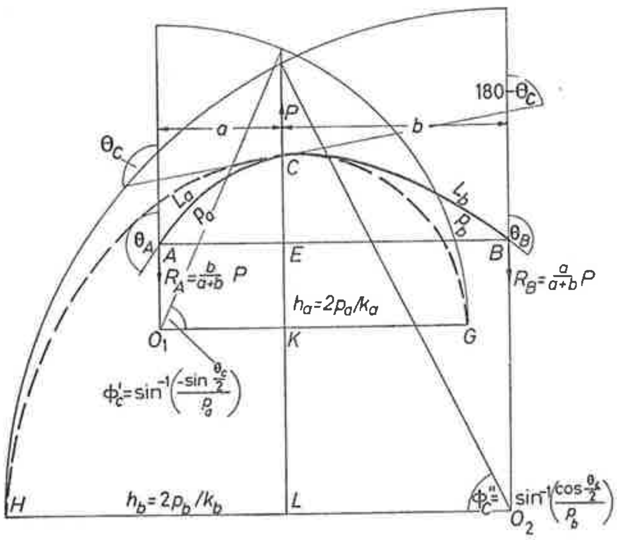

Figure 3.13

Making use of the principle of elastic similarity we transform the bar into two basic struts. The first strut, ACG, is fixed at G, carries a load $R_A = bP/(a+b)$ at A and its slope at C is θ_C. The shape is governed by the modulus p_a and we have for the length L_a,

$$L_a = \frac{1}{k_a}\left\{K(p_a) - F\left[p_a, \sin^{-1}\left(\frac{\sin(\theta_C/2)}{p_a}\right)\right]\right\} \tag{3.48}$$

where $$k_a = \left(\frac{bP}{EI(a+b)}\right)^{\frac{1}{2}}$$

The radius of the auxiliary circle belonging to strut ACG is $h_a = 2p_a/k_a$. As seen from *Figure 3.13*, $a = h_a \cos \phi'$. From

$$\sin \phi'_C = \frac{\sin(\theta_C/2)}{p_a}$$

the horizontal projection of L_a,

$$a = \frac{2}{k_a}[p_a^2 - \sin^2(\theta_C/2)]^{\frac{1}{2}} \tag{3.49}$$

Turning now to the second strut BCH, we note that it is fixed at H and is acted upon by the vertical load $R_B = aP/(a+b)$ at B. For the length of segment CB we write

$$L_b = \frac{1}{k_b}\left\{K(p_b) - F\left[p_b, \sin^{-1}\left(\frac{\cos(\theta_C/2)}{p_b}\right)\right]\right\} \tag{3.50}$$

where $k_b = \left(\frac{aP}{EI(a+b)}\right)^{\frac{1}{2}}$ and p_b is the modulus of the shape.

The horizontal projection of L_b is found from

$$b = \frac{2}{k_b}[p_b^2 - \cos^2(\theta_C/2)]^{\frac{1}{2}} \tag{3.51}$$

The reason for using $\sin^2(\theta_C/2)$ for strut ACG and $\cos^2(\theta_C/2)$ in the case of the second strut is that the slope of the first strut is θ_C while for strut BCH the slope is $\pi - \theta_C$ (*Figure 3.13*). Hence

$$\sin \phi''_C = \frac{\sin[\pi - (\theta_C/2)]}{p_b} = \frac{\cos(\theta_C/2)}{p_b}$$

For the solution of the unknowns a, b, p_a, p_b and θ_C we have, so far, four equations. A fifth equation can be found by noting that the deflection of C, CE, is the same whether derived from strut ACG or from strut BCH. Therefore,

$$CE = KC - EK = LC - LE \tag{3.52}$$

Since from (1.20) $KC - EK = q/k_a$ and $LC - LE = t/k_b$,

$$\frac{q}{t} = \frac{k_a}{k_b} \tag{3.53}$$

where $$q = \Phi\left[p_a, \sin^{-1}\left(\frac{\sin(\theta_C/2)}{p_a}\right)\right]$$

and $$t = \Phi\left[p_b, \sin^{-1}\left(\frac{\cos(\theta_C/2)}{p_b}\right)\right]$$

There is also $$k_a^2 + k_b^2 = k^2$$

in which $$k = (P/EI)^{\frac{1}{2}}$$

If, therefore, we find an angle α such that

$$\tan\alpha = \frac{k_a}{k_b} = \left(\frac{b}{a}\right)^{\frac{1}{2}}$$

we get $$k_a = k\sin\alpha \tag{3.54}$$

and $$k_b = k\cos\alpha$$

This enables us to reduce the number of equations from five to four since the unknowns a and b can be replaced by the single unknown α. Hence our problem rests with the solution of the following simultaneous equations:

$$L_a = \frac{1}{k\sin\alpha}\left\{K(p_a) - F\left[p_a, \sin^{-1}\left(\frac{\sin(\theta_C/2)}{p_a}\right)\right]\right\} \tag{3.55}$$

$$L_b = \frac{1}{k\cos\alpha}\left\{K(p_b) - F\left[p_b, \sin^{-1}\left(\frac{\cos(\theta_C/2)}{p_b}\right)\right]\right\} \tag{3.56}$$

$$\frac{q}{t} = \tan\alpha \tag{3.57}$$

$$\tan\alpha = \left(\frac{p_b^2 - \cos^2(\theta_C/2)}{p_a^2 - \sin^2(\theta_C/2)}\right)^{\frac{1}{2}} \tag{3.58}$$

Regarding the coordinates of the elastic line, for part AC we adopt AE as the x-axis and the origin of the x and y axes will be at A. We have

$$x = \frac{2}{k_a}\left[p_a^2 - \sin^2(\theta/2)\right]^{\frac{1}{2}} \tag{3.59}$$

and

$$y = \frac{1}{k_a}\Phi\left[p_a, \sin^{-1}\left(\frac{\sin(\theta/2)}{p_a}\right)\right]$$

for values $\theta_A < \theta < \theta_C$

where $\theta_A = 2\sin^{-1} p_a$

For part BC the coordinate system will be similar, excepting x will begin at B. There is

$$x = \frac{2}{k_b}\left[p_b^2 - \cos^2(\theta/2)\right]^{\frac{1}{2}}$$

and

$$y = \frac{1}{k_b}\Phi\left[p_b, \sin^{-1}\left(\frac{\cos(\theta/2)}{p_b}\right)\right] \tag{3.60}$$

for values $\theta_C < \theta < \theta_B$

where $\theta_B = 2\sin^{-1} p_b$

As an example take a flexible bar 104·6 in. long with a cross-section of 1·0 by 0·05 in. The bar is simply supported and carries a vertical load $P = 0{\cdot}5$ lb at 40 in. from the left support. The deflection under the load is required.

With $E = 3 \times 10^7$ lb/in.^{2}, $k = 1/25$. Also, $L_a = 40$ and $L_b = 64{\cdot}6$. Substituting these values in equations (3.55–58) we find that they are satisfied by

$$\theta_C/2 = 53^\circ,\ \tan\alpha = 1{\cdot}37,$$
$$p_a = \sin 70^\circ, \text{ and } p_b = \sin 65^\circ.$$

Inserting these values in equations (3.49, 51 and 59) we obtain

$$a = 31 \text{ in.},\quad b = 57{\cdot}5 \text{ in.},\quad \text{and}\quad CE = 23{\cdot}8 \text{ in.}$$

The slopes at the supports are $\theta_A = 140^\circ$, and $\theta_B = 130^\circ$. The approximate theory gives

$$\delta = \frac{P L_a^2 L_b^2}{3 L E I}$$

for the deflection under the load. This would amount to $CE =$ 34·03 in. in the present example.

REFERENCES

[1] Gospodnetic, D. Deflection curve of a simply supported beam, *J. appl. Mech.* **26,** *Trans. ASME* **81,** *Ser. E* (1959) 675

[2] Timoshenko, S. *Theory of Elastic Stability*, 1st edition, p. 28, McGraw-Hill, New York, 1936

[3] Frisch-Fay, R. Particular cases of large deflections, *Aust. J. appl. Sci.* **11,** 4, (1960) 443

[4] Sonntag, R. Der beiderseits gestuezte, symmetrisch belastete Stab mit endlicher Durchbiegung und seine Stabilität, *Ingen.-Arch.* **12** (1942) 283

[5] Biezeno, C. B. On a special case of bending, *Proc. Acad. Sci. Amst.* **45** (1942) 438

[6] Liebold, R. Die Durchbiegung einer beidseitig fest eingespannten Blattfeder, *Z. angew. Math. Mech.* **28** (1948) 247

4

INITIALLY CURVED BAR UNDER POINT LOADS

4.1. Basic Equations

The main problem in the theory of nonlinear bending is that in which the free (unloaded) shape of the bar for a particular load is given and the deflected shape is sought. The problem can, however, be reversed; that is, the deflected shape corresponding to a particular load may be given and the free (unloaded) shape be required. Consider, for example, the curved bar in *Figure 4.1*. The line a represents the free shape of the cantilever fixed at 0 and its intrinsic equation is $\eta = \eta(s)$. The loaded shape (line b) is expressed by $\psi = \psi(s)$. The bar is assumed to be inextensible, hence s is the

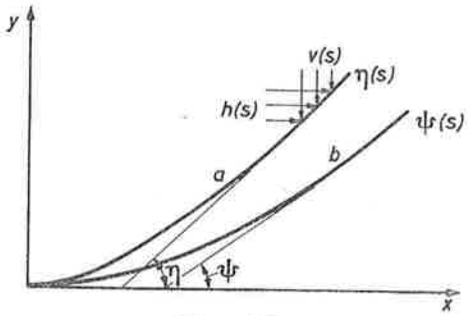

Figure 4.1

same in both equations. An arbitrary load distribution is assumed and is given in the form $v(s)$ vertically and $h(s)$ horizontally (*Figure 4.1*). The bending of an arbitrary plane curve under an arbitrary coplanar loading is expressed by

$$\frac{d}{ds}\left[EI\left(\frac{d\psi}{ds} - \frac{d\eta}{ds}\right)\right] - V(s)\cos\psi - H(s)\sin\psi = 0 \quad (4.1)$$

where $$V(s) = \int_s^L v(s)\,ds$$

and $$H(s) = \int_s^L h(s)\,ds$$

if L is the length of the bar. Equation (4.1) states that at any point of the bar the rate of change in the bending moment in the s direction is equal to the shear at that point. For a bar of constant flexural rigidity, equation (4.1) takes the form

$$EI\frac{d^2\psi}{ds^2} - V(s)\cos\psi - H(s)\sin\psi = EI\frac{d^2\eta}{ds^2} \qquad (4.2)$$

If the shape of the loaded bar $\psi = \psi(s)$ is known the free shape is found from equation (4.1):

$$\eta(s) = \psi(s) - \frac{1}{EI}\int_0^s ds \int_L^s [V(s)\cos\psi + H(s)\sin\psi]\, ds \qquad (4.3)^1$$

Equation (4.2) has, in general, no closed form solution. If, however, the free shape is circular and the load consists of concentrated forces, the analysis of the problem can be simplified to a large extent. This will be shown in the next section.

4.2. Initially Curved (Circular) Bar under Vertical Load at the Free End

Consider a bar, initially curved to form the arc of a circle of radius R, clamped at A and loaded by P at the end (*Figure 4.2*). The differential equation expressing the bending moment is, from equation (4.2),

$$EI\frac{d^2(\pi/2 - \theta)}{ds^2} - P\cos(\pi/2 - \theta) = 0$$

since, for a circle, $d^2\eta/ds^2 = 0$. Rearranging this equation,

$$\frac{d^2\theta}{ds^2} = -k^2\sin\theta \qquad (4.4)$$

Integrating equation (4.4)

$$\frac{1}{2}\left(\frac{d\theta}{ds}\right)^2 = k^2\cos\theta + C \qquad (4.5)$$

The constant of the integration is found from the boundary condition

$$\left(\frac{d\theta}{ds}\right)_{\theta=\gamma} = \frac{1}{R}$$

which states that at the free end of the bar the bending moment is zero; hence the curvature remains the original curvature $1/R$ of the unrestricted bar. Therefore,

$$C = \frac{1}{2R^2} - k^2 \cos\gamma$$

and

$$\frac{1}{2}\left(\frac{d\theta}{ds}\right)^2 = k^2(\cos\theta - \cos\gamma) + \frac{1}{2R^2} \tag{4.6}$$

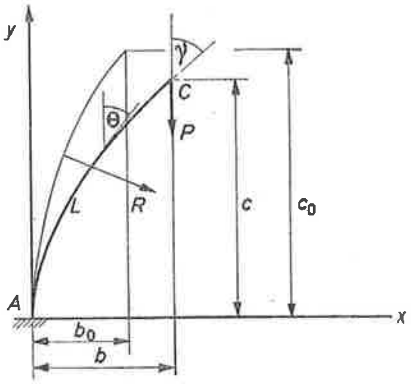

Figure 4.2

At the clamped end the bending moment $M = Pb = k^2bEI$,

hence
$$\left(\frac{d\theta}{ds}\right)_{\theta=0} = \frac{1}{R} + k^2 b$$

and
$$\frac{1}{2}\left(\frac{1}{R} + k^2 b\right)^2 = k^2(1 - \cos\gamma) + \frac{1}{2R^2}$$

or
$$b^2 \frac{1}{R^2} + b\frac{2}{k^2 R^3} - \frac{2}{k^2 R^2}(1 - \cos\gamma) = 0 \tag{4.7}$$

Once γ is known this equation may be used for finding b. The angle α is now introduced such that

$$\cos\alpha = \cos\gamma - \frac{1}{2k^2R^2} \tag{4.8}$$

Then, from equation (4.6)

$$L = \int_0^{\gamma} ds = \frac{1}{k\sqrt{2}} \int_0^{\gamma} \frac{d\theta}{(\cos\theta - \cos\alpha)^{\frac{1}{2}}} \tag{4.9}$$

This can be reduced to standard elliptic forms by selecting a new variable ϕ according to the equations

$$1 - \cos\theta = 2p^2 \sin^2\phi = (1 - \cos\alpha)\sin^2\phi \qquad (4.10)^2$$

In terms of ϕ, equation (4.9) becomes

$$L = \frac{1}{k}\int_0^{\phi_1} \frac{d\phi}{(1 - p^2\sin^2\phi)^{\frac{1}{2}}} = F(p, \phi_1)/k \tag{4.11}$$

where ϕ_1 is the value of the new parameter corresponding to γ. From equation (4.10)

$$\cos\alpha = 1 - 2p^2$$

and from equation (4.8)

$$\cos\gamma = 1 - 2p^2 + \frac{1}{2k^2R^2}$$

Therefore, $\sin^2\phi_1 = \dfrac{1 - \cos\gamma}{1 - \cos\alpha} = \dfrac{2p^2 - 1/2k^2R^2}{2p^2} = 1 - \left(\dfrac{1}{2pkR}\right)^2$

and

$$\phi_1 = \cos^{-1}\left(\frac{1}{2pkR}\right) \tag{4.12}$$

Equation (4.11) can be expressed as

$$L = F\left[p, \cos^{-1}\left(\frac{1}{2pkR}\right)\right]\Big/k \tag{4.13}$$

containing p as the only unknown.

It is noted that

$$c = \int_0^{\gamma} dy = \frac{1}{k\sqrt{2}}\int_0^{\gamma} \frac{\cos\theta\, d\theta}{(\cos\theta - \cos\alpha)^{\frac{1}{2}}}$$

With the substitutions of (4.10) this reduces to

$$c = [2E(p, \phi_1) - F(p, \phi_1)]/k \qquad (4.14)$$

The horizontal deflection b can now be calculated from equation (4.7) since γ may be obtained from

$$\cos\gamma = 1 - 2p^2 + \frac{1}{2k^2 R^2}$$

A closer inspection of equation (4.8) reveals that

$$\cos\gamma = \cos\alpha + \frac{1}{2k^2 R^2} \qquad (4.15)$$

fails for small values of P since $-1 \leqslant \cos\gamma \leqslant 1$ for real γ. To overcome this difficulty, let

$$p \sin\phi = \sin\phi' \quad \text{where } p > 1$$

The elliptic integral F changes into

$$F(p, \phi) = F\left[\frac{1}{p}, \sin^{-1}(p \sin\phi)\right] \Big/ p$$

since

$$\frac{d\phi}{d\phi'} = \frac{(1 - \sin^2\phi')^{\frac{1}{2}}}{(p^2 - \sin^2\phi')^{\frac{1}{2}}}$$

Similarly, for $p > 1$, $E(p, \phi)$ becomes

$$E(p, \phi) = pE\left[\frac{1}{p}, \sin^{-1}(p\sin\phi)\right] - \left(p - \frac{1}{p}\right)F\left[\frac{1}{p}, \sin^{-1}(p\sin\phi)\right]$$

The physical explanation of the failure of equation (4.15) is that for small P the elastic shape becomes a segment of the nodal elastica for which other equations are needed. This statement will more readily be understood if we begin the analysis of our problem from the basic strut. Consider a straight, vertical strut subject to a load P on the top and a clockwise couple $M = EI/R$ acting at the same point (*Figure 4.3* (*a*)). The action of the couple M will bend the strut into a circular arc of radius R, while the load P is still acting on the free end (*Figure 4.3* (*b*)). This bar is, therefore, the circular bar of our original problem. The couple M and the load P will now be replaced by a force P acting on a rigid lever of length $e = M/P$ (*Figure 4.3* (*c*)), and, so far as the shape AC is concerned, it does not matter whether the load acts on the bar ACD or through the lever e. We have

$$e = \frac{EI}{RP} = \frac{1}{k^2 R}, \; p = \sin(\alpha/2), \text{ and } \sin(\gamma/2) = p \sin\phi_1$$

Since
$$e = h\cos\phi_1,$$

$$\cos\phi_1 = \frac{1}{2pkR}$$

which is identical with equation (4.12).

Also,
$$\cos\alpha = 1 - 2\sin^2(\alpha/2) = 1 - 2p^2$$

and
$$\cos\gamma = 1 - 2\sin^2(\gamma/2) = 1 - 2p^2\sin^2\phi_1$$

$$= 1 - 2p^2 + \frac{1}{2k^2R^2} = \cos\alpha + \frac{1}{2k^2R^2}$$

$$\left(\text{from} \quad \sin^2\phi_1 = 1 - \frac{1}{4p^2k^2R^2}\right)$$

This shows that the auxiliary angle α in equation (4.8) is actually the end slope of the imaginary extension of the basic strut.

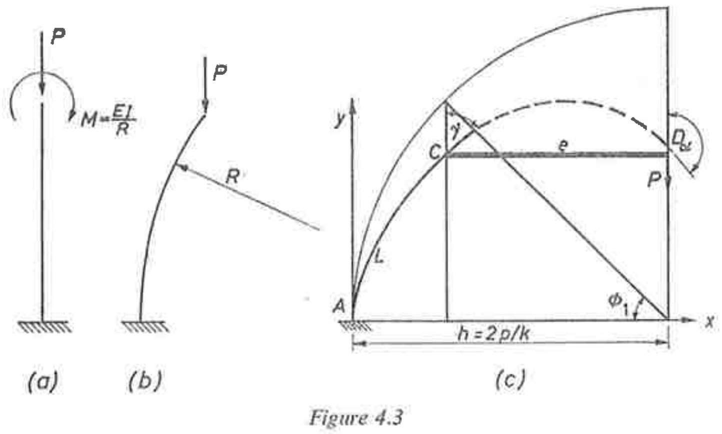

Figure 4.3

The length of the bar can be obtained from *Figure 4.3* (c):

$$L = F(p, \phi_1)/k \qquad \text{(as in equation (4.13))}$$

Having expressed the modulus p in terms of the basic strut, the slope, arc length and coordinates can be calculated without difficulty from the equations of the undulating elastica in section 1.3. It will become necessary, however, to establish the range of these equations. As seen clearly from *Figure 4.3* (*c*) a decreasing P means an increasing e, since M depends on EI and R only, and these are given. On the other hand, e cannot grow indefinitely as at some value of e the line of action of P will bypass the imaginary extension of the bar. We note that e will increase with α, but $\alpha \leqslant \pi$, hence $p_{max} = 1$. With $p = 1$, equation (4.13) reduces to

$$kL = \int_0^{\phi_1} \sec\phi = \ln\tan(\pi/4 + \phi_1/2) = \lambda(\phi_1) \qquad (4.16)$$

Since $\phi_1 = \cos^{-1}(1/2kR)$, equation (4.16) can be solved for k and hence for $P = P_0$. P_0 marks the limit of the applicability of the equations corresponding to the undulating elastica and derived at the beginning of this section. For $P < P_0$ the basic strut becomes a segment of the nodal elastica (*Figure 4.4*). We have

$$\phi_1' = \sin^{-1}[p\sin(\gamma/2)] \text{ and } e = \frac{1}{k^2R} = h[1 - p^2\sin^2(\gamma/2)]^{\frac{1}{2}}$$

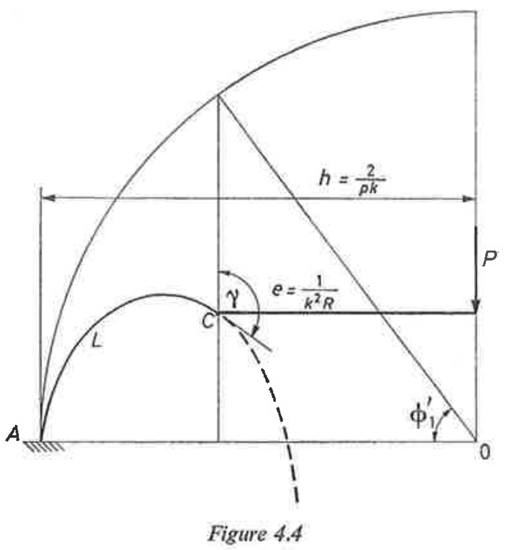

Figure 4.4

The second equation leads to

$$\sin(\gamma/2) = \left[\left(\frac{1}{p}\right)^2 - \left(\frac{1}{2kR}\right)^2\right]^{\frac{1}{2}} \tag{4.17}$$

This equation, unlike (4.15), will not fail for small values of P because p decreases with P at such a rate that the expression under the square root remains positive for, no matter how small P is chosen, there is always a positive p for which

$$2R\sqrt{P/EI} > p$$

The modulus of the shape when $P < P_0$ can be found from

$$L = \frac{p}{k} F(p, \gamma/2) \tag{4.18}$$

where $\gamma/2$ is given in equation (4.17). Once p is known, the equations of the nodal elastica in section 1.5 will give the answers for the slopes and the deflection coordinates.

4.3. Initially Curved (Circular) Bar under Horizontal Load

We shall now consider the same bar as in *Figure 4.2* but replace the vertical load with a horizontal P (*Figure 4.5*). In this case equation (4.2) becomes

$$\frac{d^2\theta}{ds^2} = -k^2\cos\theta \tag{4.19}$$

Integration yields $\frac{1}{2}\left(\frac{d\theta}{ds}\right)^2 = -k^2\sin\theta + C$ (4.20)

At $y = c,\ \theta = \gamma,$ and $\frac{d\theta}{ds} = \frac{1}{R}$

From these boundary conditions one obtains the constant

$$C = \frac{1}{2R^2} + k^2\sin\gamma$$

and equation (4.20) becomes

$$\frac{1}{2}\left(\frac{d\theta}{ds}\right)^2 = k^2(\sin\gamma - \sin\theta) + \frac{1}{2R^2} \tag{4.21}$$

Since the tangent to the bar is vertical at the fixed end and the bending moment at the same point is $M = Pc = k^2cEI$,

$$\left(\frac{d\theta}{ds}\right)_{\substack{\theta=0\\y=0}} = \frac{1}{R} + k^2 c,$$

and from equation (4.21)

$$\frac{1}{2}\left(\frac{1}{R} + k^2 c\right)^2 = k^2 \sin\gamma + \frac{1}{2R^2} \tag{4.22}$$

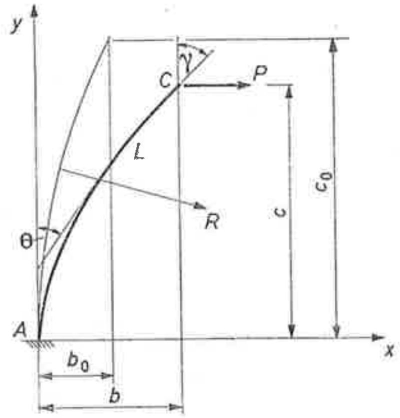

Figure 4.5

This equation may be reduced to

$$\frac{c^2}{R^2} + \frac{2c}{k^2R^3} - \frac{2}{k^2R^2}\sin\gamma = 0 \tag{4.23}$$

from which c may be obtained once $\sin\gamma$ has been found. By introducing the auxiliary angle β given by

$$\sin\beta = \sin\gamma + \frac{1}{2k^2R^2} \tag{4.24}$$

into equation (4.21), one obtains

$$L = \frac{1}{k\sqrt{2}}\int_0^{\gamma} \frac{d\theta}{(\sin\beta - \sin\theta)^{\frac{1}{2}}} \tag{4.25}$$

The integral in equation (4.25) will be reduced to Legendre's standard form if one changes to a new variable ϕ such that

$$1 + \sin\theta = 2p^2 \sin^2\phi = (1 + \sin\beta)\sin^2\phi \tag{4.26}$$

This substitution changes equation (4.25) into

$$L = \frac{1}{k}\int_{\phi_2}^{\phi_1} \frac{d\phi}{(1 - p^2 \sin^2\phi)^{\frac{1}{2}}} \tag{4.27}$$

In this integral ϕ_1 and ϕ_2 have to be found before the unknown modulus p can be evaluated. From equation (4.26)

$$\sin\beta = 2p^2 - 1$$

and from equation (4.24)

$$\sin\gamma = 2p^2 - 1 - \frac{1}{2k^2 R^2}$$

Therefore, $$\sin^2\phi_2 = \frac{1}{2p^2},$$

giving $$\phi_2 = \sin^{-1}\left(\frac{0{\cdot}707}{p}\right)$$

Further, $$\sin^2\phi_1 = \frac{1 + \sin\gamma}{1 + \sin\gamma + 1/2k^2 R^2} = 1 - \frac{1}{4p^2 k^2 R^2},$$

hence $$\phi_1 = \cos^{-1}\left(\frac{1}{2pkR}\right)$$

Equation (4.27) can now be written with p as the only unknown,

namely $$L = [F(p, \phi_1) - F(p, \phi_2)]/k \tag{4.28}$$

The horizontal displacement of the free end can be found from

$$b = \int_0^{\gamma} dx = \frac{1}{k}\int_{\phi_2}^{\phi_1} \frac{(2p^2 \sin^2 \phi - 1)\, d\phi}{(1 - p^2 \sin^2 \phi)^{\frac{1}{2}}} \tag{4.29}$$

This expression for b can be written in terms of the standard elliptic integrals:

$$b = \{F(p, \phi_1) - 2E(p, \phi_1) - F(p, \phi_2) + 2E(p, \phi_2)\}/k \tag{4.30}$$

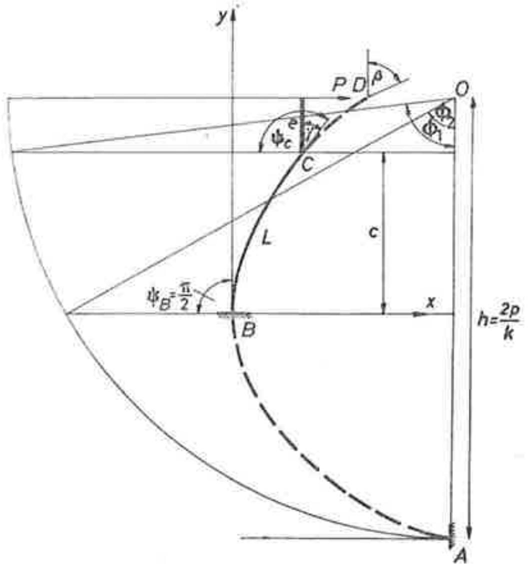

Figure 4.6

Equation (4.24) indicates that, for small values of P, $\sin \beta$ might become larger than unity in which case the substitution fails. The reason for this is similar to the explanation given in section 4.2, namely the transformation of the elastic shape into a segment of the nodal elastica. This can be seen from *Figure 4.6*. We have at once

$$\cos \phi_1 = \frac{e}{h} = \frac{1}{2pkR}, \text{ and } \phi_2 = \sin^{-1}\left(\frac{\sin (\pi/4)}{p}\right)$$

Hence
$$c = 2p(\cos \phi_2 - \cos \phi_1)/k \tag{4.31}$$

From equation (4.23) the vertical coordinate of C is

$$c = \frac{2}{k}\left[\left(\frac{2p^2 - 1}{2}\right)^{\frac{1}{2}} - \frac{1}{2kR}\right]$$

and it is easy to see that this expression is identical with equation (4.31) since

$$\cos\phi_1 = \frac{1}{2pkR} \quad \text{and} \quad \cos\phi_2 = \left(\frac{2p^2 - 1}{2p^2}\right)^{\frac{1}{2}}$$

Also, from equation (4.26)

$$p = [2(1 + \sin\beta)]^{\frac{1}{2}}/2 = \sin(\pi/4 + \beta/2)$$

which shows that the auxiliary angle β is the end slope of the imaginary extension of the bar (measured from the vertical).

As mentioned before, difficulties arise for small values of P. A decreasing P means an increasing e and an increasing β, which, however, cannot be more than $\pi/2$. Hence $p_{\max} = 1$. Equation (4.28) thus becomes

$$kL = \int_{\phi_2}^{\phi_1} \sec\phi \, d\phi = \ln\tan(\pi/4 + \phi_1/2) - \\ - \ln\tan(\pi/4 + \phi_2/2) = \lambda(\phi_1) - \lambda(\pi/4) \qquad (4.32)$$

since $\phi_2 = \pi/4$.

Equation (4.32) is a function of k because ϕ_1 depends on k; hence it can be solved for $P = P_0$. If the load on the circular bar is less than P_0 the equations derived previously cannot be used and we have to turn to the nodal elastica (*Figure 4.7*). Employing the notation of *Figure 4.7*

$$\sin\phi_2' = p\sin(\pi/4), \quad \sin\phi_1' = p\sin(\pi/4 + \gamma/2)$$

also, $$\frac{1}{k^2R} = h[1 - p^2\sin^2(\pi/4 + \gamma/2)]^{\frac{1}{2}}$$

from which $$\sin\gamma = \frac{2}{p^2} - 1 - \frac{1}{2k^2R^2} \qquad (4.33)$$

Equation (4.33) assures that γ will always be real. The modulus will be found from

$$L = p\{F[p,(\pi/4+\gamma/2)] - F(p,\pi/4)\}/k \qquad (4.34)$$

For slopes and coordinates the reader is referred to section 1.5.

When the force in *Figure 4.5* is acting in the opposite direction the analysis will reach a stage when a point of contraflexure has to be assumed. This problem will be discussed in section 4.10.

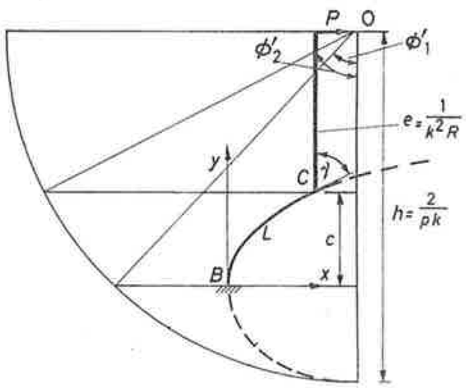

Figure 4.7

4.4. Circular Cantilever with Inclined Load

Consider now a circular bar with a horizontal end tangent at the fixed end A and subject to an inclined load P at the free end (*Figure 4.8*). Equation (4.2) becomes

$$EI\frac{d^2\psi}{ds^2} - P\sin\alpha\cos\psi + P\cos\alpha\sin\psi = 0 \qquad (4.35)$$

If the following substitutions are introduced,

$$u = \frac{s}{L}, \quad c = k^2L^2, \quad \text{and} \quad \xi = \psi - \alpha \qquad (4.36)$$

equation (4.35) changes into

$$\frac{d^2\xi}{du^2} + c\sin\xi = 0 \qquad (4.37)$$

Equation (4.37) is formally identical with equation (2.56) but the boundary conditions are here different since now

$$\left(\frac{d\psi}{ds}\right)_{s=L} = \frac{1}{R} \quad \text{that is,} \quad \left(\frac{d\xi}{du}\right)_{\xi=\psi_0-\alpha} = \frac{L}{R}$$

The solution of equation (4.37) is

$$u = \int_{-\alpha}^{\xi} \left[\left(\frac{L}{R}\right)^2 - 2c\cos\xi_L + 2c\cos\xi\right]^{-\frac{1}{2}} d\xi \qquad (4.38)$$

where $\xi_L = \psi_0 - \alpha.$

Extending the integration from $-\alpha$ to $\psi_0 - \alpha$, one obtains

$$\left.\begin{aligned} L &= p[F(p, \xi_L/2) + F(p, \alpha/2)]/k \\ p &= \frac{2k}{\{(1/R)^2 + [2k\sin(\xi_L/2)]^2\}^{\frac{1}{2}}} \end{aligned}\right\} \qquad (4.39)$$

where

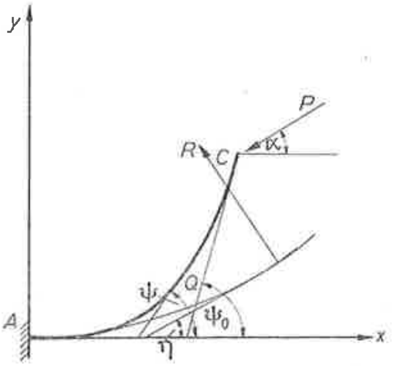

Figure 4.8

The derivation of these equations is due to Mitchell[1]. From these equations p and ξ_L can be evaluated, so that the shape is determined. The form of equation (4.39) suggests that the elastic shape is made up of segments of a nodal elastica. This becomes evident if one realizes that as k (and P) tends to zero, p also tends to zero; but for $p = 0$, the undulating elastica is a straight line while the nodal elastica degenerates into a circle of which the unloaded bar is a segment. It also appears that k and α may assume values for which equation (4.39) cannot be solved for a real ξ_L. A very detailed discussion on this subject is given by Wijngaarden[3].

Assuming that equation (4.39) can be solved for a real ξ_L the coordinates of the cantilever are

$$\left.\begin{aligned} x = {} & \frac{2}{pk}\cos\alpha\{E(p,\xi/2) + E(p,\alpha/2) - \\ & - (1-p^2/2)[F(p,\xi/2) + F(p,\alpha/2)]\} - \\ & - \frac{2}{pk}\sin\alpha\{[1-p^2\sin^2(\alpha/2)]^{\frac{1}{2}} - [1-p^2\sin^2(\xi/2)]^{\frac{1}{2}}\} \\ \text{and}\quad y = {} & \frac{2}{pk}\sin\alpha\{E(p,\xi/2) + E(p,\alpha/2) - \\ & - (1-p^2/2)[F(p,\xi/2) + F(p,\alpha/2)]\} + \\ & + \frac{2}{pk}\cos\alpha\{[1-p^2\sin^2(\alpha/2)]^{\frac{1}{2}} - [1-p^2\sin^2(\xi/2)]^{\frac{1}{2}}\} \end{aligned}\right\} \quad (4.40)$$

The slope ξ can be found in terms of s from

$$s = p[F(p,\xi/2) + F(p,\alpha/2)]/k \quad (4.41)$$

This equation contains only one unknown, ξ.

Let us assume that equation (4.39) cannot be solved for a real ξ_L. With the aid of the principle of elastic similarity the problem will be analysed with reference to *Figure 4.9*. As mentioned before, equation (4.39) will have a real solution for ξ_L provided the elastic shape is made up of segments of nodal elasticas. The deflected shape in *Figure 4.9* will, therefore, represent parts of an undulating elastica. The bar will be extended over the portion CE until it intersects the line of action of P. A tangent parallel to this line of action touches the curve at B; this now becomes the clamped end of the basic strut. The rest of *Figure 4.9* is self explanatory and the relationship between length and modulus is given by

$$L = [F(p,\ \phi_{\psi_0-\alpha}) + F(p,\phi_\alpha)]/k \quad (4.42)$$

where $\sin\phi_\alpha = \dfrac{\sin(\alpha/2)}{p}$, and $\sin\phi_{\psi_0-\alpha} = \dfrac{\sin[(\psi_0-\alpha)/2]}{p}$

Two unknowns are involved, p and ψ_0. A second equation is obtained from

$$\cos\phi_{\psi_0-\alpha} = \frac{e}{h} = \frac{1}{2pkR} \quad (4.43)$$

These two equations will yield p and ψ_0. The relationship between slope and arc length, once p is known, is found from

$$s = [F(p, \phi_{\psi-\alpha}) + F(p, \phi_\alpha)]/k \qquad (4.44)$$

where
$$\sin \phi_{\psi-\alpha} = \frac{\sin[(\psi - \alpha)/2]}{p}$$

It will be noticed that for $\psi < \alpha$, $\phi_{\psi-\alpha}$ is negative. Since $F(p, -\phi) = -F(p, \phi)$, the point will be located on the AB portion.

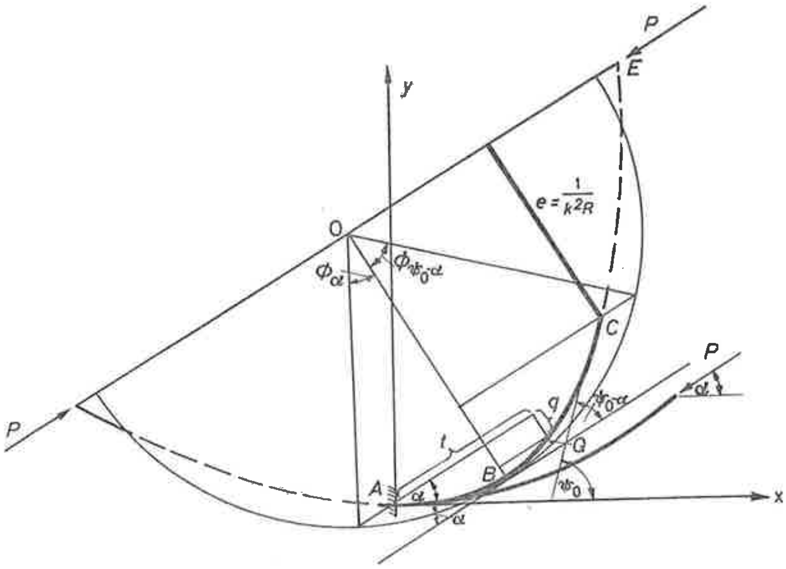

Figure 4.9

The coordinates can be seen by inspection (*Figure 4.9*) to be

$$\left.\begin{aligned} x &= t\cos\alpha + q\sin\alpha \\ y &= t\sin\alpha - q\cos\alpha \end{aligned}\right\} \qquad (4.45)$$

where t and q are made up from the vertical and horizontal co-ordinates of the basic case and may be calculated from the equations given in section 1.3.

Depending on the value of P and α the deflected shape may have a point of inflection (*Figure 4.10*). The length of the cantilever is now

$$L = [2K(p) - F(p, \phi_A) - F(p, \phi_C)]/k \tag{4.46}$$

where $\sin \phi_A = \dfrac{\sin(\alpha/2)}{p}$, $\sin \phi_C = \dfrac{\sin(\theta_C/2)}{p}$, and $\cos \phi_C = \dfrac{1}{2kpR}$

Equation (4.46) constitutes the solution of the problem. With p and θ_C, solved we proceed to evaluate the slope and the coordinates in terms of the arc length.

$$\left.\begin{aligned} s &= [2K(p) - F(p, \phi_A) - F(p, \phi)]/k \\ &\qquad \text{if } s > AJ \\ \text{and} \quad s &= [F(p, \phi) - F(p, \phi_A)]/k \\ &\qquad \text{if } s < AJ \end{aligned}\right\} \tag{4.47}$$

The slope and the coordinates will be calculated from

$$\left.\begin{aligned} \sin(\theta_B/2) &= p \sin \phi_B \\ x_B &= t \cos \alpha + q \sin \alpha \\ y_B &= t \sin \alpha - q \cos \alpha \end{aligned}\right\} \tag{4.48}$$

in which t and q can be obtained from the equations of the undulating elastica.

In the present case,

$$t = [2K(p) - 4E(p) + 2E(p, \phi_B) - F(p, \phi_B) + \\ + 2E(p, \phi_A) - F(p, \phi_A)]/k$$

and

$$q = 2p(\cos \phi_A + \cos \phi_B)/k$$

4.5. Buckled Shape of a Flat Spring

Consider a flexible leaf spring initially curved to form the arc of a circle (*Figure 4.11*). Suppose now that the spring is forced to buckle inward, as shown, and the ends are fitted between two supports[4]. The various shapes and their stability will be investigated.

Let $2L$ be the length of the spring and R the radius. Because of symmetry the spring may be considered fixed at A and the analysis can be restricted to the upper half of the curved bar.

The bar AB is transformed into a basic strut if an anticlockwise couple $M = EI/R$ is applied at the ends of a straight bar of equivalent

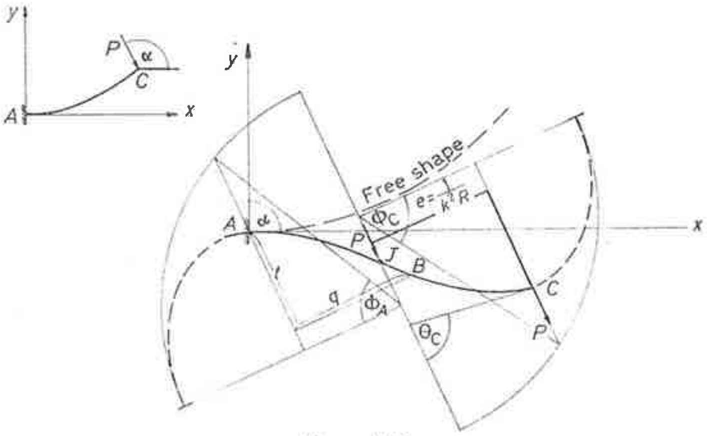

Figure 4.10

length and a load P is applied at B. This is equivalent to a load acting through a lever whose length is $e = 1/k^2R$. Inspection of *Figure 4.12* shows that the modulus of the bent shape can be obtained by solving

$$L = [2K(p) - F(p, \phi_B)]/k \tag{4.49}$$

where $\cos \phi_B = 1/2kpR$

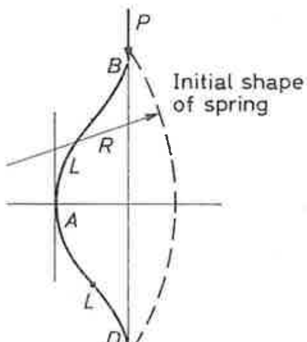

Figure 4.11

The limiting case where equilibrium is possible occurs when $\theta_B = 0$. Equation (4.49) becomes then

$$4pK(p) = \frac{L}{R} \tag{4.50}$$

since $\phi_B = 0$.

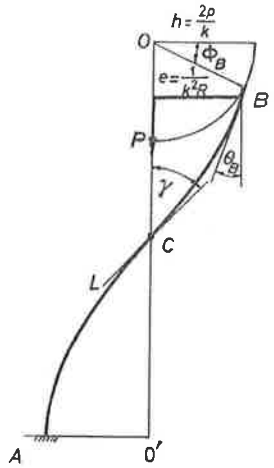

Figure 4.12

Also, $k = 1/2pR$, which gives us the load necessary to keep the bar in this shape (*Figure 4.13* (*a*)). Let this load be P_0. By bending the spring toward the right, the modulus will increase and tend toward $p = 1$. It is obvious that the point of inflexion, which for P_0 lay halfway between B and A, will move toward B with increasing deflections. It is noted, however, that the horizontal projection of CB, that is the lever arm e, does not decrease monotonously with the decrease in length of CB. Actually, according to the slopes in *Figure 4.13* (*a*), the lever arm e increases from P_0 to P_3 and decreases thereon. This is of great importance because it follows from $e = M/P$ that by bending the spring from P_0 to P_3 the forces are changing in the order $P_0 > P_1 > P_2 > P_3 < P_4 < P_5$ etc.; hence the spring is unstable for the first four shapes. Assume now that $P_3 = P_{\min}$. Then, by applying a load $P_0 > P > P_{\min}$, there will be two distinct shapes of the spring capable of balancing the load. Obviously, only the lower shape is stable because the upper shape, when subject to the slightest displacement, will not return and the spring will bend into the corresponding lower shape. This behaviour is in contrast to the properties of a straight flexible strut (*Figure 4.13* (*b*)) which needs increasing loads to produce increasing vertical deflections. Hence in *Figure 4.13* (*b*) all shapes are stable.

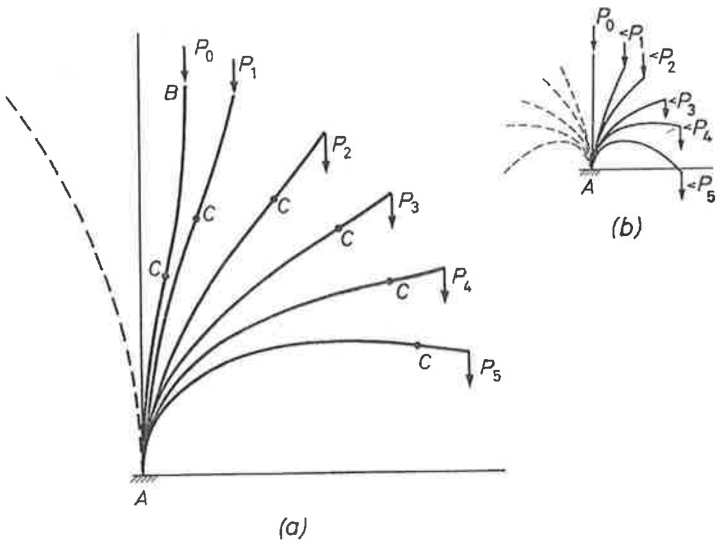

Figure 4.13 (From Hymans[4])

The shape corresponding to P_0 is analogous to the straight bar subject to $P > P_{cr}$; it can sway to either side.

Assume now the spring (*Figure 4.13* (*a*)) to be in the shape of P_4 and let P_4 be suddenly reduced to $P' < P_{min}$. The spring will then snap back toward its initial unstressed shape. Since $P' - P_{min}$ can be made arbitrarily small, vigorous snap action can be obtained by a slight reduction of the load.

Consider next the spring in its unstable equilibrium position under P_0, and apply a small anticlockwise couple at B. This will increase the lever arm and will cause the spring to sway toward the left. It can be prevented by increasing the load, thereby reducing e. This shape is shown in *Figure 4.14*. The governing equation is

$$L = [2K(p) + F(p, \phi_B)]/k \tag{4.51}$$

where $\cos \phi_B = 1/2kpR$.

By applying increasing loads $P_a < P_b < P_c < P_d$, etc., the shapes belonging to the loads are shown in *Figure 4.15*. As seen, increasing forces mean increasing deflections, hence all shapes are stable. The loads P_a, P_b, etc., corresponding to the slopes in *Figure 4.15* are larger than those in *Figure 4.13* (*a*). The reason for this is that in *Figure 4.15* the basic strut (which, in the last analysis, balances the load) is smaller than the basic strut in *Figure 4.13* (*a*). Also, the curvatures in *Figure 4.15* are, generally, larger than before, hence the spring can store more strain energy. Numerical results have been obtained by Hymans[4].

The slopes and coordinates of the spring can be calculated without difficulty by applying the formulae of the undulating elastica.

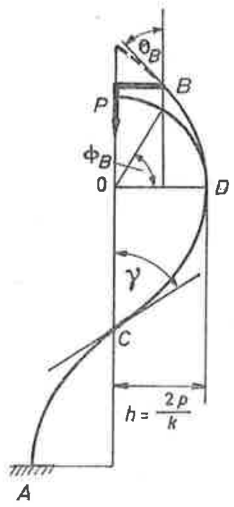

Figure 4.14

4.6. Circular Ring. Ring in Tension

Consider the closed circular ring in *Figure 4.16* (*a*) subject to two equal and opposite radial forces. This ring is statically indeterminate to the first degree. By placing hinges at *A* and *C*, two equal and opposite couples are needed to ensure that the tangents at *A* and *C* of the upper and lower parts remain vertical. If the resulting deflections are small compared with other dimensions of the ring it is found that the bending moments at *A* and *B* under the action of the loads in *Figure 4.16* (*b*) are

$$M_A = +\,0{\cdot}364\,Pr \quad \text{and} \quad M_B = -\,0{\cdot}636\,Pr$$

(These values apply to an initially stressless ring, that is, not to one that has been bent from a straight bar into a circular shape.) If compressive forces act on the ring the signs of these moments will change. The results are based on the principle of superposition and are sufficiently accurate only for relatively stiff rings. Flexible rings, however, are capable of deflections of magnitudes which are of the same order as the radius; it follows that the deformations in *Figure 4.16* (*b*) and (*c*) can be analysed in the nonlinear framework only.

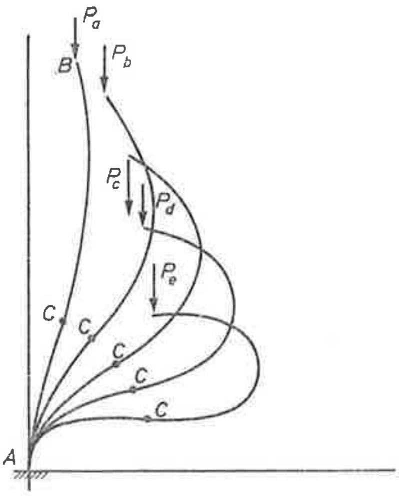

Figure 4.15 (From Hymans[4])

Before beginning our investigation of the deformations, we note that a circular ring may be conceived as stressless in the circular shape (the assumption made in the linear theory), but we can also imagine that the ring was originally straight and has been bent into shape by applying a couple $M_r = EI/r$ at the ends. The following discussion will be based on a ring bent into shape from a straight bar. We can easily change over to the initially stressless ring by increasing the bending moment at any point by M_r.

The case of tensile forces is considered first. Because of symmetry, only the deflections of one quadrant need to be considered. The deformed shape of the top right-hand quadrant of the circle is shown in *Figure 4.17*. This deformed quadrant will now be considered as an originally vertical strut of length $L = r\pi/2$, subject to P and M_B at the free end and having a horizontal tangent at B. The relationship between the curvature and the bending moment at any point may be expressed by the nonlinear differential equation[5,6]

$$\frac{x''}{[1+(x')^2]^{3/2}} = \frac{1}{EI}(Px - M_B)$$

or

$$\frac{x''}{[1+(x')^2]^{3/2}} = k^2(x - m) \tag{4.52}$$

where

$$k = \left(\frac{P}{EI}\right)^{\frac{1}{2}} \quad \text{and} \quad m = \frac{M_B}{P}$$

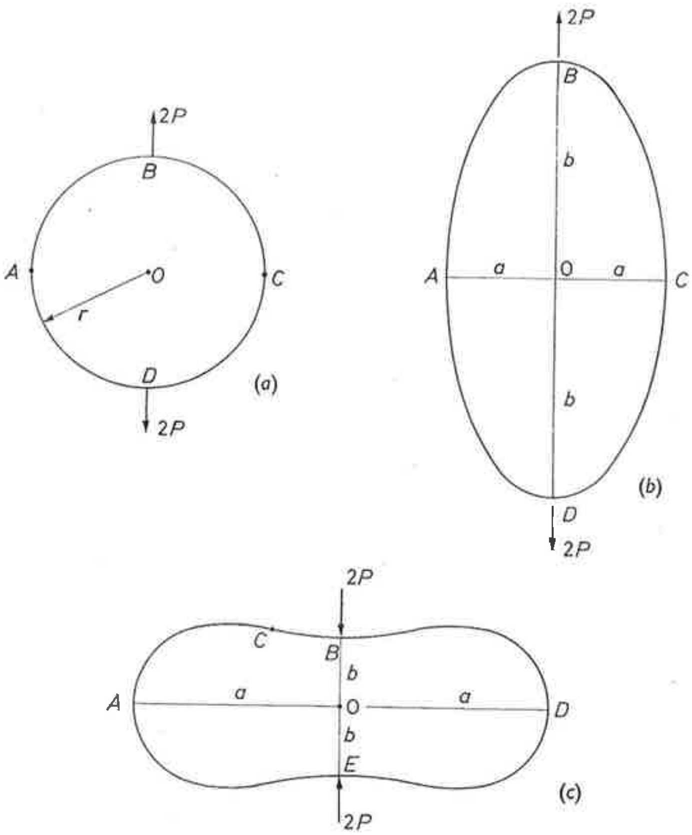

Figure 4.16

After integration we have

$$\frac{1}{[1+(x')^2]^{\frac{1}{2}}} = -\,k^2(z^2-m^2)/2 \tag{4.53}$$

in which $z = x - m$ and the integration constant has been found from

$$(x')_{x=0} = \infty$$

Let $$k^2(z^2-m^2)/2 = \cos 2\theta \tag{4.54}$$

so that $$[1+(x')^2]^{\frac{1}{2}} = -\,1/\cos 2\theta = 1/(2\sin^2\theta - 1) \tag{4.55}$$

If $x = 0$, $(z = -m)$ then from (4.54)

$$\cos 2\theta_0 = 0, \text{ hence } \theta_0 = \pi/4$$

If $x = a$ then $x' = 0$, hence $\theta_a = \pi/2$.
From equations (4.54 and 55) it follows that

$$z = -\,2(1-p^2\sin^2\theta)^{\frac{1}{2}}/kp \tag{4.56}$$

if one writes $$\frac{1}{p^2} = \frac{1}{2}\left(\frac{k^2m^2}{2}+1\right) \tag{4.57}$$

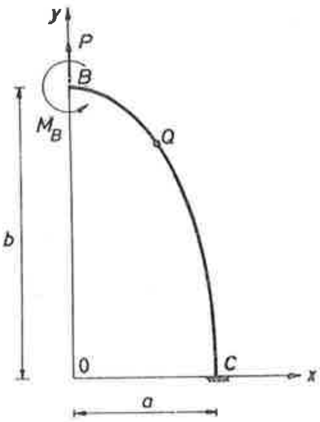

Figure 4.17

Also, from equation (4.55)

$$\frac{dx}{dy} = \frac{dz}{dy} = \frac{2\sin\theta\cos\theta}{2\sin^2\theta - 1} = -\,\tan 2\theta \tag{4.58}$$

Further, from equation (4.56)

$$\frac{dz}{d\theta} = \frac{p}{k} \frac{2 \sin \theta \cos \theta}{(1 - p^2 \sin^2 \theta)^{\frac{1}{2}}}$$

Writing
$$dy = \frac{dy}{dx}\frac{dz}{d\theta}\,d\theta = \frac{p}{k}\frac{(2 \sin^2 \theta - 1)\,d\theta}{(1 - p^2 \sin^2 \theta)^{\frac{1}{2}}} \tag{4.59}$$

and expressing the length of the curve in the well-known form

$$L = \sqrt{[1 + (x')^2]}dy$$

yields

$$L = \frac{r\pi}{2} = \int_0^b \left[1 + \left(\frac{dx}{dy}\right)^2\right]^{\frac{1}{2}} dy = \frac{p}{k}\int_{\pi/4}^{\pi/2} \frac{d\theta}{(1 - p^2 \sin^2 \theta)^{\frac{1}{2}}} =$$

$$= \frac{p}{k}\,[K(p) - F(p, \pi/4)] \tag{4.60}$$

Equation (4.60) shows that the shape in *Figure 4.17* is a segment of the nodal elastica. Regarding the range of P we see at once that if

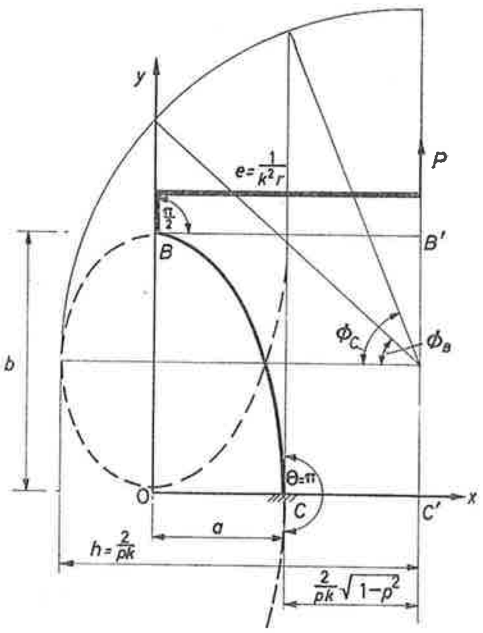

Figure 4.18

$k = 0, p = 0$; and if $k = \infty, p = 1$; it follows that equation (4.60) covers the whole range of tensile forces.

The segment of the nodal elastica that coincides with the deformed quadrant can be had by applying the load P on a lever $e = 1/k^2r$ long as shown in *Figure 4.18*. This figure shows clearly how, once p is known, the coordinates of any point can be calculated. For example

$$a = \frac{2}{kp}[\cos\phi_B - \sqrt{(1 - p^2)}] \tag{4.61}$$

where $\cos\phi_B = \sqrt{(1 - p^2/2)}$, since $\sin\phi_B = p\sin(\pi/4)$

Regarding b, we have

$$b = \frac{2}{kp}\{(1 - p^2/2)[K(p) - F(p, \pi/4)] - [E(p) - E(p, \pi/4)]\} \tag{4.62}$$

The bending moment along BC varies like the abscissae in the area $BB'C'C$, (*Figure 4.18*); hence M_{max} occurs at B and M_{min} at C. We get,

$$M_B = -\frac{2}{p}[PEI(1 - p^2/2)]^{\frac{1}{2}}, \quad \text{and} \quad M_C = -\frac{2}{p}[PEI(1 - p^2)]^{\frac{1}{2}} \tag{4.63}$$

We have seen before that p tends to 1 as P increases to infinity. Equation (4.61) shows that a is decreasing with increasing load; while equation (4.63) indicates that

$$\lim_{P\to\infty} M_C = 0, \quad \text{and} \quad \lim_{P\to\infty} M_B = -\infty$$

As a practical example, consider a circular ring with a radius of 10 in. and a flexural rigidity of $EI = 20$ lb in². Assume that the ring has been bent from a straight bar and is acted upon by tensile forces $2P$ (*Figure 4.16* (*b*)). In order to find the shapes corresponding to different loads, equation (4.60) has to be solved for p. It is easier, however, to assign values to p and calculate P from equation (4 60). The minor and major axes of the deformed circle are then found from equations (4.61 and 62). *Table 3* gives tabulated values for this case while *Figure 4.19* shows the different shapes.

Table 3. Force, modulus, and coordinates of the ring; ring in tension

Shape	$\sin^{-1}p$	P (lb)	a (in.)	b (in.)	M_C (lb in.)	M_B (lb in.)	h (in.)
1	20°	0·00648	9·9667	10·0389	−1·979	−2·043	325·0
2	30°	0·016	9·8866	10·1068	−1·974	−2·155	142·5
3	40°	0·0313	9·782	10·2231	−1·884	−2·191	78·46
4	50°	0·0578	9·611	10·4016	−1·807	−2·364	48·59
5	60°	0·1037	9·3203	10·678	−1·663	−2·629	32·076
6	70°	0·192	8·7978	11·1504	−1·425	−3·114	21·707
7	80°	0·408	7·738	11·976	−1·007	−4·107	14·225
8	85°	0·70	6·674	12·67	−0·654	−5·326	10·72
9	87°	0·968	5·972	12·948	−0·456	−6·180	9·0175
10	89°	1·682	4·758	13·6848	−0·202	−8·205	6·898
11	89°54′	3·814	3·23	14·388	−0·030	−12·377	4·5895

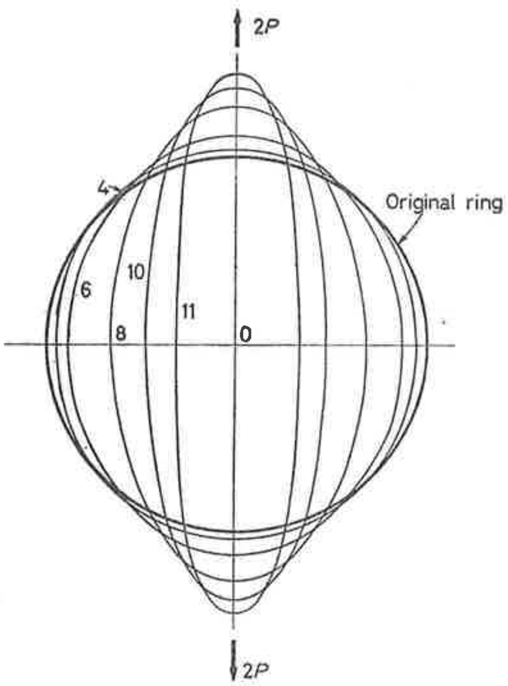

Figure 4.19

The functions

$$\frac{Pr^2}{EI} = f_1\left(\frac{a}{r}\right) \quad \text{and} \quad \frac{Pr^2}{EI} = f_2\left(\frac{b}{r}\right)$$

are plotted in *Figure 4.20* showing the nonlinear relationship between load and deflection.

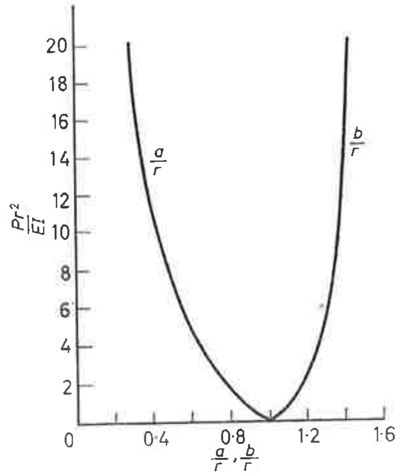

Figure 4.20

4.7. Ring in Compression

Consider the same circular ring as in section 4.6 to be acted upon by the radial compressive forces shown in *Figure 4.16 (c)*, and let the discussion be restricted to deformations in the initial plane of the ring[7]. For the generalized problem, that is, when the question of the elastic stability of the ring is involved, the reader may consult the work by Carrier[8], and by Biezeno and Koch[9]. The basic differential equation is similar to equation (4.52). It will be found, however, that the range of the forces (and the solutions) is restricted between certain limits. A further difficulty is the presence of a point of contraflexure in the quadrant for values of P in excess of a certain force. Thus, the equations necessary for the solution of the ring will be derived with the aid of the principle of elastic similarity.

At the outset, consider that a very small load, P, is applied to the ring, that is, on the quadrant in *Figure 4.21*. The clockwise couple at B and the simultaneously acting force P can be replaced by a force acting through a long lever whose length is $e = M_r/P$. The relationship between length, load and modulus is expressed by

$$r\pi/2 = p\,F(p, \pi/4)/k \tag{4.64}$$

By increasing P gradually e will decrease and the line of action of P will eventually touch the extension of the nodal elastica in *Figure*

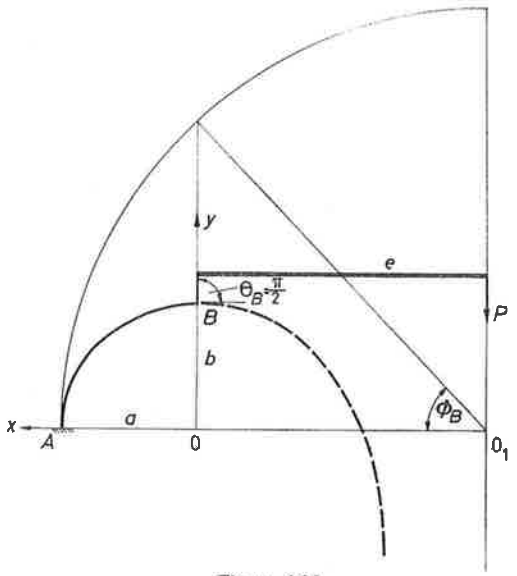

Figure 4.21

4.21. This represents the border case between the nodal and undulating elastica; the bar becomes infinitely long and $p = \sin(\pi/2)$. The load causing this condition is found from

$$r\pi/2 = F(\pi/2, \pi/4)/k$$

whence

$$P = 0{\cdot}316\, EI/r^2 \tag{4.65}$$

This load represents the end of the applicability of the nodal elastica in the compressive range. For the semi-major axis we have

$$a = 2[1 - \sqrt{(1 - p^2/2)}]/kp \tag{4.66}$$

and the semi-minor axis is calculated from

$$b = 2[E(p, \pi/4) - (1 - p^2/2)\, F(p, \pi/4)]/kp \tag{4.67}$$

If a load $P > 0{\cdot}316\, EI/r^2$ is now applied, the force P will act on the imaginary extension of the elastic line AB (*Figure 4.22*). This shape is governed by

$$r\pi/2 = F\left[p, \sin^{-1}\left(\frac{0{\cdot}707}{p}\right)\right]\Big/ k \tag{4.68}$$

It is obvious that an increasing load will cause P to move toward B. The load will reach B when $M = 0$, that is, when the presence

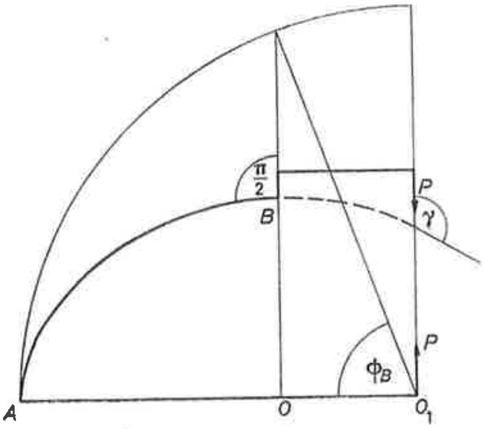

Figure 4.22

of a couple is not necessary to secure a horizontal end tangent at B. In this case $p = \sin(\pi/4)$ and P is expressed by the equation

$$r\pi/2 = K(\pi/4)/k \tag{4.69}$$

whence

$$P = 1{\cdot}39\, EI/r^2 \tag{4.70}$$

This load and the shape corresponding to it are shown in *Figure 4.23 (a)*. It follows from this figure that the curvature at B is zero. The bending moment corresponding to this case is drawn in *Figure 4.23 (b)*. The semi-major and minor axes for this border case are

$$a_0 = 1{\cdot}199\, r \quad \text{and} \quad b_0 = 0{\cdot}7185\, r$$

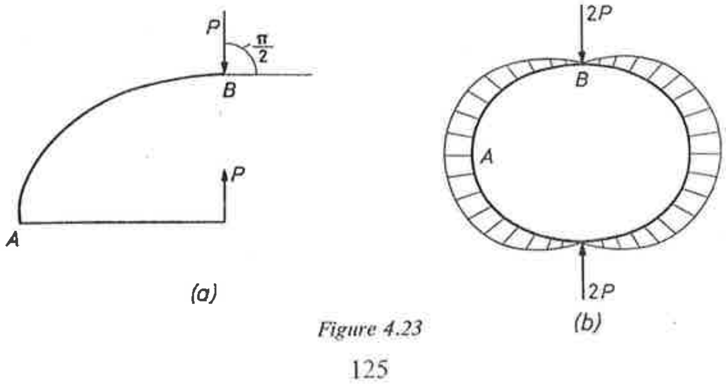

Figure 4.23

If $$0{\cdot}316\frac{EI}{r^2} < P < 1{\cdot}39\frac{EI}{r^2}$$

these axes are calculated from

$$\left.\begin{aligned} a &= 2k[1 - \sqrt{(1 - 1/2p^2)}]/p \\ b &= [2E(p, \phi_B) - F(p, \phi_B)]/k \end{aligned}\right\} \quad (4.71)$$

and

where $$\sin \phi_B = \frac{\sin(\pi/4)}{p}$$

It has been seen that as P increases from $P = 0$ to $P = 1{\cdot}39\ EI/r^2$, the curvature at B varies from $1/r$ to 0. Further increase in P will mean a negative curvature at B, hence the quadrant will have a point of contraflexure. To analyse this case assume that the point of contraflexure is at C (*Figure 4.24*). A straight, flexible bar is placed between A and H and is clamped so that the end tangents at A and H are vertical. The length of the bar has been selected such that there is a point of inflection at C. A load P, acting on a lever, is required to hold ACB in position when the portion BH is removed.

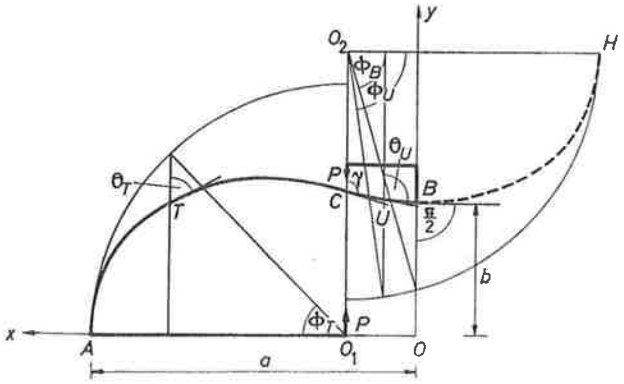

Figure 4.24

The lever is attached at B where, as seen, the tangent is horizontal. Since the only load between A and H acts through C the parts CH and AC are placed symmetrically about C. The full line in *Figure 4.24* is the length of the quadrant, $r\pi/2$. Applying the formulae derived for the undulating elastica and noting that $ACB = ACBH - BH$, one obtains:

$$r\pi/2 = [2K(p) - F(p, \phi_B)]/k \tag{4.72}$$

where $\quad p = \sin(\gamma/2) \quad$ and $\quad \phi_B = \sin^{-1}\left(\dfrac{0{\cdot}707}{p}\right)$

Equation (4.72) will yield p. The main dimensions are

$$\left.\begin{aligned} a &= 2p[1 + \sqrt{(1 - 1/2p^2)}]/k \\ \text{and} \quad b &= [4E(p) - 2K(p) - 2E(p, \phi_B) + F(p, \phi_B)]/k \end{aligned}\right\} \tag{4.73}$$

The coordinates of any point T on ACB can be given in terms of the slope θ once p is known. It will be necessary, however, to distinguish between the line AC and the line CB. For a point lying on AC

$$\left.\begin{aligned} x &= 2p(\cos\phi_B + \cos\phi_T)/k \\ \text{where} \quad \phi_T &= \sin^{-1}\left(\frac{\sin(\theta_T/2)}{p}\right) \\ \text{and} \quad y &= [2E(p, \phi_T) - F(p, \phi_T)]/k \end{aligned}\right\} \tag{4.74}$$

If the point is on portion CB

$$\left.\begin{aligned} x &= 2p(\cos\phi_B - \cos\phi_U)/k \\ \text{and} \quad y &= [4E(p) - 2K(p) - 2E(p, \phi_U) + F(p, \phi_U)]/k \\ \text{where} \quad \phi_U &= \sin^{-1}\left(\frac{\sin(\theta_U/2)}{p}\right) \end{aligned}\right\} \tag{4.75}$$

and $\quad \gamma > \theta > \pi/2$

If P is increased gradually from $p = 0$, a will increase first but will contract past a certain value of P. From equation (4.73) it is seen that a is a function of p, that is,

$$a = \eta(p)$$

hence, a_{max} may be obtained by differentiating $\eta(p)$ with respect to p and equating to zero.

$$\frac{d}{dp}\eta(p) = 1 + \sqrt{(1 - 1/2p^2)} - \frac{1}{2p\sqrt{(p^2 - 1/2)}} = 0$$

This equation is satisfied by $p = (2/3)^{1/2}$, hence $\phi_B = 60°$. The force necessary to cause a_{max} is

$$P = 3{\cdot}33\,\frac{EI}{r^2}$$

This result has been obtained from equation (4.72) by substituting $p = \sin 54°44'$. Further,

$$a_{max} = 1{\cdot}341\ r$$

from equation (4.73).

An important force P is the one which will compress the circle so that B and E are brought into contact (*Figure 4.16* (*c*)). The equation which must be solved for p is

$$b = [4E(p) - 2K(p) - 2E(p, \phi_B) + F(p, \phi_B)]/k = 0$$

The solution of this equation is $p = \sin 58°47'$ and $\phi_B = 55°46{\cdot}4'$. The force necessary to compress the ring is

$$P = 4{\cdot}02\,\frac{EI}{r^2}$$

Remembering that the ring is subject to a force $2P$ it can be seen that the critical load of a strut that has the same length and flexural rigidity as the quadrant and is hinged at both ends, is only $\frac{1}{2}$ per cent less than the force that causes the full compression of the ring. There is also $a = 1{\cdot}34\ r$.

Table 4 gives tabulated values for compressive forces acting on the ring, previously considered for tensile forces (*Table 3*). The corresponding shapes are shown in *Figure 4.25*. The graph in *Figure 4.26* shows the comparison in bending moments between the stiff ring (analysed according to the classical theory) and the initially

Table 4. Force, modulus and coordinates of the ring; ring in compression[7]

Shape	$\sin^{-1} p$	P (lb)	h (in.)	a (in.)	b (in.)	M'_A (lb in.)	M'_B (lb in.)	M^*_A (lb in.)	M^*_B (lb in.)	Remarks
1	37°30′	0·02	103·6	10·12	9·80	−2·072	−1·87	−0·072	+0·13	Nodal elastica
2	90°	0·063	35·6	10·38	9·50	−2·23	−1·59	−0·23	+0·41	$P = 0{\cdot}316EI/r^2$
3	85°	0·0638	35·2	10·40	9·48	−2·24	−1·58	−0·24	+0·42	
4	80°	0·0656	34·4	10·45	9·45	−2·26	−1·57	−0·26	+0·43	
5	70°	0·0743	30·8	10·51	9·39	−2·29	−1·51	−0·29	+0·49	No point of inflection (shapes 2–8)
6	60°	0·094	25·3	10·68	9·25	−2·38	−1·375	−0·38	+0·625	
7	55°	0·113	21·8	10·80	8·91	−2·46	−1·24	−0·46	+0·76	
8	45°	0·278	11·99	11·99	7·19	−3·31	0·00	−1·31	+2·00	$P = 1{\cdot}39EI/r^2$
9	50°	0·52	9·50	13·16	3·76	−4·94	+1·90	−2·94	+3·90	
10	54°44′	0·666		13·41						$a = a_{max}$, $P = 3{\cdot}33EI/r^2$
11	55°	0·677	8·90	13·40	2·10	−6·03	+2·98	−4·03	+4·98	
12	58°47′	0·804	8·55	13·39	0·00					$b = 0$, $P = 4{\cdot}02EI/r^2$
13	60°	0·845	8·44	13·31	−0·493	−7·13	+4·11	−5·13	+6·11	
14	70°	1·328	7·29	12·09	−4·30	−9·70	+6·38	−7·70	+8·38	Point of inflection between A and B (shapes 9–16)
15	80°	2·36	5·74	9·74	−7·85	−13·5	+9·44	−11·5	+11·44	
16	85°	3·72	4·62	7·87	−9·62	−17·2	+12·1	−15·2	+15·1	

* M'_A and M'_B apply to a ring having an initial bending moment of $EI/r = -2{\cdot}00$ lb in. at every point; M_A and M_B apply to an initially stressless ring.

stressless flexible ring (analysed within the nonlinear framework). The straight lines referring to the stiff ring are valid for all rings with $r = 10$ in., while the curves apply to a particular ring only (the one given in the example), since the deformations and hence the

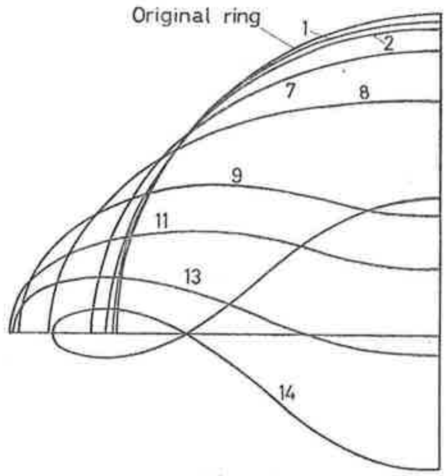

Figure 4.25

moments depend on $\sqrt{(P/EI)}$. The smaller this value the more closely will the curves approach the straight lines.

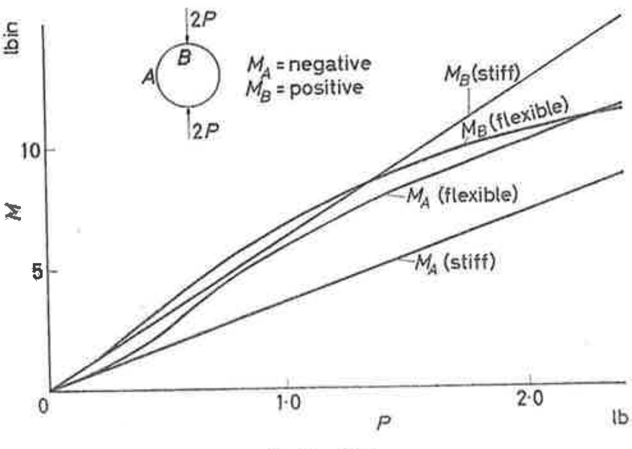

Figure 4.26

The functions $Pr^2/EI = f_1(a/r)$ and $Pr^2/EI = f_2(b/r)$ are plotted in *Figure 4.27* showing the relationship between load and deflection.

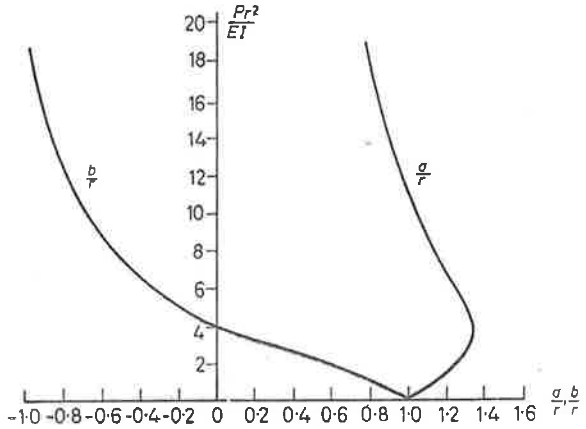

Figure 4.27

4.8. Approximate Analysis of the Circular Ring

Let the dotted line in *Figure 4.28* represent the left half of the unloaded circle bent from a straight bar, and let the heavy line *ACB* represent the deformed shape of the left half of the ring under tensile forces acting at *A* and *B*. For moderate loads the radial deviation of the elastic line from the circular arc is small. This arc has a radius R and length $r\pi$ and passes through A and B. The central angle of this arc is 2σ. The radial deflection y is found from

$$\frac{d^2y}{d\phi^2} + y = -\frac{R^2}{EI} M_\phi \tag{4.76}$$

If b is given, the radius of the auxiliary circle R and its central angle can be obtained from $2\sigma R = r\pi$, and $b = R \sin \sigma$, where r is the radius of the closed ring.

The problem is to find the force P. The elastic shape of the half ring in *Figure 4.28* may be conceived as follows. On a straight bar $r\pi$ long, the end moments

$$M_1 = \frac{EI}{R} - \frac{2EI}{r\pi}\sigma$$

are acting, which will bend the bar into an arc of radius R between A and B. This circular arc, hinged at A and B, is now subject to further couples at the ends. These moments M_2 (which turn the same way as M_1) are selected such that the end tangents of the arc become horizontal, and the vertical forces that have been created during this second rotation are identical with those acting on the elastic shape[5].

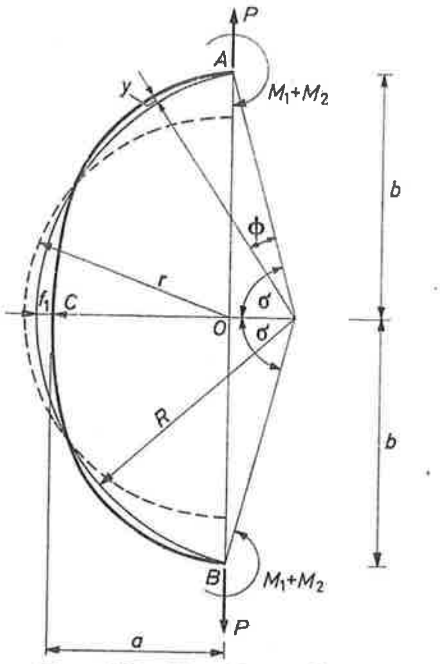

Figure 4.28 (From Sonntag[5])

The strain energy in bending stored in the bar during this second rotation is:

$$U = \frac{1}{2EI}\int_0^{\sigma}(M_{2\phi})^2\,R\,d\phi$$

where $$M_{2\phi} = M_2 - PR\left[\cos(\sigma-\phi) - \cos\sigma\right]$$

The statically indeterminate force P and the moment M_2 can be obtained by Castigliano's theorem, according to which

$$\frac{\partial U}{\partial P} = 0 \quad \text{and} \quad \frac{\partial U}{\partial M_2} = \pi/2 - \sigma$$

This calculation leads to

$$\frac{Pr^2}{EI} = \frac{4\sigma^2(\sin\sigma - \sigma\cos\sigma)(\pi/2 - \sigma)}{\pi^2(\sigma/4)\sin 2\sigma - \sin^2\sigma + \sigma^2/2} \tag{4.77}$$

The horizontal semi-axis a can be obtained from

$$a = \frac{r\pi}{2\sigma}(1 - \cos\sigma) - f_1$$

where f_1 is a *small deflection*.

We find that $f_1 = \dfrac{r\pi}{2\sigma}\left(\dfrac{2Pr^2}{EI}\dfrac{\Lambda_2}{\sigma^2} - \alpha\Lambda_4\sin^2\sigma\right)$

where
$$\alpha = \frac{Pr^2}{EI}\frac{\pi^2}{4}\frac{\Lambda_1}{\sigma^2\sin^2\sigma} + \frac{(\pi/2) - \sigma}{\sigma}$$
$$= \left(\frac{\Lambda_1^2}{\Lambda_3\sigma\sin^4\sigma - \Lambda_1^2} + 1\right)\left(\frac{\pi}{2\sigma} - 1\right)$$

and Λ_1, Λ_2, and Λ_4 are as in section 3.1.
We have thus expressed a as a function of σ. The bending moment at any cross section ϕ is

$$M_\phi = M_1 + M_{2\phi}$$

or
$$M_\phi = \frac{EI}{r}\left\{\frac{2\sigma}{\pi}(1 + \alpha) - \frac{Pr^2}{EI}\frac{\pi}{2\sigma}\left[\cos(\sigma - \phi) - \cos\sigma\right]\right\}$$

The expression for the moment at A ($\phi = 0$) is

$$M_A = \frac{2EI}{r\pi}(1 + \alpha)\sigma$$

This bending moment becomes zero for $\alpha = -1$, hence

$$\frac{\Lambda_1}{\Lambda_3\sin^4\sigma} = \pi/2 \tag{4.78}$$

The smallest root of equation (4.78) is $\sigma = 1{\cdot}98$. From equation (4.77)

$$\frac{Pr^2}{EI} = 1{\cdot}464$$

The rigorous investigation has shown that the curvature (and bending moment) is zero for a compressive force $P = 1{\cdot}39\ EI/r^2$, hence the approximate result is only 5 per cent above the correct value.

The approximate analysis may be used in both tension and compression, provided

$$\frac{Pr^2}{EI} < 1{\cdot}464$$

It cannot be applied for shapes with a point of contraflexure.

4.9. Flexible Ring Compressed between Plates

Suppose that instead of a point load $2P$ the ring is being compressed between two horizontal plates (*Figure 4.29* (*a*)). For a force $P < 1{\cdot}39\ EI/r^2$, the plates will touch the circle tangentially in one point only. Once $P > 1{\cdot}39\ EI/r^2$ the deflected shape of the quadrant will consist of the straight portion t in contact with the plates and the curved part whose length is $L_{r0} = r\pi/2 - t$. The reaction

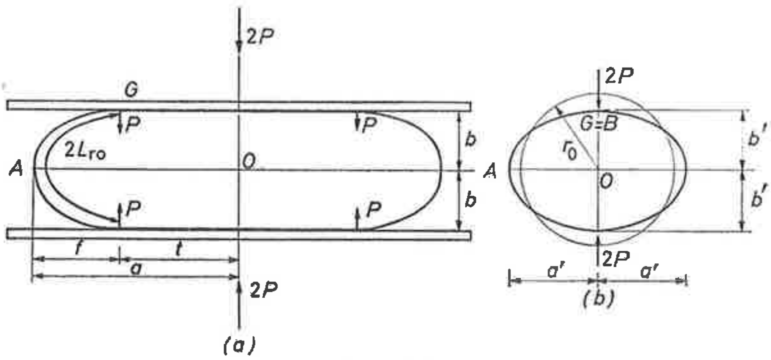

Figure 4.29

between plate and ring is P and this force acts at G, the end of the straight section. Imagine now that there is a circular bar of the same EI but with a circumference $4L_{r0}$. The radius of this reduced ring is then

$$r_0 = r - 2t/\pi$$

Let this ring be compressed by two radial forces until the curvature becomes zero at the point of application of the force. The elastic shape corresponding to this load is shown in *Figure 4.29 (b)*. It is obvious that the quadrant of the reduced ring of radius r_0 is identical with the free elastic line L_{r0} of the ring between the plates[5]. The reduced ring has zero curvature at B if $Pr^2/EI = 1{\cdot}39$, hence

$$\frac{Pr^2}{EI}\left[1 - \frac{4}{\pi}\cdot\frac{t}{r} + \frac{4}{\pi^2}\cdot\frac{t^2}{r^2}\right] = 1{\cdot}39$$

The solution of this quadratic in t/r yields

$$\frac{t}{r} = \frac{\pi}{2}\left[1 - 1{\cdot}18\left(\frac{EI}{Pr^2}\right)^{\frac{1}{2}}\right]$$

From the expression for the radius of the reduced ring

$$\frac{t}{r} = \frac{\pi}{2}\left(1 - \frac{r_0}{r}\right)$$

hence

$$\frac{r_0}{r} = 1{\cdot}18\left(\frac{EI}{Pr^2}\right)^{\frac{1}{2}} \tag{4.79}$$

It may be shown (section 4.6) that when the curvature is zero at B,

$$\frac{b}{r} = 0{\cdot}7185$$

For the reduced ring $\dfrac{b'}{r_0} = 0{\cdot}7185,$

hence

$$\frac{b'}{r} = 0{\cdot}846\left(\frac{EI}{Pr^2}\right)^{\frac{1}{2}} \quad \text{or} \quad P = \frac{0{\cdot}7157}{(b')^2}EI \tag{4.80}$$

Finally

$$\frac{a}{r} = \frac{t}{r} + \frac{f}{r_0}\cdot\frac{r_0}{r} = \frac{\pi}{2} - 0{\cdot}441\left(\frac{EI}{Pr^2}\right)^{\frac{1}{2}}$$

since

$$\frac{a'}{r_0} = \frac{f}{r_0} = 1{\cdot}199$$

when the curvature at B is zero.

The most important equation is (4.79) since this shows the transformation from the basic ring to the reduced ring. Once r_0 is known, all slopes and coordinates can be calculated as in the basic ring if we write $r = r_0$, and $p = \sin(\pi/4)$, and use the equations of the oval shape. An adjustment has to be made in the abscissae to allow for t.

The maximum bending moment occurs at A and equals

$$M_A = \sqrt{2PEI} \tag{4.81}$$

The nondimensional values of a/r and b/r are plotted in *Figure 4.30* as a function of Pr^2/EI.

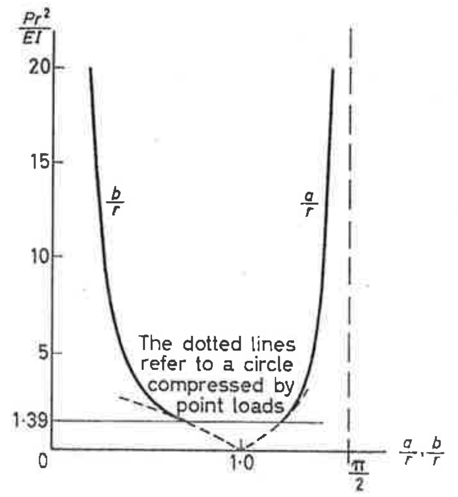

Figure 4.30

4.10. Leaf Spring

Two identical, circular leaf springs, $2L$ long, face each other (*Figure 4.31*), and are attached by means of frictionless hinges. The forces $2P$ act halfway between A and C. Dealing with tensile forces first, consider the upper right-hand bar fixed at B and carrying P at the free end. The initially circular bar is now replaced with a straight one, to which the force on a lever (*Figure 4.32*) is applied. The transformation of the cantilever into a basic strut is shown on *Figure 4.32*. At the outset a small load is applied at the end of the rigid bar. Since $e = 1/rk^2$, where r is the radius of the springs, and

$k = \sqrt{P/EI}$, a small load means a large lever and hence, at the beginning at least, a nodal elastica has to be considered.

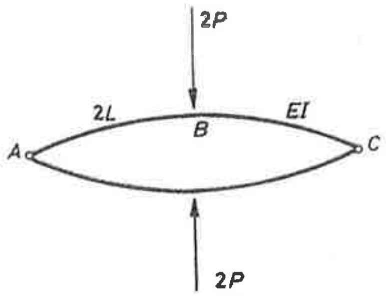

Figure 4.31

The equation for the solution of p is

$$L = p[F(p, \theta_C/2) - F(p, \pi/4)]/k \tag{4.82}$$

where $$\sin(\theta_C/2) = \left[\left(\frac{1}{p}\right)^2 - \left(\frac{1}{2kr}\right)^2\right]^{\frac{1}{2}}$$

This follows from

$$e = \frac{1}{rk^2} = \frac{2}{kp}[1 - p^2 \sin^2(\theta_C/2)]^{\frac{1}{2}}$$

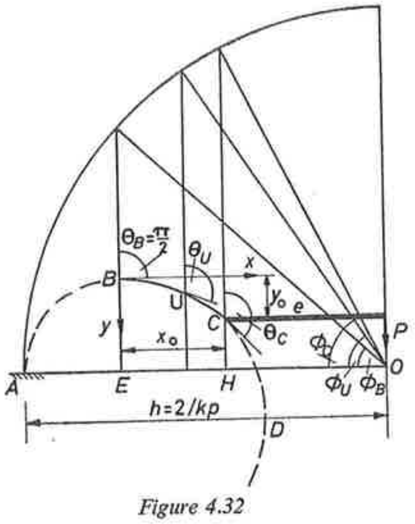

Figure 4.32

Regarding the range of the applicability of equation (4.82) it is noted that a gradually increasing P will lead to a shortening of e and to an increase of θ_C. It can be said, therefore, that by increasing P gradually, C will move toward D in *Figure 4.32*, and θ_C will tend to π. In this case

$$e = \frac{2}{kp}(1 - p^2)^{\frac{1}{2}}$$

hence

$$p = \frac{2rk}{[1 + (2rk)^2]^{\frac{1}{2}}} \tag{4.83}$$

The relationship between p and k is given by

$$L = p[K(p) - F(p, \pi/4)]/k \tag{4.84}$$

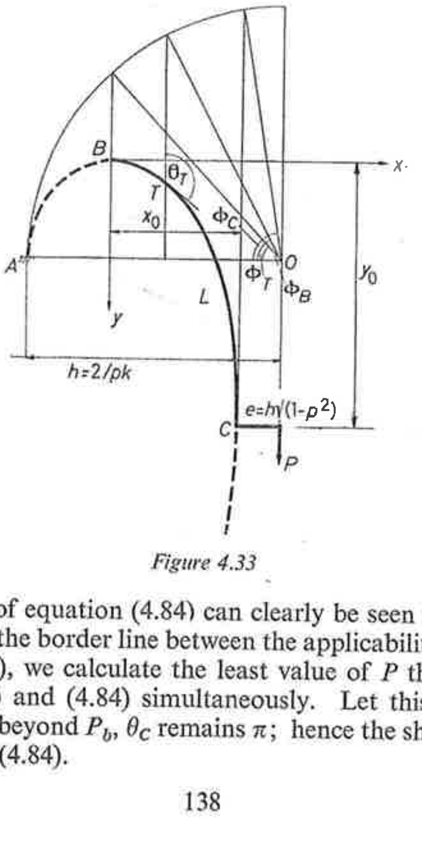

Figure 4.33

The derivation of equation (4.84) can clearly be seen in *Figure 4.33*. In order to find the border line between the applicability of equations (4.84) and (4.82), we calculate the least value of P that will satisfy equations (4.83) and (4.84) simultaneously. Let this value be P_b. By increasing P beyond P_b, θ_C remains π; hence the shape is governed by equation (4.84).

The slopes and coordinates of any point can now be expressed in terms of the arc lengths s by using the equations of the nodal elastica. Of particular interest are x_0 and y_0. For $P < P_b$

$$\left.\begin{aligned} x_0 &= 2[(1-p^2/2)^{\frac{1}{2}} - p/2rk]/kp \\ y_0 &= 2\{E(p,\pi/4) - E(p,\theta_C/2) + \\ &\quad + (1-p^2/2)[F(p,\theta_C/2) - F(p,\pi/4)]\}/kp \end{aligned}\right\} \qquad (4.85)$$

where $\theta_C/2$ may be found from equation (4.82).

If $P > P_b$, the coordinates of C are

$$\left.\begin{aligned} x_0 &= 2[(1-p^2/2)^{\frac{1}{2}} - p/2rk]/kp \\ y_0 &= 2\{E(p,\pi/4) - E(p) + (1-p^2/2) \times \\ &\quad \times [K(p) - F(p,\pi/4)]\}/kp \end{aligned}\right\} \qquad (4.86)$$

If the spring is in compression the force P will act upward (*Figure 4.34*), hence the rigid lever points to the opposite direction as shown

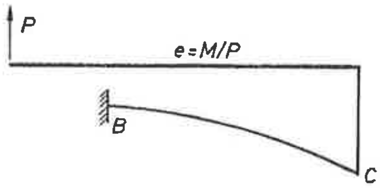

Figure 4.34

in *Figure 4.32*. Beginning with a small force P, the large lever arm e will turn the cantilever into a segment of a nodal elastica as shown in *Figure 4.35*. The connection between length and modulus is

$$L = p[F(p,\pi/4) - F(p,\theta_C/2)]/k$$

in which

$$\sin(\theta_C/2) = \left[\left(\frac{1}{p}\right)^2 - \left(\frac{I}{2kr}\right)^2\right]^{\frac{1}{2}} \qquad (4.87)$$

Gradual increase of P will cause it to move toward C (*Figure 4.35*) and will lead to an increase of p. The limit is reached when $p = 1$. Then, from equation (4.87),

$$L = \left\{F(\pi/2,\pi/4) - F\left[\pi/2, \cos^{-1}\left(\frac{1}{2rk}\right)\right]\right\}\Big/k$$

or

$$0{\cdot}8814 - L\left(\frac{P_b'}{EI}\right)^{\frac{1}{2}} = \lambda\left\{\cos^{-1}\left[\frac{1}{2r}\left(\frac{EI}{P_b'}\right)^{\frac{1}{2}}\right]\right\} \qquad (4.88)$$

Equation (4.88) will yield P'_b, the tensile force representing the border case between the nodal and the undulating elastica[10].

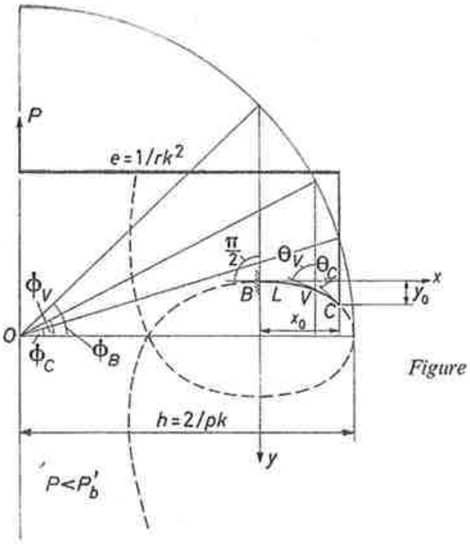

Figure 4.35

When P increases past P'_b, two cases will have to be considered separately; in the first, the line of action of P, due to the shortening

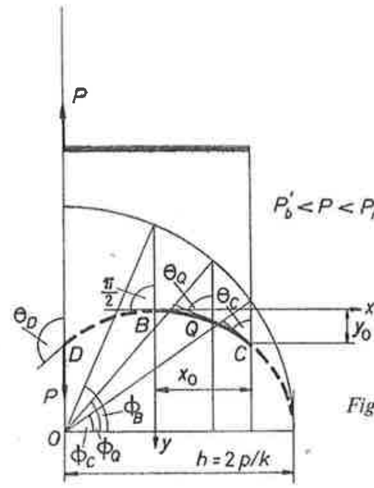

Figure 4.36

of e, intersects the imaginary extension of the elastic line (*Figure 4.36*) and in the second case, due to further decrease of e, P will intersect the bar itself (*Figure 4.37*). The border line between the two cases shown in *Figures 4.36* and *4.37* is reached when P acts through B (*Figure 4.38*). We have then

$$L = [K(\pi/4) - F(\pi/4, \phi_C)]/k \tag{4.89}$$

where $\quad \cos\phi_C = 1/rk\sqrt{2}$

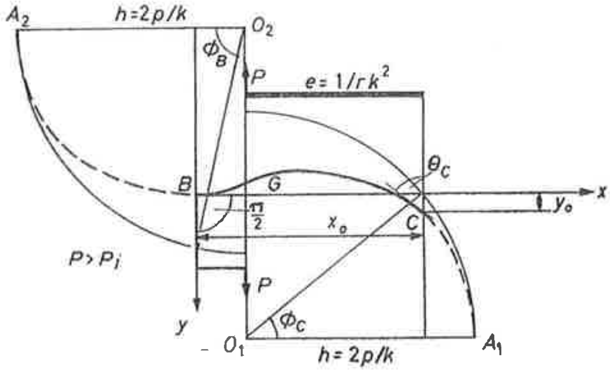

Figure 4.37

Equation (4.89) was obtained by considering that for the case shown in *Figure 4.38*

$$p = \frac{\sqrt{2}}{2}, \quad \text{and} \quad \frac{1}{rk^2} = \frac{2p}{k}\cos\phi_C$$

We need the unknown k in equation (4.89) to establish $P = P_i$, the border load between the two possible shapes in *Figures 4.36* and *4.37*. For the solution of P_i we have

$$L\left(\frac{P_i}{EI}\right)^{\frac{1}{2}} = 1{\cdot}8541 - F\left\{\pi/4, \cos^{-1}\left[\frac{1}{r}\left(\frac{EI}{2P_i}\right)^{\frac{1}{2}}\right]\right\} \tag{4.90}$$

It is clear, therefore, that in the compressed stage the force P falls into three ranges, namely

$$0 < P \leqslant P_b'$$

$$P_b' < P \leqslant P_i$$

and $\quad P > P_i$

If $0 < P \leqslant P_b'$, the coordinates of C are

$$x_0 = 2[p/2rk - \sqrt{(1 - p^2/2)}]/kp$$

and
$$y_0 = \frac{2}{kp}\{E(p, \pi/4) - E(p, \theta_C/2) + (1 - p^2/2)[F(p, \theta_C/2) - F(p, \pi/4)]\}$$

where $\theta_C/2$ and p are found from equation (4.87).

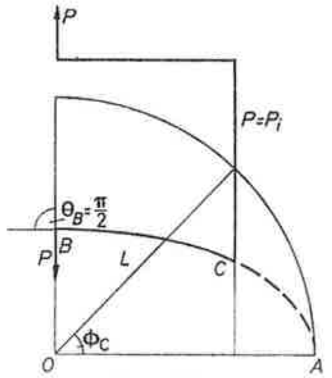

Figure 4.38

For other coordinates or slopes the basic equations of the nodal elastica may be used.

If $P_b' < P < P_i$, the elastic shape will be an undulating elastica without a point of contraflexure. The modulus of this shape can be obtained from the solution of

$$L = \frac{1}{k}\left\{F\left[p, \sin^{-1}\left(\frac{0{\cdot}707}{p}\right)\right] - F\left[p, \cos^{-1}\left(\frac{1}{2rkp}\right)\right]\right\} \quad (4.91)$$

and the coordinates of C are

$$\left.\begin{aligned} x_0 &= 2p[1/2rkp - (1 - 1/2p^2)^{\frac{1}{2}}]/k \\ \text{and} \quad y_0 &= [2E(p, \phi_B) - F(p, \phi_B) + F(p, \phi_C) - 2E(p, \phi_C)]/k \\ \text{where} \quad \cos\phi_B &= (1 - 1/2p^2)^{\frac{1}{2}}, \text{ and } \cos\phi_C = 1/2rkp \end{aligned}\right\} \quad (4.92)$$

If finally, $P > P_i$, the spring will have a point of contraflexure at G (*Figure 4.37*). The elastic line A_2BGCA_1 is symmetrical about G, hence the modulus p is the same for both parts. This modulus will be evaluated from

$$L = [2K(p) - F(p, \phi_B) - F(p, \phi_C)]/k \tag{4.93}$$

where $\phi_B = \sin^{-1}\left(\frac{0\cdot707}{p}\right)$ and $\phi_C = \cos^{-1}\left(\frac{1}{2rkp}\right)$

The coordinates of C are

$$\left.\begin{aligned} x_0 &= 2p(1/2rkp + \cos\phi_B)/k \\ \text{and} \quad y_0 &= [4E(p) - 2E(p, \phi_B) - 2E(p, \phi_C) - Lk]/k \end{aligned}\right\} \tag{4.94}$$

The force that is needed to press the springs together until they touch at B (*Figure 4.31*) may be obtained from the simultaneous solution of equation (4.93) and

$$4E(p) - 2E\left[p, \sin^{-1}\left(\frac{0\cdot707}{p}\right)\right] = Lk + 2E\left[p, \cos^{-1}\left(\frac{1}{2rkp}\right)\right] \tag{4.95}$$

Having found p and $k = k_0$ from these two equations,

$$2P_0 = 2k_0^2 EI$$

will close the springs.

All equations discussed in this article have been derived for the end slope and end coordinates. In a similar manner, by selecting any slope θ, the corresponding parameter ϕ and hence the arc length s and the coordinates of the corresponding point may be calculated.

As an example, the behaviour of a spring having the following data will be investigated:

$$r = 7\cdot5 \text{ in.}, \; L = 6\cdot5 \text{ in.}, \text{ and } EI = 10 \text{ lb in.}^2$$

For the case of tensile forces, one finds that $P_b = 0\cdot995$ lb (from equations 4.83 and 84). By separating the tensile forces into $P < 0\cdot995$ and $P > 0\cdot995$, the shapes in the tensile region can be worked out. The loads and coordinates are tabulated in *Table 5* and the shapes corresponding to the different loads are shown in *Figure 4.39*.

Table 5. Force, modulus, and coordinates of the spring: spring in tension[19]

Shape	P (lb)	p	θ_C	x_0 (in.)	y_0 (in.)	h (in.)	Remarks
0	0·00	sin 0°	139°36′	5·71	2·636	∞	Original circle
1	0·0143	sin 30°	140°22′	5·64	2·661	105·8	p and P have been calculated from equation (4.82)
2	0·056	sin 50°	144°54′	5·51	3·00	34·9	
3	0·078	sin 55°	147°12′	5·43	3·14	27·66	
4	0·111	sin 60°	150°18′	5·31	3·29	21·85	
5	0·165	sin 65°	153°48′	5·11	3·66	17·18	
6	0·275	sin 70°	160°00′	4·74	3·84	12·83	
7	0·578	sin 75°	172°08′	3·98	4·54	8·61	
8	0·995	sin 78°	180°00′	3·52	4·88	6·48	
9	1·18	sin 80°	180°00′	3·37	4·97	5·92	p and P have been calculated from equation (4.84)
10	2·05	sin 85°	180°00′	2·38	5·17	4·42	
11	4·9	sin 89°	180°00′	1·75	5·67	2·86	
12	8·99	sin 89°48′	180°00′	1·34	5·85	2·11	
13	11·07	sin 89°54′	180°00′	1·22	5·96	1·90	

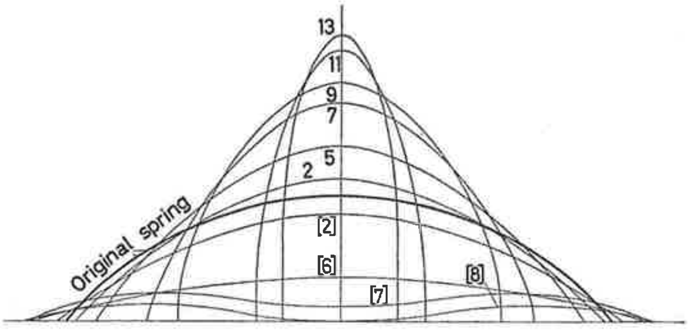

Figure 4.39

For the case of compressive loads, the ranges are as follows:

$$0 < P \leqslant 0{\cdot}0525 \text{ lb} = P_b'$$
$$0{\cdot}0525 \text{ lb} < P \leqslant 0{\cdot}208 \text{ lb} = P_t$$
$$P > 0{\cdot}208 \text{ lb}$$

These values of P have been found from equations (4.88 and 90). The loads and coordinates are tabulated in *Table 6* and the shapes corresponding to the different loads are shown in *Figure 4.39.* To facilitate numerical work in both the tensile and compressive regions, the modulus p has been assumed at certain values and the corresponding value of P calculated.

Table 6. Force modulus, and coordinates of the spring: spring in compression[10]

Shape	P (lb)	p	x_0 (in.)	y_0 (in.)	h (in.)	Remarks
1	0·0373	sin 60°	5·84	2·40	37·8	Nodal elastica
2	0·0525	sin 90°	5·90	2·25	27·6	
3	0·0545	sin 80°	5·91	2·22	26·7	Undulating elastica with no point of contraflexion
4	0·0614	sin 70°	5·92	2·195	23·98	
5	0·0760	sin 60°	6·11	2·15	19·88	
6	0·208	sin 45°	6·40	0·95	9·80	
7	0·275	sin 46°	6·44	0·32	8·66	Undulating elastica with point of contraflexion
8	0·312	sin 47°10′	6·48	0·00	8·30	

4.11. Semicircular Ring Fixed at both Ends

In the problems discussed in this chapter we have investigated shapes having one point of contraflexure. The circular ring, it is true, had four points of contraflexure when compressed beyond a certain stage, but because of symmetry the problem reduced to one with one inflection point only. There are problems, however, where the number of inflection points is more than one. Take, for example, the semicircular ring in *Figure 4.40* (*a*), clamped at both ends and carrying a compressive load $2P$ applied at the axis of symmetry. A

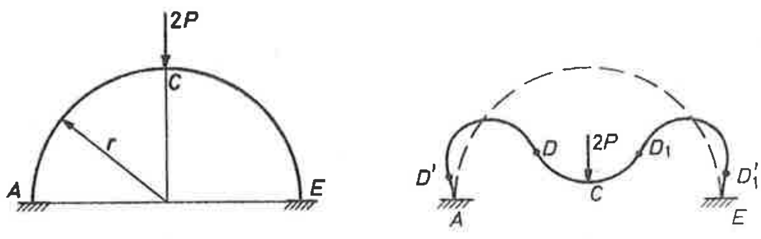

(*a*) (*b*)

Figure 4.40

method, employing slowly converging series, was used by Biezeno and Koch[11], and also by Wijngaarden[3], for the solution of this problem. The present discussion will take advantage of the geometrical properties of the compressed ring. It will be realized that at a certain stage the deflected shape has four points of contraflexure, but now, unlike the problem in section 4.7, there are two quadrants only, hence each will have two inflection points (*Figure 4.40* (*b*)).

The investigation is commenced by applying a small load. Let AC be the deformed shape of the quadrant (*Figure 4.41*). The deformed shape must fulfil the following conditions: its length remains $r\pi/2$, the slope at C is horizontal and AQ equals the radius

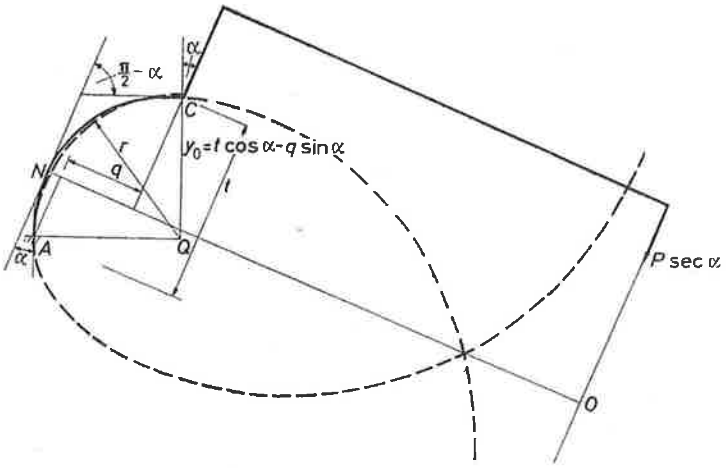

Figure 4.41

r. In order to satisfy the second and third conditions, a couple M and a horizontal force H is needed at C. The presence of P and H means that the force acting at C is inclined at an angle α to the vertical and the combined effect of this inclined load and the couple M is equivalent to a force $P \sec \alpha$ acting on a rigid lever (*Figure 4.41*). For small P the lever is large, hence the portions NC and NA are segments of a nodal elastica placed symmetrically about the base NO. The relationship between the modulus of the shape and the length of the quadrant is expressed by

$$r\pi/2 = p\{F[p,(\pi/4 - \alpha/2)] + F(p,\alpha/2)\}/k \tag{4.96}$$

where $$k = \left(\frac{P \sec \alpha}{EI}\right)^{\frac{1}{2}}$$

This equation has two unknowns, p and α. The second equation will stipulate that $AQ = r$. It is seen from *Figure 4.41* that

$$r = t \sin \alpha + q \cos \alpha \tag{4.97}$$

Here, t and q are the sum and the difference of the vertical and horizontal coordinates of C and A with respect to the base line NO and can be expressed as functions of p and α by applying the basic equations of the nodal elastica.

If the load increases from $P = 0$, the modulus will vary from zero until it reaches its maximum value of unity.

The force P that causes the modulus to become unity (in the nodal shape) will mark the end of the applicability of equations (4.96 and 97).

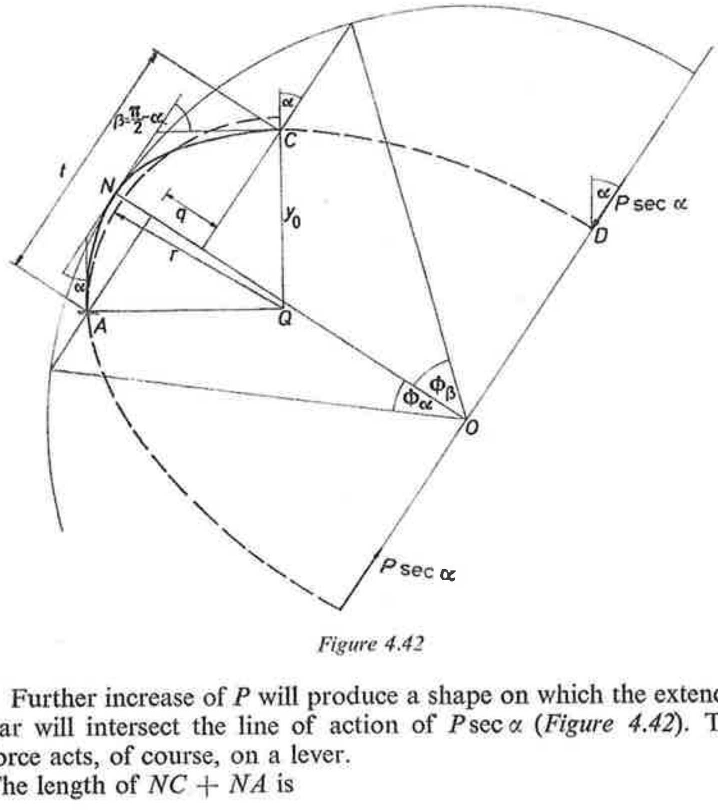

Figure 4.42

Further increase of P will produce a shape on which the extended bar will intersect the line of action of $P \sec \alpha$ (*Figure 4.42*). This force acts, of course, on a lever.

The length of $NC + NA$ is

$$r\pi/2 = [F(p, \phi_\beta) + F(p, \phi_\alpha)]/k \qquad (4.98)$$

in which $k = \left(\dfrac{P \sec \alpha}{EI}\right)^{\frac{1}{2}}$, $\phi_\alpha = \dfrac{\sin(\alpha/2)}{p}$ and $\phi_\beta = \dfrac{\sin(\pi/4 - \alpha/2)}{p}$

The second equation is again

$$r = t \sin \alpha + q \cos \alpha$$

t and q having the same meaning as before, but now the coordinates of C and A are calculated from the equations of the undulating elastica.

The shape in *Figure 4.42* requires a decreasing p for an increasing $P \sec \alpha$. This force moves gradually toward C and will eventually reach it. When this happens (*Figure 4.43*) the curvature at C is zero, hence further deflection will introduce a point of contraflexure near C. Since in this case $p = \sin(\pi/4 - \alpha/2)$, the range of the inflectionless undulating elastica is

$$1 > p > \sin(\pi/4 - \alpha/2)$$

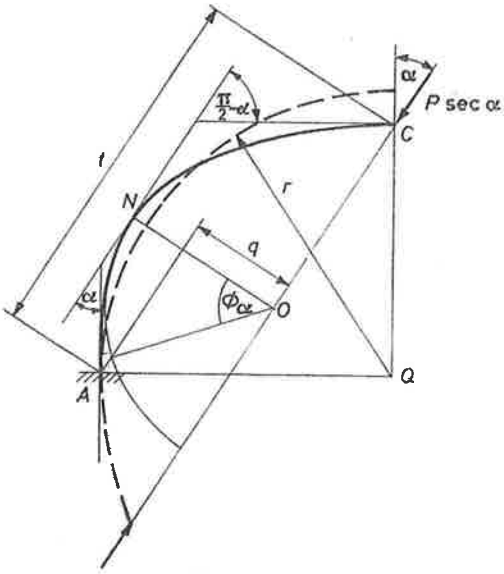

Figure 4.43

The force giving zero curvature at C may be obtained by solving

$$r\pi/2 = [K(p) + F(p, \phi_\alpha)]/k$$

where $\quad p = \sin(\pi/4 - \alpha/2) \quad$ and $\quad \sin \phi_\alpha = \dfrac{\sin(\alpha/2)}{\sin(\pi/4 - \alpha/2)}$

With an increase in the load a stage is reached where a point of inflection occurs near the load (*Figure 4.44*). The governing equation is

$$r\pi/2 = [2K(p) - F(p, \phi_{\pi/2-\alpha}) + F(p, \phi_\alpha)]/k \qquad (4.99)$$

with the second equation expressing again $AQ = r$. This shape with one point of inflection will last until the increase of P and α will

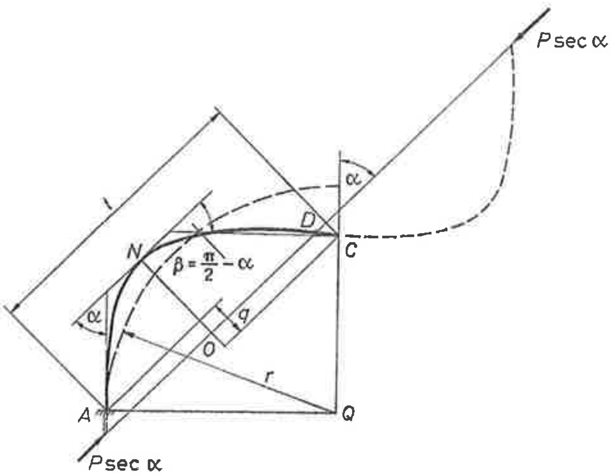

Figure 4.44

cause the line of action of $P \sec\alpha$ to pass through A. If this line of action tilts any more due to increase in α, the deflected shape will have two points of contraflexure. Therefore, equation (4.99) can be used for values of p

$$\sin(\pi/4 - \alpha/2) < p < \sin(\alpha/2)$$

The shape of the deflected ring having two points of contraflexure is shown in *Figure 4.45*. This stage will last with increasing deflections until p reaches its maximum value (somewhere between $\sin(\alpha/2)$ and 1) and thereupon drops back to $p = \sin(\alpha/2)$. The second point of inflection near A will stay only as long as the line of action of $P \sec\alpha$ intersects the deflected shape at two points.

Increasing deflection of C means that $P \sec \alpha$ will pass below A (*Figure 4.46*) so that the point of inflection near A will travel back again toward the fixed end and then disappear. In *Figure 4.45* the equations needed for the solution of p and α are

$$\left.\begin{aligned} & r\pi/2 = [4K(p) - F(p, \phi_\alpha) - F(p, \phi_\beta)]/k \\ \text{and} \quad & t \sin \alpha + q \cos \alpha = r \\ \text{where} \quad & \sin \phi_\alpha = [\sin(\alpha/2)]/p, \ \sin \phi_\beta = [\sin(\pi/4 - \alpha/2)]/p, \end{aligned}\right\} \quad (4.100)$$

$$t = \{8E(p) - 4K(p) - [2E(p, \phi_\alpha) - F(p, \phi_\alpha)] - \\ - [2E(p, \phi_\beta) - F(p, \phi_\beta)]\}/k,$$

and

$$q = 2p(\cos \phi_\beta - \cos \phi_\alpha)/k$$

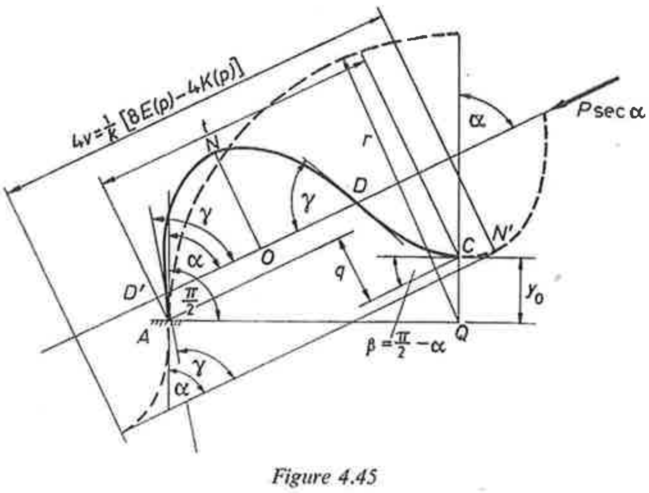

Figure 4.45

The deflection of C is $\qquad y_0 = t \cos \alpha - q \sin \alpha \qquad (4.101)$

As mentioned before, in the stage with two inflection points, p begins with $p = \sin(\alpha/2)$, reaches p_{max} and falls back to $\sin(\alpha/2)$. The second point of contraflexure (near A) disappears then and the deformed shape has once more one inflection point only (*Figure*

4.46). This last stage is marked by a decreasing modulus and an increasing P. The governing equation is

$$
\left.
\begin{aligned}
r\pi/2 = \Big\{2K(p) + F\Big[p, \sin^{-1}\Big(\frac{\sin(\alpha/2)}{p}\Big)\Big] - \\
- F\Big[p, \sin^{-1}\Big(\frac{\sin(\pi/4 - \alpha/2)}{p}\Big)\Big]\Big\}\Big/k \\
\text{while, again,} \quad r = t\sin\alpha + q\cos\alpha
\end{aligned}
\right\} \quad (4.102)
$$

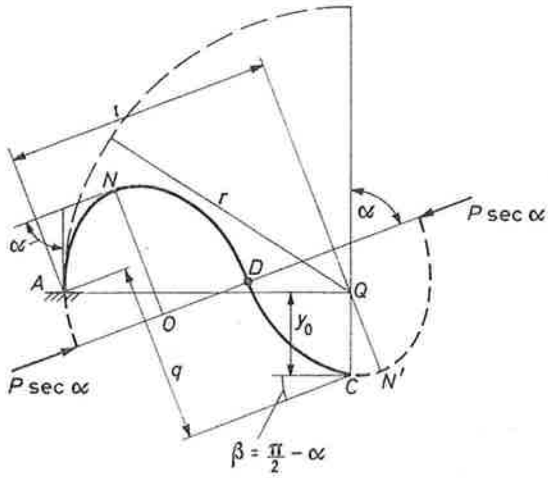

Figure 4.46

4.12. Numerical-Analysis of Curved Bars with Point Loads

It has been pointed out in section 4.1 that the differential equation governing the deflection of bars is not readily solved except for straight and circular bars. When the shape of the unloaded bar falls into neither of the above-mentioned categories, closed form solutions are extremely difficult to get and hence numerical methods will have to be employed[12]. In accordance with the conventional analysis,

$$\frac{1}{r} = \frac{M}{EI} + \frac{1}{R}$$

where r is the radius of curvature of the loaded shape, and R is the radius of the unloaded bar.

Consider the bar as initially straight and that the elastic shape is as shown in *Figure 4.47*. Replace the axis of the bent bar by a set

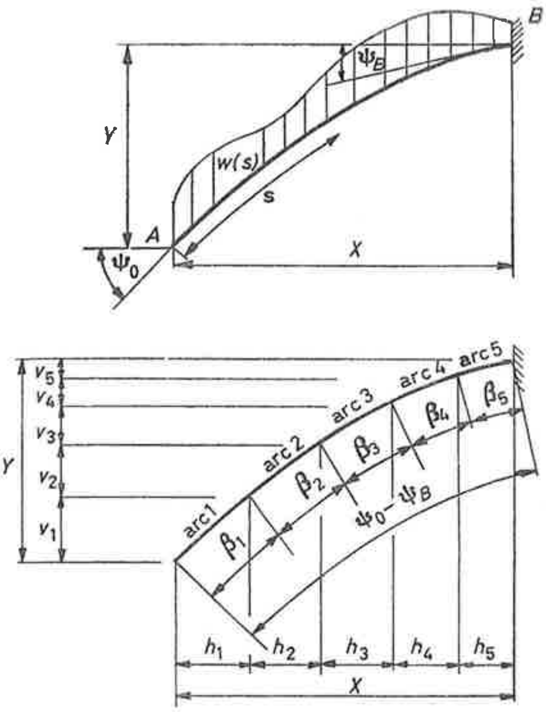

Figure 4.47 (From Seames and Conway[12])

of n circular arcs tangential to one another at the points of intersection. Then, from the geometry of an elemental arc we have for the ith element (*Figure 4.48*)

$$\left.\begin{aligned} \frac{1}{r_i} &= \frac{M_i'}{EI} \\ s_i &= \beta_i r_i \\ h_i &= r_i\left[\sin\left(\psi_0 - \sum_{j=1}^{i-1}\beta_j\right) - \sin\left(\psi_0 - \sum_{j=1}^{i}\beta_j\right)\right] \\ v_i &= r_i\left[\cos\left(\psi_0 - \sum_{j=1}^{i}\beta_j\right) - \cos\left(\psi_0 - \sum_{j=1}^{i-1}\beta_j\right)\right] \end{aligned}\right\} \quad (4.103)$$

For n arcs the subscript i takes all values from 1 to n beginning at the free end. M_i' is the average bending moment and depends on the type of loading.

The numerical work is commenced by assuming a value ψ_0 for the end slope; after that h_1, h_2, etc., are selected arbitrarily. r_i, β_i, v_i, and s_i are calculated from equation (4.103). The loaded shape is determined from

$$\left.\begin{aligned} Y &= \sum_{j=1}^{n} v_j \\ X &= \sum_{j=1}^{n} h_j \\ L &= \sum_{j=1}^{n} s_j \\ \psi_0 - \psi_B &= \sum_{j=1}^{n} \beta_j \end{aligned}\right\} \qquad (4.104)$$

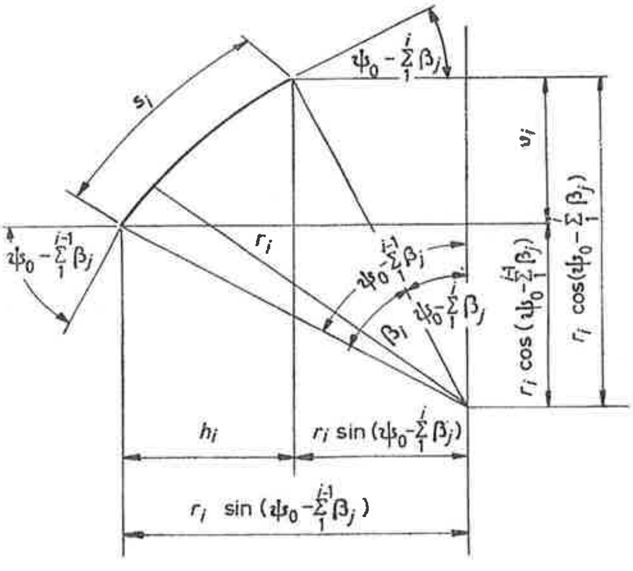

Figure 4.48 (From Seames and Conway[18])

The method is of the trial and error type since the successful calculation depends on the correct assessment of ψ_0 at the beginning. Only for an accurately assumed ψ_0 will

$$\sum_{j=1}^{n} s_j \approx L$$

If the deviation between $\sum_{j=1}^{n} s_j$ and L is too great, ψ_0 has to be adjusted accordingly and the procedure started anew. This will be shown on the following examples.

Consider a horizontal, straight cantilever: $L = 8{\cdot}25$ in. carrying $P = 1$ lb vertical load at the free end. The flexural rigidity of the bar is $EI = 20$ lb in^2.

The average bending moment for the ith arc is

$$M_i' = P(h_1 + h_2 + h_3 + \ldots + h_{i-1} + h_i/2)$$

Assume that $\psi_0 = 0{\cdot}8$ and select $h_1 = h_2 = h_3 \ . \ . \ = h_i = 1$ in. *Table 7* shows the tabulated calculation. Starting from the free end $1/r$, r, h/r, and $\psi_0 - \sum_{j=1}^{i} \beta_j$ are introduced. After that

$$\sin\left(\psi_0 - \sum_{j=1}^{i} \beta_j\right) = -\frac{h}{r} + \sin\left(\psi_0 - \sum_{j=1}^{i-1} \beta_j\right)$$

is calculated. Note that the first figure in column 5 is ψ_0. ψ_i is found from

$$\left(\psi_0 - \sum_{j=1}^{i-1} \beta_j\right) - \left(\psi_0 - \sum_{j=1}^{i} \beta_j\right)$$

Column 12 equals the difference between columns 11 and 10. The elemental arc length $s_i = \psi_i r_i$ is given in the last column. The continuation of the calculations from arc to arc shows (see the last row of *Table 7*) that h_6 cannot be taken as 1 in. as were the rest of the h's because

$$\frac{h_6}{r_6} > \left[\sin\left(\psi_0 - \sum_{j=1}^{5} \beta_j\right) - \sin\left(\psi_0 - \sum_{j=1}^{6} \beta_j\right)\right]$$

Table 7. (From Seames and Conway[12])

Column No.	1	2	3	4	5	6	7
Arc No.	h	$1/r$	r	h/r	$\psi_0-\sum_{j=1}^{i-1}\beta_j$	$\sin\left[\psi_0-\sum_{j=1}^{i-1}\beta_j\right]$	$\sin\left[\psi_0-\sum_{j=1}^{i}\beta_j\right]$
1	1	0·02500	40·0000	0·02500	0·80000	0·71736	0·69236
2	1	0·07500	13·3333	0·07500	0·76475	0·69236	0·61736
3	1	0·12500	8·0000	0·12500	0·666538	0·61736	0·49236
4	1	0·17500	5·7143	0·17500	0·51460	0·49236	0·31736
5	1	0·22500	4·4444	0·22500	0·32294	0·31736	0·09236
6	0·3615	—	3·914	0·09236	0·09249	0·09236	0·00000

Column No.	8	9	10	11	12	13	14
Arc No.	$\psi_0-\sum_{j=1}^{i}\beta_j$	β_j	$\cos\left[\psi_0-\sum_{j=1}^{i-1}\beta_j\right]$	$\cos\left[\psi_0-\sum_{j=1}^{i}\beta_j\right]$	v/r	v	s
1	0·76475	0·03525	0·69671	0·72156	0·02485	0·99400	1·4100
2	0·666538	0·09937	0·72156	0·78668	0·06512	0·86836	1·3250
3	0·51460	0·15078	0·78668	0·87049	0·08410	0·67284	1·2062
4	0·32294	0·19166	0·87049	0·94831	0·07782	0·44467	1·0952
5	0·09249	0·23045	0·94831	0·99573	0·04742	0·21075	1·0242
6	0·00000	0·09249	0·99573	1·00000	0·00427	0·01662	0·3620
							$\sum_{1}^{6} s_j = 6{\cdot}4226$

where the second sine in the bracket equals zero. This indicates that $h_6 < 1$ in. Since

$$\frac{h_6}{r_6} = \sin\left(\psi_0 - \sum_{j=1}^{5} \beta_j\right) = \frac{M'_6}{EI} h_6$$

we have for the solution of h_6

$$\sin\left(\psi_0 - \sum_{j=1}^{5} \beta_j\right) = \frac{P}{EI} (5 + h_6/2) h_6$$

This equation yields $h_6 = 0{\cdot}3615$.

When all values have been tabulated the addition of the last column shows that

$$L = \sum_{1}^{6} s_j = 6{\cdot}4226 \text{ in.}$$

while the correct length is $L = 8{\cdot}25$ in. This means that ψ_0 has been assumed too small.

For the second trial assume $\psi_0 = 1{\cdot}05$. The calculations based on this new end slope are tabulated in *Table 8*. It is found that for this value

$$\sum_{1}^{6} s_j = 8{\cdot}2169 \text{ in.}$$

which is close enough to the real $L = 8{\cdot}25$ in. Also,

$$Y = \sum_{1}^{6} v_j = 5{\cdot}182 \text{ in.}$$

and

$$X = \sum_{1}^{6} h_j = 5{\cdot}891 \text{ in.}$$

The exact solution of this cantilever (from equations 2.24, 29, and 30) is $\psi_0 = 1{\cdot}047$, $Y = 5{\cdot}23$ in., and $X = 5{\cdot}88$ in.

As a further example of the numerical method a cantilever, initially curved as a circular arc, will be considered. The deflection curve will again be approximated by a number of circular arcs tangential to each other at their intersection (*Figures 4.47* and *4.48*). Equations (4.103) are valid with the exception of the first expression which is modified to

$$\frac{1}{r_i} = \frac{M'_i}{EI} + \frac{1}{R_0}$$

Table 8

Column No.	1	2	3	4	5	6	7
Arc	h	$1/r$	r	h/r	$\psi_0-\sum_{j=1}^{i-1}\beta_j$	$\sin\left[\psi_0-\sum_{j=1}^{i-1}\beta_j\right]$	$\sin\left[\psi_0-\sum_{j=1}^{i}\beta_j\right]$
1	1	0·02500	40·0000	0·02500	1·05000	0·86748	0·84248
2	1	0·07500	13·3333	0·07500	1·00182	0·84248	0·76748
3	1	0·12500	8·0000	0·12500	0·87499	0·76748	0·64248
4	1	0·17500	5·7143	0·17500	0·69784	0·64248	0·46748
5	1	0·22500	4·4444	0·22500	0·48637	0·46748	0·24248
6	0·891	—	3·6745	0·24248	0·24493	0·24248	0·00000
	$\sum_1^6 h_j = 5{\cdot}891$						

Column No.	8	9	10	11	12	13	14
Arc	$\psi_0-\sum_{j=1}^{i}\beta_j$	β_j	$\cos\left[\psi_0-\sum_{j=1}^{i-1}\beta_j\right]$	$\cos\left[\psi_0-\sum_{j=1}^{i}\beta_j\right]$	v/r	v	s
1	1·00182	0·04818	0·49748	0·53877	0·04129	1·65160	1·9272
2	0·87499	0·12683	0·53877	0·64100	0·10223	1·36306	1·69110
3	0·69784	0·17715	0·64100	0·76623	0·12523	1·00184	1·4172
4	0·48637	0·21147	0·76623	0·88404	0·11781	0·67320	1·2084
5	0·24493	0·24144	0·88404	0·97015	0·08611	0·38270	1·0731
6	0·00000	0·24493	0·97015	1·00000	0·02985	0·10968	0·8999
		1·05000				$\sum_1^6 v_j = 5{\cdot}18208$	$\sum_1^6 s_j = 8{\cdot}2169$

where R_0 is the radius of the unstressed cantilever. The horizontal and vertical deflections of the free end are

$$H = R_0 \sin\left(\frac{L}{R_0}\right) - \sum_{j=1}^{n} h_j$$

$$V = \sum_{j=1}^{n} v_j - R_0\left[1 - \cos\left(\frac{L}{R_0}\right)\right]$$

The calculation proceeds in a similar manner as for the straight cantilever. The success of the approximation depends on the accurate choice of ψ_0. Adopt $h_1 = h_2 = \ldots$ etc., $= 1$ in. It is noted that the ith average bending moment is

$$M_i' = P(h_1 + h_2 + h_3 + \ldots + h_{i-1} + h_i/2)$$

that is, the same as before. The difference between the present problem and the previous one is in the evaluation of $1/r$. For a correctly assumed ψ_0,

$$\sum_{j=1}^{n} s_j = L$$

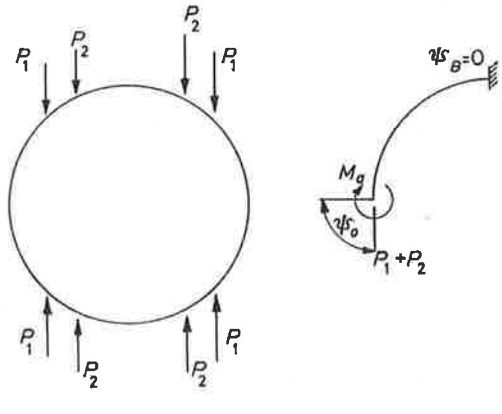

Figure 4.49

This method of substituting the deflected shape by a set of continuous circular arcs may be used for the calculation of closed rings too. In the case of a symmetrically loaded ring only one quadrant need be considered (*Figure 4.49*). The statically indeterminate moment M_a is unknown, but ψ_0 is known and equals

$\pi/2$. Hence no guesswork is involved in the selection of the initial slope; it is M_a whose value must be correctly assumed, otherwise

$$\sum_{j=1}^{n} s_j \neq R_0 \pi/2$$

The average bending moment of the ith arc is

$$M_i' = P(h_1 + h_2 + h_3 + \ldots + h_{i-1} + h_i/2) - M_a$$

while the rest of the calculations is similar to the procedure for the curved cantilever.

As an example, consider the case of a closed circular ring (*Figure 4.16 (a)*) according to the following data: $R_0 = 10$ in., $P = 0{\cdot}2$ lb, and $EI = 20$ lb in^2. Suppose that two trial-and-error calculations have already been carried out and that they lead to the conclusion that M_a is slightly above 0·60 lb in. Assume $M_a = 0{\cdot}61$ lb in. and calculate accordingly. Adopting $h_1 = h_2 = \ldots$ etc., $= 1$ in., *Table 9* has been prepared. It is noted that in the first row

$$\psi_0 - \sum_{j=1}^{n} \beta_j = \pi/2 = 1{\cdot}57080$$

The horizontal projection of the last arc, h_9, is found from

$$\sin\left(\psi_0 - \sum_{j=1}^{8} \beta_j\right) = \left[\frac{P}{EI}(8 + h_9/2) - \frac{M_a}{EI}\right] h_9 + \frac{h_9}{R_0}$$

This equation gives $h_9 = 0{\cdot}8069$ in. Adding up column 10 gives

$$L = \sum_{j=1}^{9} s_j = 15{\cdot}69 \text{ in.} \approx R_0 \pi/2, \text{ hence } M_a = 0{\cdot}61 \text{ was correct.}$$

The horizontal semi-diameter of the deformed ring is

$$\sum_{j=1}^{9} h_j = 8{\cdot}8069 \text{ in.}$$

while, from column 11, we find that the vertical semi-diameter is

$$\sum_{j=1}^{9} v_j = 11{\cdot}0867 \text{ in.}$$

The accurate solution (section 4.6) is 8·74 in., and 11·20 in. for the horizontal and vertical semi-diameters respectively.

Table 9. (From Seames and Conway[12])

Column No.	1	2	3	4	5	6	7
Arc No.	h	M'/EI	$1/r$	h/r	$\psi_0-\sum_{j=1}^{i-1}\beta_j$	$\sin\left[\psi_0-\sum_{j=1}^{i-1}\beta_j\right]$	$\sin\left[\psi_0-\sum_{j=1}^{i}\beta_j\right]$
1	1	−0·0255	0·07450	0·07450	1·57080	1·00000	0·92550
2	1	−0·0155	0·08450	0·08450	1·18237	0·92550	0·84100
3	1	−0·0055	0·09450	0·09450	0·99931	0·84100	0·74650
4	1	0·0045	0·10450	0·10450	0·84279	0·74650	0·64200
5	1	0·0145	0·11450	0·11450	0·69710	0·64200	0·52750
6	1	0·0245	0·12450	0·12450	0·55566	0·52705	0·40300
7	1	0·0345	0·13450	0·13450	0·41480	0·40300	0·26850
8	1	0·0445	0·14450	0·14450	0·27184	0·26850	0·12400
9	0·8069	—	0·15367	0·12400	0·12433	0·12400	0·00000

Column No.	8	9	10	11	12	13	14
Arc No.	$\psi_0-\sum_{j=1}^{i}\beta_j$	β_j	s	$\cos\left[\psi_0-\sum_{j=1}^{i-1}\beta_j\right]$	$\cos\left[\psi_0-\sum_{j=1}^{i}\beta_j\right]$	v/r	v
1	1·18237	0·38843	5·2138	0·00000	0·37873	0·37873	5·0836
2	0·99931	0·18306	2·1664	0·37873	0·54090	0·16217	1·9192
3	0·84279	0·15652	1·6563	0·54090	0·66538	0·12448	1·3172
4	0·69710	0·14569	1·3942	0·66538	0·76671	0·10133	0·9697
5	0·55566	0·14144	1·2353	0·76671	0·84955	0·08284	0·7235
6	0·41480	0·14086	1·1314	0·84955	0·91519	0·06565	0·5273
7	0·27184	0·14296	1·0628	0·91519	0·96327	0·04808	0·3575
8	0·12433	0·14751	1·0208	0·96327	0·99228	0·02901	0·1385
9	0·00000	0·12433	0·8091	0·99228	1·00000	0·00772	0·0502
			$L=\Sigma s=15{\cdot}69$ in.				

The method outlined in this section can be used for any curved bar provided the geometry of the free shape allows us to calculate R_0 for the elemental arcs. The procedure is the same as for circular bars except that R_0 has a different value for every segment.

Suitable modifications of this method will permit the approximate analysis of a bar whose deformed shape contains one or more points of inflection.

REFERENCES

[1] Mitchell, T. P. The nonlinear bending of thin rods, *J. appl. Mech.* **26**, *Trans. ASME*, **81**, *Ser. E* (1959) 40

[2] Conway, H. D. The nonlinear bending of thin circular rods, *J. appl. Mech.* **23**, *Trans. ASME*, **78**, *Ser. E* (1956) 7

[3] van Wijngaarden, A. Large distortions of circular rings and straight rods, *Proc. Acad. Sci. Amst.* **49** (1946) 648

[4] Hymans, F. Flat springs with large deflections, *J. appl. Mech.* **13**, *Trans. ASME*, **68**, *Ser. E* (1946) 223

[5] Sonntag, R. Zur Theorie des geschlossenen Kreisringes mit grosser Formaenderung, *Ingen.-Arch.* **13** (1943) 380

[6] Biezeno, C. B. and Koch, J. J. The circular ring under the combined action of compressive and bending loads, *Proc. Acad. Sci. Amst.* **49** (1946) 3

[7] Frisch-Fay, R. The deformation of elastic circular rings, *Aust. J. appl. Sci.* **11** (1960) 329

[8] Carrier, G. F. On the buckling of elastic rings, *J. Math. Phys.* **26** (1947) 94

[9] Biezeno, C. B. and Koch, J. J. The generalized buckling problem of the circular ring, *Proc. Acad. Sci. Amst.* **48** (1945) 445

[10] Frisch-Fay, R. The flexible leaf spring, *Aust. J. appl. Sci.* **11** (1960) 341

[11] Biezeno, C. B. and Koch, J. J. On the nonlinear deflection of a semicircular ring clamped at both ends, *Proc. Acad. Sci. Amst.* **49** (1946) 139

[12] Seames, A. E. and Conway, H. D. A numerical procedure for calculating the large deflections of straight and curved beams, *J. appl. Mech.* **24**, *Trans. ASME*, **79**, *Ser. E* (1957) 289

5

APPLICATION OF POWER SERIES. DISTRIBUTED LOADS

5.1. Horizontal Cantilever under Point Load

The methods used so far in the solution of cantilevers have been based either on the application of complete and incomplete elliptic integrals or on a numerical procedure giving approximate results only. In the present chapter, power series will be employed in analysing the elastic shape of the bar. This method will yield the solution to any desired degree of accuracy; also, the solutions can be given in a form similar to those used in the elementary theory. In other words, the solutions will take the form of equations depending directly on the load, the length of the bar, and on the flexural rigidity. The application of power series does away with the solution of transcendental equations where the finding of the modulus p might become cumbersome. Power series solution is, in certain cases, the only analytical approach, particularly when the basic differential equation does not lend itself to a closed form solution.

Take the horizontal cantilever in *Figure 2.2.* The basic differential equation of this problem is, (2.10),

$$\frac{d^2\psi}{ds^2} = -k^2 \cos\psi \tag{5.1}$$

Let ψ_0 be the slope at the free end and let s be the arc length measured from the free end. (In *Figure 2.2*, s is measured from the fixed end.) The boundary conditions are

$$\left(\frac{d\psi}{ds}\right)_{s=0} = 0$$

$$(\psi)_{s=0} = \psi_0$$

and

$$(\psi)_{s=L} = 0$$

We wish to express ψ as a function of s. Expanding this function into Maclaurin's series,

$$\psi(s) = \psi(0) + s\,\psi'(0) + \frac{s^2}{2!}\psi''(0) + \frac{s^3}{3!}\psi'''(0) + \ldots. \tag{5.2}$$

From the first and second boundary conditions we have

$$\psi(0) = \psi_0$$

and
$$\psi'(0) = 0$$

Inserting the second boundary condition in equation (5.1)

$$\psi''(0) = -k^2 \cos\psi_0$$

Differentiation of equation (5.1) gives

$$\psi''' = \psi' k^2 \sin\psi$$

hence
$$\psi'''(0) = 0$$

Differentiating again,

$$\psi^{(4)} = k^2 [\psi' \sin\psi + (\psi')^2 \cos\psi]$$

hence
$$\psi^{(4)}(0) = -k^4 \sin\psi_0 \cos\psi_0$$

Continuing this way we obtain

$$\psi^{(5)}(0) = 0$$
$$\psi^{(6)}(0) = k^6 (3\cos^3\psi_0 - \sin^2\psi_0 \cos\psi_0)$$
$$\psi^{(7)}(0) = 0$$
$$\psi^{(8)}(0) = k^8 (33 \sin\psi_0 \cos^3\psi_0 - \sin^3\psi_0 \cos\psi_0)$$

We can now express equation (5.2) up to terms containing s^8 as

$$\psi = \psi_0 - \frac{k^2 \cos\psi_0}{2} s^2 - \frac{k^4 \sin 2\psi_0}{48} s^4 + + k^6 \left[\frac{\cos^3\psi_0}{240} - \frac{\sin^2\psi_0 \cos\psi_0}{720} \right] s^6 + + k^8 \left[\frac{11 \sin\psi_0 \cos^3\psi_0}{13440} - \frac{\sin^3\psi_0 \cos\psi_0}{40320} \right] s^8 + \dots \quad (5.3)$$

Introducing a_2, a_4, a_6, etc., for the coefficients of s^2, s^4, s^6, etc., we get

$$\psi = \psi_0 + \beta$$

where
$$\beta = a_2 s^2 + a_4 s^4 + a_6 s^6 + \dots$$

Since $(\psi)_{s=L} = 0$, we have for the end slope

$$\psi_0 = -\sum_{n=1}^{\infty} a_{2n} L^{2n} \tag{5.4}$$

For small deflections ψ_0 is small, hence $\sin\psi_0 \approx \psi_0$ and $\cos\psi_0 \approx 1$. By taking the first term only in the series (5.4)

$$\psi_0 = k^2 L^2/2 = PL^2/2EI$$

which is in agreement with the elementary theory.

The bending moment at any point of the cantilever may be expressed as

$$M = EI\frac{d\psi}{ds} = EI(2a_2 s + 4a_4 s^3 + 6a_6 s^5 + \ldots.)$$
$$= EI \sum_{n=1}^{\infty} 2n\, a_{2n} s^{2n-1} \tag{5.5}$$

Taking the origin of the rectangular coordinate system at the free end of the cantilever, the vertical deflection of a point can be found from

$$y = \int_0^s dy = \int_0^s \sin\psi\, ds = \int_0^s (\sin\psi_0 \cos\beta + \cos\psi_0 \sin\beta)\, ds \tag{5.6}$$

since $$\frac{dy}{ds} = \sin\psi$$

Similarly, the horizontal deflection is

$$x = \int_0^s (\cos\psi_0 \cos\beta - \sin\psi_0 \sin\beta)\, ds \tag{5.7}$$

We get an expression for $\int \cos\beta\, ds$ by expanding $\cos\beta$ into a series and integrating term by term. Thus

$$\int_0^s \left(1 - \frac{\beta^2}{2} + \frac{\beta^4}{24} - \ldots\right) ds$$
$$= \int_0^s \left[1 - \frac{a_2^2 s^4}{2} - a_2 a_4 s^6 - \left(\frac{a_4^2}{2} + a_2 a_6 - \frac{a_2^4}{24}\right) s^8\right] ds$$
$$= s - \frac{a_2^2}{10} s^5 - \frac{a_2 a_4}{7} s^7 - \left(\frac{a_4^2}{18} + \frac{a_2 a_6}{9} - \frac{a_2^4}{216}\right) s^9 \tag{5.8}$$

up to terms containing s^9.

Expanding $\sin\beta$ now up to terms containing s^8 and integrating, we find

$$\int_0^s \sin\beta\, ds = \frac{a_2}{3}s^3 + \frac{a_4}{5}s^5 + \left(\frac{a_6}{7} - \frac{a_2^3}{42}\right)s^7 + \left(\frac{a_8}{9} - \frac{a_2^2 a_4}{18}\right)s^9 \tag{5.9}$$

The vertical and horizontal deflection of a point represented by $\psi = \psi(s)$ can now be obtained if we express a_2, a_4, a_6, etc., in terms of ψ_0 and P/EI and substitute these values into equations (5.8 and 9); then equations (5.6 and 7) will yield x and y. The maximum deflection is calculated by the substitution $s = L$. For small deflections we find

$$y_0 = y_{\max} = \sin\psi_0 \int_0^L \cos\beta\, ds + \cos\psi_0 \int_0^L \sin\beta\, ds$$
$$= \psi_0\left[L - \frac{k^4 L^5}{40}\right] - \frac{k^2}{6}L^3 = \frac{PL^3}{3EI} - \left(\frac{P}{EI}\right)^3 \frac{L^7}{80} \tag{5.10}$$

This result shows agreement in the first term with the small deflection theory.

5.2. Buckling of Bar under Own Weight

Problems involving the elastic stability of a structure are usually analysed within the framework of the approximate theory, that is, by applying the approximate formula for the curvature. This problem will be examined by using first the approximate theory and later by applying the rigorous solution.

Consider the vertical bar in *Figure 5.1*, fixed at the bottom, free at the top, and subject to a uniformly distributed load w. The basic equation in the approximate theory is

$$EI\frac{d^2y}{dx^2} = -M \tag{5.11}$$

where the origin of the xy coordinate system is at the fixed end. The problem was first solved by Greenhill[1] although it was first considered by Euler[2]. By taking the weight per unit volume as unity, Euler gives the following equation:

$$EI\frac{d^2y}{dx^2} + A\,x\,dy = 0$$

If $m = EI/A$, where A is the cross-sectional area of the strut, the critical height for which the column will bend is the least root of

$$0 = 1 - \frac{l^3}{4\,!\,m} + \frac{1.4.l^6}{7\,!\,m^2} - \frac{1.4.7.l^9}{10\,!\,m^3} + \frac{1.4.7.10.l^{12}}{13\,!\,m^4} - \ldots$$

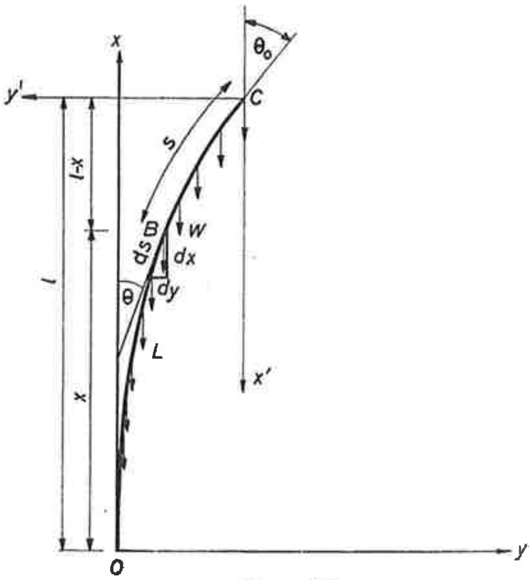

Figure 5.1

This equation has, however, no real root and Euler arrives at the absurd result that the height of the column does not influence its stability. Euler was more successful in finding the curve which the column would assume when bent by its own weight.

Differentiating the equation given by Euler and letting

$$dy/dx = u, \quad \text{and} \quad z = x/m^{1/3}$$

we arrive at

$$\frac{d^2 u}{dz^2} + zu = 0$$

The general solution of this equation is

$$u = \sqrt{z}\,[C_1 J_{1/3}(2z^{3/2}/3) + C_2 J_{-1/3}(2z^{3/2}/3)]$$

It may be shown that $C_1 = 0$, hence

$$\frac{dy}{dx} = C_2 \frac{1}{3\Gamma(2/3)}\left(1 - \frac{z^3}{2.3} + \frac{z^6}{2.3.5.6} - \frac{z^9}{2.3.5.6.8.9} + \ldots\right)$$

Integrating,

$$y = C_2 \frac{1}{3\Gamma(2/3)}\left(x - \frac{x^4}{4\,!\,m} + \frac{4x^7}{7\,!\,m^2} - \frac{4.7\,x^{10}}{10\,!\,m^3} + \ldots\right)$$

which agrees with Euler's results[3].

Returning now to the basic equation (5.11), differentiation with respect to x yields

$$EI\frac{d^3y}{dx^3} = -S = -w(L-x)\sin\theta \tag{5.12}$$

Since the elementary theory deals with flat curves only, $l \approx L$. Also, for the same reason

$$\sin\theta \approx \tan\theta = \frac{dy}{dx} = u(z) \tag{5.13}$$

in which $\quad z = l - x \approx L - x \approx s$

Combining equations (5.12 and 13), we get

$$EI\frac{d^2}{dx^2}\,u(z) = -w(L-x)\,u(z) \tag{5.14}$$

This last equation reduces to

$$\frac{d^2u}{dz^2} + m^2 zu = 0 \tag{5.15}$$

if we write $\quad \dfrac{w}{EI} = m^2$

The general solution of this linear differential equation is

$$u(z) = \sqrt{z}\left[C_1 J_{1/3}\left(\frac{2}{3}mz^{3/2}\right) + C_2 J_{-1/3}\left(\frac{2}{3}mz^{3/2}\right)\right] \tag{5.16}$$

where $J_{1/3}$ is the Bessel function of order 1/3 of the first kind. We note that the tangent at the fixed end is zero and that the curvature at the top is also zero. Hence the boundary conditions are

$$\left(\frac{dy}{dx}\right)_{x=0} = 0, \quad \text{or} \quad [u(z)]_{z=L} = 0$$

and
$$\left(\frac{d^2y}{dx^2}\right)_{x=L} = 0, \quad \text{or} \quad \left(\frac{du}{dz}\right)_{z=0} = 0$$

It can be shown that the second boundary condition is satisfied for $C_1 = 0$ only. Applying now the first boundary condition

$$C_2\sqrt{L}J_{-1/3}(2mL^{3/2}/3) = 0$$

If $C_2 = 0$ the bar remains straight and no buckling will occur. Therefore, we require that

$$J_{-1/3}(2mL^{3/2}/3) = 0 \tag{5.17}$$

The smallest zero of $J_{-1/3}$ is 1·87, hence

$$(wL)_{cr} = 7{\cdot}84\frac{EI}{L^2} \tag{5.18}$$

From $(\theta)_{z=0} = \theta_0$, and equation (5.16), we find that

$$\theta_0 = C_2\frac{(m/3)^{-1/3}}{\Gamma(2/3)}$$

and by solving m from equation (5.17) and substituting it in the above expression of θ_0, we get

$$C_2 = \frac{1{\cdot}32\,\theta_0}{\sqrt{L}}$$

The above solution was based on the elementary theory, and therefore it is valid for small deflections only. In the approximate theory of a bar buckling under its own weight θ_0 is a small but indeterminate angle, just as in the approximate theory of a bar buckling under a concentrated load, it is the horizontal movement of the top that is indeterminate. In section 1.7 we discussed the latter problem and found that by applying the exact differential equation of bending, the horizontal deflection can be defined uniquely for $P > P_{cr}$. Similarly, by applying the rigorous solution of the bar buckling under its own weight, the angle θ_0 will not be indeterminate but rather a function of wL.

In order to solve this problem according to the exact theory we first transfer the coordinate system into the $x'y'$ position (*Figure 5.1*). Using equation (2.8) to express the equilibrium of the bar and noting that $\theta = \pi/2 - \psi$,

$$S_0 = T_0 = q_x = 0$$

and

$$q_y = w$$

With these conditions, equation (2.8) reduces to

$$EI \frac{d^2}{ds^2}(\pi/2 - \theta) = -\, ws \cos(\pi/2 - \theta)$$

or

$$EI \frac{d^2\theta}{ds^2} = -\, ws \sin\theta \tag{5.19}$$

We now introduce the nondimensional quantities

$$c = \left(\frac{EI}{w}\right)^{1/3}, \quad q = \frac{s}{c}$$

and equation (5.19) becomes

$$\frac{d^2\theta}{dq^2} = -\, q \sin\theta \tag{5.20}$$

since

$$\frac{d^2\theta}{ds^2} = \frac{1}{c^2}\frac{d^2\theta}{dq^2}$$

The boundary conditions are

$$\left(\frac{d\theta}{ds}\right)_{s=0} = 0, \quad \text{or} \quad \frac{1}{c}\left(\frac{d\theta}{dq}\right)_{q=0} = 0$$

and

$$(\theta)_{q=0} = \theta_0$$

Equation (5.20) does not seem to admit of a finite solution. An approximation of its integral can be obtained by expanding the unknown function $\theta(q)$ into Maclaurin's series and find θ', θ'', etc., in conformity with the boundary conditions. We have

$$\begin{aligned}
\theta'(0) &= 0\\
\theta''(0) &= 0\\
\theta'''(0) &= -\sin\theta_0\\
\theta^{(4)}(0) &= 0\\
\theta^{(5)}(0) &= 0\\
\theta^{(6)}(0) &= 2\sin 2\theta_0\\
\theta^{(7)}(0) &= 0\\
\theta^{(8)}(0) &= 0\\
\theta^{(9)}(0) &= 70\sin^3\theta_0 - 14\cos\theta_0\sin 2\theta_0
\end{aligned}$$

Let $q^3 = r$, and substitute these derivatives into a Maclaurin series:

$$\theta(q) = \theta_0 - \frac{r}{6}\sin\theta_0 + \frac{r^2}{360}\sin 2\theta_0 + \frac{r^3}{5184}\sin^3\theta_0 - \\ - \frac{r^3}{25920}\cos\theta_0\sin 2\theta_0 + \ldots \tag{5.21}$$

According to the elementary theory buckling occurs at small values of θ_0. In this case $\theta_0 \approx \sin\theta_0$ and $\cos\theta_0 \approx 1$. Introducing these values in (5.21) and noting that $(\theta)_{q=L/c} = 0$,

$$1 - \frac{r_L}{6} + \frac{r_L^2}{180} - \frac{r_L^3}{12960} + \ldots. = 0 \tag{5.22}$$

where $$r_L = \frac{L^3}{c^3} = \frac{wL^3}{EI}$$

We now expand the Bessel function in equation (5.17) into a power series:

$$J_{-1/3}(2mL^{3/2}/3) = \frac{(mL^{3/2}/3)^{-1/3}}{\Gamma(2/3)}\left\{1 - \frac{(mL^{3/2}/3)^2}{2/3} + \right. \\ \left. + \frac{(mL^{3/2}/3)^4}{2\,!\frac{2}{3}\cdot\frac{5}{3}} - \frac{(mL^{3/2}/3)^6}{3\,!\frac{2}{3}\cdot\frac{5}{3}\cdot\frac{8}{3}} + \ldots\right\}$$

The series in the bracket may be written as

$$1 - \frac{m^2L^3}{2.3} + \frac{m^4L^6}{2.3.5.6} - \frac{m^6L^9}{2.3.5.6.8.9} + \ldots. = 0 \tag{5.23}$$

Since $m^2 = w/EI$ it can be seen that the series (5.22 and 23) are identical. This, however, applies to small values of θ_0 only where the powers of sin θ_0 become infinitesimally small.

The lowest root of (5.23) is

$$r_L = \frac{L^3 w}{EI} = 7{\cdot}81$$

if, however, we include the next term in the series (5.23)

$$\frac{m^8 L^{12}}{2.3.5.6.8.9.11.12}$$

we get $r_L = 7{\cdot}84$ which is the correct value of the critical load according to the elementary theory.

By using the exact differential equation (5.20) for the deflection, the notion of $(wL)_{cr}$ becomes meaningless in the ordinary sense. The strut will not collapse if wL reaches the critical value nor will the strut remain in an indeterminately, though slightly, bent shape. When wL increases beyond $(wL)_{cr}$, θ_0 may be calculated from

$$\theta_0 - \frac{r_L}{6}\sin\theta_0 + \frac{r_L^2}{360}\sin 2\theta_0 + \frac{r_L^3}{5184}\sin^3\theta_0 - \frac{r_L^3}{25920}\cos\theta_0 \sin 2\theta_0 = 0$$

If
$$\frac{wL}{(wL)_{cr}} = n = 1 + \Delta \tag{5.24}$$

where Δ is small compared with unity,

$$\theta_0 \approx 2{\cdot}1\sqrt{\Delta}$$

This approximate result has been obtained by neglecting the 4th term in equation (5.24) and by expanding sin θ_0 into $\theta_0 - \theta_0^3/6$; a term containing r_L^4 has also been included. Accordingly[4],

if $\Delta = 0{\cdot}001$, $\theta_0 = 0{\cdot}067$,

and if $\Delta = 0{\cdot}01$, $\theta_0 = 0{\cdot}21$

Once θ_0 is known, θ (q) can be solved for any value of q (and hence of s too) from equation (5.21). The coordinates of the deflected shape may be calculated from

$$x' = \int_0^s \cos\theta\, ds = c\int_0^q \cos\theta\, dq$$

and
$$y' = \int_0^s \sin\theta\, ds = c\int_0^q \sin\theta\, dq \tag{5.25}$$

In cases dealt with before, ds had a formal solution in terms of a parameter, hence in terms of the slope too. In this case, however, dq (and ds) have no finite solution in terms of θ or any other variable. Numerical integration is, therefore, necessary to solve equations (5.25). An alternative method would be to expand $\sin\theta$ and $\cos\theta$ and solve the deflection in a series form. This method will be demonstrated in the next section.

5.3. Horizontal Cantilever under Distributed Load

This problem, like the one discussed in the previous section, has shown considerable resistance to a closed form solution and all investigations dealing with it have employed approximate methods only[5]. The approach adopted in this discussion for the solution of our case is clearly indicated in *Figure 5.2.* We note that $\theta_0 - \pi/2 = \alpha$ hence, from equation (5.21),

$$\theta(n) = (\alpha + \pi/2) - \frac{n}{6}\sin(\alpha + \pi/2) + \frac{n^2}{360}\sin(2\alpha + \pi) + \\ + \frac{n^3}{5184}\sin^3(\alpha + \pi/2) - \\ - \frac{n^3}{25920}\cos(\alpha + \pi/2)\sin(2\alpha + \pi) + \dots \qquad (5.26)$$

where $$n = \frac{s^3}{c^3}$$

After some reduction, equation (5.26) becomes

$$\theta(n) = (\alpha + \pi/2) - \frac{n}{6}\cos\alpha - \frac{n^2}{360}\sin 2\alpha + \frac{n_L^3}{5184}\cos^3\alpha - \\ - \frac{n_L^3}{25920}\sin\alpha\sin 2\alpha \qquad (5.27)$$

From the boundary condition $(\theta)_{s=L} = \pi/2$ we get

$$\alpha - \frac{n_L}{6}\cos\alpha - \frac{n_L^2}{360}\sin 2\alpha + \frac{n_L^3}{5184}\cos^3\alpha - \frac{n_L^3}{25920}\sin\alpha\sin 2\alpha = 0 \qquad (5.28)$$

for the solution of α. Here $n_L = \dfrac{L^3}{c^3}$

The coordinates of the cantilever can be found from

$$x' = \int_0^s \cos\theta\, ds = -\int_0^s \sin\psi\, ds$$

and $$y' = \int_0^s \sin\theta\, ds = \int_0^s \cos\psi\, ds \tag{5.29}$$

Now, from equation (5.27), $\psi = \alpha + \beta$

where[6] $\beta = a_3 s^3 + a_6 s^6 + a_9 s^9 + \ldots = \sum_{k=1}^{\infty} a_{3k} s^{3k}$

and the coefficients of s are

$$a_3 = -\frac{w}{EI}\frac{\cos\alpha}{2.3}$$

$$a_6 = -\left(\frac{w}{EI}\right)^2 \frac{\sin\alpha\cos\alpha}{2.3.5.6}$$

$$a_9 = \left(\frac{w}{EI}\right)^3 \left[-\frac{\sin^2\alpha\cos\alpha}{2.3.5.6.8.9} + \frac{5}{2}\cdot\frac{\cos^3\alpha}{2.3.5.6.8.9}\right], \text{ etc.}$$

Hence, from equations (5.29) and from the expansion of $\sin\beta$ and $\cos\beta$ we finally have the deflection coordinates. They are

$$-x' = s\sin\alpha - \frac{w}{EI}\frac{\cos^2\alpha}{24}s^4 - \left(\frac{w}{EI}\right)^2\frac{\sin\alpha\cos^2\alpha}{360}s^7 - \\ -\frac{13}{129600}\left(\frac{w}{EI}\right)^3 \sin^2\alpha\cos^2\alpha\, s^{10} + \\ + \frac{1}{10368}\left(\frac{w}{EI}\right)^3 \cos^4\alpha\, s^{10} \tag{5.30}$$

$$y' = s\cos\alpha + \frac{w}{EI}\frac{\sin 2\alpha}{48}s^4 + \left(\frac{w}{EI}\right)^2 \frac{\sin\alpha\sin 2\alpha}{2520}s^7 - \\ -\left(\frac{w}{EI}\right)^2\frac{\cos^3\alpha}{504}s^7 - \frac{49}{259200}\left(\frac{w}{EI}\right)^3 \sin\alpha\cos^3\alpha\, s^{10} + \\ + \left(\frac{w}{EI}\right)^3 \frac{\sin^3\alpha\cos\alpha}{129600}s^{10} \tag{5.31}$$

If $s = L$ and α is small we have from equation (5.28)

$$\alpha = \frac{wL^3}{6EI},$$

which agrees with the elementary theory. The vertical deflection in this case is

$$-x' = \alpha L - \frac{wL^4}{24EI} = \frac{wL^4}{8EI} \text{ (same as in the elementary theory).}$$

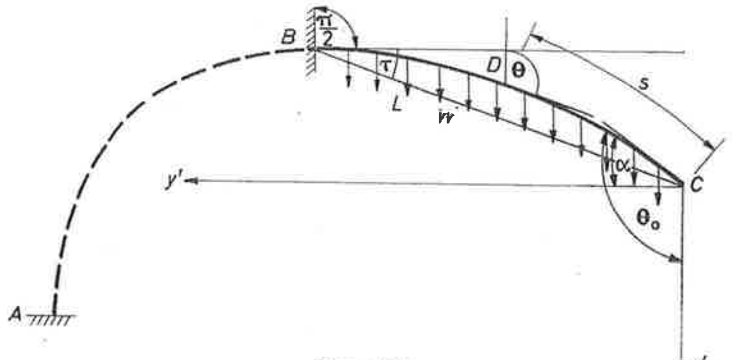

Figure 5.2

The bending moment can also be represented as a power series.

$$M = EI\frac{d\psi}{ds} = EI(3a_3 s^2 + 6a_6 s^5 + 9a_9 s^8 + \ldots)$$

$$= EI\sum_{k=1}^{\infty} 3ka_{3k} s^{3k-1}$$

From previous calculations we find for α

$$\alpha = -\sum_{k=1}^{\infty} a_{3k} L^{3k}$$

For small values of α, $\tan\alpha = \dfrac{wL^3}{6EI}$

and the slope of the chord BC (*Figure 5.2*) is

$$\tan\tau = -\frac{x'}{L} = \frac{wL^3}{8E}$$

As a result, $$\tau = 3\alpha/4 \tag{5.32}$$

Investigations[7] have shown that equation (5.32), which has been derived for small deflections only, holds very closely for $0° < \alpha < 20°$ and begins to deviate for $\alpha > 20°$, but even then the accurate value of τ/α at $\alpha = 70°$ is only 8 per cent in excess of 3/4.

The elementary theory applies as long as α is small and $\cos\alpha \approx 1$. Under these conditions the difference between the first two terms and the first five terms in (5.27) is 0·12 per cent if $L/c = 1$. This difference decreases further with the decrease of L/c.

If a horizontal cantilever bent under its own weight has a rectangular cross section of depth $2b$ and an arbitrary width, and its weight per unit volume is σ, the conditions of $L/c < 1$ and $f < f_{\text{yield}}$ are

$$\zeta > \left(\frac{3}{\eta}\right)^{\frac{1}{2}}$$

and

$$\zeta > \frac{3L\sigma}{2f_y}$$

where $\zeta = b/L$, and $\eta = E/\sigma L$. If $\zeta < (3/\eta)^{\frac{1}{2}}$, the deflections are too large for the simplified theory and will have to be analysed within the nonlinear framework.

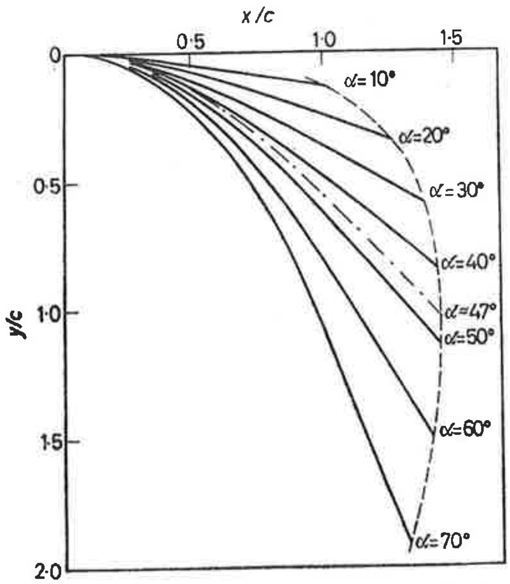

Figure 5.3 (From Lippmann, Mahrenholtz and Johnson[8])

Consider now a flexible strip pushed through a horizontal clamp. Let the strip be uniform and let $c = (EI/w)^{\frac{1}{3}}$. The shapes of the overhanging strip as the material is gradually fed through the clamp are shown in *Figure 5.3*. The lengths are selected so that the end slopes are $\alpha = 10°$, $20°$, etc. The strip whose end is most distant from the vertical through 0 has the following parameters: $\alpha \approx 47°$, $x/c = 1{\cdot}45$, $y/c = 1{\cdot}03$, and $L/c = 1{\cdot}84$. These results have been obtained by using an analogue computer[8].

Consider next a cantilever of unit length and increase the weight w without altering its flexural rigidity. The effect of this is shown in *Figure 5.4*.

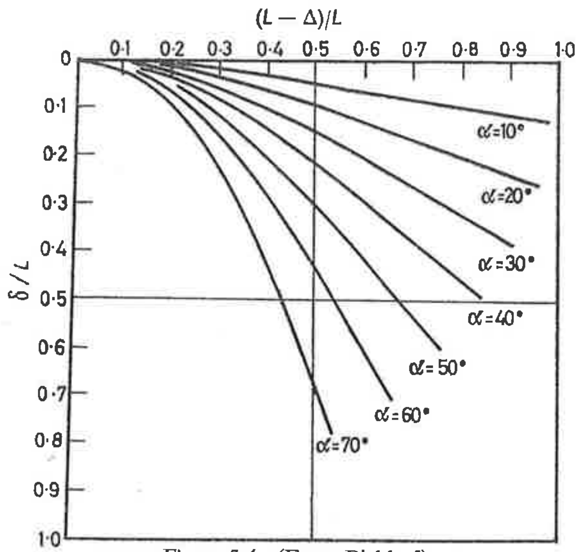

Figure 5.4 (From Bickley[7])

The deflections of the free end are found from the graph in *Figure 5.5*. In terms of wL^3/EI, the ratios δ/L and $(L - \Delta)/L$ are plotted, also, the ratio δ'/L, where δ' is the deflection according to the elementary theory.

When the initial shape of the cantilever is circular, the investigation of the bar under a uniformly distributed load takes a course similar to the straight cantilever. Let R be the radius of the free shape. We note that in this case the first boundary condition is

$$\frac{d\psi}{ds} = \pm \frac{1}{R}$$

at $s = 0$, depending on whether the cantilever is convex upward or downward. For a free shape convex downward, the final (loaded) shape might have a point of inflection. Assuming first that the loaded shape will have no point of inflection, we put

$$\psi = \sum_{n=0}^{\infty} a_n s^n$$

and find the coefficients

$$a_0 = \alpha, \quad a_1 = -\frac{1}{R}, \quad a_2 = 0,$$

$$a_3 = \frac{w}{EI}\cos\alpha, \quad a_4 = \frac{1}{12R}\frac{w}{EI}\sin\alpha, \quad a_5 = -\frac{1}{40R^2}\frac{w}{EI}\cos\alpha,$$

$$a_6 = -\left(\frac{w}{EI}\right)^2 \frac{\sin 2\alpha}{360} - \frac{1}{180R^3}\frac{w}{EI}\sin\alpha, \quad \text{etc.}^9$$

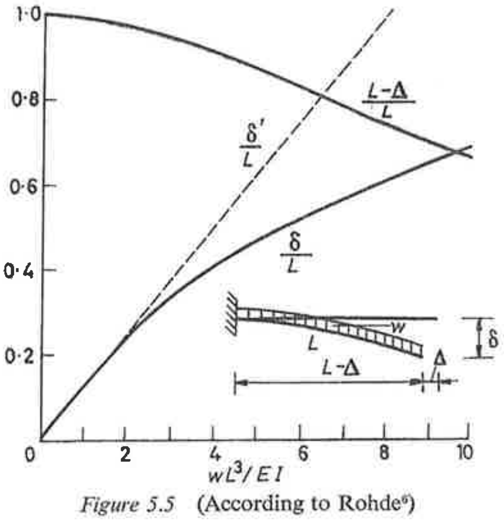

Figure 5.5 (According to Rohde[6])

Comparing these coefficients with those obtained for the straight bar, we find that, with the exception of a_2, $a_n \neq 0$; also, that R enters all coefficients a_n for $n \geqslant 4$. The loaded shape will have no point of inflection if

$$\frac{d^2\psi}{ds^2} = \sum_{n=2}^{\infty} n(n-1)\, a_n s^{n-2} \neq 0$$

If there is a point of contraflexure, the problem can be treated as two straight cantilevers of lengths s_1 and s_2, subject to w distributed load, $W = ws_1$ concentrated load and a couple $M = EI/R$ at the ends where s_1 is the distance from the point of contraflexure to the free end measured along the arc. The problem is solved if the slope ψ_0, satisfying both cantilevers, is found and if $s_1 + s_2 = L$.

5.4. Cantilever under Normal, Uniformly Distributed Load

On referring to equation (4.2) it becomes obvious that, generally speaking, problems in nonlinear bending dealing with distributed loads are more complicated than under point loads. In this section we shall consider a special case for which a closed form solution is available.

Take a straight cantilever on which the load is uniformly distributed and acts normal to the deflected shape[10]. The origin of

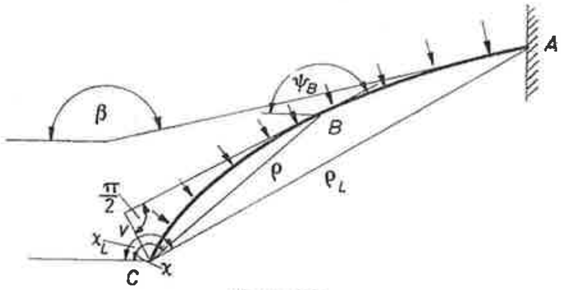

Figure 5.6

the polar coordinates (ρ, χ) is at the free end A (*Figure 5.6*). The bending moment at B equals

$$M_B = w\rho^2/2,$$

hence, in polar coordinates

$$\frac{1}{r} = \frac{M}{EI} = \frac{1}{\rho}\frac{dv}{d\rho} = \frac{w\rho^2}{2EI} \tag{5.33}$$

where
$$v = \rho\left[1 + \left(\frac{1}{\rho}\frac{d\rho}{d\chi}\right)^2\right]^{-\frac{1}{2}}$$

Integrating equation (5.33), we have at once

$$v = \frac{w\rho^4}{8EI} \tag{5.34}$$

The deflected shape is determined from

$$3\chi = \sin^{-1}(nv^3) - 4\sin^{-1}(nv_L^3) + 3\beta \tag{5.35}$$

and $$F(p,\Omega) = 2\sqrt[3]{n}\sqrt[4]{3} \tag{5.36}$$

where $$p = \tfrac{1}{2} - \tfrac{1}{4}\sqrt{3} = \sin 3°54',$$

$$\Omega = \cos^{-1}\left[\frac{1-(\sqrt{3}+1)\,n^{2/3}\,v_L^2}{1+(\sqrt{3}-1)\,n^{2/3}\,v_L^2}\right],$$

$$v = \frac{\rho}{L}, \quad v_L = \frac{\rho_L}{L}, \quad \text{and} \quad n = \frac{wL^3}{8EI}$$

The trial and error solution of equation (5.36) will yield ρ_L and then, from equation (5.35), we have a relationship between χ and ρ.

There is also $$\chi_L = \beta - \sin^{-1}(nv_L^3)$$

In terms of $\rho = \rho_B$ the shape at B is

$$\psi_B = \chi_B + \sin^{-1}\left(\frac{w\rho_B^3}{8EI}\right)$$

If the loaded shape of the cantilever under a normal, uniformly distributed load is given, and the free shape is needed, the polar inertia method may be used[11]. Let $z = z(s)$ be the free shape of the bar and $r(s)$ its radius of curvature at any point (*Figure 5.7*), and let $Z = Z(S)$ be the shape of the loaded bar whose radius of curvature is $R(S)$. The bending moment at B is

$$M_B = wC^2/2$$

where $C = C(S)$ is the chord length. It follows from Euler's law that

$$\frac{1}{r} = \frac{1}{R} + \frac{wC^2}{2EI} \tag{5.37}$$

Since C and R are functions of S (that is, of the assigned shape of the loaded bar), equation (5.37) is the intrinsic equation of the free bar.

Equation (5.37) changes into

$$\frac{d\theta}{dS} = \frac{d\Theta}{dS} + \frac{wC^2}{2EI}$$

where θ and Θ are the slopes on the free and the loaded bar respectively; also, $ds = dS$, since there is no extension. Integration yields

$$\theta = \Theta + \frac{w}{2EI}\int_0^S C^2\, dS \tag{5.38}$$

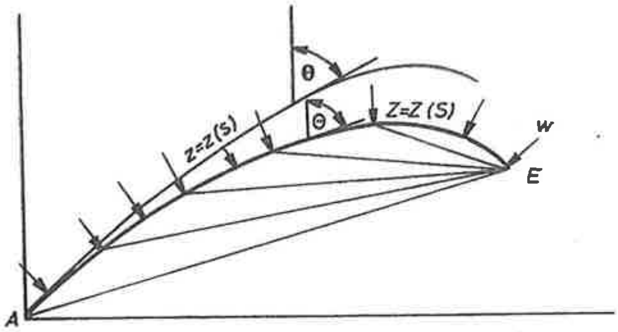

Figure 5.7

The physical meaning of the integral in equation (5.38) is the geometric polar moment of inertia of the bar segment AB with respect to an axis through E, perpendicular to its plane. Equation (5.38) becomes

$$\theta = \Theta + bI_p$$

if we put $b = w/2EI$, and $I_p = I_p(S)$ is the polar moment of inertia.

In the complex plane the free shape is represented by

$$z = f(Z) = e^{ibI_p}\,dZ \tag{5.39}$$

where $z = x + iy$, and the integration is carried out along the desired form.

5.5. Heart Loop

The heart loop (*Figure 5.8*) is used for finding the elastic properties of a very flimsy material, since in a cantilever form it would fall nearly vertically. Let $2L$ be the length of the loop. The equilibrium of the loop is expressed (from equation 2.8) by

$$\frac{d^2\psi}{dq^2} = t_0 \sin\psi - q\cos\psi \qquad (5.40)^7$$

Here $\quad q = \frac{s}{c}, \quad c = \left(\frac{EI}{w}\right)^{1/3} \quad$ and $\quad t_0 = \frac{T_0}{wc}$

(T_0 is the axial force at A).

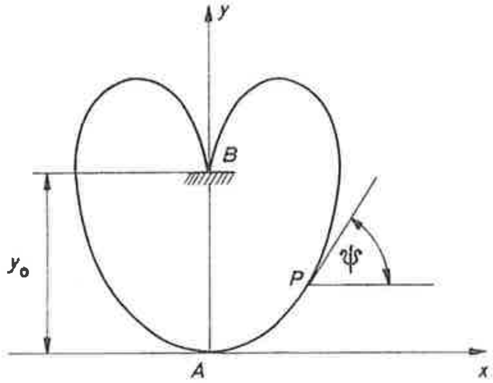

Figure 5.8

The solution of this differential equation is more complicated than in the case of the cantilever because there is no free end at which the conditions are known in advance. Each value of t_0 defines a shape of the loop and t_0 depends on c. For a numerical integration we need

$$\frac{d\psi}{dq} = c\frac{M_0}{EI} \qquad \text{at } A$$

but M_0, the bending moment at A, can be found by trial and error only. If we assume M_0 for every value of t_0, the integration can be carried out until ψ reaches $2\pi/3$. After this we find

$$\xi = \frac{x}{c} = \int_0^{q_1} \cos\psi \, dq$$

where $q_1 = (q)_{\psi=2\pi/3}$. For a correctly assumed M_0 the parameter ξ is zero.

The measurable quantities are L, y_0 and w. To find c the graphs in *Figure 5.9* have been drawn; this enables experimental results to be used for the evaluation of the flexural rigidity of the material.

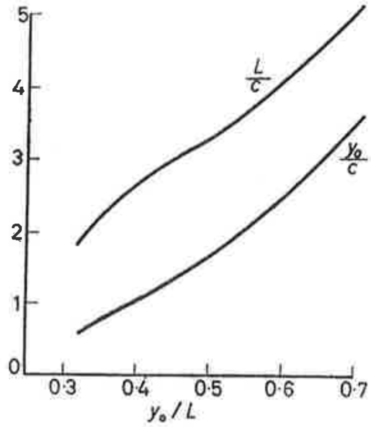

Figure 5.9 (According to Bickley[7])

The shapes corresponding to different values of t_0 are shown in *Figure 5.10*. They were first calculated by Bickley[7]; similar shapes have been obtained on the oscilloscope of an electronic computer[8].

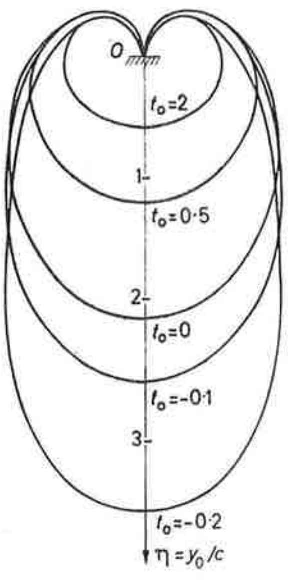

Figure 5.10 (From Bickley[7])

A more detailed analysis shows that no loop exists below $t_0 \approx -0{\cdot}37$. This follows from the fact that for long loops the ratio L/y_0 must approach unity. If we plot L/y_0 against t_0 (y_0 is found from $c \int_0^{q_1} \sin \psi \, dq$), the graph in *Figure 5.11* will result, which explains the lower limit of t_0.

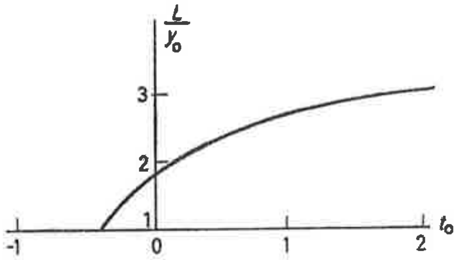

Figure 5.11 (From Bickley[7])

5.6. Simply Supported Bar under Uniformly Distributed Load

For reasons of symmetry, only the right-hand side of the bar will be analysed (*Figure 5.12*). If the length of the bar is $2L$ we can change the problem into a cantilever L long, subject to w distributed load acting downward and Lw point load acting upward. Taking these two loads separately, the cantilevers have been dealt with in sections 5.1 and 5.3 respectively. Since the deflections are large the superposition of the two cases does not avail.

The basic differential equation is

$$EI\frac{d^2\psi}{ds^2} = w(L-s)\cos\psi \qquad (5.41)$$

where s is measured from C.

Let $$\psi(s) = a_0 + a_1 s + a_2 s^2 + a_3 s^3 + \ldots . \qquad (5.42)^{12,13}$$

Since $(\psi)_{s=0} = \psi_0$ and $\left(\dfrac{d\psi}{ds}\right)_{s=0} = 0$, equation (5.42) becomes

$$\psi(s) = \psi_0 + \beta$$

where $$\beta = a_2 s^2 + a_3 s^3 + a_4 s^4 + \ldots . .$$

From (5.41) we have

$$EI(2a_2 + 6a_3 s + 12a_4 s^2 + 20a_5 s^3 + \dots) = w(L-s)\cos(\psi_0 + \beta) \tag{5.43}$$

Expanding $\sin\beta$ and $\cos\beta$ in terms of s and comparing the coefficients in equation (5.43), we find

$$a_2 = \frac{wL}{2EI}\cos\psi_0, \qquad a_3 = -\frac{w}{6EI}\cos\psi_0,$$

$$a_4 = -\frac{w^2L^2}{48(EI)^2}\sin 2\psi_0, \qquad a_5 = \frac{w^2L}{60(EI)^2}\sin 2\psi_0,$$

$$a_6 = -\frac{w^3L^3}{240(EI)^3}\cos^3\psi_0 - \frac{w^2}{360(EI)^2}\sin 2\psi_0 + \\ + \frac{w^3L^3}{720(EI)^3}\sin^2\psi_0\cos\psi_0, \text{ etc.}$$

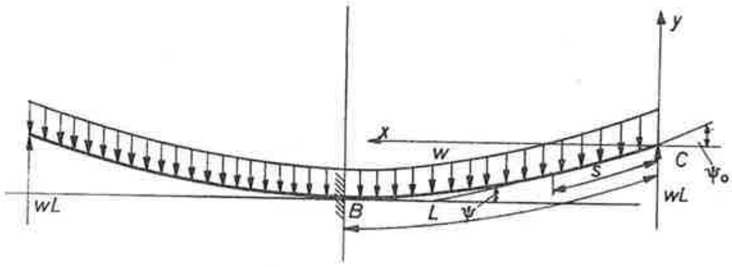

Figure 5.12

Since $(\psi)_{s=L} = 0$,

$$-\psi_0 = k_w\frac{\cos\psi_0}{3} - k_w^2\frac{\sin\psi_0\cos\psi_0}{72} - k_w^3\frac{\cos^3\psi_0}{240} + \\ + k_w^3\frac{\sin^2\psi_0\cos\psi_0}{720} + \dots \tag{5.44}$$

where $$k_w = \frac{wL^3}{EI}$$

As a first approximation $$\psi_0 = \frac{wL^3}{3EI}$$

which is in agreement with the small deflection theory.

The coordinates of any point are obtained from

$$y = \int_0^s \sin(\psi_0 + \beta)\, ds$$

and

$$x = \int_0^s \cos(\psi_0 + \beta)\, ds$$

The maximum deflection is

$$y_B = \int_0^L \sin(\psi_0 + \beta)\, ds$$

$$= L\left[\sin\psi_0 + \frac{k_w}{8}\cos^2\psi_0 - \frac{k_w^2}{60}\sin\psi_0\cos^2\psi_0 + \ldots\right] \quad (5.45)$$

If ψ_0 is small $\quad y_B = -L\dfrac{wL^3}{3EI} + \dfrac{wL^4}{8EI} = -\dfrac{5}{24}\dfrac{wL^4}{EI}$

5.7. Calculation of Deflections from Chart

Consider the strut in *Figure 5.13*, fixed at the bottom at an angle θ_0 to the vertical and carrying a vertical load P at the free end. Instead of using elliptic integrals this problem can be solved in terms of a special function that satisfies a nonlinear partial differential equation; in other words, a function is sought whose partial derivatives will give the coordinates of the deflected shape[14].

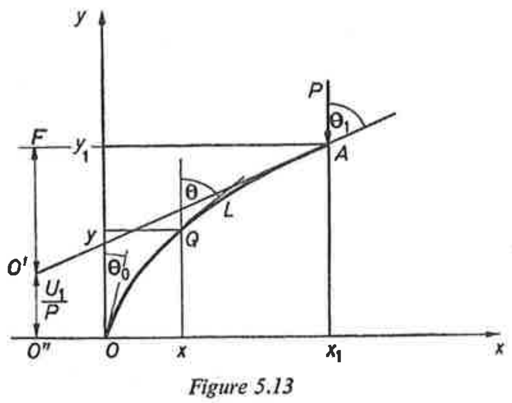

Figure 5.13

The length of the strut OA is L. This length is also shown as $O'A$. In terms of L, EI, P and θ_0 we wish to find as dependent variables the unknowns x_1, y_1, θ_1 and U_1, the strain energy of the bar.

From
$$P(x_1 - x) = EI \sin\theta \frac{d\theta}{dx} \tag{5.46}$$

we get, after integration, the first algebraic equation

$$Px_1^2 = 2EI(\cos\theta_0 - \cos\theta_1) \tag{5.47}$$

The constants have been found from the boundary conditions

$$(\theta)_{x=x_1} = \theta_1 \quad \text{and} \quad (\theta)_{x=0} = \theta_0$$

The second algebraic relationship is based on the strain energy of the bar. The strain energy due to bending of an element of length ds is

$$dU = \frac{EI}{2}\left(\frac{d\theta}{ds}\right)^2 ds$$

Combining this expression with equation (5.46) and applying the first boundary condition we get, after eliminating $x_1 - x$,

$$dU = P(dy - \cos\theta_1 \, ds) \tag{5.48}$$

We integrate equation (5.48) along the whole length of the bar and arrive at

$$U_1 = P(y_1 - L\cos\theta_1) \tag{5.49}$$

which is the second algebraic equation for the solution of the unknowns.

From *Figure 5.13*

$$\frac{U_1}{P} = y_1 - L\cos\theta_1 = O''F - O'F$$

Hence, if we lay off $O'A = L$ along the tangent at A, then the projection of OO' on the line of thrust of P is U_1/P. Consideration of equation (5.48) shows that a similar geometric interpretation of strain energy holds in any segment of the strut.

Suppose now that we vary P and θ_0. This will result in a change of U_1 too. Let this change be ΔU_1; it must equal the work done by P at A and by the bending moment Px_1 at O.

$$\Delta U_1 = -P\Delta y_1 - Px_1 \Delta\theta_0$$

(The negative sign means that the energy increases, while y_1 and θ_0 decrease.)

Take now the derivative of U_1 with respect to P and also with respect to θ_0.

$$\frac{\partial U_1}{\partial P} = -P\frac{\partial y_1}{\partial P} \tag{5.50}$$

and

$$\frac{\partial U_1}{\partial \theta_0} = -P\frac{\partial y_1}{\partial \theta_0} - Px_1 \tag{5.51}$$

Equations (5.47, 49, 50 and 51) are the four fundamental relationships for the calculation of the unknowns x_1, y_1, U_1 and θ_1. Replacing the independent variables P and θ_0 by

$$t = L(P/EI)^{\frac{1}{2}} \quad \text{and} \quad \alpha = \cos\theta_0 \tag{5.52}$$

and the dependent variables by

$$X = \frac{x_1}{L},\ Y = \frac{y_1}{L},\ Z = \cos\theta_1 \quad \text{and} \quad W = \frac{U_1}{PL} \tag{5.53}$$

Substitution of equations (5.52 and 53) in (5.47 and 49) yields

$$\left.\begin{aligned} t^2 X^2 &= 2(\alpha - Z) \\ W &= Y - Z \end{aligned}\right\} \tag{5.54}$$

and

From equation (5.50), we find

$$\frac{\partial U_1}{\partial P} = L\left[W\frac{\partial P}{\partial t} + P\frac{\partial W}{\partial t}\right]\frac{\partial t}{\partial P} \quad \text{and} \quad -P\frac{\partial y_1}{\partial P} = -\frac{EI}{L}t^2\frac{\partial Y}{\partial t}\cdot\frac{\partial t}{\partial P}$$

Noting that

$$\frac{\partial P}{\partial t} = 2t\frac{EI}{L^2},$$

$$2W = -t\left[\frac{\partial W}{\partial t} + \frac{\partial Y}{\partial t}\right] \tag{5.55}$$

Analysing equation (5.51), we find that

$$\frac{\partial U_1}{\partial \theta_0} = -LP\frac{\partial W}{\partial \alpha}\sin\theta_0$$

or,

$$-P\frac{\partial y_1}{\partial \theta_0} = LP\frac{\partial W}{\partial \alpha}\sin\theta_0$$

Hence

$$X = \beta\left[\frac{\partial W}{\partial \alpha} + \frac{\partial Y}{\partial \alpha}\right] \tag{5.56}$$

where

$$\beta = \sin\theta_0 = (1-\alpha^2)^{\frac{1}{2}}$$

The next step is to find a function S of variables α and t such that the unknowns X, Y, Z, and W can be expressed in terms of this function.

Let S be defined as follows:

$$\mathrm{S} = \mathrm{S}(\alpha, t) = t(1 + Y + W) = \left(L + y_1 + \frac{U_1}{P}\right)\left(\frac{P}{EI}\right)^{\frac{1}{2}} \tag{5.57}$$

The partial derivatives of S can be obtained with reference to equations (5.54, 55, 56). We have

$$\frac{\partial \mathrm{S}}{\partial t} = 1 + Y + W + t\left(\frac{\partial Y}{\partial t} + \frac{\partial W}{\partial t}\right) = 1 + \mathrm{Z} \tag{5.58}$$

and

$$\frac{\partial \mathrm{S}}{\partial \alpha} = \frac{\partial Y}{\partial \alpha} + \frac{\partial W}{\partial \alpha} = t\frac{X}{\beta} \tag{5.59}$$

In terms of S and its partial derivatives the unknowns are

$$\left.\begin{aligned} X &= \frac{\partial \mathrm{S}}{\partial \alpha}\cdot\frac{\beta}{t} \\ Y &= \frac{1}{2}\left(\frac{\mathrm{S}}{t} + \frac{\partial \mathrm{S}}{\partial t} - 2\right) \\ \mathrm{Z} &= 1 - \frac{\partial \mathrm{S}}{\partial t} \\ W &= \frac{1}{2}\left(\frac{\mathrm{S}}{t} - \frac{\partial \mathrm{S}}{\partial t}\right) \end{aligned}\right\} \tag{5.60}$$

The problem is now reduced to that of finding the function $S = S(\alpha, t)$. Substituting equations (5.58 and 59) into

$$t^2 X^2 = 2(\alpha - Z)$$

$$\frac{\partial S}{\partial t} = 1 + \alpha - \frac{\beta^2}{2}\left(\frac{\partial S}{\partial \alpha}\right)^2 \tag{5.61}$$

results. $S(\alpha, t)$ must satisfy this nonlinear partial differential equation. The boundary conditions are

$$S(\alpha, 0) = 0$$

and

$$S(-1, t) = 0$$

The first equation follows from equation (5.57). The second equation becomes evident if one realizes that for $\cos\theta_0 = -1$, $\theta_0 = \pi$, hence

$$S = \frac{t}{L}\left(L + y_1 + \frac{U_1}{P}\right)$$

But if $\theta_0 = \pi$, L equals $-y_1$ and U_1/P is zero; the expression in the bracket also becomes zero.

$S(\alpha, t)$ is shown as a function of t in *Figure 5.14* for different values of α. The value of S, also that of $\partial S/\partial t$ can be found from these curves if we draw a tangent to the curve in question. $\partial S/\partial \alpha$ cannot be found directly but since X is the only unknown which depends on $\partial S/\partial \alpha$, we calculate X from

$$t^2 X^2 = 2(\alpha - Z)$$

once Z is found from equation (5.60).

It follows from equation (5.61) that the slope of every curve in *Figure 5.14* is $1 + \alpha$ at the origin.

For a vertical strut $\theta_0 = 0$ and $\alpha = 1$. If $P < P_{cr}$ the strut will remain straight, that is, $\cos\theta_1 = Z = 0$ and, from equation (5.60),

$$\frac{\partial S}{\partial t} - 1 = 0$$

The curve is, therefore, straight between O and E. E lies at $S(1, \pi/2) = t(1 + Y + W) = \pi$, since $P = t^2EI/L^2 = P_{cr}$.

When using *Figure 5.14* we first find $t = L(P/EI)^{\frac{1}{2}}$. Selecting the proper curve for a given θ_0 we read S on the left-hand scale. The tangent at $S(\alpha, t)$ gives $\partial S/\partial t$. Y and Z are then found from equation (5.60). Finally, X is calculated from equation (5.54).

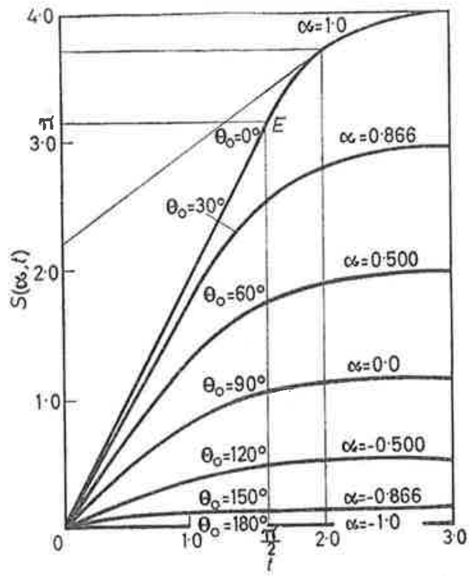

Figure 5.14 (According to Beth and Wells[14])

As a comparison with the methods outlined in Chapters 1 and 2, let us investigate a vertical strut with a large value for L^2/EI. If L tends to infinity, θ_1 tends to π, hence $Z = -1$. From equation (5.54)

$$t^2 X^2 = 4, \quad \text{or} \quad x_1 = 2(EI/P)^{\frac{1}{2}}$$

This agrees with equation (1.23).

For a finite L, $\theta_1 < \pi$ provided the strut was initially vertical. For this case we have from equation (5.54)

$$X^2 = \frac{2(1 - \cos\theta_1)}{t^2}, \text{ or } x_1 = \left[\frac{2(1 - \cos\theta_1)EI}{P}\right]^{\frac{1}{2}}$$

Since $\cos\theta_1 = 1 - 2p^2$ where $p = \sin(\theta_1/2)$, we get

$$x_1 = 2p(EI/P)^{\frac{1}{2}}$$

which is the result obtained for h in section 1.3.

S (α, t) can be expressed as a power series with coefficients which are functions of α. The coordinates x and y, also $\cos\theta_1$, can be expressed as a power series in terms of P. Hence the series for X, Y, and Z will contain only even powers of t. It is clear from equation (5.60) that S will have only odd powers of t. We note from the condition $S(\alpha, 0) = 0$ that only positive powers of t will occur in S, for, if there were negative powers as well $[S(\alpha, t)]_{t=0} \neq 0$. Therefore, S will be assumed in the form

$$S = a_0 t + a_1 t^3 + a_2 t^5 + \ldots\ldots = \sum_{n=0}^{\infty} a_n(\alpha)\, t^{2n+1} \qquad (5.62)$$

The partial derivatives of S are

$$\frac{\partial S}{\partial t} = a_0 + \sum_{n=1}^{\infty} (2n+1)\, a_n t^{2n}$$

$$\frac{\partial S}{\partial \alpha} = b_0 t + b_1 t^3 + b_3 t^5 + \ldots\ldots = \sum_{n=0}^{\infty} b_n t^{2n+1}$$

$$\left(\frac{\partial S}{\partial \alpha}\right)^2 = b_0^2 t^2 + 2b_0 b_1 t^4 + (2b_0 b_1 + b_1^2)\, t^6 + \ldots$$

$$= \sum_{m=0}^{m=n-1} b_m b_{n-1-m} t^{2n}, \text{ for } n = 1, 2, 3, \text{etc.}$$

where $$b_n = \frac{\partial a_n}{\partial \alpha}$$

Substitution of these derivatives in equation (5.61), and the comparison of the coefficients of t^{2n} in that equation leads to

$$a_0 = 1 + \alpha$$

and $$a_n = \frac{\alpha^2 - 1}{2(2n+1)} \sum_{m=0}^{m=n-1} b_m b_{n-1-m} \qquad \text{for } n = 1, 2, 3, \text{etc.}$$

These formulae enable us to determine a_1, a_2, a_3, etc., and b_1, b_2, b_3, etc., recursively. We have

$$b_0 = 1, \qquad a_1 = \frac{\alpha^2 - 1}{6}, \qquad b_1 = \frac{\alpha}{3},$$

$$a_2 = \frac{\alpha^2 - 1}{2.5}\left(\frac{\alpha}{3} + \frac{\alpha}{3}\right) = \frac{\alpha^2 - 1}{15}, \; b_2 = \frac{\partial a_2}{\partial \alpha} = \frac{3\alpha^2 - 1}{15},$$

$$a_3 = \frac{\alpha^2 - 1}{2.7}\left[2\frac{3\alpha^2 - 1}{15} + \left(\frac{\alpha}{3}\right)^2\right] = (\alpha^2 - 1)\frac{23\alpha^2 - 6}{630}, \text{ etc.}$$

The power series for S (α, t) can now be written:

$$S = (1 + \alpha)t + \frac{\alpha^2 - 1}{6}t^3 + \frac{\alpha^2 - 1}{15}\alpha t^5 + \frac{\alpha^2 - 1}{630}(23\alpha^2 - 6)t^7 + \ldots \tag{5.63}$$

This series satisfies the boundary conditions since S $(\alpha, t = 0) = 0$, and S $(\alpha = -1, t) = 0$.

Equation (5.60) will supply the coordinates in a power series form:

$$\left.\begin{aligned}
X &= \beta \sum_{n=0}^{\infty} b_n t^{2n} \\
Y &= \frac{1}{2}\left[\sum_{n=0}^{\infty} a_n t^{2n} + a_0 + \sum_{n=1}^{\infty} (2n + 1) a_n t^{2n}\right] - 1 \\
&= \alpha - (1 - \alpha^2)\left(\frac{t^2}{3} + \frac{\alpha}{5}t^4 + \frac{46\alpha^2 - 12}{315}t^6 + \ldots\right) \\
Z &= \alpha + \sum_{n=1}^{\infty} (2n + 1) a_n t^{2n} = \alpha - (1 - \alpha^2) \times \\
&\quad \times \frac{1}{2}t^2\left(\frac{\alpha}{3}t^4 + \frac{23\alpha^2 - 6}{90}t^6 + \ldots\ldots\right)
\end{aligned}\right\} \tag{5.64}$$

For a vertical strut with P_{cr} at the free end

$$t = \pi/2, \; \theta_0 = 0, \; \alpha = 1, \text{ and } \beta = 0,$$

hence $$X = \frac{x_1}{L} = 0, \qquad \text{and} \qquad Y = \frac{y_1}{L} = 1$$

These are correct results if $t < \pi/2$. For $t > \pi/2$, the strut becomes unstable but X and Y still show a vertical line since disturbing forces are not considered here.

For the horizontal cantilever with P at the free end

$$\theta_0 = \pi/2, \quad \alpha = 0, \quad \text{and} \quad \beta = 1,$$

hence

$$X = 1 - \frac{t^4}{15} + \frac{36}{2835}t^8 - \ldots.$$

$$Y = -\frac{t^2}{3} + \frac{12}{315}t^6 + \ldots$$

and the vertical deflection at the end is

$$y_1 = -\frac{PL^3}{3EI} + \frac{12}{315}\left(\frac{P}{EI}\right)^3 L^7 + \ldots.$$

The first term agrees with the small deflection theory.

5.8. Numerical Analysis of Bars under Distributed Loads

This type of analysis for the deflection of a bar has already been mentioned in section 4.12 where the method was explained for point loads. The same general lines will be followed when the bar carries a distributed load although M'_i, the average bending moment, needs special consideration.

Consider the bar in *Figure 4.47* subject to a distributed load $w = w(s)$ and let w_1, w_2, w_3, etc., be the average load intensity over arcs 1, 2, 3, and so on. The average bending moment for a general arc is

$$\left.\begin{aligned} M'_i = w_1 s_1 (h_1/2 + h_2 + h_3 + \ldots\ldots.. h_{i-1} + h_i/2) &+ \\ + w_2 s_2 (h_2/2 + h_3 + \ldots\ldots.. h_{i-1} + h_i/2) &+ \\ + w_3 s_3 (h_3/2 + \ldots\ldots.. h_{i-1} + h_i/2) &+ \\ + w_{i-1} s_{i-1} (h_{i-1}/2 + h_i/2) &+ \\ + \frac{w_i s_i^2}{8} \cos\left(\psi_0 - \sum_{j=1}^{i-1} \beta_j\right) & \end{aligned}\right\} \quad (5.65)$$

Since M' is a function of both h and s the value of s is approximated by[15]

$$h\Big/\left[\cos\left(\psi_0 - \sum_{j=1}^{i-1}\beta_j\right)\right]$$

in the first step of the iteration.

$$\begin{aligned} M'_{i\ \text{approx}} = {} & w_1 s_1 (h_1/2 + h_2 + h_3 + \ldots\ldots h_{i-1} + h_i/2) + \\ & + w_2 s_2 (h_2/2 + h_3 + \ldots\ldots h_{i-1} + h_i/2) + \\ & + w_3 s_3 (h_3/2 + \ldots\ldots h_{i-1} + h_i/2) + \\ & + w_{i-1} s_{i-1} (h_{i-1}/2 + h_i/2) + \\ & + w_i h_i^2 \Big/ \left[8\cos\left(\psi_0 - \sum_{j=1}^{i-1}\beta_j\right)\right] \end{aligned}$$

The calculation proceeds as follows: h_1 is assumed (h_1 = say 1 in.) and $M'_{1\ \text{approx}}$ is calculated from

$$\frac{w_1 h_1^2}{8\cos\psi_0}$$

where ψ_0 is the end slope, unknown for the time being. After that we find $1/r_1$, r_1, and h_1/r_1. This is followed by ψ_0, $\sin\psi_0$,

$$\sin\left(\psi_0 - \sum_{j=1}^{1}\beta_j\right) = \sin\psi_0 - \frac{h_1}{r_1},\ \psi_0 - \sum_{j=1}^{1}\beta_j,$$

$$\text{and } \psi_j = \psi_0 - \left[\psi_0 - \sum_{j=1}^{1}\beta_j\right] \text{ (see section 4.12).}$$

Finally, we obtain $s_1 = r_1\beta_1$. This s_1 will now be used in equation (5.65) for the exact average bending moment. From

$$M'_1 = \frac{w_1 s_1^2}{8}\cos\psi_0$$

$1/r_1$, r_1, and h_1/r_1 is recomputed for arc 1 (b). This process is now repeated several times until s remains constant.

When $$\frac{h_k}{r_k} > \sin\left(\psi_0 - \sum_{j=1}^{k-1}\beta_j\right)$$

Table 10. (From Seames and Conway[15])

Column No.	1	2	3	4	5	6	7
Arc No.	h	$1/r$	r	h/r	$\psi_0-\sum_{j=1}^{i-1}\beta_j$	$\sin\left[\psi_0-\sum_{j=1}^{i-1}\beta_j\right]$	$\sin\left[\psi_0-\sum_{j=1}^{i}\beta_j\right]$
1a	1	0·01515	66·027	0·01515	0·60000	0·56464	0·54949
1b	1	0·01498	66·756	0·01498	0·60000	0·56464	0·54966
2a	1	0·13539	7·3860	0·13539	0·58196	0·54966	0·41427
2b	1	0·13408	7·4582	0·13408	0·58196	0·54966	0·41558
3a	1	0·36899	2·7101	0·36899	0·42858	0·41558	0·04659
3b	1	0·36743	2·7216	0·36743	0·42858	0·41558	0·04815
4	0·0893	—	1·8548	0·04815	0·04817	0·04815	0·00000

Column No.	8	9	10	11	12	13	14
Arc No.	$\psi_0-\sum_{j=1}^{i}\beta_j$	β_i	$\cos\left[\psi_0-\sum_{j=1}^{i-1}\beta_j\right]$	$\cos\left[\psi_0-\sum_{j=1}^{i}\beta_j\right]$	v/r	v	s
1a	0·58176	0·01824	—	—	—	—	1·2050
1b	0·58196	0·01804	0·82534	0·83537	0·01003	0·66956	1·2043
2a	0·42714	0·15482	—	—	—	—	1·1435
2b	0·42858	0·15338	0·83537	0·90956	0·07419	0·55332	1·1439
3a	0·04661	0·38197	—	—	—	—	1·0352
3b	0·04817	0·38041	0·90956	0·99884	0·08928	0·24298	1·0353
4	0·00000	0·04817	0·99884	1·00000	0·00116	0·00215	0·0893

the last arc has been reached and h_k has been chosen too large. h_k is found from solving

$$\sin\left(\psi_0 - \sum_{j=1}^{k-1} \beta_j\right) = \frac{M'_k}{EI} h_k$$

For a correctly assumed ψ_0, $\sum_{j=1}^{n} s_j = L$.

As an example take a cantilever 3·48 in. long with a flexural rigidity $EI = 20$ lb in.^{2} and a uniformly distributed load $w = 2$ lb/in. Let us assume that previous calculations have already been carried out and that they suggest that $\psi_0 = 0{\cdot}6$ would probably be correct. A calculation based on $\psi_0 = 0{\cdot}6$ is shown in a tabulated form in *Table 10*. We find that

$$\sum_1^4 s_j = 3{\cdot}47 \text{ in.} \approx L, \quad Y = \sum_1^4 v_j = 1{\cdot}47 \text{ in.},$$

and

$$X = \sum_1^4 h_j = 3{\cdot}09 \text{ in.}$$

If the cantilever is curved, the radius of curvature R_i of every elemental arc in the unloaded stage must be known in advance. The calculation follows similar lines to those outlined for the straight bar and the average bending moment for a general arc is the same as before. Again, M' is a function of both s and h, hence the approximate average bending moment is used as the first step of the iteration. The calculation follows *Table 10*, except that

$$\frac{1}{r_1} = \frac{M'_i}{EI} + \frac{1}{R_i}$$

takes the place of

$$\frac{1}{r_i} = \frac{M'_i}{EI}$$

REFERENCES

[1] Greenhill, A. G. On height consistent with stability, *Proc. Camb. phil. Soc.* 4 (1881)

[2] Euler, *Mém. Acta. Acad. St-Petersb.*, 1780

[3] Todhunter, J. and Pearson, K. *History of the Theory of Elasticity*, Cambridge, 1886

REFERENCES

[4] Frisch-Fay, R. The analysis of a vertical and a horizontal cantilever under a uniformly distributed load, *J. Franklin Inst.* **271** (1961) 192

[5] Hummel, F. H. and Morton, W. B. *loc. cit.* page 72

[6] Rohde, F. V. Large deflections of a cantilever beam with a uniformly distributed load, *Quart. appl. Math.* **11** (1953) 337

[7] Bickley, W. G. The heavy elastica, *Phil. Mag. Ser.* 7, **17** (1934) 603

[8] Lippmann, H., Mahrenholtz, O. and Johnson, W. Thin heavy elastic strips at large deflections, *Int. J. Mech. Sci.* **2** (1961) 294

[9] Sato, K. Large deflections of a circular cantilever beam, *Ingen.-Arch.* **27** (1959) 195

[10] Mitchell, T. P. *loc. cit.* page 161

[11] Truesdell, C. A new chapter in the theory of the elastica, *Proc. First Midwestern Conf. Solid Mech.* (1955) 52

[12] Sundara Raya Iyengar, K. T. Large deflections of cantilever beans, *J. Indian Inst. Sci.* Annual Report of Civil and Hydraulic Engineering Section (1954) 27

[13] Sundara Raya Iyengar, K. T. and Lakshmana Rao, S. K. Large deflections of simply supported beams, *J. Franklin Inst.* **259** (1955) 523

[14] Beth, R. A. and Wells, C. P. Finite deflections of a cantilever strut, *J. appl. Phys.* **22** (1951) 742

[15] Seames, A. E. and Conway, H. D. *loc. cit.* page 161

6

THREE-DIMENSIONAL DEFORMATIONS OF A BAR

6.1. Generalized Kinetic Analogy

It has been mentioned in section 1.6 that the pendulum swinging in a vertical plane about a horizontal axis is the kinetic analogy of a thin, prismatic bar, initially straight, that is bent in a principal plane by forces and couples applied at the ends only. Since no torque is present the elastic line is a plane curve. Kirchhoff, and later Clebsch[1], pointed out that the equations referring to a thin, prismatic bar, straight when unstressed, and bent and twisted by a force, couple, and torque applied at the ends, are analogous with the equations of motion of a rigid body turning about a fixed point. The same bar when bent and twisted by a couple and a torque at the ends is analogous with a rigid body rotating about its centre of gravity G. In the last two cases the deflected shape of the bar becomes a space curve and we need a three-dimensional coordinate system to analyse it.

In the unstressed state the thin bar is straight and its axis coincides with the coordinate axis Z; X and Y are parallel to the principal axes of the cross-section. After the application of a force, couple, and torque (or a force and a couple whose plane is not a principal plane) the direction of the deflected shape changes from point to point; hence it becomes necessary to select a coordinate system for every cross-section. The tangent of an element ds of the bar will be called the Z' axis, while the X' and Y' axes will coincide with the principal axes of the cross-section. Since adjacent cross-sections in the deflected shape bend about two axes and twist about the third, the $X'Y'Z'$ coordinate system (moving system) will change its position with respect to the XYZ coordinate system (fixed axes) as we traverse the length of the bar. The fixed and moving coordinates are linked together by the following direction cosines

	X	Y	Z
X'	l	m	n
Y'	l'	m'	n'
Z'	l''	m''	n''

(6.1)

The direction cosines can be expressed in terms of three angles, θ, ψ, and ϕ. As seen from *Figure 6.1*, θ is the angle between Z and Z', ψ is the angle between the fixed plane XZ and ZZ' plane, and ϕ is the angle between the same ZZ' plane and the moving plane $Z'X'$. All these angles are functions of s, measured from the free end of the bar. The direction cosines are:

$$\left.\begin{aligned} l &= -\sin\psi\sin\phi + \cos\psi\cos\phi\cos\theta, \\ l' &= -\sin\psi\cos\phi - \cos\psi\sin\phi\cos\theta, \\ l'' &= \sin\theta\cos\psi, \\ m &= \cos\psi\sin\phi + \sin\psi\cos\phi\cos\theta, \\ m' &= \cos\psi\cos\phi - \sin\psi\sin\phi\cos\theta, \\ m'' &= \sin\theta\sin\psi, \\ n &= -\sin\theta\cos\phi, \\ n' &= \sin\theta\sin\phi, \\ n'' &= \cos\theta \end{aligned}\right\} \quad (6.2)^2$$

Let us assume that the bar is acted upon by couples **M** at the ends; the axis of the couple is in the plane in which the principal axes of the two bending rigidities and the torsional rigidity have the maximum and minimum values respectively[3]. In this case every element of the bar will undergo bending as well as twist. The kinetically analogous case, the rotation of a rigid body about G, is governed by Euler's equations:

$$\left.\begin{aligned} A\frac{du}{dt} + (B - C)\,vw &= 0 \\ B\frac{dv}{dt} + (C - A)\,wu &= 0 \\ C\frac{dw}{dt} + (A - B)\,uv &= 0 \end{aligned}\right\} \quad (6.3)$$

In this equation, A, B and C are the moments of inertia of the rotating body about the principal axes X', Y', and Z'; u, v, and w

are the angular velocities about X', Y', and Z' at the time t. Au, Bv, and Cw are the components of the impulse of torque about X', Y', and Z', resulting in the angular velocities u, v, and w about the instantaneous position of the moving coordinate axes.

Equations (6.3) can be applied for the solution of the bar mentioned before if t is replaced by the length s; if A, B, C designate the resistance against bending about X' and Y', and against torsion about Z'; if u, v, w are replaced by the curvature components p and q for bending about X' and Y', and r for twist about Z'; and finally, if Ap, Bq, and Cr are the components of the couple $\mathbf{M}$ necessary to cause the curvatures p, q, and r about X', Y', and Z' respectively.

A, B, and C of the rotating body correspond in the bar to the flexural and torsional rigidities EI_x, EI_y, and αGA_c (GI_p for a circular wire) where G is the modulus of shear, A_c the cross-sectional area and I_p the polar moment of inertia of the cross section about the longitudinal axis of the bar.

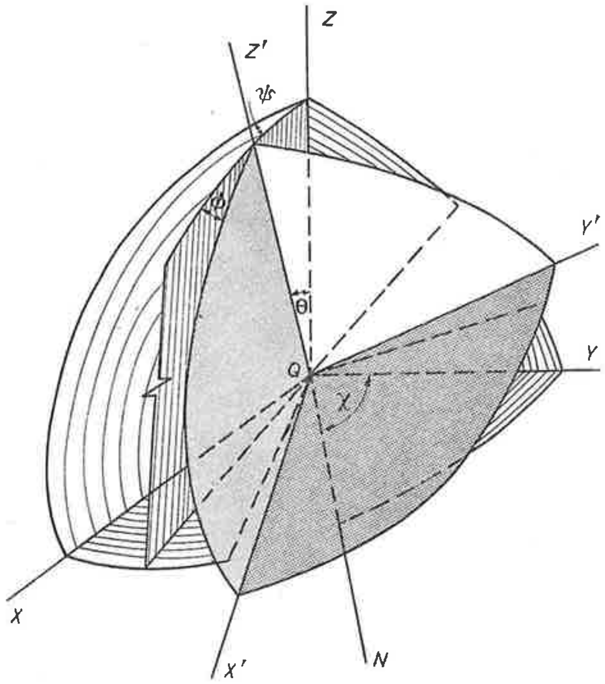

Figure 6.1

The curvature components can be expressed in terms of the derivatives of θ, ψ, and ϕ with respect to s. We have

$$\left.\begin{aligned} p &= \frac{d\theta}{ds}\sin\phi - \frac{d\psi}{ds}\sin\theta\cos\phi \\ q &= \frac{d\theta}{ds}\cos\phi + \frac{d\psi}{ds}\sin\theta\sin\phi \\ r &= \frac{d\phi}{ds} + \frac{d\psi}{ds}\cos\theta \end{aligned}\right\} \tag{6.4}$$

From the condition that the axes X, Y, Z are fixed while X', Y', Z' are moving with the angular velocities p, q, r, we obtain

$$\left.\begin{aligned} \frac{dl}{ds} &= l'r - l''q \\ \frac{dm}{ds} &= m'r - m''q \\ \frac{dn}{ds} &= n'r - n''q \\ \frac{dl'}{ds} &= l''p - lr, \quad \text{etc.,} \end{aligned}\right\} \tag{6.5}$$

altogether 9 equations for the solution of the direction cosines. They are interrelated through the orthogonal substitutions

$$\left.\begin{aligned} l &= m'n'' - n'm'' \\ m &= n'l'' - l'n'' \\ n &= l'm'' - m'l'', \\ &\text{etc.} \end{aligned}\right\} \tag{6.6}$$

The coordinates of a point Q on the bar are found from the differential equations

$$dx = l''\,ds, \quad dy = m''\,ds, \quad dz = n''\,ds \tag{6.7}$$

Integration of (6.7) will give the coordinates x, y, z in the XYZ fixed coordinate system.

6.2. The Curvatures p, q, and r

By adding the triad of curvature components vectorially, we have $\Theta = (p^2 + q^2 + r^2)^{\frac{1}{2}}$, where Θ is the magnitude of the total curvature at a point of the bar measured along the instantaneous radius of curvature Θ. There is also $M = (A^2p^2 + B^2q^2 + C^2r^2)^{\frac{1}{2}} = \mathbf{M}$, the magnitude of the internal resisting couple about the instantaneous axis of torque. The curvature due to pure bending is $\Theta' = (p^2 + q^2)^{\frac{1}{2}}$; this magnitude is the component of the instantaneous curvature Θ in the $X'Y'$ plane.

If we multiply the equations in (6.3) by Ap, Bq, and Cr, and then add them, we arrive at

$$A^2 p^2 + B^2 q^2 + C^2 r^2 = \text{const.} = \mathbf{M}^2 \tag{6.8}$$

Next, we multiply the three equations in (6.3) by l, l', l'' and add them together. We obtain

$$Apl + Bql' + Crl'' = \text{const.} = \mathbf{M}_1 \tag{6.9a}$$

Similar operations with m, m', m'', and with n, n', n'' result in

$$Apm + Bqm' + Crm'' = \text{const.} = \mathbf{M}_2$$
$$Apn + Bqn' + Crn'' = \text{const.} = \mathbf{M}_3 = (\mathbf{M}^2 - \mathbf{M}_1^2 - \mathbf{M}_2^2)^{\frac{1}{2}} \tag{6.9b}$$

These equations state that the internal resistance at any cross-section due to the applied couple at the end of the bar is equivalent to $\mathbf{M}$.

Let us conceive the instantaneous curvature axis made up of the curvature components $p(s)$, $q(s)$, and $r(s)$; all these axes are parallel to the generating lines of a cone $\mathbf{P}$ of the second degree; in the aggregate these axes produce a warped surface ($\mathbf{P}$). The locus of the centres of curvature on these axes is a transcendental line $\mathbf{p}$. The equation of the cone $\mathbf{P}$ is

$$Ap^2(Ah - \mathbf{M}^2) + Bq^2(Bh - \mathbf{M}^2) + Cr^2(Ch - \mathbf{M}^2) = 0 \tag{6.10}$$

where $$h = Ap^2 + Bq^2 + Cr^2$$

The cone $\mathbf{P}$ is always real, hence not all the differences in the three brackets of equation (6.10) can have identical signs. It follows that if the flexural and torsional rigidities are of the magnitudes $A > B > C$, then $Ah - \mathbf{M}^2 > 0$, $Ch - \mathbf{M}^2 < 0$, and $Bh - \mathbf{M}^2 \lesseqgtr 0$. According to Jacobi the curvature components can be expressed through elliptic functions. For the case $A > B > C$, and $Bh - \mathbf{M}^2 > 0$ the modulus of the functions is[4]

$$\mu = \left[\frac{(A - B)(\mathbf{M}^2 - Ch)}{(B - C)(Ah - \mathbf{M}^2)}\right]^{\frac{1}{2}} = \left[\frac{C(A - B)}{A(B - C)}\right]^{\frac{1}{2}} \tan \phi_0$$

where ϕ_0 is the angle between the axis of the applied couple $\mathbf{M}$ and the principal axis of the least rigidity. The problem considered by Jacobi refers to a rotating body, but the analogy that exists between angular velocity components and curvature enables us to use equations (6.11).

The curvature components are

$$\left.\begin{aligned} p &= \frac{\mathbf{M}}{A} \sin \phi_0 \operatorname{cn} u\,, \\ q &= \frac{\mathbf{M}}{A} \sin \phi_0 \left[\frac{A\,(A - C)}{B\,(B - C)}\right]^{\frac{1}{2}} \operatorname{sn} u\,, \\ r &= \frac{\mathbf{M}}{C} \cos \phi_0 \operatorname{dn} u \end{aligned}\right\} \quad (6.11)$$

The argument in the elliptic functions is $u = js$, where s is the length from the free end to the point in question, and

$$j = \frac{\mathbf{M}}{C}\left[\frac{(B - C)(A - C)}{AB}\right]^{\frac{1}{2}} \cos \phi_0$$

It should be noted that the conditions of $A > B > C$; $Bh - \mathbf{M}^2 > 0$ are not the only ones that will make the cone $\mathbf{P}$ real. In fact, there are six combinations between A, B, C, h, and $\mathbf{M}$ which will produce a real cone $\mathbf{P}$, and for those cases the expressions for p, q, and r are different from those listed in (6.11).

Inspection of equations (6.11) shows that p, q, and r are, generally speaking, periodical with $4K(\mu)$. It is also apparent that, neglecting the sign, (6.11) will yield the same values for u and for $u \pm 2K(\mu)$. Consequently, the absolute values of bending and torsion need be calculated for a length K/j only. Assuming again that $A>B>C$ and $Bh - \mathbf{M}^2>0$, the curvature components will vary with the parameter u as follows:

$u = 0$	$< K$	$= K$	$< 2K$	$= 2K$	$< 3K$	$= 3K$	$< 4K$	$= 4K$
p_{max}	$+ p$	0	$- p$	p_{min}	$- p$	0	$+ p$	p_{max}
0	$+ q$	q_{max}	$+ q$	0	$- q$	q_{min}	$- q$	0
r_{max}	$+ r$	$+r_{min}$	$+ r$	r_{max}	$+ r$	$+r_{min}$	$+ r$	r_{max}

Similar tables apply for the other five cases.

Some important features of the behaviour of bars loaded in this way can be learnt from these tables. If, for instance, the torsional rigidity is the second largest of the three, the twist of the bar cannot proceed in the same direction all the way. There will be cross-sections on the deflected bar having no torsion at all (only bending), and cross-sections lying at an equal distance to the right and left from these ' points of torsional contraflexure ' will have twists of identical magnitude but opposite directions.

If the torsional rigidity is the least of the three and if $Bh - \mathbf{M}^2 > 0$, the bar will always be twisted in the same direction, although the intensity of the twist will oscillate between a positive maximum and minimum; if $Bh - \mathbf{M}^2 < 0$, the direction of the twist will alternate.

Regarding now the bending components, if one of the flexural rigidities, say A, is the second largest, the sign of the bending about X' will alternate.

If C is the second largest rigidity, pure bending will reach its maximum value at points belonging to $u = 0$, $2K$, $4K$, etc.; Θ' will be a minimum at the same points if C is the smallest of the three rigidities. If the torsional rigidity is the largest, we have a maximum or a minimum bending moment at $u = 0$, $2K$, $4K$, etc., depending on whether or not $C > A + B$ or $C < A + B$.

6.3. The Cones P and H

Let the solid body rotate about the instantaneous axis $G\Theta$ during the time dt and let Θ_1 be the angular velocity. In this case an axis $G\Theta_2$, adjacent to $G\Theta_1$, will move into position $G\beta_2$ and become itself the instantaneous axis of rotation. The solid now rotates about $G\beta_2$ with a velocity Θ_2, while another $G\Theta_3$ axis rotates about $G\Theta_2$ and will soon be displaced into position $G\beta_3$, only to become the new instantaneous axis of rotation itself. It appears, therefore, that the cone $G\Theta_1\Theta_2\Theta_3$ . . . of the instantaneous axes of rotation (which can be composed from u, v, w) will roll without slipping on another cone $G\beta_1\beta_2\beta_3$ . . . and that both cones at every instant have a common generator which is the instantaneous axis of rotation. These two cones are called **P** and **H** respectively.

Applying the foregoing to the elastic bar, take the straight, untwisted bar and attach to every point Q the resultant of the curvature components p, q and r. This will give us the instantaneous curvature Θ in magnitude and direction; hence $Q\Theta$ is the axis about which the element ds will deform. Beginning from the free end we turn the bar element Q_1Q_2 about the axis of curvature $Q_1\Theta_1$ by the amount $\Theta_1 ds$. We do this by bending the element to the amount of $\Theta_1' ds$ about the axis of pure bending and, in addition, twist it to the amount of $r_1 ds$ about the axis of ds, that is, about Z'. After that Q_1Q_2 is locked in position and a deformation $\Theta_2 ds$ is applied on the element Q_2Q_3 about its axis of curvature $Q_2\Theta_2$; Q_2Q_3 is then locked again and Q_3Q_4 will be bent and twisted along $Q_3\Theta_3$ to the combined amount of $\Theta_3 ds$, etc. In the end, the initially straight and untwisted bar is transformed into the equilibrium shape of the bent and twisted bar. As mentioned before, the axes $Q_1\Theta_1$, $Q_2\Theta_2$, $Q_3\Theta_3$, ... generate the surface (**P**); but now these axes lie on a new warped surface whose directrix is the bent bar. Let this warped surface be called (**H**). As seen, therefore, the transformation of the straight, untwisted bar into its final bent and twisted shape can be visualized by unwrapping the flexible warped surface (**P**) on the fixed warped surface (**H**). The two surfaces will, during unwrapping, touch each other along the instantaneous axis of curvature. The directrices of (**P**) and (**H**) are the straight bar and the bent elastic shape, respectively.

When the bar is acted upon by couples only, the generators of the flexible surface (**P**) are parallel to the generators of a second degree cone, while those of the surface (**H**) are parallel to the generators of a transcendental cone.

6.4. Coordinates of the Elastic Shape

It will be remembered that the periods of p, q, and r vary as the period of $K(\mu)$ of u, hence all points whose parameters differ by a multiple of $4K(\mu)$ possess identical curvatures, and arc lengths limited by such points are congruent.

The magnitude of the curvature of pure bending, $\Theta' = (p^2+q^2)^{\frac{1}{2}}$ can never become zero, except for $p = q = 0$. This would mean that the axis of the applied couple is the axis of the straight bar; the twisted bar remains straight too. Hence, apart from this particular case, the elastic curve has no points of contraflexure. In the following discussion the axis of the applied couple **M** will coincide with the fixed coordinate axis Z and the plane of **M** will be the XY plane. The Y axis is selected to coincide with the axis of the second largest rigidity of the cross-section at the free end.

From (6.4) and (6.5)

$$m'' \frac{dl''}{ds} - l'' \frac{dm''}{ds} = np + n'q \tag{6.12}$$

It can be shown that

$$n = Ap/\mathbf{M}, \quad n' = Bq/\mathbf{M}, \quad n'' = Cr/\mathbf{M} \tag{6.13}$$

After substituting (6.13) in (6.12)

$$-(l'')^2 \frac{d(m''/l'')}{ds} = \frac{Ap^2 + Bq^2}{\mathbf{M}} \tag{6.14}$$

However, $\quad (l'')^2 + (m'')^2 = 1 - (n'')^2 = \dfrac{A^2p^2 + B^2q^2}{\mathbf{M}^2}$

hence, by introducing the auxiliary angle χ (*Figure 6.1*)

$$l'' = (A^2 p^2 + B^2 q^2)^{\frac{1}{2}} \cos \chi/\mathbf{M}$$

and

$$m'' = (A^2 p^2 + B^2 q^2)^{\frac{1}{2}} \sin \chi/\mathbf{M}$$

Inserting these values in equation (6.14) and writing $u/j = s$, we obtain

$$d\chi = -\frac{\mathbf{M}}{j}\left(\frac{Ap^2 + Bq^2}{A^2p^2 + B^2q^2}\right) du \tag{6.15}$$

The auxiliary angle χ is the angle between the intersection line of plane $X'Y'$ of a point Q on the fixed plane XY on the one hand, and the fixed Y axis on the other.

From equation (6.7)

$$z = \int n'' \, ds = \frac{C}{\mathbf{M}j} \int r \, du \tag{6.16}$$

In this expression, r can have different values depending on the relative magnitudes of the principal rigidities of the bar. For the case to which the discussion is restricted, that is, for $A > B > C$ and $Bh - \mathbf{M}^2 > 0$,

$$r = \frac{\mathbf{M}}{C} \cos \phi_0 \operatorname{dn} u ,$$

and since $\int \operatorname{dn} u \, du = \operatorname{am} u$, z may be expressed as

$$z = \frac{\cos \phi_0}{j} \operatorname{am} u$$

However, j depends on ϕ_0, on $\mathbf{M}$, and on the principal rigidities; inserting j into the expression of z above yields

$$z = \frac{C}{\mathbf{M}} \left[\frac{AB}{(A - C)(B - C)} \right]^{\frac{1}{2}} \operatorname{am} u \tag{6.17}$$

The function $\operatorname{am} u$ can be expanded into a Fourier Series[5]. Accordingly

$$z = \frac{1}{D} \left[v + 4 \sum_{\nu=1}^{\nu=\infty} \frac{q^{\nu} \sin (\nu v)}{(1 + q^{2\nu})} \right] \tag{6.18}$$

where $$D = \frac{2\mathbf{M}}{C} \left[\frac{(A - C)(B - C)}{AB} \right]^{\frac{1}{2}}, \quad v = \pi u / K,$$

$$q = e^{-(\pi K'/K)} = \textit{nome } q,$$

and K' is the complete elliptic integral of the first kind with the complementary modulus $\mu' = (1 - \mu^2)^{\frac{1}{2}}$.

Regarding the angle χ, it has been found that in the case of a solid rotating about its centroid, χ is the angle between the nodal line and the Y axis (*Figure 6.1*) (the nodal line N is the intersection between the plane of torque and the $X'Y'$ plane). This angle has been analysed by Jacobi[4], who expressed it as

$$\chi = \chi' + j' u \tag{6.19}$$

where $$\chi' = \frac{1}{2i} \ln \frac{\vartheta_0 (u + ia)}{\vartheta_0 (u - ia)}, \quad j' = \frac{\mathbf{M}}{Aj} + \left(\frac{d}{dt} \ln \vartheta_0 (it) \right)_{t=a}$$

Here a is defined from

$$a = \int_{\beta}^{\pi/2} \frac{d\phi}{[1-(k')^2\sin^2\phi]^{\frac{1}{2}}}, \text{ where } \sin\beta = \left[\frac{A(B-C)}{B(A-C)}\right]^{\frac{1}{2}}$$

Having determined χ, l'' and m'' may be obtained without difficulty. According to Jacobi the direction cosines of Z' with respect to X and Y are

$$\begin{aligned} l'' &= f\cos(j'u) + g\sin(j'u) \\ m'' &= -f\sin(j'u) + g\cos(j'u) \end{aligned} \tag{6.20}$$

where $$f = \frac{\vartheta_2(0)}{2i\vartheta_2(ia)\vartheta_0(u)}[\vartheta_0(u+ia) - \vartheta_0(u-ia)]$$

and $$g = \frac{\vartheta_2(0)}{2\vartheta_2(ia)\vartheta_0(u)}[\vartheta_0(u+ia) + \vartheta_0(u-ia)] \tag{6.21}$$

The x and y coordinates in the XYZ system can now be found by performing the integrations $x = \int l''ds$ and $y = \int m''ds$, if the Theta functions ϑ_0 and ϑ_2 in (6.21) are replaced by infinite series. Introducing the substitutions

$$b = \frac{a}{K'}, \text{ and } c = \frac{j'K}{\pi}, \text{ the coordinates are}$$

$$\begin{aligned} x = \frac{1}{D}\Bigg\{&\frac{2q^{b/2}}{c(1-q^b)}\sin(cv) + 2q^{b/2}\sum_{\nu=1}^{\nu=\infty}\frac{q^\nu\sin[(c-\nu)v]}{(c-\nu)(1-q^{2\nu+b})} - \\ &- 2q^{-b/2}\sum_{\nu=1}^{\nu=\infty}\frac{q^\nu\sin[(c+\nu)v]}{(c+\nu)(1-q^{2\nu-b})}\Bigg\} \\ y = \frac{1}{D}\Bigg\{&\frac{4q^{b/2}}{c(1-q^b)}\sin^2(cv/2) + 4q^{b/2}\sum_{\nu=1}^{\nu=\infty}\frac{q^\nu\sin^2[v(c-\nu)/2]}{(c-\nu)(1-q^{2\nu+b})} - \\ &- 4q^{-b/2}\sum_{\nu=1}^{\nu=\infty}\frac{q^\nu\sin^2[v(c+\nu)/2]}{(c+\nu)(1-q^{2\nu-b})}\Bigg\} \end{aligned} \tag{6.22}$$

The discussion in the last three sections has shown that the analogy between the rotating body has to be studied carefully; for, while in the case of the rotating body it is immaterial which of the principal axes has the largest, the second largest, and the least moment of inertia, the relative magnitudes of the flexural rigidities and of the torsional resistance are of great importance in the analysis of the bar.

Let a bar be subject to forces and couples at the free end. If two principal rigidities are equal, and if the axis of the applied couples coincides with the axis of the third principal rigidity, the problem becomes analogous to the gyroscope[6].

6.5. The Spiral Spring

Let a straight, prismatic bar with two identical flexural rigidities be wound along a helix on a circular cylinder; this case is analogous to the steady motion of a symmetrical top, its axis of rotation inclined at $\theta = \pi/2 - \alpha$ to the fixed Z axis, where α is the angle which the tangent at any point of the helix makes with a plane normal to the axis of the cylinder. The configuration of the helical bar can be kept in equilibrium if a force P and a torque M_t act on the end of the rigid lever shown in *Figure 6.2*. Since θ is constant, $d\theta/ds = 0$.

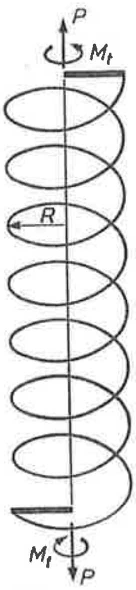

Figure 6.2

Also, from equation (6.4),
$p = 0$, $q = \cos^2 \alpha/R$, $r = \sin \alpha \cos \alpha/R$, since $\phi = \pi/2$, $d\phi/ds = 0$,

and $d\psi/ds = \cos\alpha/R$. R is the radius of the cylinder. The force and torque necessary to hold the spring in helical form are

$$P = -(B - C)\sin\alpha\cos^2\alpha/R^2,$$

and

$$M_t = (B\cos^2\alpha + C\sin^2\alpha)\cos\alpha/R \qquad (6.23)^7$$

Suppose now that the unstressed form of a bar is a helix of radius R and incline α, and that $A = B$. In this case

$$p_0 = 0,\ q_0 = \cos^2\alpha/R, \text{ and } r_0 = \sin\alpha\cos\alpha/R$$

Applying a force and a torque at the ends of a rigid lever (*Figure 6.2*), the radius and the incline of the spring will change to R_1 and α_1 respectively. The force and torque necessary for this change are

$$\left.\begin{aligned} P &= C\frac{\cos\alpha_1}{R_1}(V_1 - V) - B\frac{\sin\alpha_1}{R_1}(W_1 - W) \\ M_t &= C\sin\alpha_1(V_1 - V) + B\cos\alpha_1(W_1 - W) \end{aligned}\right\} \qquad (6.24)$$

where $V = \sin\alpha\cos\alpha/R$, $V_1 = \sin\alpha_1\cos\alpha_1/R_1$,

$W = \cos^2\alpha/R$, $W_1 = \cos^2\alpha_1/R_1$

6.6. Large Deflection of a Spiral Spring

As a first approach, the coiled spring can be treated as a bar of identical flexural rigidity. Then, by fixing the spring at A, the central line of the deflected shape will be as shown in *Figure 6.3*. Since the axial force at every cross-section depends on θ, the pitch of a spring in the deformed shape ABC will vary from point to point. This makes the spring equivalent to a bar with a varying flexural rigidity. There is present, however, a shear force too, whose influence on the curvature cannot be neglected as in the case of a flexible bar. In addition, the shear rigidity varies along ABC due to the variation of the pitch. Finally, the inextensibility of the bar on which the analysis of the flexible bar was based cannot be accepted here because the lengths of the loaded and unloaded spring differ considerably[8].

Let s, L, and b denote the arc length AB, the length ABC, and the pitch when P has been applied; s_0, L_0, and b_0 will denote the same dimensions on the unloaded spring. The axial, flexural, and shear rigidities of the spring in the unloaded condition are

$$\mathbf{A}_0 = \frac{GIb_0}{\pi R^3}, \quad \mathbf{B}_0 = \frac{2EGIb_0}{\pi R(E+2G)} \quad \text{and} \quad \mathbf{C}_0 = \frac{EIb_0}{\pi R^3} \quad \text{respectively}$$

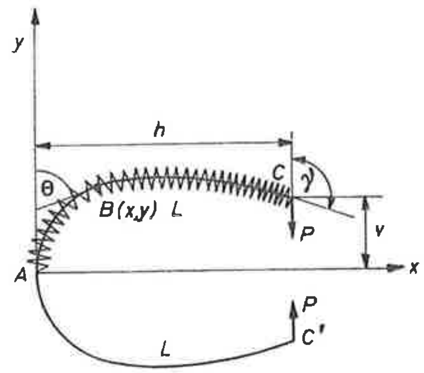

Figure 6.3

where R is the radius of the coil, and I is the moment of inertia of the cross-section of the wire with respect to a diameter[9]. The formulae apply to a coil made of circular wire. If the cross-section of the wire is not circular a shape factor is included in the formulae of the rigidities[10].

Let T, S, and M be the axial force, shear force, and bending moment respectively at B.

$$T = -P\cos\theta, \quad S = P\sin\theta, \quad M = P\int_s^L \sin\theta\, ds \tag{6.25}$$

Let **A**, **B**, and **C** denote the rigidities at point B when the spring is under load P. It follows from $T/\mathbf{A}_0 = (b - b_0)/b_0$, that

$$\mathbf{A} = \mathbf{A}_0\frac{b}{b_0} = \mathbf{A}_0\left[1 - \frac{P}{\mathbf{A}_0}\cos\theta\right], \quad \mathbf{B} = \mathbf{B}_0\frac{b}{b_0} = \mathbf{B}_0\left[1 - \frac{P}{\mathbf{A}_0}\cos\theta\right],$$

$$\text{and} \quad \mathbf{C} = \mathbf{C}_0\frac{b}{b_0} = \mathbf{C}_0\left[1 - \frac{P}{\mathbf{A}_0}\cos\theta\right] \tag{6.26}$$

The rigidities are thus a function of θ. The differential equation of the deflected axis of the coil is

$$\frac{d\theta}{ds} = \frac{M}{\mathbf{B}} + \frac{1}{\mathbf{C}}\frac{dS}{ds} \tag{6.27}$$

Substitution of (6.25) and (6.26) in (6.27) gives

$$(1 - \tau\cos\theta)\frac{d\theta}{d\sigma} = \beta\int_{\sigma}^{1}\sin\theta\, d\sigma \tag{6.28}$$

where $\sigma = \dfrac{s}{L}$, $\lambda = \dfrac{P}{\mathbf{A}_0}$, $\beta = \dfrac{L^2 P}{\mathbf{B}_0}$, $\nu = \dfrac{P}{\mathbf{C}_0}$,

and $\lambda + \nu = \tau = \dfrac{P\pi R^3}{EIb_0}(3 + 2\mu)$ (μ is Poisson's ratio).

Taking the derivative with respect to σ and integrating, we get

$$(1 - \tau\cos\theta)^2\left(\frac{d\theta}{d\sigma}\right)^2 = \beta(2\cos\theta - \tau\cos^2\theta + H) \tag{6.29}$$

H is the constant of the integration; it is found from the boundary condition

$$\frac{d\theta}{d\sigma} = L\left(\frac{d\theta}{ds}\right)_{\theta=\gamma} = 0$$

Accordingly, $H = [(1 - \tau\cos\gamma)^2 - 1]/\tau$. Hence equation (6.29) becomes

$$(1 - \cos\theta)^2\left(\frac{d\theta}{d\sigma}\right)^2 = \frac{\beta}{\tau}[(1 - \tau\cos\gamma)^2 - (1 - \tau\cos\theta)^2] \tag{6.30}$$

However, from previous notations,

$$\left(\frac{\tau}{\beta}\right)^{\frac{1}{2}} = \frac{R}{L}\left(\frac{3 + 2\mu}{2 + \mu}\right)^{\frac{1}{2}};\ \text{hence}$$

$$d\sigma = \sqrt{f}\,\frac{R}{L}\,\frac{(1 - \tau\cos\theta)\, d\theta}{[(1 - \tau\cos\gamma)^2 - (1 - \tau\cos\theta)^2]^{\frac{1}{2}}} \tag{6.31}$$

where $\quad f = \dfrac{3 + 2\mu}{2 + \mu}$

Let $\quad U(\theta) = (1 - \tau\cos\gamma)^2 - (1 - \tau\cos\theta)^2$

Equation (6.31) thus reduces to

$$ds = \sqrt{f}\,R\,\frac{(1 - \tau\cos\theta)\,d\theta}{[U(\theta)]^{\frac{1}{2}}} \tag{6.32}$$

and gives

$$L = \sqrt{f}\,R\int_0^{\gamma}\frac{(1 - \tau\cos\theta)\,d\theta}{[U(\theta)]^{\frac{1}{2}}} \tag{6.33}$$

Since $\dfrac{b - b_0}{b_0} = \dfrac{ds - ds_0}{ds_0} = \dfrac{T}{A_0}$, we have $\dfrac{ds}{ds_0} = 1 - \lambda\cos\theta$, and it follows that

$$L_0 = \sqrt{f}\,R\int_0^{\gamma}\frac{(1 - \tau\cos\theta)\,d\theta}{(1 - \lambda\cos\theta)[U(\theta)]^{\frac{1}{2}}} \tag{6.34}$$

The solution of this equation will yield γ.

In order to reduce equation (6.34) to standard elliptic integrals, put $z = \cos\theta$; then

$$d\theta = -\frac{dz}{(1 - z^2)^{\frac{1}{2}}}$$

The resulting expression is

$$L_0 = \sqrt{f}\,\frac{R}{\lambda\tau}\int_1^{\cos\gamma}\frac{(1 - \tau z)\,dz}{(z - 1/\lambda)[(z-1)(z+1)(z-\cos\gamma)(z+\cos\gamma - 2/\tau)]^{\frac{1}{2}}} \tag{6.35}$$

This integral can be reduced to elliptic integrals of the third kind[11].

Another way of finding γ is to expand the integral in equation (6.33) into a series. It may be shown that

$$\left.\begin{aligned} &2\sqrt{\beta} = \pi(1 - \tau)^{-\frac{1}{2}} S_1 \\ &\text{where} \\ &S_1 = (1 - \tau) + \frac{1}{4}\sin^2(\gamma/2) + \frac{1}{64}\frac{9 - 8\tau}{1 - \tau}\sin^4(\gamma/2) + \ldots \end{aligned}\right\} \tag{6.36}$$

Expansion of equation (6.34) leads to

$$\left.\begin{aligned} &L_0/L = (1 - \lambda)^{-1}(1 - S_2/S_1) \\ &\text{where} \\ &S_2 = \lambda\frac{1 - \tau}{1 - \lambda}\sin^2(\gamma/2) + \\ &\qquad + \frac{\lambda}{8}\frac{(3 - 15\lambda + 2\tau + 10\lambda\tau)}{(1 - \lambda)^2}\sin^4(\gamma/2) + \ldots \end{aligned}\right\} \tag{6.37}$$

By multiplying together equations (6.36) and (6.37)

$$\left.\begin{aligned} 2\sqrt{\beta}\,(L_0/L) &= \pi(1-\lambda)^{-1}(1-\tau)^{-\frac{1}{2}}(S_1 - S_2) \\ \text{or}\quad \frac{2}{\pi\sqrt{f}}\frac{L_0}{R}[\tau(1-\tau)]^{\frac{1}{2}}(1-\lambda) &= S_1 - S_2 \\ &= (1-\tau) + a_1\sin^2(\gamma/2) + a_2\sin^4(\gamma/2) + \ldots \end{aligned}\right\} \quad (6.38)$$

It appears from (6.38) that γ depends on λ and τ only, since

$$\left(\frac{\tau}{\beta}\right)^{\frac{1}{2}} = \frac{R}{L}\sqrt{f}$$

By taking $S_1 - S_2$ to terms containing $\sin^4(\gamma/2)$ only,

$$\sin^2(\gamma/2) \approx \frac{-a_1 + (a_1^2 + 4a_0a_1)^{\frac{1}{2}}}{2a_2} \quad (6.39)$$

If μ is given, a_0, a_1, and a_2 depend on τ only since $\lambda = c\tau$. For example, if $\mu = 0{\cdot}3$, $\lambda = 0{\cdot}722\,\tau$, and $\sqrt{f} = 1{\cdot}25$. With these values

$$a_0 = \frac{2}{\pi}\cdot\frac{1}{1{\cdot}25}\,\frac{L_0}{R}\,[\tau(1-\tau)]^{\frac{1}{2}}(1 - 0{\cdot}722\,\tau) - (1-\tau)$$

$$a_1 = \frac{1}{4} - 0{\cdot}722\,\tau\,\frac{1-\tau}{1 - 0{\cdot}722\,\tau}$$

$$a_2 = \frac{1}{64}\,\frac{9 - 8\tau}{1-\tau} - \frac{0{\cdot}722}{8}\,\tau\,\frac{3 - 8{\cdot}33\,\tau + 7{\cdot}22\,\tau^2}{(1 - 0{\cdot}722\,\tau)^2}$$

In order to facilitate the calculation of $\sin^2(\gamma/2)$ a chart is given in *Figure 6.4*. As seen, the value of $\sin^2(\gamma/2)$ depends on $2L_0/R$ and on the parameter $t = P/P_{cr}$, where P_{cr} is the critical load at buckling. This critical load may be found from equation (6.40).

When $\gamma = 0$, the greatest load which the spring can carry is the buckling load P_{cr}. Hence, $S_1 = 1 - \tau_{cr}$, and $2\sqrt{\beta_{cr}} = \pi(1 - \tau_{cr})^{\frac{1}{2}}$. After some reductions

$$\frac{1}{4\beta_{cr}/\pi^2 + \nu_{cr}} = \frac{1}{\lambda_{cr}}\left(\frac{1}{1-\lambda_{cr}} - 1\right)$$

From $\quad \lambda_{cr} = \dfrac{P_{cr}}{\mathbf{A}_0},\ \beta_{cr} = \dfrac{P_{cr}}{\mathbf{B}_0}L_{cr}^2,\ \nu_{cr} = \dfrac{P_{cr}}{\mathbf{C}_0},$

and from $L_{cr} = (1 - \lambda_{cr})L_0$, the critical load is

$$P_{cr} = \frac{\pi^2 \mathbf{B}_0}{L_{cr} L_0} \frac{1}{4 + (\pi^2 \mathbf{B}_0 / L_{cr}^2 \mathbf{C}_0)} \tag{6.40}$$

L_{cr} is, for the time being, unknown. Since

$$P_{cr}/\mathbf{A}_0 = \lambda_{cr} = (L_0 - L_{cr})/L_0,$$

by putting $1 - \lambda_{cr} = L_{cr}/L_0 = j$, equation (6.40) reduces to

$$4j^3 - 4j^2 + \frac{\pi^2 \mathbf{B}_0}{L_0^2} j \left(\frac{1}{\mathbf{C}_0} + \frac{1}{\mathbf{A}_0}\right) - \frac{\pi^2 \mathbf{B}_0}{L_0^2 \mathbf{C}_0} = 0 \tag{6.41}$$

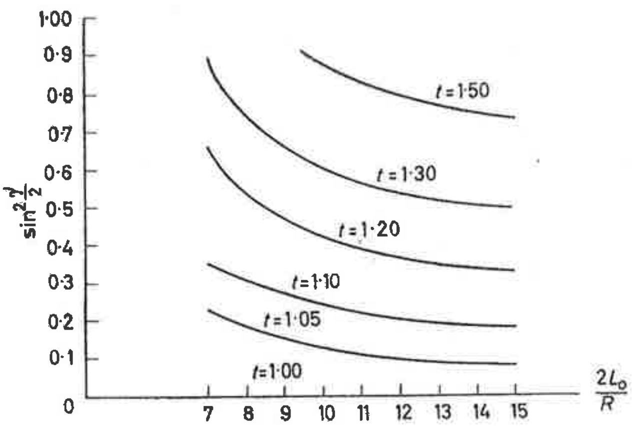

Figure 6.4 (From Mizuno[8])

This equation can be solved for j, hence P_{cr} may be found from (6.40).

When $\gamma = 0$, that is, before the spring buckles, $S_2 = 0$, and therefore $L_0/L = 1/(1 - \lambda)$. This leads to the following expression for the shortening of the spring before buckling occurs,

$$\delta_y = 2(L_0 - L) = 2\lambda L_0 = 2L_0 \frac{P}{\mathbf{A}_0} = 2P \frac{\pi R^3 L_0}{G I b_0}$$

If $n = 2L_0/b_0$ = number of coils, and d = diameter of the wire,

$$\delta_y = P \frac{64 n R^3}{d^4 G},$$

which agrees with the conventional analysis.

Regarding the coordinates of the central line of the spring once $P > P_{cr}$, we note that

$$h = \int_0^L \sin\theta \, ds = R\sqrt{f}\int_0^{\gamma} \frac{(1 - \tau\cos\theta)\sin\theta \, d\theta}{[U(\theta)]^{\frac{1}{2}}}$$

$$= \sqrt{f}\frac{R}{\tau}[(1 - \tau\cos\gamma)^2 - (1 - \tau)^2]^{\frac{1}{2}} \tag{6.42}$$

The vertical deflection v may be obtained by changing $\sin\theta$ to $\cos\theta$ in the integral of (6.42). Therefore,

$$v = R\sqrt{f}\int_0^{\gamma} \frac{(1 - \tau\cos\theta)\cos\theta \, d\theta}{[U(\theta)]^{\frac{1}{2}}} \tag{6.43}$$

By substituting $z = \cos\theta$, equation (6.43) can be reduced to elliptic integrals of the type

$$\int_1^z \frac{z}{[V(z)]^{\frac{1}{2}}} dz \quad \text{and} \quad \int_1^z \frac{z^2}{[V(z)]^{\frac{1}{2}}} dz$$

where $V(z)$ is a quartic in z.

Alternatively,

$$v = L_0(1 - \lambda)\left(\frac{S_1 - S_3}{S_1 - S_2}\right) \tag{6.44}$$

where $\quad S_3 = (1 - \tau)\sin^2(\gamma/2) + \frac{1}{8}(3 + 2\tau)\sin^4(\gamma/2) + \ldots$

The length of the spring after buckling may be found from equation (6.33).

This discussion applies to helical springs where the coils do not touch each other during deflection. The analysis also assumes that the radius of the coils remains unchanged or, at least, does not differ greatly in the loaded and unloaded conditions. If the spring is deformed solely by an axial compressive force $P < P_{cr}$, we have $M_t = 0$ in equation (6.24). If R is the radius of the helix and α its incline, the new radius R_1 and the new incline α_1 may be found from the simultaneous solution of

$$\left.\begin{aligned} P\cos\alpha_1 &= \frac{\mathbf{C}}{R_1}(V_1 - V) \\ P\sin\alpha_1 &= \frac{\mathbf{B}}{R_1}(W_1 - W) \end{aligned}\right\} \quad (6.45)$$

REFERENCES

[1] Clebsch, A. *Theorie der Elasticität fester Koerper*, Leipzig, 1862
[2] Love, A. E. H. *Mathematical Theory of Elasticity*, 4th Ed., p. 385. Dover Publications, New York, 1944
[3] Hess, W. Ueber die Biegung und Drillung eines duennen Stabes, *Math. Ann.* **23** (1884) 181
[4] Jacobi, C. G. J. Sur la Rotation d'un Corps. Jacobi's gesammelte Werke, vol. 2, pp. 289–352. (G. Reiner, Berlin, 1882)
[5] Byrd and Friedman. *Handbook of Elliptic Integrals*, p. 303, Springer Verlag, Berlin, 1954
[6] Hess, W. Ueber die Biegung und Drillung eines unendlich duennen Stabes mit zwei gleichen Widerstaenden, *Math. Ann.* **25** (1885) 1
[7] Love, A. E. H. *Mathematical Theory of Elasticity*, 4th Ed., p. 415
[8] Mizuno, M. Problem of large deflection of coiled spring, *Bull. Japan Soc. Mech. Eng.* **3**, 9 (1960) 95
[9] Timoshenko, S. *Theory of Elastic Stability*, 1st Ed., p. 165, McGraw-Hill Book Company, New York, 1936
[10] Biezeno and Grammel. *Engineering Dynamics*, vol. 2, p. 432, Blackie & Son Limited, London, 1956
[11] Byrd and Friedman. *Handbook of Elliptic Integrals*

INDEX